

Precision in RNA Molecular Measurement

Rebecca Sanders

School of Biosciences
Cardiff University

A thesis submitted for the degree of
Doctor of Philosophy
2016

Supervisor: Dr Deborah Mason (Cardiff University)

Second supervisor: Dr Jim Huggett (LGC)

Advisor: Dr Peter Kille (Cardiff University)

Joint project: Cardiff University and LGC

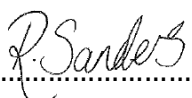


Declaration

I, Rebecca Sanders, confirm that the studies presented in this thesis were the unaided work of the author except for the following:


1. Some of the culture of Hep-G2, Hs 683 and SaOS-2 cell lines was performed by Dr Gary Morley and Dr Sabhi Rahman, LGC, Teddington (as detailed in corresponding Chapters).
2. Detailed in Chapter 6, the culture of MLO-Y4 and SaOS-2 cells, generation of 3D gel co-cultures and subsequent mechanical loading experiments were performed by Dr Cleo Bonnet, Cardiff University. Downstream processing (including RNA extraction) was performed by this author.
3. Statistical analysis was performed in collaboration with Dr. Simon Cowen, Dr. Steve Ellison and Dr. Jesus Minguez, Statisticians, LGC, Teddington.

This work has not been submitted in substance for any other degree or award at this or any other university or place of learning, nor is being submitted concurrently in candidature for any degree or other award.

Signed..... (candidate) Date25/05/16.....

STATEMENT 1


This thesis is being submitted in partial fulfillment of the requirements for the degree of PhD.

Signed  (candidate) Date25/05/16.....

STATEMENT 2


This thesis is the result of my own independent work/investigation, except where otherwise stated.

Other sources are acknowledged by explicit references. The views expressed are my own.

Signed  (candidate) Date25/05/16.....

STATEMENT 3

I hereby give consent for my thesis, if accepted, to be available for photocopying and for inter-library loan, and for the title and summary to be made available to outside organisations.

Signed  (candidate) Date25/05/16.....

Acknowledgements

I am grateful to my supervisors, Dr Jim Huggett (LGC) and Dr Deborah Mason (Cardiff University), for continued guidance and support. I would also like to thank my team leader, Dr Alison Woolford, for unwavering support and encouragement throughout my time at LGC. Colleagues Dr Simon Cowen, Dr Steve Ellison and Dr Jesus Minguez (LGC) for Statistical input. Dr Alison Devonshire, Dr Gavin Nixon and Dr Alexandra Whale (LGC) for experimental contributions. Dr Gary Morley and Dr Sabhi Rahman (LGC) for preparation of cell lysates. Dr Cleo Bonnet (Cardiff University) for generation of 3D co-cultures and help with bone core experiments. Prof. Lynda Bonewald (University of Missouri, USA) for the generous donation of MLO-Y4 osteocyte-like cells. The multi-functional team at the Arthritis Research UK Biomechanics and Bioengineering Centre in Cardiff involved in obtaining the clinical bone core samples (Dr Andrea Longman, Dr Helen Roberts, Dr Deborah Mason, Dr Cleo Bonnet, and surgeons Rhys Williams, Chris Wilson and Sanjeev Argawal). Dr Marc Salit (NIST, USA) for kind provision of ERCC plasmid DNA reference standards. Furthermore, I would like to voice my appreciation to all my colleagues, both at LGC and at Cardiff University, for shared knowledge and expertise, encouragement and a friendly and collaborative working environment. This study was partly funded by the UK National Measurement System.

I would also like to thank my family, and in particular my Mother, who has always believed in me; an incredible woman and my role model.

Table of Contents

Declaration	i
Acknowledgements	iii
Table of Contents	iv
I. List of Abbreviations	x
II. List of Figures	xiii
III. List of Tables	xvi
IV. Manuscripts	xviii
Abstract	xix
1 Introduction	1
1.1 Introduction to Metrology	1
1.1.1 The Need for Standardisation	1
1.1.2 Accuracy and Measurement Uncertainty	3
1.2 Reference materials	6
1.2.1 Traceability.....	7
1.2.2 Accurate Measurement in Molecular Biology	7
1.3 RNA Molecular Measurement	10
1.3.1 Sources of Variability.....	10
1.3.1.1 Sample Source and Storage	13
1.3.1.1.1 Cell Line Treatment	14
1.3.1.2 RNA Extraction	14
1.3.1.3 Reverse Transcription Quantitative PCR.....	15
1.3.1.3.1 Reverse Transcription Priming	17
1.3.1.3.2 Reverse Transcription Enzymes	18
1.3.1.4 Inhibition.....	20
1.3.1.4.1 One-Step versus Two-Step RT-qPCR	22
1.3.1.4.2 Reagents and Equipment	25
1.3.1.4.3 Estimating Copy Number	26
1.3.1.5 Other Molecular Methods	28
1.3.1.5.1 Digital PCR	29

1.3.1.5.2	Next Generation Sequencing (NGS)	29
1.3.1.6	Normalisation	31
1.3.1.6.1	RNA Mass Quantity	31
1.3.1.6.2	Internal Reference Genes	33
1.3.1.6.3	External Standards	36
1.3.1.6.4	Measurement Controls	38
1.3.1.7	Other Considerations	39
1.4	Clinical Relevance	41
1.4.1	Biological Variability	42
1.4.2	Tissue Variability	43
1.4.3	Patient Variability	44
1.4.4	Musculoskeletal Disease	44
1.4.4.1	Important Clinical Questions in the Musculoskeletal System.....	46
1.4.4.2	Additional Cell Lines.....	47
1.4.5	Practical Clinical Challenges	47
1.5	Conclusion	49
1.6	Scope.....	50
1.7	Aims and Hypothesis.....	50
2	Materials & Methods	54
2.1	Materials	54
2.1.1	Synthetic RNA Transcripts.....	54
2.1.2	Cell Lines.....	55
2.1.2.1	Carrier Options.....	55
2.2	Production of RNA	56
2.2.1	ERCC RNA: Plasmid DNA Digest & IVT.....	56
2.2.1.1	Secondary Structure Prediction	57
2.2.2	Cell Line RNA Production for Complex Background.....	57
2.3	Preparation of Transcriptomic Calibration Material (TCM).....	58
2.3.1	Endogenous Target Selection.....	59
2.3.1.1	Reference Genes.....	59
2.3.1.2	Genes of Interest	60
2.3.2	Assay Design.....	60
2.3.3	Measurement Uncertainty Budget	61

2.4	Reverse-Transcription Quantitative PCR Analysis	61
2.4.1	Two-step RT-qPCR.....	62
2.4.2	One-step RT-qPCR	62
2.4.3	qPCR Analysis	63
2.4.4	dPCR Analysis	63
2.4.4.1	dPCR Calculations Explained	65
2.5	Experimental Details – RT-qPCR Kit Comparison.....	67
2.5.1	One-Step RT-qPCR Kit Comparison by dPCR	67
2.5.2	Comparison between dPCR and UV Measurement	68
2.5.3	Linearity and Sensitivity of RT-dPCR	68
2.6	Experimental Details – Extraction Kit Comparison	68
2.6.1	Lysate Preparation	68
2.6.2	Total RNA Extraction using TRIzol Reagent.....	69
2.6.3	Total RNA Extraction using RNeasy Mini Kit	69
2.6.4	Total RNA Extraction using MasterPure RNA Purification Kit	69
2.6.5	Post-Extraction Treatment.....	70
2.6.6	RNA Quality Metrics.....	70
2.6.6.1	Nanodrop.....	70
2.6.6.2	Bioanalyzer.....	70
2.6.6.3	Qubit	71
2.6.6.4	Alu PCR.....	71
2.7	Experimental Details - Sample Source and Type	72
2.7.1	2D Culture Model – SaOS-2 Mineralisation	72
2.7.2	3D Co-Culture Model.....	73
2.7.2.1	Cell Lines	73
2.7.2.2	3D Collagen Co-Cultures	73
2.7.2.3	Mechanical Loading of 3D Co-cultures	74
2.7.2.4	TRIzol Treatment of 3D Co-cultures.....	76
2.7.3	Clinical Samples – Total Knee Replacement Bone Cores	76
2.7.3.1	Dismembrator.....	78
2.7.4	Quality Metrics	78
2.7.5	Dynamic Array.....	79
2.7.5.1	Preamplification.....	79
2.7.5.2	Dynamic Array Analysis.....	80

3	Production & Validation of Novel Transcriptomic Calibration Material.....	82
3.1	Introduction.....	82
3.2	Material & Methods.....	83
3.2.1	DNA Contamination Assessment	84
3.2.2	Assay Cross-Reactivity with Human Targets	85
3.2.3	Carrier Optimisation.....	85
3.2.4	RNA Stability Analysis.....	85
3.2.5	RT Variability	86
3.2.6	Endogenous Target Selection.....	86
3.2.7	Transcriptomic Calibration Material Homogeneity and Stability.....	86
3.3	Results & Discussion.....	88
3.3.1	ERCC IVT RNA Quality Control.....	88
3.3.1.1	Assay Validation	88
3.3.1.2	Cell Line RNA Quality	92
3.3.2	DNA Contamination Assessment	96
3.3.3	Assay Cross-Reactivity with Human Targets	101
3.3.4	Carrier Optimisation.....	101
3.3.5	RNA Stability Analysis.....	106
3.3.6	RT Variability	111
3.3.7	Endogenous Target Selection.....	115
3.3.8	Transcriptomic Calibration Material Homogeneity and Stability.....	118
3.3.9	Measurement Uncertainty.....	127
3.4	Conclusions.....	127
4	Comparison of Different Reverse Transcriptases by Digital PCR.....	130
4.1	Introduction.....	130
4.2	Materials & Methods	132
4.2.1	Statistical Methods.....	132
4.3	Results & Discussion.....	133
4.3.1	One-Step RT-qPCR Kit & Format Comparison by dPCR using Synthetic RNA Targets 133	
4.3.2	Comparison Between dPCR and UV Measurement of Synthetic RNA Targets ...	136
4.3.3	Linearity and Sensitivity of RT-dPCR of Synthetic RNA Targets	138

4.3.4	Evaluation of Reverse Transcriptase’s Targeting Endogenous mRNA Transcripts 141	
4.3.5	Causes of Differing RT-dPCR Results	143
4.4	Conclusions.....	149
5	Evaluation of the Impact of Extraction Protocol on Target Quantification	151
5.1	Introduction.....	151
5.2	Materials & Methods	152
5.2.1	Lysate preparation	152
5.2.2	Total RNA Extraction using TRIzol	153
5.2.3	Total RNA Extraction using RNeasy Mini Kit	154
5.2.4	Total RNA Extraction using MasterPure RNA Purification Kit	154
5.2.5	Post-Extraction Treatment.....	155
5.3	Results & Discussion.....	155
5.3.1	Effect of Extraction Protocol on RNA Yield	155
5.3.2	Effect of Extraction Protocol on RNA Quality.....	158
5.3.2.1	Assessment of gDNA Contamination	162
5.3.3	Effect of Quality Assessment Method on RNA Yield	164
5.3.4	Effect of Quality Assessment Method on RNA Quality	173
5.3.5	Influence of Different Cell Batches	175
5.4	Conclusions.....	180
6	The Influence of Sample Type on Measurement Variability.....	185
6.1	Introduction.....	185
6.1.1	2D Culture Model	188
6.1.2	3D Co-Culture Model.....	189
6.1.3	Clinical Samples	190
6.2	Materials & Methods	191
6.2.1	2D Culture Model – SaOS-2 Mineralisation	191
6.2.2	3D Co-Culture Model.....	191
6.2.3	Clinical Samples	192
6.2.4	RT-qPCR: Dynamic Array	193
6.3	Results & Discussion.....	193
6.3.1	Comparison of RNA Yield and Quality from Different Sample Sources	193

6.3.1.1	RNA Yield and Precision	194
6.3.1.1.1	2D Culture Model	194
6.3.1.1.2	3D Co-Culture Model	199
6.3.1.1.3	Clinical Samples.....	200
6.3.1.2	RNA Extraction Process Precision Factors.....	202
6.3.1.3	Alu PCR.....	204
6.3.1.3.1	3D Co-Culture Model	204
6.3.1.3.2	Clinical Samples.....	206
6.3.2	Comparison of mRNA Expression Variability from Different Sample Sources....	206
6.3.2.1	Preamplification.....	206
6.3.2.2	Reference Gene Determination	208
6.3.2.2.1	3D Co-Culture Model	208
6.3.2.2.2	Clinical Samples.....	210
6.3.2.3	mRNA Quantification Process Precision Factors.....	211
6.3.2.3.1	3D Co-Culture Model	211
6.3.2.3.2	Clinical Samples.....	211
6.3.2.4	Comparison of Factor Variability	215
6.3.2.4.1	3D Co-Culture Model	215
6.3.2.4.2	Clinical Samples.....	221
6.3.2.5	Assay Troubleshooting.....	227
6.4	Conclusions.....	232
7.	Final Discussion & Overall Conclusions	238
7.1.	Future Work	244
7.2.	Overall Impact	246
8.	References	248
9	Appendices	280
9.1	Appendix 1 – Assay Information	280
9.2	Appendix 2 –Endogenous and ERCC Transcript Predicted Secondary Structures	289
9.3	Appendix 3 – Measurement Uncertainty Budgets.....	301
9.4	Appendix 4 – Pilot Reference Material Composition.....	322
9.5	Appendix 5 – Typical dPCR Output Data.....	323
9.6	Appendix 6 – Digital MIQE.....	327

List of Abbreviations

Abbreviation	Meaning
A_{260}	Absorbance at wavelength 260 nm
AL	Anterior lateral
ALP	Alkaline phosphatase
AM	Anterior medial
AMV	Avian myeloblastosis virus
ANOVA	Analysis of variance
BMP	Bone morphogenic protein
CASC3	Cancer susceptibility candidate 3
CCQM	Consultative Committee for Amount of Substance — Metrology in Chemistry
cDNA	Complementary DNA
CI	Confidence interval
CNS	Central nervous system
ColI	Type I collagen
C_q	Quantification threshold (formally C_t or C_p)
CRM	Certified reference material
C_t	Cycle threshold (C_q)
CV	Coefficient of variation
DFBS	Dialysed fetal bovine serum
dMIQE	Minimum Information for Publication of Quantitative Digital PCR Experiments
DNA	Deoxyribose nucleic acid
DNase	Deoxyribonuclease
dPCR	Digital PCR
dsDNA	Double-stranded DNA
EAAT1	Excitatory amino acid transporter 1 (also known as SLC1A3, GLAST1)
EAR	Expressed <i>Alu</i> repeat
ELISA	Enzyme-linked immunosorbent assay
ENCODE	Encyclopedia of DNA Elements
ERCC	External RNA Control Consortium
ERS	Expressed repetitive elements
FFPE	Formaldehyde-fixed paraffin-embedded
FISH	Fluorescent in-situ hybridisation
GAPDH	Glyceraldehyde-3-phosphate dehydrogenase
gDNA	Genomic DNA
GEUVADIS	Genetic European Variation in Disease
GLAST1	Glutamate/aspartate transporter 1 (also known as EAAT1, SLC1A3)
GMO	Genetically modified organism

GOI	Gene of interest
HBSS	Hanks Balanced Salt Solution
Hep-G2	Hepatocyte cell line
HER2	Human epidermal growth factor 2
HIFBS	Heat inactivated fetal bovine serum
HINBCS	Heat inactivated newborn calf serum
HP-ICP-OES	High-performance inductively coupled plasma optical emission spectrometry
HPLC	High-performance liquid chromatography
HPRT1	Hypoxanthine phosphoribosyl-transferase 1
Hs 683	Glial cell line
IGF-I	Insulin-like growth factor I
IHC	Immunohistochemistry
IRC	Inter-run calibrator
ISO	International Organization for Standardization
IU	International unit
IVT	<i>In vitro</i> transcription
LOQ	Limit of quantification
MIAME	Minimum Information About a Microarray Experiment
MIQE	Minimum standard for the provision of information for publications utilising qPCR experiments
MLO-Y4	Osteocyte-like cells
MMLV	Moloney murine leukemia virus
MMP1	Matrix metalloproteinase 1
mRNA	Messenger RNA
Mw	Molecular weight
NES	Nestin
NGS	Next Generation Sequencing
NIST	(American) National Institute of Standards and Technology
NMI	National Measurement Institute
NTC	No template control
OCN	Osteocalcin
OPN	Osteopontin
PCR	Polymerase chain reaction
PL	Posterior lateral
PM	Posterior medial
Poly (A) tail	Polyadenylated tail
PreAmp	Preamplification
qPCR	Real-time quantitative polymerase chain reaction
RCT	Randomised controlled trials

rDNase I	Recombinant DNase I
RIN	RNA integrity number
RM	Reference material
RNA	Ribose nucleic acid
RNase H	Ribonuclease H
RNA-seq	RNA sequencing
RQ	Relative quantification
RQI	RNA quality indicator
RT	Reverse transcription
RTase	Reverse transcriptase
rRNA	Ribosomal RNA
RSD	Relative standard deviation
RSS	RNA storage solution
RT-dPCR	Reverse transcriptase digital PCR
RT-qPCR	Reverse transcriptase quantitative PCR
SaOS-2	Osteoblastic cell line
SD	Standard deviation
SEM	Standard error of the mean
SI	Système International d'Unités
SLC1A3	Solute carrier family 1 (glial high affinity glutamate transporter), member 3 (also known as EAAT1, GLAST1)
ssDNA	Single-stranded DNA
sTCM	Synthetic-only transcriptomic calibration material
TCM	Transcriptomic calibration material
TGF	Transforming growth factor
TKR	Total knee replacement (surgery)
tRNA	Transfer RNA
U	Expanded uncertainty
UBC	Ubiquitin C
u _c	Combined standard uncertainty
UNG	Uracil N-glycosylase
UTR	Untranslated region
UV	Ultraviolet
VEGF	Vascular endothelial growth factor
WHO	World Health Organization

I. List of Figures

Figure 1.1 Effect of varying conditions on precision measurement.	5
Figure 1.2 Cause & Effect: Uncertainty Contributions for mRNA Analysis.	11
Figure 1.3 Schematic representation of variability observed between cDNA and RNA standard curves.	16
Figure 1.4 Schematic representation of different experimental designs representing biological versus technical replication.	23
Figure 1.5 Proposed experimental strategy for investigating contributors to variability.	51
Figure 2.1 Fluidigm Biomark chips.	64
Figure 2.2 Schematic representation of 3D gel co-cultures.	75
Figure 2.3 Positional schematic of clinical sample regions.	77
Figure 3.1 Quality control of ERCC IVT RNA.	90
Figure 3.2 RNA yields pre- and post-DNase treatment.	94
Figure 3.3 Quality control of cell line total RNA.	95
Figure 3.4 DNA Contamination Assessment.	98
Figure 3.5 Carrier optimisation.	104
Figure 3.6 RNA Stability Analysis.	110
Figure 3.7 RNA versus cDNA Standard Curves.	113
Figure 3.8 Comprehensive gene stability, generated from RefFinder output.	116
Figure 3.9 Results of Homogeneity study.	119
Figure 3.10 Results of Short-Term Stability study.	122
Figure 3.11 Results of Long-Term Stability study.	124
Figure 4.1 One-step kit comparison.	134
Figure 4.2 dPCR versus UV quantification.	137

Figure 4.3 dPCR sensitivity for RNA measurement.	140
Figure 4.4 Evaluation of Reverse Transcriptases.	142
Figure 5.1 Average total RNA extracted by each extraction method.	156
Figure 5.2 RNA Nanodrop quality absorbance assessment.	159
Figure 5.3 <i>Alu</i> PCR analysis of samples extracted using different methods.	163
Figure 5.4 RNA yields according to different metrics.	166
Figure 5.5 Quality Metric Correlation Plots of Yield Estimates.	171
Figure 5.6 Representative Bioanalyzer electropherogram.	174
Figure 5.7 RNA Bioanalyzer quality assessment.	176
Figure 5.8 Batch Analysis.	177
Figure 5.9 <i>Alu</i> PCR analysis of different cell batches.	179
Figure 5.10 <i>Alu</i> PCR cell batch analysis: genome equivalents.	181
Figure 6.1 Total RNA yields.	196
Figure 6.2 SaOS-2 mineralisation process precision contributed by different factors.	203
Figure 6.3 <i>Alu</i> PCR expression.	205
Figure 6.4 Comprehensive gene stability, generated from RefFinder output.	209
Figure 6.5 3D Gel co-culture process precision contributed by different factors.	213
Figure 6.6 Clinical bone core process precision contributed by different factors.	214
Figure 6.7 3D co-culture treatment variability.	217
Figure 6.8 3D Gel co-culture variability distributions.	219
Figure 6.9 Clinical bone core patient variability.	222
Figure 6.10 Clinical bone core anatomical position variability.	223

Figure 6.11 Clinical bone core SLC1A3 anatomical position expression variability.....	225
Figure 6.12 RT-qPCR test for abundance.	229
Figure 6.13 EAAT1/SLC1A3 RNA Secondary Structure Prediction from mFold.	231
Figure 9.1 RNA Secondary Structure Predictions from mFold.	300
Figure 9.2 Calibrant Unit Measurement Uncertainty Contributing Factors.	307
Figure 9.3 Unknown 1 Unit Measurement Uncertainty Contributing Factors.	314
Figure 9.4 Unknown 2 Unit Measurement Uncertainty Contributing Factors.	321
Figure 9.5 Typical dPCR output data from Chapter 4.	326

II. List of Tables

Table 1.1 Factors Contributing Bias to an RT-qPCR Measurement.....	12
Table 2.1 dPCR Specifications	66
Table 3.1 IVT ERCC RNA standards.	89
Table 3.2 ERCC Assay Efficiencies.	91
Table 3.3 Cell line RNA quantity	93
Table 3.4 Carrier optimisation.	102
Table 3.5 RNA stability analysis.....	107
Table 3.6 Endogenous reference genes and GOI selected and validated	117
Table 3.7 Assigned values and measurement uncertainty of ERCC standards.	125
Table 4.1 Three one-step kit comparison with uniplex and duplex formats.	135
Table 5.1 Nanodrop quality assessment based on UV absorbance ratios at 260/280 and 260/230 nm.	160
Table 5.2 qPCR measurement bias introduced by standard curve value assignment.	168
Table 6.1 Accuracy and Precision between PreAmplified and Non-PreAmplified cDNA.	207
Table 9.1 Primer and probe sequences	280
Table 9.2 Human endogenous control assays	282
Table 9.3 Human endogenous GOI assays	283
Table 9.4 Assay Positions	284
Table 9.5 Sample dilutions analysed during study.....	285
Table 9.6 ERCC RNA concentration and copy number estimates	288
Table 9.7 Calculation of Calibrant assigned value and measurement uncertainty.....	301

Table 9.8 Calculation of Unknown 1 assigned value and measurement uncertainty.....	308
Table 9.9 Calculation of Unknown 2 assigned value and measurement uncertainty.....	315
Table 9.10 Proportions of each cell line included in the pilot RMs.....	322
Table 9.11 dMIQE checklist for authors, reviewers and editors.	327

IV. Manuscripts

1. Considerations for accurate gene expression measurement by reverse transcription quantitative PCR when analysing clinical samples. **Sanders R**, Mason DJ, Foy CA, Huggett JF. *Anal Bioanal Chem.* 2014 May 25. doi: 10.1007/s00216-014-7857-x.
2. The need for transparency and good practices in the qPCR literature. Bustin SA, Benes V, Garson J, Hellemans J, Huggett J,....., **Sanders R**, *et al.* *Nat Methods.* 2013 Nov;10(11):1063-7. doi: 10.1038/nmeth.2697.
3. Evaluation of digital PCR for absolute RNA quantification. **Sanders R**, Mason DJ, Foy CA, Huggett JF. *PLoS One.* 2013 Sep 20;8(9):e75296. doi: 10.1371/journal.pone.0075296. eCollection 2013.
4. Application of next generation qPCR and sequencing platforms to mRNA biomarker analysis. Devonshire AS, **Sanders R**, Wilkes TM, Taylor MS, Foy CA, Huggett JF. *Methods.* 2013 Jan;59(1):89-100. doi: 10.1016/j.ymeth.2012.07.021. Epub 2012 Jul 24. Review.

Accepted for Publication

1. An international comparability study on quantification of mRNA gene expression ratios: CCQM-P103.1. Devonshire AS, **Sanders R**, *et al.* *Accepted for publication by BDQ.*

Abstract

Measurement of gene expression profiles represents a snapshot of cellular metabolism or activity at the molecular scale. This involves measurement of messenger (m)RNA employing techniques such as reverse transcription quantitative polymerase chain reaction (RT-qPCR). To truly assign biological significance to associated findings, researchers must consider the idiosyncrasies of this method and associated technical error, termed measurement uncertainty. Significant error can occur at sample source, RNA extraction, RT and qPCR levels. This thesis explores the steps which may introduce potential bias. It is hypothesised that error in mRNA measurement can be partitioned across different experimental stages. Within this thesis, RNA measurement from sample source to qPCR has been analysed at each stage to delineate variability contributions attributed to specific steps using synthetic and validated endogenous reference genes, single cell lines, 3D models and complex bone tissue. These data determined that total RNA yields remained consistent between treatment (2D cell mineralisation, 3D co-culture mechanical loading) and control groups ($p > 0.06$). Sample complexity was positively correlated with RNA extraction yield variability. Evaluation of different extraction methods demonstrated that total RNA yields differed between methods ($p < 0.001$). Assessing total RNA quantity and quality, different metrics (Bioanalyzer, Nanodrop and Qubit) generated different yield estimates ($p < 0.05$), although quality estimates from different metrics were found to be comparable. In addition, different cell batches (cultures of the same cells from different cryo vials) generated disparate total RNA yields ($p < 0.02$), with variable quality estimates, despite normalisation for cell count. RT-digital PCR analysis revealed quantification differences and detection sensitivity biases between different RT enzymes ($p < 0.0001$), suggesting cDNA prepared using different RT enzymes cannot be meaningfully compared. The ERCC synthetic targets were variable under the model conditions assessed and therefore not suitable as normalisers in these circumstances. This work provides a guide for the approaches necessary to reduce error, improve experimental design and minimise uncertainties.

Chapter 1

Introduction

1 Introduction

This chapter is adapted from the peer-reviewed publication: Considerations for accurate gene expression measurement by reverse transcription quantitative PCR when analysing clinical samples. **Sanders R, Mason DJ, Foy CA, Huggett JF.** Anal Bioanal Chem. 2014 May 25. doi: 10.1007/s00216-014-7857-x.

1.1 Introduction to Metrology

Metrology is the science of measurement. A theme in constant flux and development, metrological challenges are fundamental to every scientific field. The primary goal for all forms of measurement is accuracy, to address the question whether the measured value is a true representation of the actual value. These queries can be partially satisfied by the assignment of uncertainty values to express the confidence in a result. Methodological and technological innovations fuel an ever-progressing capability to improve measurement accuracy and precisely assign values to measurands of otherwise unknown quantities.

1.1.1 The Need for Standardisation

Throughout the history of civilisation, as modern societies evolved each developed their own unique numbering systems. For as long as these measurement systems have been in place, standardisation practices have been developed in order to aid social development through trade and commerce. An agreed set of measurement units recognised throughout the world was essential for the evolution of international trade. Since 1670, when a comprehensive decimal measurement system was proposed, modern society has been on a journey towards the development of a globally recognised metric system. However, it was not until 1790, in the midst of the French Revolution, when the National Assembly of France requested the French Academy of Science to ‘deduce an invariable standard for all the measures and all the weights’, that a simple and scientific system was put in

Chapter 1 Introduction

place. The consequence of this development came to fruition in 1960, when the General Conference on Weights and Measures revised the system and established seven base units: the metre (for length); the kilogram (for weight); the second (for time); the ampere (for electric current); the kelvin (for thermodynamic temperature); the mole (for amount of substance); and the candela (for luminous intensity). Together, these base units form the foundation of the *Système International d'Unités* – the international metric system of units known throughout the world as SI. A further 22 derived units complete the complement of the SI system [1,2]. The metric system is widely used in science, engineering and medicine. Today, standardisation of measurement is fundamental to all facets of civilisation and is particularly well established within the scientific and engineering communities.

The National Measurement Institutes (NMIs) that lie within many of the countries throughout the world develop and maintain national measurement standards. LGC, the UK's NMI for chemical and bioanalytical measurement, supports the measurement infrastructure in the UK by producing reference materials which allow other laboratories to ensure the traceability of measurement results through instrument calibration and method validation.

This level of measurement standardisation is crucial to almost all aspects of modern-day life. Architecture; superconductors; GPS; transport systems; finance; the internet; all these endeavours would be unsuccessful without modern metrology standards. Failure to meet these standards can be very costly, financially and otherwise. Human health and safety depend on reliable measurements in medical diagnosis and therapy. The reliability of these measurements must be beyond reproach, because errors can have devastating consequences. These factors taken together necessitate sustained efforts to improve the reliability of such measurements and play a key role in the continual development of effective healthcare systems.

1.1.2 Accuracy and Measurement Uncertainty

Accuracy is essentially how close the measurement is to the truth and is influenced by both precision and bias [3]. The challenge when measuring patient samples is that the truth is often a moving target that can vary from patient to patient and within patient, over time. As measurement systems improve they may often lead to increased measurement precision. The added danger with high precision is that it can lead to considerable bias. This can manifest results that are difficult to reproduce, either simply as a result of repeat measurements providing different estimations of the truth or, potentially worse, results that are reproducible but still biased and therefore all incorrect; this situation is problematic because agreement between laboratories leads to further confidence that the wrong result is correct.

To further understand measurement accuracy, considerations of uncertainty should be applied to indicate scientific confidence. Uncertainty has two components: systematic and random variation. Systematic errors lead to bias in the measurement. These error components are fixed and predictable and may be inherent to various instruments and methods. Random variation occurs when making repeated measurements (related to precision; a measure of the degree of agreement between replicate measurement results obtained for the same sample). Contributing factors are multitude and include issues of sampling, different analysts as well as each stage of the stepwise protocol necessary for a measurement [4].

The concept of accuracy includes the effect of both precision and bias and describes how close a single result is to the true value. While it cannot be given a numerical value, measurement results are said to be 'more accurate' when measurement errors are reduced. Results with a small bias that are also very precise are considered highly accurate, i.e., the average result is close to the true value and the data spread (standard deviation) is small. Equally, methods generating data with a large bias (large difference between true value and average

Chapter 1 Introduction

value of results), or imprecision (large variance), or both, would be considered inaccurate.

It is also prudent to introduce and define precision terms (**Figure 1.1**). Repeatability represents the tightest extreme of independent precision measurements, describing the sort of precision one might expect from a set of replicate measurements made one after the other, in a single laboratory, by a single analyst on a single instrument, with a short time interval [3,5]. Over such conditions, one would not expect results to be affected by drift. Intermediate precision represents mid-range precision, where a single laboratory uses several analysts or equipment sets for a particular method, over different days, and may give the most appropriate precision value for setting quality control limits [3,5]. Various combinations of conditions are user defined. Reproducibility represents the widest extreme of precision, describing the variation that one might expect within a set of measurements made on a sample over an extended time period, in several laboratories, by a number of different analysts and different instruments [3,5]. One would expect reproducibility to reflect variation in the method from all possible sources, i.e. the sort of variation expected in a method used to measure a sample in several different laboratories.

As discussed in subsequent sections, the science of measurement is well established in the fields of physics and chemistry. In molecular analysis however, the concept of 'true value' is relatively new and hampered by the fact that there is no agreement on how such a value might be obtained [4]. Despite this, bias must still be considered in the form of standardisation and mechanisms put in place to ensure the robustness of results between laboratories can be assessed. Accordingly, variability at each stage of an experimental process needs to be taken into account. This allows a comprehensive assessment of the confidence in a result and enables inter- and intra-laboratory comparison of data, especially if different measurement equipment and/or methods are utilised.

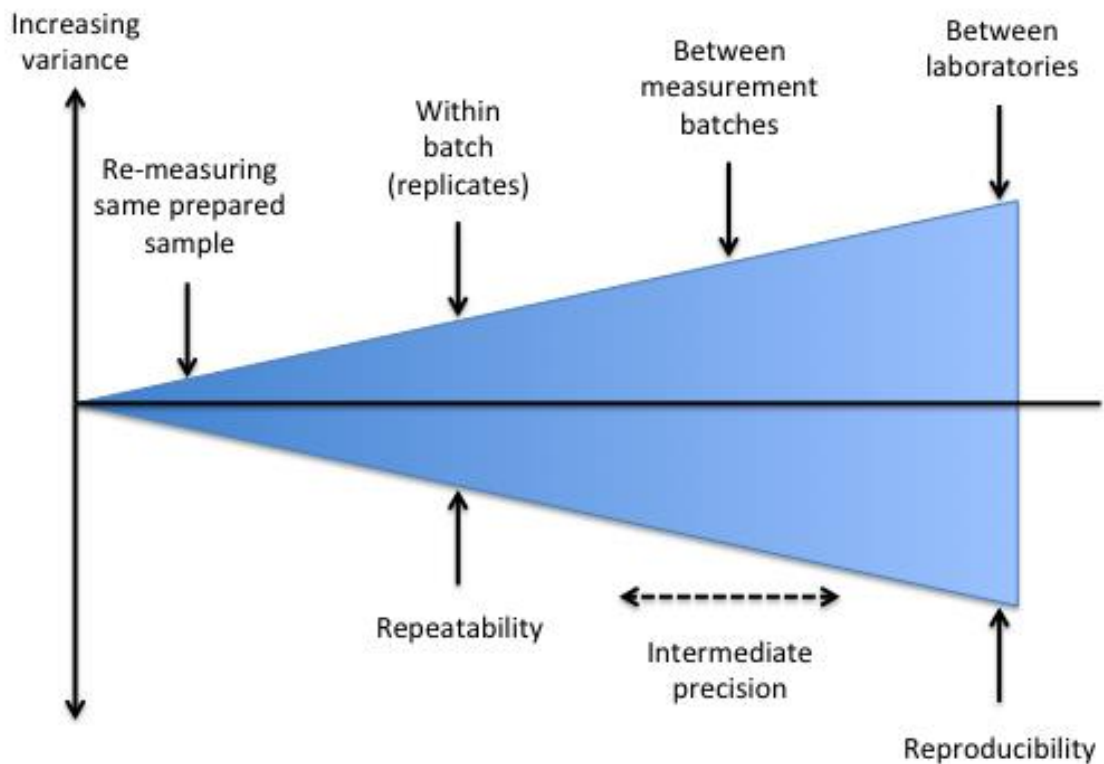


Figure 1.1 Effect of varying conditions on precision measurement. In general, the more conditions you vary within a particular method the larger the precision value will become. Thus you will normally expect repeatability precision to be smaller (i.e. more precise) than intermediate precision, which will in turn be smaller than reproducibility. To get a representative estimate of the precision of an analytical method, the replicate determinations made must be sufficiently independent. A failure to analyse replicates that are appropriately independent will lead to misleadingly good precision data. Figure modified from [5].

1.2 Reference materials

“Reference materials are important to ensure the necessary sensitivity, specificity and level of reproducibility of intra- and inter-laboratory test results. The best approach to achieve consistent and comparable quantitative data amongst laboratories is by the use of internationally established reference reagents.”

Dr Karen Mann, President of the Association of Molecular Pathology, in her testimony before Congress (Feb 24, 2010). Source: <http://www.amp.org>

To obtain highly accurate results, sample unknown measurements should be properly correlated to appropriate standards with a well-defined value and uncertainty [3]. The establishment of accurate and practical measurement standards linked to fundamental constants, having also the range and diversity required for the whole of modern science and technology is a major undertaking. Measurement standards, also known as reference materials, are not static. They evolve continually to reflect advances in science and in response to changing industrial and other needs [1,6,7].

A reference material (RM) is defined as “a material or substance one or more of whose property values are sufficiently homogeneous and well established to be used for the calibration of an apparatus, the assessment of a measurement method, or for assigning values to materials” [8,9]. A certified reference material (CRM) is defined as a “reference material, accompanied by a certificate, one or more of whose property values are certified by a procedure which establishes its traceability to an accurate realisation of the unit in which the property values are expressed, and for which each certified value is accompanied by an uncertainty at a stated level of confidence” [9,10].

In any long-term programme to observe small changes in critical parameters, such as monitoring viral loads in disease states, the measurements made at the beginning of the study must be compatible with those made at the end, i.e. the measurement standards used to calibrate them must have long-term stability [1].

1.2.1 Traceability

A given result obtained in terms of measurement units that are linked by an unbroken chain of calibrations or comparisons to national measurement standards, in practical terms to SI units, is known as traceability of measurement results [1]. The uncertainty of the calibration or comparison must be given at each link of the chain. An appropriate uncertainty of the final measurement in terms of SI units can then be achieved. Only when the uncertainty has been properly calculated is it possible to estimate the measurement's reliability and decide whether or not it is suitable for the application in hand [1], or its 'fitness for purpose'. In this way, measurement traceability facilitates appropriate data comparison.

1.2.2 Accurate Measurement in Molecular Biology

When used appropriately, RMs and CRMs allow value assignment for a measurand in SI units [9,11]. However, molecular biology is a comparatively new discipline, particularly in terms of the development of measurement standards. This is additionally hindered by the fact that, while some biological methods may be traceable to the SI via the Mole (for example, accurate estimation of total DNA mass concentration, e.g. ng/ μ L) [12], current SI units and their derivatives may in fact not be apposite for the description of all biological measurement as indirect conversions and various assumptions are necessary for reporting according to SI. For example, whilst estimation of total DNA mass concentration by UV spectrophotometry may be converted to the Mole, this method does not take into account presence of intact target or the capacity of any given target to undergo

Chapter 1 Introduction

successful PCR amplification. These are assumptions that must be made in order to assign a value. An inability to measure directly to SI affects traceability and uncertainty considerations. Several studies have highlighted the lack of standards in this discipline, which leads to difficulties in comparing results from different laboratories or between different methods [13-16].

The three central components of molecular biology measurement encompass DNA, RNA and proteins. In these terms, a development of an appropriate RM may require the application of non-SI derived standardised measurement; such as based on enumeration principles, for example DNA copy number (such enumeration units can be linked back to SI, but several assumptions must be made that may compromise uncertainty estimates). An international unit (IU), officially defined by the International Conference for Unification of Formulae, is an internationally accepted amount of a substance. This arbitrary measure may be used to standardise measurements where the amount of a substance cannot be traced back to SI. The IU is utilised for fat-soluble vitamins (such as vitamins A, D and E) and certain hormones, enzymes, and biologicals (such as vaccines and viral RMs [17]). DNA RMs certified for their DNA mass concentration, with an estimated measurement uncertainty and traceable to the SI, are beginning to emerge for the purpose of measurement standardisation in molecular biology. Current examples include human cytomegalovirus [18], BCR-ABL [19] and GMO analysis [20]. However, appropriate CRMs are necessary for effective comparison of quantitative measurements, method validation, and quality control in routine analysis [12]. To improve biological measurement capabilities, DNA (or RNA) reference materials are required which have been certified for total DNA (or RNA) concentration [12]. Over the last ten years, international measurement institutes have collaborated to build an improved support infrastructure for biological measurement. This work is coordinated by the Nucleic Acids (formerly Bioanalysis) Working Group, part of the CCQM (Consultative Committee for Amount of Substance — Metrology in Chemistry [21]) of the International Committee for Weights and Measures. This relatively new field of science is referred to as biometrology and has applications

Chapter 1 Introduction

in fields as diverse as agricultural biotechnology, diagnostics, forensic science, pharmaceuticals and speciation.

The real-time quantitative polymerase chain reaction (qPCR) [22], developed from the revolutionary method of PCR pioneered by Kary Mullis in the 1980s [23-25], has emerged as a widely used method for biological investigation because it can detect and precisely quantify very small amounts of specific nucleic acid sequences. This is coupled to an inherent simplicity that makes qPCR assays straightforward to design and perform. The characterisation of gene expression patterns through quantification of messenger RNA (mRNA), by coupling reverse transcription with PCR, as a surrogate of cell metabolism is a major application of this technology. Reverse transcription quantitative PCR (RT-qPCR) enables rapid and precise assessment of changes in mRNA levels as a result of physiology, pathophysiology or development [26]. However, for RNA analyses to be clinically informative, reliable measurements that are reproducible between laboratories are essential. As much as 30% of the costs of medical care budgets are in measurements and tests related to diagnosis [1]. This necessitates sustained efforts to improve the reliability of such measurements and tests, which play a key role in the continual development of effective healthcare systems.

In research studies, RT-qPCR has been used to measure bacterial mRNA levels [27,28] or RNA viral loads [29-32], to evaluate cancer status or to track disease progression and response to treatment [33-35]. As a consequence, this method is being applied to the discovery and development of putative biomarkers. An example of successful translation of an RT-qPCR method to patient is the OncotypeDx assay, which predicts the potential benefits of chemotherapy and likelihood of cancer recurrence [36-39] and thus can be used to stratify patients to different treatment regimens [40]. Furthermore, viral load monitoring using RT-qPCR is now routine for a number of RNA viruses [41].

1.3 RNA Molecular Measurement

As with other approaches, accurate quantification of RNA demands a comprehensive assessment of uncertainty. To facilitate this, we must first undertake a consideration of those factors within the measurement process that may contribute variability to that measurement. Only then can we proceed with the assignment of uncertainty.

1.3.1 Sources of Variability

The route from sample to accurate quantification of mRNA levels is a multi-component process each with its own experimental uncertainty. There can be numerous factors that need to be considered (**Figure 1.2**) [42]. Such cause and effect diagrams are widely used in measurement uncertainty and the field of metrology [43,44]. There are several sources of bias in an RNA measurement by RT-qPCR, the main culprits are summarised in **Table 1.1** [42].

RT-qPCR techniques have the ability to quantify nucleic acids over a wide dynamic range (at least eight logarithms) and are precise (DNA and RNA measurements can typically be optimised to have a coefficient of variation of < 5% or < 10%, respectively [45]). Routine detection of fewer than five target copies make it possible to analyse small samples such as clinical biopsies or miniscule lysates from laser capture microdissection [7,26,46]. But measurements using this precise technique are only as robust as the upstream processes used to sample, store and prepare the RNA. Precision is a measure of the degree of agreement between replicate measurement results obtained for the same sample [3,4]. However, what is often overlooked is that the whole stepwise procedure contributes to the experimental precision.

Variability in qPCR results obtained from identical samples assayed in different laboratories is a problem [46-48]. The use of distinct instruments, software,

Chapter 1 Introduction

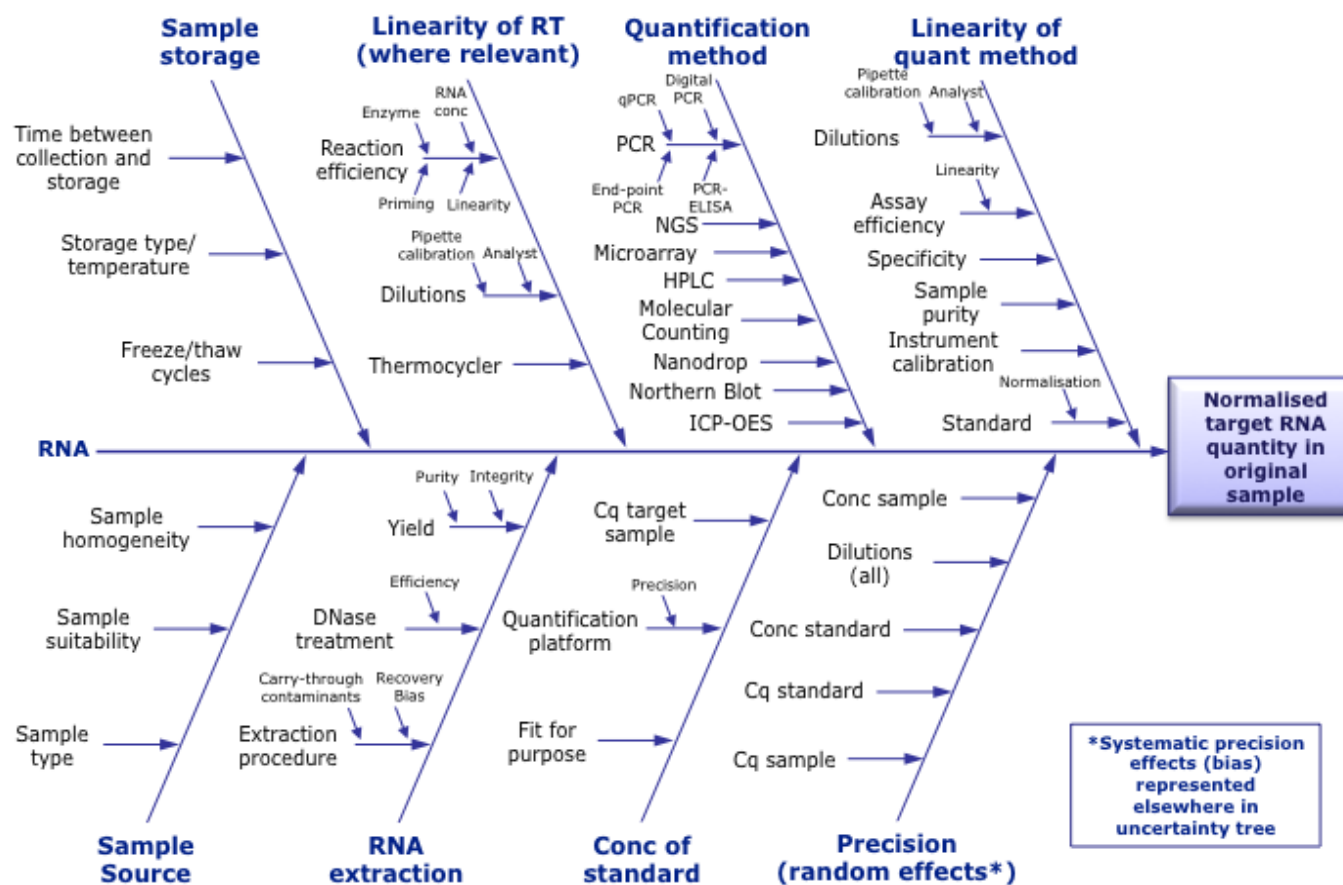


Figure 1.2 Cause & Effect: Uncertainty Contributions for mRNA Analysis. The central arrow represents the experimental process from RNA to quantification. Branches feeding into experimental progression characterise sources of variability that contribute to uncertainty at various stages of the process. There are numerous methodologies available for the final quantification step. Concentration (conc), quantification (quant).

Table 1.1 Factors Contributing Bias to an RT-qPCR Measurement

Source of Bias	Details/Solution
Sample	Sampling. Inhomogeneous samples (e.g. whole tissue biopsies comprising multiple cell populations) may lead to an average mRNA profile across multiple cell types. Particularly important for disease states such as cancer where only the tumour itself should be processed. Optimise sample collection, using cellular separation where appropriate. Care should be taken to obtain samples when multiple factors can be controlled for (e.g. time of collection, time post treatment, gender, race, age, etc.).
RNA not efficiently extracted	Will limit the amount of RNA available. May bias towards more abundant targets making minority target measurement difficult/impossible. Optimise sample collection and extraction process.
RNA degraded	Bias cDNA production and detection sensitivity. May affect some targets more than others. Avoid multiple freeze-thaw cycles. Use RNase/DNase free plastics or DEPC treated labware and RNase decontaminating solutions and sprays. Use RNase inhibitors during sample preparation. Change gloves frequently. Sample analysis by gel electrophoresis or a lab-on-a-chip platform can reveal RNA degradation before the RT step.
RNA storage	Optimise storage conditions to preserve RNA integrity
Non-linearity of method	Caused by inhibition, enzyme inefficiency (e.g. resulting in not all RNA being converted to cDNA in RT reaction), etc. Choose an RTase that is more tolerant of inhibitors typically found in RNA preparations (e.g., salt, phenol, proteins, etc.). Validate RTase for sample type. Include appropriate controls. Too little or too much RNA or widely varying amounts of RNA in RT reactions will result in inefficient or biased results (non-linearity), with saturation at the extremes. Quantify the amount of RNA in each sample and add the same amount to each RT reaction.
Inappropriate calibrator	For example, DNA standard is used when measuring RNA. Calibrator prepared in different background material/matrix to unknown samples. Where possible, ensure that calibrators are validated as appropriate for sample type and are spiked into sample matrices.
Instrument bias	Ensure instrument maintenance and calibration is up to date.
Operator	Different operators can introduce significant bias. Where possible, ensure operator consistency throughout an experimental protocol. When analysing data from different operators, the appropriate consideration of intermediate precision and/or reproducibility should be made. Operator bias can be tested by comparing different operators.

reagents, plates or seals can often lead to underestimated run-to-run differences that need to be compensated in order to allow data reproducibility [49]. Indeed, the single most likely source of data variation is due to variability introduced by the analyst [46-48]. Since there are so many steps involved in taking a tissue sample to a 'quantitative' result (**Figure 1.2**), it is not surprising that this variation is problematic [47] and factors that more comprehensively estimate error will lead to a better estimation of the variation and increase the likelihood of making accurate measurements.

1.3.1.1 Sample Source and Storage

Samples may be obtained from a wide variety of biological sources: from animal and plant material, to bacteria and viruses. Each sample type will have its own qualities, which will contribute to variability. For example, extraction of high quality RNA is particularly challenging in bone as it contains low cell numbers embedded within a highly mineralised tissue [50]. It is important to recognise and account for these differences in order to correctly design experiments that will generate meaningful data.

The surgical removal of tissue or the collection of cells from a plate can introduce variability. The transcriptome is dynamic [51] and highly sensitive to environmental factors [52] such as tissue removal, washing plated cells, or tissue-handling methods [53]. Harvesting samples via a highly reproducible method in the shortest possible time frame will minimise transcriptional changes induced by the manipulation of the samples, and can dramatically reduce the expression variability between biological replicates. Flash freezing of tissue samples in liquid nitrogen immediately upon isolation is typically recommended. For cell-based assays, the initial RNA extraction buffer should be added from a kit directly to the washed cells on the plate with scraping and mixing to form a stable homogenate that can be frozen at -20°C or -80°C [53].

1.3.1.1.1 Cell Line Treatment

Treating cells, tissue, or animals with intervention can be a common source of error due to the varying post-treatment incubation times [51,53]. Transcription of mRNA is dynamic such that a treatment-induced transcriptional effect can be observed only during a particular time frame. Thus, sampling a series of time points maybe the difference between valid results, less than optimal data, or no data at all [53].

Due to the dynamic nature of the transcriptome, many researchers plan experiments to sample different time points; however, some may fail during implementation [53]. A good example is the addition of a compound to several plates of cells that will be used in a time-course study in which all the plates are treated at precisely the same initial time. Under this circumstance, it would be difficult, or impossible, to stop the treatment for several replicates at each time point due to the time required to manipulate each replicate plate of cells. A more accurate approach is to stagger the treatments between each replicate to allow enough time to stop treatment at precisely the same time for each plate in a replicate group [53].

1.3.1.2 RNA Extraction

RNA is extremely labile compared with DNA, which is mainly due to its susceptibility to RNase degradation. RNases are very stable and RNA isolation must therefore be carefully performed to ensure both RNA integrity and the removal of contaminating nucleases, genomic DNA (gDNA) and RT or PCR inhibitors. This can be a problem with any sample source, but clinical samples are of special concern because of their complexity and potential inconsistencies in sample size, collection, storage and transport can lead to variable quality of RNA templates [26]. The mRNA used for clinical diagnostics and research may be derived from various tissues including biopsies, lumbar puncture, blood, urine or buccal swabs: each posing their own challenges for accurate measurement. In each case, the

limitations of sample handling in real life clinical situations will be different. It is well known that RNA is sensitive to degradation by post-mortem processes and inadequate sample handling or storage [6,54].

As with other molecular biology processes (e.g. DNA or protein extraction), there are a multitude of kits and protocols available on the market. While this availability of choice has undeniable benefits, it also creates problems that can only be solved by experimental compliance with the utilisation of appropriate RMs. By definition, RMs are designed to enable researchers to identify and account for these differences in data interpretation. The impact these variabilities can exert should not be taken lightly.

1.3.1.3 Reverse Transcription Quantitative PCR

When performing RT-qPCR it may be widespread practice to focus on technical replication at the qPCR stage of the process. However, many studies have shown that variability attributed to reverse transcription is far greater than the variability contribution of qPCR alone [47,48,55,56], (**Figure 1.3**). This increased variance may be caused by factors such as RT enzyme efficiency, RNA integrity and secondary structure [47]. The RT step is therefore critical for accurate RNA quantification [56,57]. Reverse transcriptase linear dynamic range is another crucial consideration for successful RT-qPCR [47] and should be demonstrated empirically. However, often it is the PCR rather than the RT step that is replicated. This has the danger of appearing to produce highly precise data, but could in fact proffer bias by masking true measurement variability. Consequently, true, meaningful and clinically significant measurement, particularly of small expression fold changes, ideally requires a discussion of the potential different sources of variance and bias.

Several factors can influence a result. For example, multiple reverse transcriptase enzymes with different characteristics exist and unintended endogenous priming

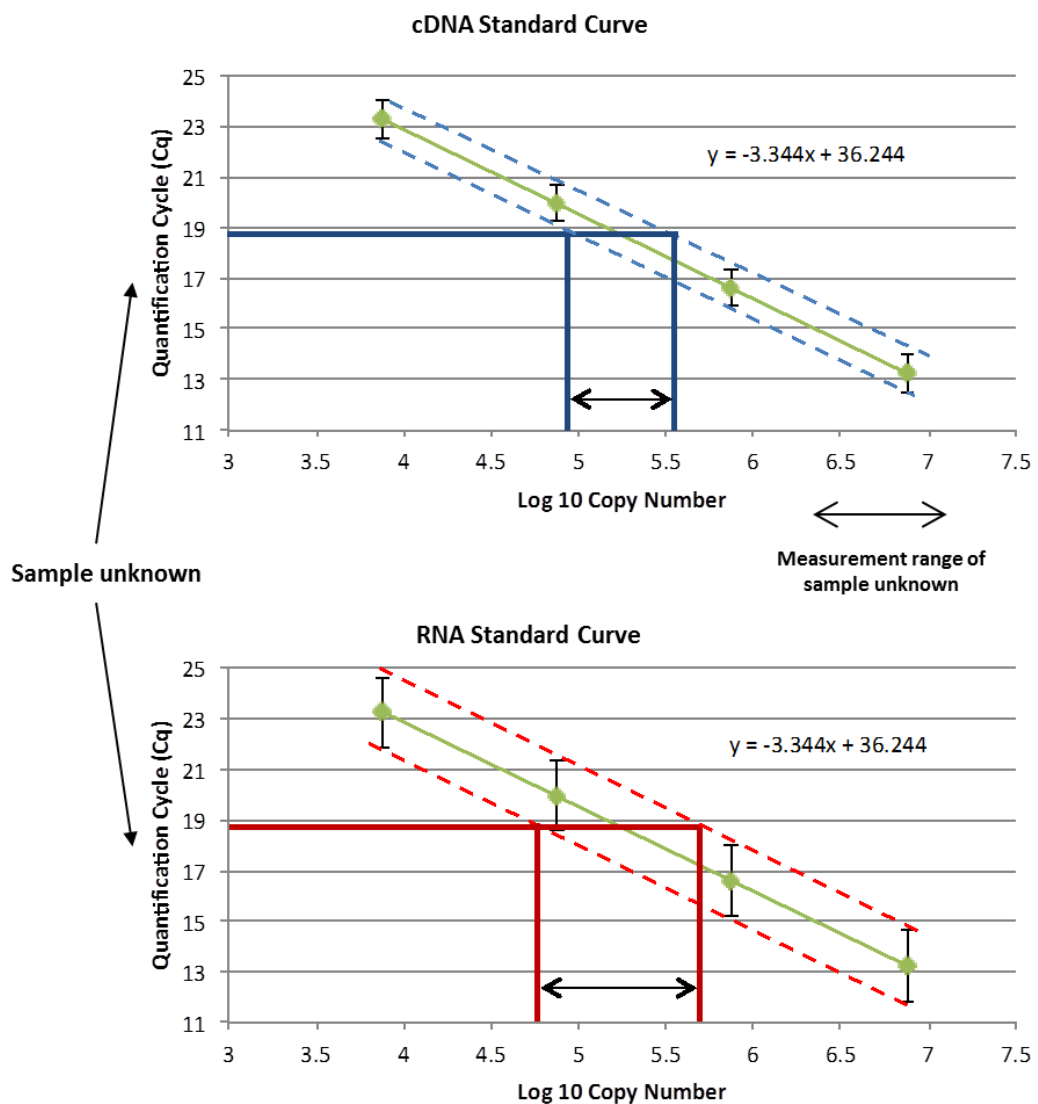


Figure 1.3 Schematic representation of variability observed between cDNA and RNA standard curves. Green points: standard curve. qPCR variability is relatively low when compared to reverse transcription variability. As a result, a standard curve generated from the dilution of cDNA indicates the variability associated with the qPCR step alone and does not represent variability associated with the RT step. Alternatively, a standard curve generated from an RNA dilution series incorporates the variability accountable to the RT step, which is intrinsically more variable than qPCR. Consequently, the range within which the unknown sample measurement can reliably lie is greater when using an RNA-based standard curve and smaller when using a DNA-based standard curve. The RNA curve will therefore provide a more accurate estimate of uncertainty, offering greater confidence in a result. Sample fold changes discerned when utilising this approach more likely represent ‘true’ measurement differences rather than insufficiently apportioned uncertainty.

can occur regardless of which primers are used to prime the RT reaction. Such non-specific priming can lead to lowered and/or variable signal in the subsequent PCR assay [26,48]. Each strategy may exert different efficiency influences over the RT reaction and as such experimental designs should be harmonised to reflect this. Equally, total RNA concentration should be similar in every sample to minimise bias. In addition, the purity of RNA can be the cause of variable C_q values from contaminants that can affect reaction efficiency [58].

RT-qPCR is used extensively in clinical research investigating putative biomarkers for disease diagnosis as well as for predictive and prognostic monitoring. However, on review of the literature, articles published reporting RT-qPCR data frequently do not report all experimental details relating to RT-qPCR experiments [59]. Fundamental experimental details are often omitted when reporting mRNA measurements, including information pertaining to RNA quality, rationale for choice of normalisation strategy, location of amplicon or detailed descriptions of the reverse transcriptase and PCR assay conditions [60,61].

1.3.1.3.1 Reverse Transcription Priming

Broadly three strategies exist for priming during cDNA synthesis. Random primers prime non-specific cDNA synthesis at multiple transcript sites and may include rRNA templates in total RNA samples. Given that total RNA contains only 3-5% mRNA [62], the potential for non-protein coding synthesis is large, which may create inconsistencies if the target of interest is present at low levels as ineffective priming will lead to non-quantitative amplification. If bias is consequently introduced, this becomes exaggerated during qPCR amplification. For low target levels it may be preferable to prime using oligo d(T)₁₆ as this will specifically amplify polyadenylated (poly(A)) tail targets, i.e. mRNA, preventing out-competition of low level targets by rRNA fractions. Target-specific primers synthesize specified cDNA sequences. However, this requires separate priming reactions for each target and gene-specific variation may be introduced [48].

1.3.1.3.2 Reverse Transcription Enzymes

Reverse transcriptase's (RT enzymes) are RNA-dependent DNA polymerases encoded by retroviruses, which convert their RNA genome into DNA prior to host genome infiltration. These RT enzymes have two functions; firstly as a DNA polymerase utilising RNA as a template in the viral life cycle, although capable of using ssDNA as an equally efficient template in the laboratory. This is due to the fact that DNA-dependent DNA polymerase activity is also present to allow synthesis of the complementary DNA strand after synthesis of the first strand using the RNA template. This intrinsic DNA-dependent DNA polymerase activity also explains in part the importance of performing efficient DNase treatment of all RNA extracts prior to the RT. Its second function is RNase H activity, or ribonuclease H activity, whereby the RNA moiety of an RNA-DNA duplex or hybrid formed following RT of an RNA template is degraded [62].

Commercially available RT enzymes are derived from one of two sources; Moloney murine leukemia virus (MMLV) or Avian myeloblastosis virus (AMV), either purified directly from the virus or expressed in *E. coli*. Fundamentally, both RT enzymes possess the same activities. However, differences include optimal experimental conditions for temperature and pH, as well as RNase H activity, which is much stronger for AMV than MMLV-derived enzymes [62].

The AMV-derived enzyme has a powerful RNase H activity that can cleave the template near the 3' terminus of the growing DNA strand if reverse transcriptase pauses during synthesis [63,64]. Thus, the high level of RNase H activity associated with the avian RT tends to suppress the yield of cDNA and restricts its length. The murine enzyme may be better suited for RT-qPCR because its RNase H activity is comparatively weak [65]. However, the MMLV enzyme reaches maximum activity at a lower temperature (37°C) than the avian enzyme (42°C), which may be a slight disadvantage if the RNA template has a high degree of secondary structure [64].

Chapter 1 Introduction

Variants of MMLV RT that lack RNase H activity have been engineered [64]. Several such enzymes are sold commercially (for example, Superscript from Life Technologies and StrataScript from Stratagene). The modified RTs transcribe a greater proportion of the template molecules and synthesize longer cDNA molecules than the WT enzyme [63,65,66]. In addition, they are capable of cDNA synthesis at higher temperatures (up to 50°C in some cases), which is an advantage when the template RNA is rucked into secondary structures [64].

Thermostable Tth DNA polymerase (or recombinant Tth, rTth), which is encoded by the thermophilic bacterium *Thermus thermophilus*, exhibits RT activity in the presence of Mn²⁺ [67]. The chief advantage of using Tth polymerase in RT-qPCR is that both stages of the reaction (RT and qPCR) are carried out in the same reaction tube [68]. As a disadvantage, the average size of the cDNA synthesised by the Tth polymerase is only ~1-2 kb, far less than can be achieved with MMLV RT (~10 kb) [64]. In addition, the use of Mn²⁺ is of concern because of the lowered fidelity of DNA synthesis in the presence of this cation. Finally, Tth cannot be used with oligo(dT) or random hexamers as primers, since the hybrids will be unstable at temperatures at which the thermostable DNA polymerase is active [64].

As for PCR enzymes for use in RT-qPCR, RT enzymes require efficiency over a wide dynamic range. This facilitates efficient conversion of both high and low abundance transcripts into cDNA and as such is one of the most crucial steps in a quantitative study [62]. RT efficiency may be influenced by total RNA content in the RT reaction [56,57], where quantification of both high and low abundance targets is positively correlated with total RNA background present in the RT reaction. In this capacity, background RNA may act as a chelator of inhibitors. When dilutions are performed at the RNA stage, in order to maintain RT reaction linearity it is suggested that a carrier RNA should be included in the reaction mix to ensure the total RNA concentration for each reaction is constant. This is particularly important for generation of standard curves for qPCR analysis.

1.3.1.4 Inhibition

Several studies have also shown that RT components may have an inhibitory effect on the subsequent qPCR reaction, the magnitude of which depends on the RT system [47,62,69-72]. This is particularly noticeable for low abundance targets within undiluted cDNA and in the absence of carrier. The inhibitory effect of reversible inhibitors decreases upon dilution of the cDNA samples for calibration curve analysis. Therefore, this should be considered when performing RNA standard curves. However, when using RNA standard curves, all standards will consequently have the same amount of RT components when used in the qPCR reaction and so the inhibitory effect should be equal across all samples. When performing a cDNA standard curve, the lowest standards are subject to the highest level of dilution and therefore more efficient in the qPCR. This disparity between samples creates a non-linear relationship between standards, which may yield a theoretical reaction efficiency of over 100%. Furthermore, if samples are compared at different dilutions, measurement differences may in part be due to variable inhibition of the PCR by RT components [62], rather than true biological variability. Sellner *et al.* [70] suggest that maintaining an RT:PCR enzyme ratio less than 3:2 alleviates the PCR inhibition caused by the RT enzyme. Moreover, this study also showed that adding non-homologous RNA improved PCR enzyme sensitivity by up to 100 fold. This reliance on unit ratios suggests an interaction between the two enzymes at a molecular level, which may take the form of direct binding between the two enzymes. The alleviation of this inhibition by the addition of extra non-homologous RNA may be due to the RNA providing an alternative binding substrate for the RT enzyme [70]. These observations strengthen the case for using RNA, rather than cDNA, dilutions in RT-qPCR experiments and this approach is recommended by the author.

Contrary to independent findings for low abundance targets [56,57], Levesque-Sergerie *et al.* [62] suggested that the presence of background does not alleviate the inhibitory effects of RT components. In fact, in those samples with higher

Chapter 1 Introduction

background concentrations, the auspicious effect of RT component dilution on PCR inhibition was muted. As different enzymes may have different reaction efficiencies, the RT component inhibitory effect may be enzyme dependent. Dilution may therefore change the efficiency ranking of compared qPCR enzymes.

Understanding the impact of sample matrix on different targets helps to identify its influence on the accuracy of analytical results [73]. In this context, matrix refers to components of a sample other than the analyte. The presence of RT or PCR enzyme inhibitors has the potential to increase measurement error, reduce assay precision and sensitivity, and produce false negative results in both quantitative and qualitative RT-qPCR assays [74]. Inhibitors can come from many sources including co-purified cellular or tissue components, carry over components from storage buffers and the extraction process and the RT reaction. For example, biological samples from different sources (human tissue from two different organs) may comprise distinct protein profiles. The inconsistency between these different 'background matrices' may alternately influence experimental outcomes. Studies show that PCR inhibition can be assay specific and PCR inhibitors co-purified during nucleic acid extraction may affect different assays to variable degrees. This highlights the importance of matched sample matrices when evaluating potential reference genes to ensure both the reference and the target gene assay are subject to the same reaction conditions [74]. Furthermore, calibration curves that are prepared in a reaction that is not affected by the inhibitor may yield biases.

All this may contribute to variation in measurement, particularly if samples are obtained and analysed periodically during a successive long-term study. Recognising the importance of matrix-specific standards helps to identify influence of sample matrix on the accuracy of analytical results [73] and ensures that temporally separated measurements may be compared meaningfully. Consequently, sampling and subsequent storage should be carefully controlled and documented in order to preserve the quality and abundance of the RNA material. This is especially important in clinical studies [75-78]. Both biological and

technical replicates are recommended for good experimental design [79], (**Figure 1.4**). The potential for the introduction of variability is greatest at the first stages in experimental process, i.e. biological variability at sample source.

1.3.1.4.1 One-Step versus Two-Step RT-qPCR

While conventional methods partition the RT and qPCR steps of the process, recent years have seen an abundance of one-step processes, where both RT and qPCR occur in the same reaction, come into common use. Using the conventional two-step method, where RT and qPCR steps are temporally and spatially separated, researchers can replicate at either or both the RT and qPCR levels. Additionally, extra handling stages are required in order to transfer the newly synthesised cDNA into the qPCR reaction mixture. This also results in a further dilution of sample and dilution of the RT reaction components before commencement of qPCR. Dilution of both potential sample/extraction contaminants and/or RT components may alleviate inhibition of the qPCR reaction. In contrast, one-step processes ensure that any sample dilution is performed at the RNA level, any replicate analyses consequently replicate the RT step; the sample does not undergo further dilution (when cDNA proceeds to qPCR amplification) and no additional handling steps are involved. This may be particularly valuable when low copy number targets are analysed. When using one-step processes, the influence of RT components and RNA contaminants on the efficiency of the qPCR reaction should be investigated to apportion these variabilities.

One-step RT-qPCR systems may circumvent the issue of RT component inhibition of PCR since equal bias introduced by RT components is maintained, as components are not attenuated in any of the standard dilutions. Thus qPCR reactions should also remain linear within the dynamic range. Furthermore, by not requiring cDNA dilution by transfer into a qPCR reaction, one-step processes may also enhance sensitivity of low abundance targets. However, to obtain highly accurate results, sample unknown measurements should be properly correlated to

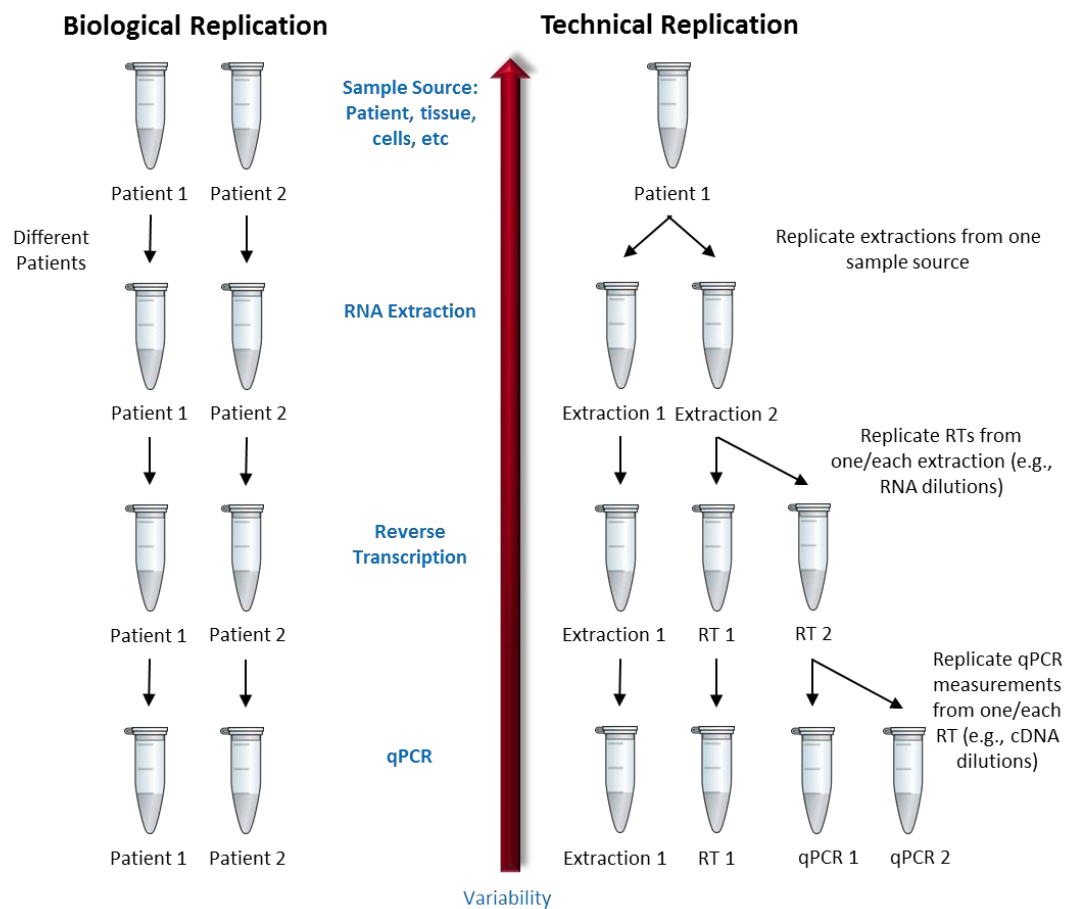


Figure 1.4 Schematic representation of different experimental designs representing biological versus technical replication. Generally, data variability increases, as replication is included from higher stages within the experimental process. For example, to ascertain true patient variability, replicate biological samples must be analysed (different samples from one patient, samples from different tissues from the same patient, or samples from different patients). The RNA extraction and reverse transcription components of the process may contribute more variability to the final measurement than qPCR alone. Definition of all sources of technical variability enables the actual biological variability to be discerned and as such, more confidence can be conferred to the results when this variability is included.

Chapter 1 Introduction

appropriate measurement standards, or RMs, with a well-defined value and uncertainty [1,6,7].

Significant differences in one-step versus two-step RT-qPCR quantification sensitivities may be observed for low copy targets or low concentration samples such as single cells [71,72,80,81]. In such observations, one-step methods display up to a 32-fold ($5 C_q$) increase in sensitivity for transcript copy number compared to two-step reactions. This sensitivity difference has been attributed to gene-specific priming in one-step protocols (as opposed to random hexamers or oligo (dT) commonly used in two-step protocols). Alternatively, there may be increased opportunity for the generation of mRNA secondary structures with some two-step RT temperature conditions. Target availability for primer annealing and the RT enzyme is diminished (random hexamers require a lower pre-incubation temperature of 25°C to aid target binding) [80,82]. Indeed, further studies show increased qPCR linearity of template dilutions when using gene-specific primers for RT rather than random hexamers [48].

Searching for the key words 'gene expression' and 'clinical diagnostics' in Pubmed (<http://www.ncbi.nlm.nih.gov/pubmed/>) yielded an approximate 579% increase in publications in 2014 compared to 2004 (364% increase from 2005 to 2015). However, upon reviewing several recent articles reporting RT-qPCR data, few articles reported all RT-qPCR experimental details [59]. The majority were deficient of several fundamental experimental details when reporting gene expression measurements, including 65% without information pertaining to RNA quality and 85% with no reference to data normalisation. Furthermore, only 20% of those articles assessed provided complete descriptions of the RT, with only 10% detailing complete PCR reaction conditions. In order to stand up to scientific rigour, key aspects of RT-qPCR experimental processes must be reported. There had been a growing consensus developing around the need to improve published information with relevant experimental detail that covers every aspect important to the qPCR assay itself, as well as issues relating to pre- and post-assay

parameters [83]. However, poor qPCR data obtained amongst a catalogue of mistakes, inaccuracies and inappropriate analysis methods as well as contamination and poor assay performance [84,85], promoted the now retracted claim of a link between the triple measles mumps and rubella (MMR) virus vaccine, gut pathology and autism [83]. It was these MMR papers and subsequent court case that were the final inspiration for the development of the MIQE guidelines (*Minimum Information for Publication of Quantitative Real-Time PCR Experiments*), which propose a minimum standard for the provision of information for publications utilising qPCR experiments [86]. These cover key aspects including sample acquisition, assay design and validation as well as details about data analysis, enabling other scientists to easily assess and, if necessary, repeat the experiment [55,86].

These issues highlight the importance of including appropriate RMs, designed to enable researchers to identify and account for these differences, and for harmonisation of experimental design. RMs enable data normalisation to alleviate technical variabilities. This can also be advanced by the application of standardised procedures, such as those outlined by the International Organization for Standardization (ISO) [87].

1.3.1.4.2 Reagents and Equipment

Other sources of RT-qPCR variability include ability of the thermocycler to maintain a consistent temperature across all sample wells, as any deviations in temperature may lead to different RT and/or PCR amplification efficiencies [26,88,89] and thus contribute to the overall variability in measurement. This extends to differences between different thermocycler platforms, with differences observed in timing and heat transfer capabilities [89]. Expectation of lot-to-lot consistency may be reason for selecting commercially available kits rather than preparing mixes in-house. In addition, maintenance of primer/probe stabilities is often assumed between different syntheses or suppliers. However, while the

multitude of commercial kits and protocols available offer undeniable benefits, reagent preparations from distinct batches have been shown to contribute significant experimental variability with up to seven-fold differences in calculated mRNA quantities observed [47,90].

For numerous commercially supplied primers and probes, the location of the amplicon selected for mRNA detection is omitted; a fact that makes it difficult to adhere to the MIQE guidelines. The problem with not providing this information means the reader does not know which part of a given transcript is being detected. This information is important for any hope of reproducibility due to transcript differences including alternative splicing, polyadenylation and alternative promoters. An amendment to the MIQE guidelines [91] offered a compromise to commercial vendors who do not disclose this information by alternatively requiring a context sequence to enable the researcher to locate which portion of a given sequence was being detected [55,86,91]. Where neither primer information nor context sequence is provided, researchers using such commercial assays are strongly advised to sequence the PCR products to obtain the location of the transcript being measured.

1.3.1.4.3 Estimating Copy Number

RT-qPCR is typically performed either by estimating copy number using a calibration curve or simply assessing the fold change without considering the absolute abundance of the respective RNAs; the latter is termed the delta (Δ) C_q (or ΔC_t) method (Livak [92] and Pfaffl [93]). Considerations around what is accurate differ between the two methods. The former has the added challenge of how appropriate and transmutable the choice of calibrator is. A calibration curve provides an estimation of the magnitude and dynamic range of a given measurement, but can reduce or increase bias of the estimated copy number (depending on the initial value assignment).

Chapter 1 Introduction

A calibration curve also provides an estimation of the PCR efficiency, which is an important source of bias both when estimating copy number as well as fold change. Consequently, while the ΔC_q method ignores magnitude, PCR efficiency must be estimated [93] to avoid biases. Where PCR efficiency is not routinely estimated, which is most common for the ΔC_q method [92], biases could be avoided by factoring in additional uncertainty to account for the unknown PCR efficiency. This would reduce the chance of measuring a significant difference, but increase the chance that when a difference is significant, it is real.

Assay efficiencies may also be estimated using amplification curve fitting algorithms, which are dependent on the number of cycles over which there is an increase in fluorescence, and several such approaches have been proposed [94-97]. These are most likely to succeed when the measurement is made using a DNA binding dye since these assays yield a greater change in fluorescence [98]. While these approaches offer an alternative to the implementation of a standard curve, the latter is still the more commonly used method for assay evaluation as it additionally provides information about working range and is conceptually easy to apply [98,99].

The evaluation of background-normalised qPCR data can be subjective, for example, assessing the quality of a curve, determining the perfect starting point of the exponential phase and where to assign the threshold for C_q generation. These elements are subject to personal judgment. For this reason, digital PCR is seen as a promising alternative, where a digital output is produced (presence or absence of target) [36,100] and the ambiguity associated with C_q measurement is negated. For RT-qPCR measurements, calibration curve estimated copy number or fold changes should be reported rather than C_q , which is an arbitrary measure, and assay efficiency should always be taken into account.

Experimental replication serves to improve confidence as it provides a better estimation of the mean provided by a given technique. Nevertheless, replication

cannot assist where systematic errors are present and may serve to make matters worse by increasing the confidence in the biased result. For RNA measurement, bias can be reduced by aiming to replicate the experimental steps that afford the highest variance from sample to analysis (**Figure 1.2**). This will reduce precision but will also reduce bias. Another essential method for reducing measurement uncertainty is to apply normalisation.

1.3.1.5 Other Molecular Methods

There are many methods in molecular biology for measuring quantities of target nucleic acid sequences. However, most of these methods exhibit one or more of the following shortcomings: they are time consuming, labour intensive, insufficiently sensitive, non-quantitative, require the use of radioactivity, or have a substantial probability of cross contamination [26,101]. These methods include, but are not limited to; Northern and Southern hybridisations, HPLC, scintillation proximity assay, PCR-ELISA, RNase protection assay, in situ hybridisation, and various gel electrophoresis PCR end-point systems [26], (see also **Figure 1.2**).

The measurement of phosphorus content of nucleotides and DNA by high-performance inductively coupled plasma optical emission spectroscopy (HP-ICP-OES) has been reported for quantifying nucleic acids. This method can provide an accurate measurement, which is traceable to the SI [14,102] provided that the material contains no other sources of phosphorus, such as contaminating RNA. However, this approach requires large amounts of material (1 to 2 mg) and sample purity is critical [12,102]. Furthermore, complete destruction of target is required in order to liberate the constituent phosphorous. Consequently, subsequent analysis of the same sample is not possible for most methods.

1.3.1.5.1 Digital PCR

Digital PCR (dPCR) is a relatively new technology which can measure both absolute and relative copy numbers of template DNA independent of external calibrators and, hence, has the potential to be used as a reference method for quantifying DNA amount (copy number) concentration (copies/ μ L) required for certification of RMs [103-105]. dPCR is based on the principle that an absolute count of amplified targets can be achieved. Single molecules are isolated by dilution and individually amplified by PCR; each product is analysed separately [103]. This process requires only small amounts of material when compared to phosphorus analysis or next generation sequencing (NGS), although the cost of dPCR analysis may be higher than some other techniques [12,106]. dPCR may also be utilised for the measurement of RNA, RT-dPCR [107-111]. The same difficulties with RT efficiency will present themselves with RT-dPCR as they do for RT-qPCR, but dPCR may be better placed as a tool to measure such variability more precisely.

Despite the commonly held belief to the contrary, several studies have shown that dPCR is subject to inhibition affects that may change the measurement result [112-115]. Increased inhibition has been shown to slow down the reaction considerably. In dPCR, inhibitors or slow starting reactions may result in misclassification as partitions fail to reach the fluorescence threshold while still containing at least one initial target copy [112]. Resulting false negatives hence reduce sensitivity for the detection of positive partitions.

1.3.1.5.2 Next Generation Sequencing (NGS)

NGS platforms share the common technological feature of being capable of massively parallel sequencing on clonally amplified or single cDNA molecules [36]. NGS technologies offer the possibility of hypothesis-neutral discovery of novel transcripts and isoforms in a fraction of the time required for genome-wide analysis performed by Sanger sequencing [116,117]. However, multiple template preparation stages, diverse sequencing chemistries and complex data processing

of NGS experiments may impact on the verification of bona fide nucleic acid biomarkers [36,116]. When applied to sequencing transcriptomes, NGS is known as RNA-seq.

RNA-Seq is the first sequencing-based method that allows a more comprehensive transcriptome to be surveyed in a very high-throughput and quantitative manner [117]. This method uses recently developed deep-sequencing technologies. In general, a population of RNA (total or fractionated, such as poly(A)+) is converted to a library of cDNA fragments with adaptors attached to one or both ends. Each molecule, with or without amplification, is sequenced in a high-throughput manner to obtain short sequences from one end (single-end sequencing) or both ends (pair-end sequencing) [117]. The reads are typically 30–400 bp, depending on the DNA-sequencing technology used. Following sequencing, the resulting reads are either aligned to a reference genome or reference transcripts, or assembled *de novo* without the genomic sequence to produce a genome-scale transcription map that consists of both the transcriptional structure and/or level of expression for each gene [117].

RNA-Seq has an upper limit for quantification, which correlates with the number of sequences obtained [117]. Consequently, it has a large dynamic range of expression levels over which transcripts can be detected: a greater than 9,000-fold range was estimated in a study that analysed 16 million mapped reads in *Saccharomyces cerevisiae* [118], and a range spanning five orders of magnitude was estimated for 40 million mouse sequence reads [119]. RNA-Seq has also been shown to be accurate for quantifying expression levels, as determined using qPCR [118] and spike-in RNA controls of known concentration [119]. The results of RNA-Seq also show high levels of reproducibility, for both technical and biological replicates [117,118,120].

1.3.1.6 Normalisation

Normalisation is an essential component of a precise mRNA measurement. Its purpose is to remove technical error. However, as with the measurement of the genes of interest (GOI), normalisation strategies are also influenced by variance and bias, so must be used with caution. Current normalisation methods include standardising tissue weight, tissue volume, cell count, RNA concentration, or using reference genes and external reference panels [7,121-123]. A standard approach relies on reducing gross variation by ensuring samples are of comparable size with more subtle variation (crucial to fine measurements) being further removed using (preferably multiple) internal reference genes, and/or synthetic internal positive controls.

Challenges associated with representative sampling of clinical samples are discussed in detail below, but ensuring samples are comparable can be a further challenge. Under controlled conditions of reproducibly extracted, good-quality RNA, initial gene transcript number is ideally standardised to cell number, but accurate enumeration of cells is often precluded when starting with solid tissue [7]. Following RNA extraction, quantity and quality of extracts may be measured [55,122,124].

1.3.1.6.1 RNA Mass Quantity

A frequently applied normalisation scalar is RNA concentration [7]. There are a number of methods for RNA quantification. Following RNA extraction, both quantity and quality of extracts should be measured [55] using metrics such as UV absorbance at 260 nm (A_{260}), RiboGreen RNA quantification assay and 'Lab-on-a-chip' based capillary electrophoresis. Each method has associated limitations. Common extraction contaminants, such as proteins, DNA/RNA and salts, can increase A_{260} nucleic acid quantity estimation [12,125,126]. Furthermore, measurement by A_{260} cannot discriminate between single-stranded DNA, double-stranded DNA or RNA in solution, or between target sequence and other

Chapter 1 Introduction

potentially contaminating sources of nucleic acid. In addition, it cannot indicate target quality or the ability of PCR to successfully amplify a DNA sample. Furthermore, small changes in the pH of the solution will cause the 260/280 absorbance ratio to vary [127]. Acidic solutions will under-represent the 260/280 ratio by 0.2-0.3, while a basic solution will over-represent the ratio by 0.2-0.3. Together, these factors may contribute to inaccuracy in nucleic acid concentration estimates [12,47,103,125,126,128].

In addition to these considerations, the five nucleotides that comprise DNA and RNA exhibit widely varying 260/280 ratios (Adenine: 4.50, Cytosine: 1.51, Guanine: 1.15, Thymine: 1.47 and Uracil: 4.00) [129]. The 260/280 ratio will therefore depend on the composition of the nucleic acid being measured. RNA will typically have a higher 260/280 ratio due to the higher ratio of Uracil compared to that of Thymine.

Alternatively, fluorescent dyes have been used for quantifying total RNA. RiboGreen (Life Technologies) RNA quantification exploits the fluorescence enhancement seen upon nucleic acid-dye association. Reagent literature states that RiboGreen reagent does not detect significant sample contamination by free nucleotides and thus more accurately measures the amount of intact RNA in potentially degraded samples than A_{260} . Despite the general assumption that A_{260} is less accurate than RiboGreen analysis, studies have shown that both methods generate comparable results when RNA concentration exceeds a minimum of 100 ng/ μ L, albeit with RiboGreen measurements registering marginally lower concentrations than spectrophotometer results. While A_{260} analysis becomes less reliable at lower RNA concentrations [47] it should be remembered that methods that use fluorescent dyes typically require a calibration curve and that the calibrator used for this must also be assigned a value (usually by A_{260} measurement). However, neither of these methods provides reliable RNA quality information, a key consideration when quantitating mRNA levels in fresh tissue [47].

Chapter 1 Introduction

When using RNA concentration to normalise, RNA quality is also an important consideration. Methods for estimating RNA quality based primarily on the detection of ribosomal (r)RNAs are very popular. Agarose gels or 'Lab-on-a-chip' based capillary electrophoresis platforms allow RNA sample quality assessment with the latter offering the integration of RNA sample quantification with a quality assessment in one rapid step [47]. rRNA ratios, with additional electrophoretic trace features, are used to calculate total RNA integrity (e.g. RIN: RNA integrity number, RQI: RNA quality indicator). However, it should be noted that rRNAs yielding similar RIN/RQI numbers generated by these instruments can contain mRNAs that differ significantly in their integrity [130], so good quality rRNA is not necessarily indicative of good quality mRNA. In some instances it is impossible to quantify this parameter, for example, when minimal RNA is available from microdissected tissues [7]. Further drawbacks to the use of 18S or 28S rRNA molecules as standards are their absence in purified mRNA samples and their high abundance compared to target mRNA transcripts. The latter makes it difficult to accurately subtract the baseline value in RT-qPCR data analysis [7].

In some cases, the validity of normalising to total RNA has been confirmed when comparing results between individuals [47]. However, there are several arguments against the use of mass quantity. Normalisation to total RNA content first requires accurate quantification of the RNA sample and as discussed above, methods utilised for this purpose have various limitations. Another important consideration when using this approach is the lack of internal control for RT or PCR inhibitors [13] and as such, the variability attributed by these factors cannot be monitored.

1.3.1.6.2 Internal Reference Genes

RT-qPCR analysis of mRNA should also be normalised using internal reference genes. While manuscripts that evaluate the stability of candidate reference genes under certain experimental conditions might provide helpful guidelines for other researchers, it has long been undisputed that the utility of chosen reference

genes must be confirmed by each research group for every experimental setup [6,86,131]. Although this may seem laborious and time-consuming in the short-term, it is key to the generation of truly meaningful data that will hold-up against scientific scrutiny. Their suitability must be validated experimentally for particular tissues or cell types on an experimental-specific basis [132].

Ideally, normalisation should be performed against validated multiple reference genes. Multiple reference genes rely on comparative expression measurements between a number of targets to estimate the error induced trends that are introduced by the experimental process; this is reported to provide considerably increased precision [7,55,133-136]. While the latter are considered the gold standard, some advocates of this approach state that it is assumption free. This is erroneous as the technical assumptions are that all RTs and PCRs are equal and we have already seen that this is not the case. A multiple reference gene approach validated on a study-specific basis should alleviate the use of inappropriate normalisers.

Further support for reference gene selection may be found using algorithms such as geNorm [7], NormFinder [137] or BestKeeper [138]. The validated geNorm approach utilises the geometric mean of multiple, carefully selected, candidate genes. The BestKeeper algorithm uses a pair-wise correlation analysis method and NormFinder uses the estimate of inter-group and intra-group values. In general, using fewer than three reference genes is not advisable [7,46,86,131,139]. Single reference genes may be used if the measurement of small differences is not necessary, but the chosen target must be validated across the range of experimental conditions under investigation [140]. Crucially, any difference that is measured would need to be sufficiently greater than the inherent variation of the single reference gene measurements (incorporating all the steps from sampling to measurement) used to normalise that data, to be sure the observation is due to the gene of interest and not the reference gene or a combination of both.

Chapter 1 Introduction

It is increasingly evident that a number of classically designated reference genes demonstrate inconsistent expression between different tissues and treatment regimens [7,86,121,132,136,139,141,142]. For example, despite continuing reports for more than a decade that emphasise the problems associated with its use, glyceraldehyde-3-phosphate dehydrogenase (GAPDH) continues to be utilised as a normaliser [47,143-145]. It is well documented that GAPDH mRNA levels are not constant [131,142,146] and it contributes to diverse cellular functions such as nuclear RNA export, DNA replication, DNA repair, exocytotic membrane fusion, cytoskeletal organisation and phosphotransferase activity [147]. It is pathologically implicated in apoptosis and neurodegenerative disease [148] and its mRNA levels are highly heterogeneous even in cellular subpopulations of the same pathological origin [47,149]. There are some instances when normalisation to GAPDH may be valid, but for most experimental conditions its use is inappropriate and should be discontinued [47]. Although studies continue to be published using one or more reference genes that have not been specifically validated for the measurement in question [59], it is encouraging that in recent years (and generally since the publication in 2009 and implementation by some of the MIQE guidelines), there has been an increase in publications directly evaluating reference gene validation [133-135,141,150-152]. However, more work is needed to ensure such guidelines are adhered to, particularly from Journals and reviewers who could make it a requirement for publication [153].

A recently described alternative normalisation technique targets expressed repetitive elements, ERS (expressed *Alu* repeats, or EARs) [130] that are abundant in the human genome (~1 million copies). This strategy uses *Alu* repeat sequences embedded in the UTRs (untranslated regions) of mRNAs, to estimate the global mRNA quantity. As a result, it has the potential to be used as a 'universal' internal target, i.e. suitable to use for normalisation in all human RT-qPCR experiments. However, further work is needed to assess the validity of this proposed method.

1.3.1.6.3 External Standards

An external standard comprises a target sequence that is present at a defined quantity and may be analysed independently of the test samples or spiked into test samples and used for value assignment and/or normalisation purposes. External standards differ from reference genes, which are usually internal targets with consistent expression levels. However, these expression levels can only be determined through comparison to a standard curve of external standards of defined concentration, or relative fold change measurements.

All quantitative methods assume that the RNA targets are reverse transcribed and subsequently amplified with similar efficiency [47]. The risk with normalisation against external standards (such as RMs) is that a proportion of the samples might contain some inhibitor that significantly reduces the RT-PCR efficiency, resulting in inaccurate quantification. This does not apply to reference genes as they are internal targets and so are subject to the same matrix effects as the unknown target genes. It is therefore necessary to develop universal well-defined and characterised standards for spiking into biological samples pre-RNA extraction [47]. This format would enable an assessment of the variability inherent to each step in the experimental process post-lysis. In contrast to internal standards/reference genes, external standards can be quantified before inclusion in test samples and so provide a means by which to absolutely quantify targets using a calibration curve. Furthermore, they also offer traceability. However, a disadvantage of external standards is their lack of commutability. They may not readily transfer from a research to a clinical setting and so therefore would not easily slot into diagnostic markets. Further research and development would be required in order to fulfil this role. It would be preferable to develop external standards that may be spiked into biological samples and measured alongside GOI targets so that (1) external spikes are subject to the same matrix effects as GOI and (2) no additional reaction wells need be accommodated, keeping costs down and improving commutability.

Chapter 1 Introduction

For this purpose, the External RNA Control Consortium (ERCC) panel of synthetic RNA oligonucleotides have been developed in collaboration with the American National Institute of Standards and Technology (NIST). The ERCC is an ad hoc group with approximately 70 members from private, public, and academic organisations, initiated in 2003 to develop a set of external RNA control transcripts that can be added to assess technical performance in gene expression assays. They have been designed to evaluate data consistencies with defined performance criteria. All ERCC work is intended to apply to RT-qPCR assays as well as one-colour and two-colour microarray experiments [154].

The use of synthetic standards raises the questions: “How similar to a ‘real’ molecule is a synthetic one?” and “Will they behave the same during analysis?” Once again, the value of experimental-specific RM validation is clear. It may potentially require a trade-off between synthetic molecule stability and trueness to ‘real life’ endogenous targets. ERCC standards have been designed to mimic endogenous mammalian mRNA targets, for example, through possession of secondary structure motifs and a poly(A) tail. The panel comprises unique control sequences inserted in common plasmid DNA engineered to be readily *in vitro* transcribed to make RNA controls. Endogenous mRNA species undergo modification to include a 5’ cap, which is important for export from the nucleus, excision of introns and stabilisation of the RNA. The synthetic ERCC transcripts lack this 5’ cap. While the related functions of nuclear export and splicing are not important for these exogenous species, transcript stabilisation is. However, using stabilising storage solutions as a diluent, storing at -80°C and making aliquots to avoid multiple freeze thaw cycles all act to maintain target stability and integrity.

It should be noted that while external RNA standards spiked into biological samples may provide an assessment of the variability within the proceeding experimental steps, they cannot account for any variability upstream (e.g. sampling or cell lysis). Also, purified RNAs may not always be compatible with a given extraction method. Consequently, application of external standards needs to

be validated empirically and a combined approach in conjunction with validated reference genes may be most effectual.

1.3.1.6.4 Measurement Controls

Studies show that PCR inhibition can be assay specific with an inhibitor completely inhibiting one assay while having no effect on another [74] so where internal positive controls are used they need to be representative of the targets of interest. The SPUD assay has been developed to estimate the extent of qPCR inhibition by measuring an external spike-in from potato (*Solanum tuberosum*) in control (water) vs. target samples [155]. This can be applied as DNA or RNA [156]. Analysis of C_q and assay efficiency between control and target samples for the SPUD assay indicates the extent of matrix inhibition [36,155]. Another method for evaluating inhibition is to perform a serial dilution of the sample of interest. A reduced delta C_q at the higher concentrations is suggestive of reversible inhibition.

External positive controls can be used more extensively to evaluate biases associated with the extraction step. In clinical virological load monitoring, control viruses can be added to the sample prior to extraction [157,158]. Extraction methods can purify different amounts of template with different variances, so this is an important step to replicate [159,160]. Quantifying total RNA is a simple method for controlling for varying yields when measuring mRNA, with the accepted potential problems discussed above. However, if further rigour is required then external RNA standards can be used. An example of such a resource is the ERCC panel of synthetic RNA oligonucleotides, which has been developed for this purpose [154].

It is also important to include negative control samples in order to evaluate the potential for contamination [79]. No template controls (NTCs) are commonly employed in RT-qPCR studies. There are no guidelines on how to report positive NTC results, although proposals have been made [48], namely that NTCs with high

Chapter 1 Introduction

C_q values, far removed from sample unknown positive results, can be legitimately ignored but should be reported when publishing data. Any C_q that differs by more than 5 from the NTC may be regarded as probably not caused by any contaminant, especially when the replicate wells also record positive, similar C_q values. However, if an NTC records a C_q less than 30, high levels of contamination are indicated.

It should be noted that false positive amplification may not always be the result of contamination, but maybe attributable to badly designed assays resulting in primer-dimer formation, amplification of pseudo genes and/or primers binding to carrier molecules. One technique to counteract contamination from previous PCR products is the application of uracil N-glycosylase (UNG). The dTTP is substituted by dUTP in the PCR mastermix, generating dUTP-containing amplicons. UNG enzyme is activated before the normal reaction thermocycling and any contaminating PCR products (containing dUTP) are digested. This is a proactive method to prevent contamination from future reactions, but will not help with a pre-existing contamination problem of standard dTTP-containing PCR products [161].

1.3.1.7 Other Considerations

In order to facilitate good repeatability (measurement made by the same operator, instrument, and conditions over a short period of time) and reproducibility (by different operators, instruments, and/or conditions) [3], key aspects of RT-qPCR experimental processes need to be reported, as outlined in the MIQE guidelines [55,86]. This is fundamental if findings are to be corroborated, which is in turn crucial for the observation to be translated into a clinically useful tool.

The MIQE guidelines encourage the use of a sample maximisation strategy, i.e., analysing as many samples as possible in the same experiment, as opposed to a gene maximisation strategy that analyses multiple genes in the same experiment

[55,86]. This is because it minimises any technical, run-to-run variation between different samples for the comparison of mRNA levels. If not all samples can be analysed in the same run, identical samples that are tested in both runs (inter-run calibrators, or IRCs) must be analysed. Measuring the difference in C_q or the normalised relative quantity between the IRCs in different runs allows the calculation of a correction or calibration factor to remove run-to-run differences [86,162].

RNA measurement on a complex biological sample (like a tissue biopsy) requires a series of steps, each of which contributes error that is often several fold greater than the difference in the mRNA to be measured. Consequently, determining differences in mRNA levels in real scenarios requires consideration of the sources of error and appropriate normalisation mechanisms to control for them. Yet measurement claims of biologically significant mRNA level differences are routinely made without apparent consideration (or reporting) of such technical factors [59]. Consequently, while often statistically significant, these results may not be due to the biological phenomenon under investigation and/or may not be reproducible. Without assessment and consideration of the technical variability introduced at each stage of the experimental process, findings may be of limited practical use in the clinic because they are difficult to reproduce.

Simple measures that will help to facilitate effective measurement capabilities include spatial separation of individual aspects of the experimental procedure. Designating separate areas for nucleic acid extraction/preparation, PCR set-up (template negative area), template addition and finally PCR (PCR positive area) will go a long way to minimise potential contamination, increasing confidence in measurement results [79].

The issues described above highlight the importance of including appropriate controls, designed to enable researchers to identify and account for these differences, and harmonisation of experimental design [122,163]. There are a

number resources that support experimental design both as basic guides [98], extensive repositories of information [164], as well comprehensive software tools including GenEx [165], qbase [166] and RealTime StatMiner ® [167].

1.4 Clinical Relevance

RT-qPCR is an important tool in the understanding of the molecular events underlying human diseases but also identifies unique biomarkers for the identification and stratification of a range of diseases [6,47]. Studies have reported applying these methods for the identification of micrometastases or minimal residual disease in colorectal cancer [168], neuroblastoma [169], prostate cancer [170] and leukaemia [171]. It has been employed to distinguish different types of lymphoma [172], for the analysis of cellular immune responses in the peripheral blood [173,174], the detection of bacterial [175] and viral [176] RNA signatures in clinical samples and for monitoring the response of human cancer to treatment [33]. Other clinically relevant applications include its use for the analysis of tissue-specific mRNA levels [177], identifying cytokine mRNA levels upon *ex vivo* stimulation of peripheral blood mononuclear cells [178] and for cytokine mRNA profiling [179]. Novel gene expression approaches are constantly being evaluated for diagnostic purposes for numerous human diseases.

These developments may ultimately lead to the implementation of truly personalised medicine, whereby the course of treatment chosen, response and prognosis may centre on molecular measurements. Yet what is ominous is that despite the vast amount of published clinical research using RT-qPCR to measure putative mRNA biomarkers, few tests have as yet been transferred to the clinic for routine use. Where RNA measurements are routinely used, such as monitoring viral loads in disease states or response to a particular treatment regime, the measurements made at the beginning of the study must be compatible with those made at the end, i.e. the measurement standards used to calibrate them must have long-term stability [1]. These considerations apply equally to gene expression

biomarkers and collectively contribute to measurable improvements in the quality of analytical results.

In terms of clinical measurement, different capabilities will be required depending on the measurement need. For example, viral load and specific gene signatures, such as the BCR-ABL fusion transcript, require differentiation between gross changes of target, whereas cellular mRNA levels are more subtle and much more challenging to measurement reproducibly. For example, clinicians will not usually alter therapy when measuring HIV viral load unless there is a change of around one order of magnitude (\log_{10} scale). However, research that measures normalised mRNA levels by RT-qPCR frequently presents much smaller significant differences (e.g. frequently less than three-fold).

1.4.1 Biological Variability

Biological variability is one of the principal unknown entities in terms of the aforementioned considerations and represents the final determining factor whether a given RNA measurement will be of clinical value, i.e. once the technical factors are resolved the measurement is still dependent on biology. Previously, it has been assumed that the findings of randomised controlled trials (RCTs) were applicable to all patients. However, it is becoming increasingly apparent that this is not the case [180,181]. Treatment outcomes as well as disease progression and manifestation have been shown to vary between patient groups, with women and ethnic minorities being under-represented in vascular surgery RCTs [182], or patient chronotype and its relationship with cancer treatment schedules [183]. The underlying cause for these findings will be due to physiological differences many of which will manifest in the mRNA profiles, suggesting that many putative surrogate mRNA biomarkers are likely to be similarly variable between different patient groups.

Chapter 1 Introduction

mRNA profiles may change on a cyclical basis, influenced by circadian rhythms, growth and development, and other environmental factors such as stress, sustenance/nutrition, physical activity and infection, in conjunction with variability attributable to gender, race, age and time of sample collection, to name a few. These factors must additionally be considered over and above general experimental issues such as choice of procedure, sources of error and sample contamination, in order to select a useful biomarker that can yield reproducible results. Unpicking the sources of biological versus technical variance represent a crucial yet frequently neglected step in translating a measurement to the clinic.

The mRNA used for clinical diagnostics and research may be derived from various tissues including biopsies, spinal taps, blood, urine or buccal swabs. As a consequence, sample handling has to be carefully controlled and regulated in order to preserve the quality and integrity of the RNA material [6,54].

1.4.2 Tissue Variability

As described above, sample source is a major contributor to measurement variation. RNA extractions and subsequent analyses performed from whole tissue biopsies with little regard for the different cell types contained within that sample, inevitably result in the averaging of the expression of different cell types and the mRNA profile of a specific cell type may be masked, lost or ascribed to and dismissed as incorrect measurement [184] because of the bulk of the surrounding cells [47,185]. When working with versatile tissues such as blood, cell number and composition may vary within two samples (even from the same patient); consequently blood volume may not be an appropriate metric to begin with and separation of the different cell types is often performed. However, it should be remembered that any processing of live cells will impact on the cellular physiology and may directly alter the expression of the genes of interest.

Cellular separation is more difficult to achieve when analysing solid tissue samples but may be important, as significant differences have been detected in the mRNA profiles between microdissected and bulk tissue samples [185,186]. This is particularly relevant when comparing mRNA profiles in complex tissue with multiple, phenotypically distinct cell types, within a given tumour or between normal and cancer tissue where phenotypically normal cells adjacent to a tumour may exhibit altered mRNA profiles due to their proximity to the tumour [47,187]. It may be possible to alleviate these pressures of sample source/cell type by performing single cell analysis. This rapidly growing field has much to offer but also comes with a multitude of unique challenges associated with sample processing, low mRNA abundance and data normalisation [188-191]. It should also be remembered that cell sizes may vary between different samples (such as tumor biopsies or where tissues are undergoing hypertrophy as part of normal physiology), which adds an additional challenge to data interpretation.

1.4.3 Patient Variability

The greatest contribution to variability in clinical measurement will be observed between different subjects (patient-to-patient). While fundamental similarities in expression may be observed, demographic, genetic and environmental factors ranging from; age; sex; and ethnicity to smoking, nutrition and medication [121] will exert considerable influences on biological flux. Expression may also be modified by disease state, during cellular proliferation, due to cellular composition, circadian fluctuations and by mitogenic stimuli (e.g. growth factors) [6,142,192].

1.4.4 Musculoskeletal Disease

The World Health Organization (WHO; <http://www.who.int/en/>, accessed May 2011) in collaboration with the Bone and Joint Decade Initiative has completed a ten-year study investigating the "Burden of Musculoskeletal Conditions at the Start of the New Millennium" [193]. Joint diseases, rheumatoid arthritis and

Chapter 1 Introduction

osteoarthritis, osteoporosis, spinal disorders, low back pain, and severe trauma are among 150 musculoskeletal conditions affecting millions of people globally. These conditions are the most frequent cause of disability severely affecting individuals' ability to carry out their activities of daily living. WHO estimates that several hundred million people already suffer from bone and joint diseases, with dramatic increases expected due to a doubling in the number of people over 50 years of age by 2020.

Diseases of the musculoskeletal system can affect the body's muscles, bones, joints, tendons, ligaments and nerves. They mostly encompass functional disorders or motion discrepancies, and those of or pertaining to the joints are the most common. The numbers of those affected are set to rise over the next few decades. In the developing world, successful treatment of communicable diseases, combined with a rapid increase in road traffic accidents, will lead to an increase in the burden of musculoskeletal conditions. In industrialised countries, the increasing numbers of elderly people is a key factor in this rise. As these conditions represent an increasingly substantial health problem, it is essential that good molecular tools are developed to provide confident measurement for the development of research as well as diagnostic and prognostic tools.

Standardisation of RNA measurement, which represents one of the greatest challenges of its type in biological measurement, is particularly difficult when studying expression in musculoskeletal tissues, especially bone and cartilage, due to difficulties in sample sourcing and RNA extraction. Obtaining intact, high quality RNA is an essential step in analysing mRNA levels. This step is particularly challenging in bone, which contains low numbers of cells embedded within a highly mineralised tissue [50]. The physical and chemical characteristics of bone hinder the access of reagents in the nucleic acid extraction process [194-196] and predispose to co-extraction of PCR inhibitory compounds [194,197-200]. Consequently, relatively specialised techniques are required for successful nucleic acid extraction from bone. Major approaches, with innumerable variations, include

organic extraction methods involving phenol/chloroform and silica-binding methods where guanidinium-based chaotropic salts are used both to disrupt proteins, as well as mediate highly specific binding of nucleic acid to silica particles via ionic salt bridges [194,201-203]. A suitable cell line model alleviates the difficulties of RNA extraction from whole bone. Osteoblastic cell lines such as SaOS-2 offer the additional benefit of being able to mineralise in culture [204,205].

1.4.4.1 Important Clinical Questions in the Musculoskeletal System

Mechanical loading regulates the shape, repair and regeneration of the skeleton. Mechanical signals are transduced through the extracellular matrices, modify cell-matrix and cell-cell interactions, and impact on transcriptional responses [206]. Mechanical behaviour of whole bone is often studied in order to obtain a greater understanding of the relationship between bone structure and functions during physiological loading. These insights can help identify areas of peak stresses that are more likely to fracture during intense activity, and allow the prediction of effects of various genetic defects, disease processes and drug treatments [207]. The complexity of bone architecture itself makes such studies difficult, as differences in for example mineralisation, can vary within a sample as well as between samples. However, load transfer between bones through joints and the implications of long-term mechanical loading may be studied by elucidating the coinciding changes in mRNA levels (mechanoresponsive signalling) and may subsequently aid patient diagnosis, treatment and tissue engineering approaches [208].

It is well established that mechanical loading is a critical factor in the maintenance of adequate bone mass in the skeleton, where various signals have been implicated. One such signal is glutamate; a major excitatory neurotransmitter in the central nervous system (CNS) [208,209]. The excitatory amino acid transporter, EAAT1 (also known as SLC1A3: solute carrier family 1 (glial high affinity glutamate transporter), member 3, or GLAST1: glutamate/aspartate

transporter1, the rat homologue) terminates glutamatergic signalling and was first implicated in mechanotransduction [208]. GLAST1 was originally discovered in a gene screening experiment looking for mechanoresponsive genes in osteocytes *in vivo* [210]. This led to the idea, later confirmed, that glutamate signals in bone [209]. Furthermore, several studies have shown evidence that glutamate release, receptors and transporters are expressed and functional in several bone cells, including osteoblasts, osteocytes and osteoclasts [209,211]. Glutamate and associated signalling mechanisms provide potential therapeutic targets in connective tissue and musculoskeletal disorders.

1.4.4.2 Additional Cell Lines

The hepatocyte-derived cell line Hep-G2 is a commonly employed *in vitro* model. Cells maintain in large part a number of cellular functions similar to those of normal hepatocytes such as expression of hepatocyte-specific cell surface receptors and synthesis and secretion of plasma proteins [212-214]. Furthermore, because of the high degree of morphological and functional differentiation *in vitro*, the Hep-G2 cell line is a suitable model to study intracellular trafficking, hepatocarcinogenesis, drug targeting and toxicogenomics *in vitro* [214-217]. These cells are relatively uncomplicated to cultivate and as such, make a useful model system.

The Hs 683 cell line, of oligodendroglial origin, has been extensively characterised and display similar expression patterns to oligodendrogliomas [218]. These cells are also known to express factors involved in glutamate signalling, and so may augment such signalling in cells of osteoblastic origin [219,220].

1.4.5 Practical Clinical Challenges

In certain clinical situations, for example where surgical sampling is required, some of the points detailed here will reflect a utopian view that will not be

practical to implement. For instance, tissue-sampling methods may vary among institutes and even across individuals within the same institution. This can be very challenging to standardise with respect to the time-span of surgery, how long it takes for a sample to be fixed or frozen, etc. To ensure data comparability and increased clinical impact within such challenging circumstances, it is crucial that such conditions are defined as accurately as possible and the associated limitations are fully considered within the discussions around a given finding.

A particular mRNA result may only be possible under a very specific sampling procedure that is not easily repeatable (due to specialist skill and/or equipment). Such findings may reveal new biological mechanisms, but unless they can be corroborated they will be of questionable value. An example by which this can be performed could be that the samples are re-analysed (ideally including re-extraction) by a different laboratory to confirm the measurement. However, such analysis may never be translated to routine clinical care as biomarkers and as mRNAs are frequently measured as surrogates for protein driven physiology, additional confirmatory experiments considering the proteins and/or physiology in question is essential.

It is also crucial that other factors within the protocol (**Figure 1.2**) that can be controlled are detailed within a given study. Factors that frequently vary but which are easily controlled, and easily reported, like storage conditions and duration may vary among laboratories, e.g. type of freezer, storage in liquid nitrogen by immersion or by vapour phase, etc. and so they must be comprehensively described. Documentation of such factors will facilitate identification of any associated discrepancies that might arise, a fact that is particularly pertinent to biobanking, which may comprise large numbers of samples that may have been stored for different durations.

1.5 Conclusion

Accurate RT-qPCR analysis and reporting could improve clinical diagnosis as well as predictive and prognostic monitoring. Furthermore, improved analytical measurement sensitivity may offer tools to detect and quantify disease markers at earlier stages of progression, facilitating earlier treatment and improved outcome. Moreover, diagnostic tests conferring superior accuracy and analytical confidence may change treatment regimens patients are offered. For example, several expensive and highly toxic cancer therapies are only effective in treating certain oncogene genotypes. As such, they are offered only to those patients that have definitive molecular proof they harbour the associated specific mutation. HER2 (human epidermal growth factor 2) status in breast cancer is one such DNA measurement example and is used as a predictive therapy-selection factor for the humanised monoclonal antibody trastuzumab (Herceptin®; Genentech) [221]. Current diagnostic methods, including fluorescent *in-situ* hybridisation (FISH) and immunohistochemistry (IHC), can be subjective and insensitive. Advances in accurate molecular quantification of RNA [222,223], could offer enhanced analytical power for this and many similar clinical challenges, and may in the future become gold standards in clinical diagnostics.

Yet for RT-qPCR to make an impact when applied to preclinical research, accuracy must be seen as more than just good precision. Accurate clinical measurement must also include considerations of both potential bias and good technical reproducibility. By applying this to the whole stepwise process for preparing the RNA sample and subsequent methods for normalisation, RT-qPCR will become more reproducible, which in turn will improve the impact and likelihood that findings will be translated to routine clinical use.

The accomplishment of such standardisation measures as detailed in this review may be problematic in practice, particularly in clinical laboratories. The key is to implement a standardised approach, to be aware of (and define) limitations and to

include appropriate calibrators or reference materials, which will allow appropriate data normalisation.

1.6 Scope

The overall objective for RMs and standardisation is to provide an appropriate and versatile solution to measurement bias. Correct interpretation of results and appropriate use of statistics will increase confidence in experimental findings and clinical relevance, aiding scientific understanding and medical innovation.

Bone represents one of the most difficult tissues in which to make accurate molecular measurements as a consequence of varying and complex matrices. However, it is included here due to its fundamental role in musculoskeletal disease and glutamate signalling crossover between mechanical loading, inflammation and brain signalling mechanisms.

Liver and brain tissues are extensively studied due to their central involvement in body homeostasis and are relatively uncomplicated to work with due to high RNA yields with straightforward extraction procedures. These will be utilised here as an additional experimental challenge.

Figure 1.5 outlines the major components of this investigative strategy. Starting with a bottom-up approach, i.e. from the end of the process (qPCR measurement and data normalisation and interpretation) through to the start (sample source and extraction of RNA), this study aims to characterise the variability inherent to various aspects of the experimental path.

1.7 Aims and Hypothesis

This thesis is based on the hypothesis that error in mRNA measurement can be partitioned across different stages of the experimental procedure. This project

Chapter 1 Introduction

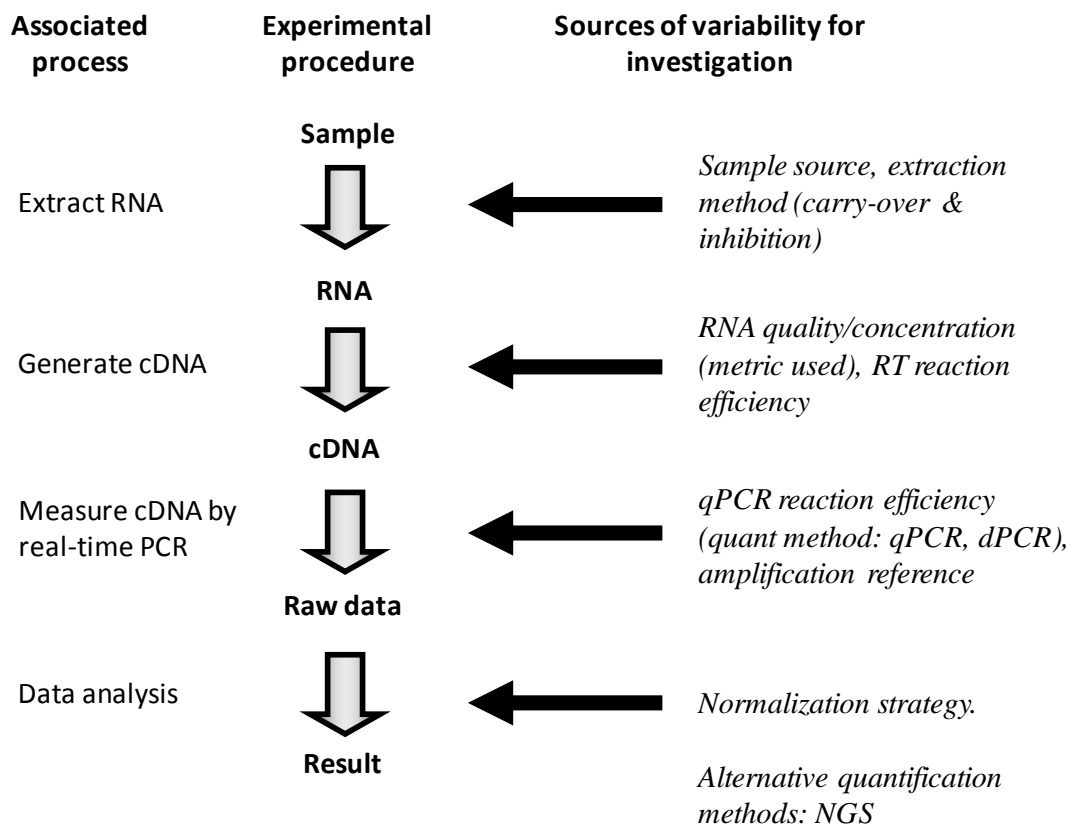


Figure 1.5 Proposed experimental strategy for investigating contributors to variability.

Chapter 1 Introduction

aims to define such error in a range of samples to improve experimental design and minimise uncertainties, alongside providing a guide on how to approach apportioning error, standardisation and validation. An ERCC RNA panel has been developed for use as an external (synthetic) RM, which was evaluated alongside validated endogenous reference genes. This thesis employs multiple bone models of differing complexity (2D cell culture model, 3D gel co-culture model and clinical samples) for the assessment of variability introduction and error propagation for RT-qPCR measurements and compares this with glial and hepatic variabilities. Additionally explored are potential clinical applications for this method.

Aims:

1. To define the experimental sources of variation during the key stages required for RNA measurement.
2. To use synthetic RNA standards, namely an ERCC RNA panel, to elucidate sources of variability in RT-qPCR measurement of mRNA levels.
3. To use human-derived cell lines as background material and as a source of endogenous reference targets and GOI for the preparation of a pilot reference material to test process variabilities and normalisation approaches.
4. To use three bone models of increasing complexity to evaluate variability contributions attributable to sample source.

Chapter 2

Materials & Methods

2 Materials & Methods

2.1 Materials

Human genomic DNA (gDNA; Promega P/N G304A) and/or human universal reference RNA (Stratagene P/N 740000) was used in qPCR assay development. LoBind® safe-lock PCR clean tubes were employed throughout this study (Eppendorf 1.5 mL P/N 0030 108.116 and 0.5 mL P/N 0030 108.035). Primer and probe sequences for qPCR and dPCR designed in-house using Primer Express, software version 3 (ABI) and ordered from Sigma, with purification by HPLC. Some experiments were performed using assay-on-demand (ABI). Sequences, gene accession numbers and assay concentrations are outlined in **9.1 Appendix 1 – Assay Information**. Total yeast RNA [from baker's yeast (*Saccharomyces cerevisiae*), Sigma P/N 26750] at 25 ng/reaction was used as carrier in this study. All samples were diluted using RNA Storage Solution, RSS (ABI P/N AM7001), unless otherwise stated.

2.1.1 Synthetic RNA Transcripts

Eight synthetic (ERCC developed targets; External RNA Control Consortium) RNA transcripts (ERCC-00013, -00025, -00042, -00084, -00095, -00099, -00113, and -00171) were selected for investigation (supplied in plasmid DNA format, courtesy of Dr Marc Salit, NIST, USA). For brevity, the ERCCs shall be subsequently identified without the preceding zeros. Concentrations of plasmid were assigned by the supplier using UV spectrophotometry and converted to copy number using published methods [224]. Copy number conversions were performed using the appropriate extinction coefficient values for dsDNA (50 ng-cm/ μ L) or RNA (40 ng-cm/ μ L). Plasmid DNA was used as template for *in vitro* transcription (IVT).

2.1.2 Cell Lines

Hep-G2-derived RNA (organ: liver, disease: hepatocellular carcinoma) was used for RNA stability experiments (ATCC P/N HB-8065). Three human cell lines were employed for production of complex background material for endogenous target selection: Hep-G2; SaOS-2 (organ: bone, disease: osteosarcoma, ATCC P/N HTB-85); and Hs683 (organ: brain, disease: glioma, ATCC P/N HTB-138).

Subculturing and propagation was performed as per manufacturer's instructions, with appropriate culture medium and serum additionally supplied from ATCC (Hep-G2: Eagle's Minimum Essential Medium (P/N 30-2003), 10% fetal bovine serum (P/N 30-2020). SaOS-2: McCoy's 5a Medium Modified (P/N 30-2007), 15% fetal bovine serum. Hs683: Dulbecco's Modified Eagle's Medium (P/N 30-2002), 10% fetal bovine serum). Prior to sub-culturing of cells in T-175 flasks (Corning, Sigma P/N CL S431079), culture medium was aspirated from cell monolayer at approximately 90% confluency, which was washed briefly in room temperature Hanks Balanced Salt Solution (HBSS; PAA Laboratories P/N H15-009) to remove serum. Five mL Trypsin/EDTA (Sigma P/N T4049) solution was added to each flask and incubated at 37°C for 5 min. After incubation, cell detachment was monitored under a light microscope until all cells had detached. Adding an equal volume of the appropriate culture media subsequently quenched trypsin activity. Cells were pooled together and re-seeded into fresh T-175 flasks containing 30 mL of the appropriate cell culture media, according to their splitting ratio. For propagating cells in culture, 100% of the media was replaced every second day.

2.1.2.1 Carrier Options

Inclusion of carrier nucleic acid (DNA or RNA not containing the target sequence) may increase experimental precision when evaluating low target copy number samples [56,69,103]. Carriers utilised in this study include: 50 ng total Hep-G2 RNA (produced in-house); 50 or 250 ng total yeast RNA; 50 or 250 ng sonicated salmon sperm DNA (Agilent P/N 201190); and no carrier (water). All were diluted

using RSS (RNA carriers) or 1× TE pH 8 (DNA carriers; Sigma P/N 93283), unless otherwise stated.

2.2 Production of RNA

2.2.1 ERCC RNA: Plasmid DNA Digest & IVT

ERCC plasmid DNA (from standards ERCC-13, 25, 42, 84, 95, 99, 113 and 171) was linearized using *Bam*HI; 0.5 µg plasmid DNA was digested with 40 U restriction endonuclease, as per manufacturer's instructions (New England Biolabs P/N R01365). Samples were purified according to manufacturer's instructions (QiaQuick DNA purification; Qiagen P/N 28104), with an elution volume of 32 µL.

IVT was performed using MEGAscript® T7 Kit (ABI P/N AM1333). Briefly; 8 µL linearized plasmid DNA template was subjected to IVT in 20 µL total reaction volume (according to manufacturer's instructions), with an overnight incubation of 37°C. Samples were treated with Turbo DNase (as per MEGAscript® T7 kit protocol, Ambion P/N AM1907M) at 37°C for 15 min, before purification using RNeasy kit (Qiagen P/N 74104) and further on-column DNase treatment (Qiagen, as per optional method in RNeasy kit protocol). The two DNase treatments were performed due to previous experience of residual DNA remaining when only one treatment was performed. However, for the pilot RM production, an alternative DNase treatment was validated. IVT ERCC RNA concentrations and insert sizes were subsequently estimated using Nanodrop UV spectrophotometry (Thermo Scientific) and 2100 Bioanalyzer (Agilent), respectively. Samples were diluted to approximately 1 ng/µL in RSS and stored at -80°C. Concentrations and copy number estimates are reported in **Table 9.6**.

An aliquot of each of the same IVT ERCC RNA transcript samples were additionally heat-treated (70°C for 2 min, before being placed on ice) before re-analysing using 2100 Bioanalyzer to test for secondary structure denaturation.

2.2.1.1 Secondary Structure Prediction

ERCC RNA sequences were subjected to *in-silico* secondary structure prediction using the online tool, MFOLD (<http://mfold.rna.albany.edu/>, accessed 2011 and 2015). Folding predictions were performed at 45°C (temperature of RT step). Predicted structures with the lowest energies (most stable) were chosen as the most probable configuration for the majority of transcript molecules within a sample (**9.2 Appendix 2 –Endogenous and ERCC Transcript Predicted Secondary Structures**).

2.2.2 Cell Line RNA Production for Complex Background

Total RNA derived from SaOS-2, Hep-G2 and Hs 683 cell lines were used for production of the complex background material. Based on confluency and cell size, eight to fourteen flasks were prepared for each cell type, as outlined above. Medium was removed, cells washed in HBSS and TRIzol (Sigma, P/N 15596-018) added directly to cell monolayers (17.5 mL per T-175 flask, 1 mL per 10 cm²) and passed three times over the entire surface of the flask to ensure cell lysis. Lysates were transferred to 50 mL round-bottomed Falcon tubes (VWR P/N 21008-951) and stored at -80°C until RNA extraction. Replicate T-175 flasks (one per cell line used) generated at the same time and under the same conditions were used for cell enumeration and viability estimates using a Vi-Cell (Beckman Coulter). For cell counting, cells were detached post HBSS wash using 5 mL Trypsin/EDTA for 5 min at 37°C and neutralised with 5 mL culture medium before Vi-Cell analysis.

Total RNA was extracted from cell lysates by following a standard TRIzol protocol (Invitrogen). Briefly, TRIzol lysates were thawed and incubated for 5 min at room temperature and harvested by centrifugation (12,000 × g for 10 min at 4°C) to pellet DNA and cell debris. Chloroform (Sigma P/N 472476-1L) was added to the supernatant (200 µL of chloroform for every 1 mL of TRIzol). Following phase separation using centrifugation (12,000 × g for 15 min at 4°C), RNA was collected in the upper aqueous phase and precipitated using 0.5 mL isopropyl alcohol

(Sigma P/N 59304) per 1 mL TRIzol. The RNA pellet was washed with 75% ethanol (Sigma P/N E7023) before resuspension in 50 μ L nuclease-free water (ABI P/N AM9937). Total RNA solutions were treated with recombinant (r)DNase I (ABI P/N AM2235), as per manufacturer's protocol (1 U rDNase I reagent added per 4 μ g of total RNA, incubated at 37°C for 30 min). These preparations were purified using RNeasy midi kit (Qiagen P/N 75144) and the total RNA eluted in varying volumes of nuclease-free water (depending on expected yield, following kit protocol), assessed for quantity (yield; Nanodrop), and subsequently pooled (per cell-type).

Following total RNA extraction, DNase treatment and purification, pooled cell line RNA samples were subjected to standard quality metrics for concentration and integrity (Nanodrop and 2100 Bioanalyzer, respectively). Neat samples (resuspended following purification in nuclease-free water, between 110-700 ng/ μ L) were stored at -80°C.

2.3 Preparation of Transcriptomic Calibration Material (TCM)

Ideally the expression ratio of two reference genes should be the same in all samples, regardless of the experimental condition or cell type, with increasing ratio variation corresponding to decreasing expression stability of one (or both) of the tested genes [7]. Based on this principle, pilot RMs were prepared using a combination of six validated synthetic and three endogenous reference genes. Different mixed ratios of the three chosen cell lines were prepared to comprise the three distinct pilot RMs, each offering a different experimental challenge, with scope for applicability to standardisation. These pilot RMs are assigned as Calibrant, Unknown 1 and Unknown 2. The unit types Unknown 1 and Unknown 2 are referred to as 'Unknown' materials, despite the fact that their composition is known to us, as their ultimate purpose is as a prototype reference material for molecular measurements, helping to determine measurement capabilities and validate measurement claims of laboratories.

Chapter 2 Materials & Methods

Each ERCC IVT RNA stock solution was diluted to $1.0E+09$ copies/ μL (Calibrant) or $1.0E+08$ copies/ μL (Unknown 1 and Unknown 2) in RSS and three, $100\times$ ERCC solutions (synthetic-only TCM, sTCM) for Calibrant, Unknown 1 or Unknown 2 containing all six ERCC transcripts at different concentrations was prepared (**Table 3.7**). Pooled cell line RNA stocks were diluted in RSS to $250\text{ ng}/\mu\text{L}$ (Hep-G2 and Hs683) or $100\text{ ng}/\mu\text{L}$ (SaOS-2), and three solutions for Calibrant, Unknown 1 or Unknown 2 prepared by mixing different proportions of each cell line RNA to a final concentration of $50\text{ ng}/\mu\text{L}$ (**9.4 Appendix 4 – Pilot Reference Material Composition**). The respective $100\times$ ERCC solution was spiked into the corresponding mixed ratio cell line solution to produce Calibrant, Unknown 1 or Unknown 2 materials. The solutions were aliquoted ($150\ \mu\text{L}$) to generate 245 replicate units for each Calibrant, Unknown 1 and Unknown 2 prior to storage at -80°C . These pilot RMs comprised the test material for determining uncertainty contributions at each stage of the experimental process.

2.3.1 Endogenous Target Selection

2.3.1.1 Reference Genes

A panel of 32 control genes were evaluated as candidates for endogenous reference genes shared between the three cell lines (ABI P/N 4391590. See **9.1 Appendix 1 – Assay Information** for candidate reference gene assay details). Reference genes with consistent/least variable expression across the three different cell types were selected for continuation, as determined by RefFinder [225] analysis.

RefFinder, accessed via the Cotton EST Database, is a web-based comprehensive tool developed for evaluating and screening reference genes from extensive experimental datasets. It integrates three computational programs (GeNorm [7], Normfinder [137], BestKeeper [226] and the comparative $\Delta\Delta C_t$ (C_q) method [227]) to compare and rank the tested candidate reference genes. Based on the rankings

from each program, it assigns an appropriate weight to an individual gene and calculates the geometric mean of their weights for the overall final ranking.

2.3.1.2 Genes of Interest

A selection of 29 candidate genes was assessed for GOI suitability. The expression of each potential target gene in each of the three cell lines (C_q values) were used to model fold changes based on different options for composition of Unknown 1 and Unknown 2 materials. See **9.1 Appendix 1 – Assay Information** for candidate GOI assay details. Based on these predictions, mixed ratio model units of the three cell lines were mocked up and tested for applicability using a subset of the GOI assays. For our purposes, GOIs simply required differential expression in each of the three cell lines and assays that performed reproducibly with high efficiency.

2.3.2 Assay Design

When designing primers for ERCC TCM targets, assays were positioned across different RNA secondary structure motifs (predicted using MFOLD [228,229]), representing both tightly folded and more open regions, depending on the target (**9.2 Appendix 2 –Endogenous and ERCC Transcript Predicted Secondary Structures**).

ERCC RNA concentration and copy number estimates are summarised in **Table 9.6**. Assay positions within the respective transcripts are detailed in **Table 9.4**.

After initial endogenous target selection, the amplicon region of both Reference and GOI assays, as detailed by the commercial assay manufacturer, was identified and used to redesign assays in-house. Assays were designed to this same region and amplification conditions optimised. These assays underwent validation as performed previously, including primer/probe concentration optimisation and cross-reactivity tests with ERCC RNA standards, before application to pilot RM evaluation.

2.3.3 Measurement Uncertainty Budget

A₂₆₀ was used for initial quantification of ERCC stock concentration. The 2100 Bioanalyzer was employed for the assignment of purity to ERCC stock solutions. These factors were additionally used for calculation of the pilot RM assigned values and associated uncertainty budgets for each ERCC transcript. Furthermore, other contributions to uncertainty calculations included volumetric dilutions of the stock solution and sample homogeneity and stability. Since all study materials were prepared from the same stock ERCC solution, transcript concentration and purity terms were the same when measuring relative expression ratios. Therefore, the associated measurement uncertainty is composed of precision terms related to the independent dilution steps performed for each Unknown unit type (Unknown 1, Unknown 2) preparation, plus sample homogeneity and stability.

Measurement uncertainty was calculated using the root sum of squares rule for combining standard uncertainties for independent variance components:

$$U_c = \sqrt{u_1^2 + u_2^2}$$

Where: U_c = combined uncertainty

u_n = uncertainty (*SD*) of a contributing factor

2.4 Reverse-Transcription Quantitative PCR Analysis

RT-qPCR experiments were performed under either one-step or two-step reaction conditions. Taqman 96-well optical plates (ABI P/N 4306737) and Taqman 96-well optical plate adhesive covers (ABI P/N 4311971) were employed for all RT-qPCR experiments.

2.4.1 Two-step RT-qPCR

For two-step RT-qPCR, the RT reaction was performed using TaqMan reverse transcription reagents (ABI P/N N8080234). Reactions performed according to supplier recommendations (final reaction concentrations given); TaqMan RT buffer, 5.5 mM MgCl₂, 500 μM each dNTP, 2.5 μM oligo d(T)₁₆, 0.4 U/μL RNase Inhibitor, 1.25 U/μL Multiscribe RTase and 5 μL RNA at various quantities (20, 2 or 0.2 ng, diluted in RSS). Sample reactions were incubated at 25°C for 10 min, 48°C for 30 min and 95°C for 5 min. Triplicate reactions per sample were performed in parallel.

Subsequent qPCR analysis employed hydrolysis probes or intercalating dye (Power SYBR Green PCR Master Mix; ABI P/N 4367659, or EvaGreen; Biotium P/N 31003-1) in a 96 well plate format with the Prism 7900 HT real-time PCR system (ABI). Reactions of 10 or 25 μL consisted of TaqMan® Universal Master Mix (ABI P/N 4304437) or Power SYBR Green Buffer or 2× Fast EvaGreen Master Mix (final concentration 1×), sequence-specific gene assay (**9.1 Appendix 1 – Assay Information**), 2-5 μL cDNA at various concentrations (20, 2 or 0.2 ng, RNA equivalent) (**Table 9.5**) and ROX (Biotium P/N 99939, EvaGreen reactions only, final concentration 1×). Level and stage of replication can also be found in **Table 9.5**. The qPCR reaction was performed using the following parameters: 50°C for 2 min (TaqMan assays only), 95°C for 10 min (2 min EvaGreen reactions only), 40-45 cycles of 95°C for 15 s and 60 °C for 1 min. SYBR Green and EvaGreen assays additionally included a dissociation step (60 to 95°C) to assess for non-specific products and/or primer-dimers (*Alu* assay). Only single product peaks were observed.

2.4.2 One-step RT-qPCR

Unless otherwise stated, one-step RT-qPCR utilised AgPath-ID one-step RT-PCR reagents (Ambion P/N 4387391) and the Prism 7900 HT real-time PCR system, in a 96 well plate format. Reactions of 10 or 25 μL comprised RT-PCR buffer/master

mix, RT enzyme (1×), sequence-specific gene assay (**9.1 Appendix 1 – Assay Information**, RT priming gene-specific due to one-step process), 25 ng/reaction carrier (unless otherwise stated) and 1-2.5 µL RNA at 50 ng/µL (unless otherwise stated). Samples were analysed in triplicate. Thermal cycling conditions: 55°C for 10 min (RT step), 95°C for 10 min, 40 cycles of 95°C for 15 s and 60°C for 45 s.

PCR efficiency estimates were derived from curves encompassing six-point (or seven-point, GAPDH assay), ten-fold serially diluted standards (incorporating triplicate measurements per dilution), utilising: ERCC IVT RNA transcripts (ERCC assays, one-step); human gDNA (*Alu* assay, qPCR only); complex background material (mixed cell line-derived total RNA from each Hep-G2, SaOS-2 and Hs 683 cells, endogenous assays, one-step), or human universal reference RNA (GAPDH assay, two-step, RT replicates).

2.4.3 qPCR Analysis

For all experiments performed on the Prism 7900 HT real-time PCR system, analysis was performed utilising SDS software (ABI), version 2.3. Assays included in this analysis typically exhibited efficiencies between 90 and 110% as a selection criterion. Systematic limit of quantification (LOQ) was not performed for all assays, however, standard curve analysis showed good linearity within the experimental range.

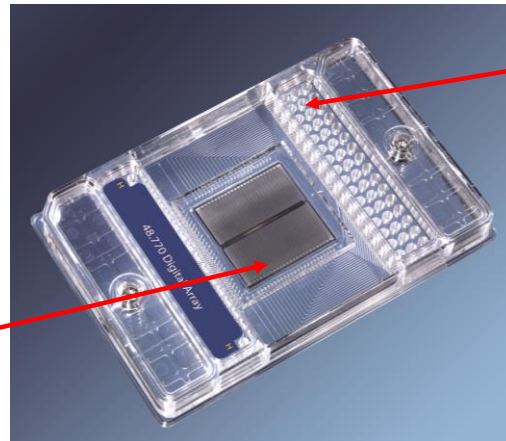
2.4.4 dPCR Analysis

dPCR experiments were performed using the Fluidigm Biomark platform. Both 12.765 (P/N BMK-M-12.765) and 48.770 (P/N BMK-M-48.770) chip formats were utilised. Assays were first optimised using the qPCR platform before transfer to the Biomark. Analysis was performed utilising dPCR analysis software (Fluidigm), version 3.0.2. Each chip contains 12 panels with 765 reaction chambers or 48 panels with 770 reaction chambers, respectively (**Figure 2.1A**). Master reactions, which additionally included GE sample loading reagent (1×, Fluidigm P/N

A

12:765 chip
765 partitions
per panel, 6 nL

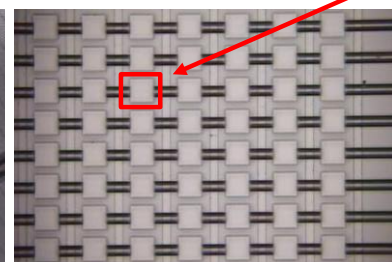
Nanofluidic
panels



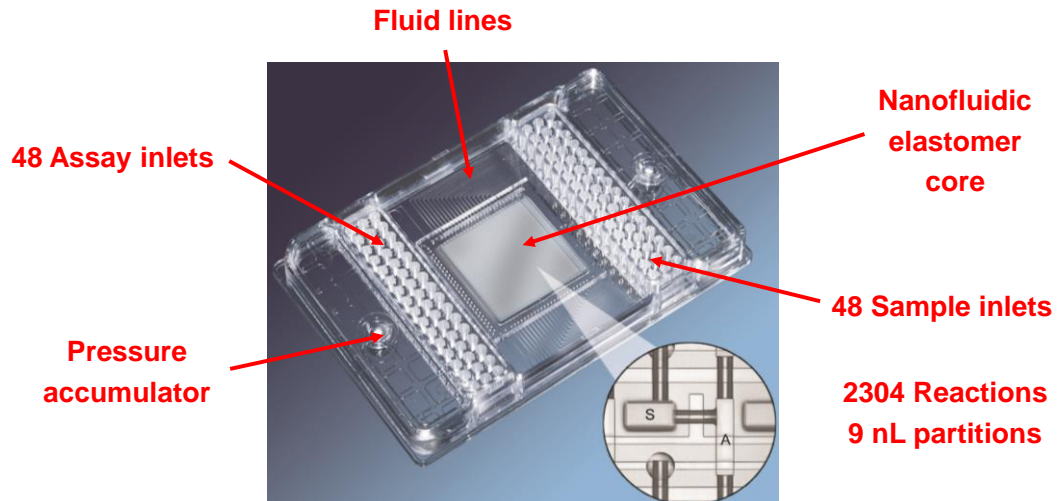
48 Sample
inlets

770 partitions
per panel

1 partition
(0.86 nL)



B



Fluid lines

48 Assay inlets

Pressure
accumulator

Nanofluidic
elastomer
core

48 Sample inlets

2304 Reactions
9 nL partitions

Figure 2.1 Fluidigm Biomark chips. (A) 48:770 digital PCR array. Each chip contains 48 panels, with 770 reaction chambers/partitions. Reaction mix is loaded into sample inlets and delivered to 0.86 nL chambers by an integrated fluidic circuit controller. 12:765 digital PCR arrays (not pictured), consist of 12 panels each with 765 reaction partitions; 6 nL per partition. (B) 48:48 Dynamic array. Each chip can analyse up to 48 different samples with 48 different assays. Assay and sample mixes are loaded into respective inlets and delivered to 9 nL reaction chambers by an integrated fluidic circuit controller.

85000735), were loaded into sample inlets and delivered to 6 nL or 1 nL chambers respectively, by an integrated fluidic circuit controller. Thermal cycling conditions as for qPCR. Analysis was performed utilising dPCR analysis software (Fluidigm), version 3.0.2. A count of partitions showing positive amplification can be made and an absolute target concentration elucidated [103]. dPCR calculations are explained in further detail below. MIQE guideline required information [230] is presented in **9.6 Appendix 6 – Digital MIQE**.

2.4.4.1 dPCR Calculations Explained

A count of partitions showing positive amplification can be made and an absolute target concentration elucidated. “Estimated copies” or “copies per panel” refer to the number of targets on the panel following a Poisson correction, to account for the fact that some positive partitions will contain more than one molecule. As the number of positive partitions increases, so does the probability that some partitions will contain more than one target molecule. The number of partitions in the dPCR chips used is sufficiently large to use Poisson probabilistic analysis to broadly estimate the mean concentration of the RNA sample using the following Excel formula [100]:

$$\lambda = -\ln(1 - k/n) \quad \text{or} \quad \lambda = m/n$$

$$N^{\circ} \text{ Copies on the panel} = (\text{LN}((C - k)/n)) * (-n)$$

$$k = n - ((\text{EXP}(N^{\circ} \text{ copies in the panel}/-n)) * n)$$

$$*\text{Target copies}/\mu\text{L} = (N^{\circ} \text{ copies on the panel}) / (\text{proportion loaded per panel})$$

$$\text{Proportion loaded per panel} = (\text{volume loaded per panel}) / (\text{volume loaded per inlet})$$

$$\text{Volume loaded per panel} = (\text{Partition volume}) \times (n)$$

Where:

λ = the mean number of molecules per partition

k = the number of positive partitions

Chapter 2 Materials & Methods

n = the number of partitions analysed per panel

m = the estimated copy number in the total volume of all partitions

N^o Copies in the panel \equiv estimated copies

Inlet = individual well for sample loading (discrete for each panel)

*Target copies/ μ L is the concentration of sample as it is added to master mix. If dilutions have been made to get to this point, these also need to be considered in your calculation of target copies/ μ L in your original sample.

Table 2.1 dPCR Specifications

	12.765	48.770
N ^o panels	12	48
n	765	770
Master reaction volume prepared per inlet	8 μ L	4 μ L
Volume of master reaction loaded per panel	4.6 μ L	0.65 μ L
Proportion loaded per panel	0.575	0.1625
Partition volume	6 nL	0.84 nL

- So for example, for a sample with 500 positive partitions (amplifications), using a 48.770 dPCR chip:

$$\text{N}^{\circ} \text{ Copies on the panel} = (\text{LN}((770 - 500)/770)) * (-770) = 806.9358$$

- Then:

$$\text{Target copies}/\mu\text{L in dilution used} = 806.9358/0.1625 = 4965.759$$

- Original sample was diluted 1:1000 for experiment. Therefore:

$$\text{Original sample concentration} = 4965.759 \times 1000 = 4965759 \text{ copies}/\mu\text{L}$$

$$= 4.97\text{E}+06 \text{ copies}/\mu\text{L}$$

Lamda (λ), defined as the number of molecules per partition or true concentration, may be determined with the least amount of relative error when there are approximately 1.6 target molecules per partition, which corresponds to approximately 80% positive partitions [231]. That equates to approximately 612 or 616 positive partitions per panel and 1231 or 1239 copies/panel, for 12:765 or 48.770 dPCR chips respectively.

2.5 Experimental Details – RT-qPCR Kit Comparison

Details pertaining to assay, replication, RT-qPCR experimental format (one-step or two-step) and sample and carrier concentrations can be found in **Table 9.5**, for each experiment.

2.5.1 One-Step RT-qPCR Kit Comparison by dPCR

Initially, quantification was assessed for two synthetic (ERCC-25 and ERCC-99) targets in both uniplex and duplex formats, between the three commercial one-step RT-qPCR kits: AgPath-ID one-step RT-PCR reagents, Quantitect Probe one-step RT-PCR Kit (Qiagen P/N 204443) and Superscript III Platinum one-step RT-qPCR system w/ROX (Invitrogen P/N 11745-100). Reactions were prepared as outlined for AgPath-ID kit in **2.4.2 One-step RT-qPCR**.

RT-dPCR was performed using Fluidigm Biomark 12.765 dPCR chips, n = 1 panel, plus three replicate experiments. Sample was diluted to approximately 1896 copies per panel (or 2062 copies/ μ L added to master mix), based on UV estimates. Thermocycling conditions were as follows: (RT) 45°C for 30 min, (RT inactivate/denature) 95°C for 15 min, (PCR) 40 cycles 95°C for 15 s and 60°C for 60 s. Yeast total RNA carrier was included at 25 ng/reaction. Following this, ERCC-25 and ERCC-99, plus two endogenous (UBC and MMP1) targets were compared between the kits. These assays were analysed in duplex: ERCC-25 with ERCC-99 (duplex A), UBC with MMP1 (duplex B), and ERCC-25 with UBC (duplex C). Sample was diluted to approximately 1886 copies per panel (or 1640 copies/ μ L added to

Chapter 2 Materials & Methods

master mix, for ERCC targets), based on UV estimates. RT-dPCR was performed using Fluidigm Biomark 12.765 dPCR chips, n = 3 replicate panels, plus two replicate experiments.

2.5.2 Comparison between dPCR and UV Measurement

Measurement variability of six ERCC targets was tested using RT-dPCR evaluated as above (AgPath-ID kit). ERCC targets were spiked into cell line-derived total RNA at approximately $1.0E+06$ copies/ μ L (estimated by UV), enabling evaluation of potential assay bias. Sample was diluted to approximately 200-400 copies per panel. RT-dPCR was performed using Fluidigm Biomark 48.770 dPCR chips, n = 3 replicate experiments, on different days. Assays were analysed in uniplex.

2.5.3 Linearity and Sensitivity of RT-dPCR

An evaluation of RT-dPCR quantification sensitivity was performed using ERCC-25 and ERCC-99 assays. Based on UV estimated values, sample was diluted in 0.5% Tween 20 (Sigma P/N P9416) to approximately 500, 250, 100, 50, 25, 10 and 5 copies per panel (equivalent to 3077, 1538, 615, 308, 154, 62 and 18 copies/ μ L, respectively). Volumetric dilutions were performed independently for each dilution, rather than sequentially, to avoid volumetric error propagation during dilution steps. RT-dPCR was performed using Fluidigm Biomark 48.770 dPCR chips, n = 6 panels per dilution, plus three replicate experiments. Assays were analysed in duplex.

2.6 Experimental Details – Extraction Kit Comparison

2.6.1 Lysate Preparation

Cell lysates of 17.5 mL were collected from T-175 flasks in aliquots for each cell line (Hs 683 and SaOS-2) and lysate buffer (for TRIzol, RNeasy and MasterPure extraction kits). Four flasks per cell line were produced; one flask per each of three

different lysis buffers plus one flask for cell enumeration. The TRIzol experiment was repeated three times for an analysis of batch variability. Seven mL of lysate were aliquoted and stored at - 80°C.

To assess the linearity of each extraction method, lysates were extracted at different dilutions: neat, 1:2 and 1:5. Prior to total RNA extraction, the 7 mL lysate aliquots were thawed, thoroughly mixed and dilutions prepared using the appropriate lysis buffer as diluent. Aliquots of total RNA were reserved for quantification and all extracts were stored at - 80°C before DNase treatment.

2.6.2 Total RNA Extraction using TRIzol Reagent

Total RNA was extracted from cell lysates by following a standard TRIzol protocol (Invitrogen). See **2.2.2 Cell Line RNA Production for Complex Background**.

2.6.3 Total RNA Extraction using RNeasy Mini Kit

Total RNA was extracted from cell lysates by following the “Purification of Total RNA from Animal Cells” protocol in the kit handbook (Qiagen P/N 74104). RLT buffer (containing 1% beta-mercaptoethanol, Sigma P/N M7154) lysates were homogenized using a QIAshredder spin column. One volume of 70% ethanol was mixed with the eluate and transferred to an RNeasy spin column. After separation using centrifugation (8,000 × g for 15 s), the silica membrane-bound RNA was washed with 700 µL of RW1 buffer followed by 500 µL of buffer RPE (both at 8,000 × g for 15 s). A further 500 µL of buffer RPE was used to wash the membrane (30 s) and the membrane spun dry for 2 min at full speed. Total RNA was eluted in 50 µL nuclease-free water.

2.6.4 Total RNA Extraction using MasterPure RNA Purification Kit

Total RNA was extracted from cell lysates by following the manufacturers’ protocol (Epicentre, Cambio, P/N MCR85102). Fifty µg Proteinase K (Epicentre P/N 56-

0002 and Qiagen P/N 19131) was added to Tissue and Cell Lysis Solution lysates and incubated at 65°C for 15 min with frequent vortexing, before placing samples on ice for 3-5 min. Addition of 175 µL MPC Protein Precipitation Reagent preceded centrifugation (10,000 × g for 10 min at 4°C). Total RNA was precipitated from the supernatant using 0.5 mL isopropyl alcohol. The RNA pellet was washed with 70% ethanol before resuspension in 35 µL of TE Buffer. Samples were incubated at 26°C for 15 min to assist resuspension of the pellet.

2.6.5 Post-Extraction Treatment

Total RNA solutions were treated with rDNase I, as per manufacturer's protocol (1 U rDNase I reagent added per 4 µg of total RNA, incubated at 37°C for 30 min). These preparations were purified using RNeasy midi kit, assessed for quantity (yield; Nanodrop). Neat samples (resuspended following purification in nuclease-free water) were stored in aliquots at -80°C.

2.6.6 RNA Quality Metrics

Following total RNA extraction, DNase treatment and purification, total RNA samples were subjected to several quality metrics for concentration and integrity.

2.6.6.1 Nanodrop

Sample concentration in ng/µL is based on absorbance at 260 nm. Volumes of 1.4 µL were measured on a NanoDrop 1000 Spectrophotometer (Thermo Scientific) in triplicate per sample. 260/280 and 260/230 absorbance ratios were also obtained and used in assessment of sample quality.

2.6.6.2 Bioanalyzer

A 2100 Bioanalyzer (Agilent) was used to assess quality and quantity of RNA samples employing both the RNA 6000 Nano kit (P/N 5067-1511) and the RNA 6000 Pico kit (P/N 5067-1513), following the manufacturers protocol. Samples

Chapter 2 Materials & Methods

were measured once each. Instrument generated RIN (RNA Integrity Number) values provided an estimate of sample quality.

2.6.6.3 Qubit

A Qubit 2.0 Fluorometer (Invitrogen) and RNA Broad Range (BR) Assay kit (Invitrogen P/N Q10210) was employed as an additional quantity metric comparison. A 1:200 working solution of Quant-iT reagent was prepared with RNA BR Buffer. The high and low standards provided in the kit were prepared by a 1:20 dilution using the working solution. RNA samples were prepared in a similar manner to the standards, before incubation in the dark for 2 min. Triplicate readings per sample were measured on the Fluorometer.

2.6.6.4 Alu PCR

The *Alu* assay was utilised for the detection of gDNA contamination of cell line-derived RNA pre- and post-DNase treatment, plus post RT. In addition, total RNA concentration as estimated by *Alu* PCR may be used for normalisation [130]. DNase untreated, DNase treated and post RT was analysed for neat SaOS-2 sample triplicates only (post RT samples were performed using RT triplicates). All other samples analysed post DNase only. RTs for *Alu* PCR analysis were performed using the Taqman Reverse Transcription Kit and 100 ng/ μ L SaOS-2 (neat lysate) RNA post DNase treatment. Twenty-five μ L reactions were prepared and analysed as outlined in **2.4.1 Two-step RT-qPCR**.

Alu PCR was performed using EvaGreen chemistry (not hydrolysis probe), due to universality of *Alu* sequence [130]. Ten μ L reactions consisted of 2 \times Fast EvaGreen Master Mix, 10 \times ROX, 250 nM (final concentration) of each forward and reverse primer (**9.1 Appendix 1 – Assay Information**) and 2 μ L RNA at 10 ng/ μ L, on a randomised 96-well plate format. Samples were measured in triplicate. A six point standard curve of human female gDNA was used with 10-fold dilutions starting at

10 ng/ μ L. Reaction conditions: 95°C for 2 min, 45 cycles of 95°C for 15 s and 60°C for 60 s.

2.7 Experimental Details - Sample Source and Type

Samples were spiked pre-extraction with synthetic-only transcriptomic calibration material (sTCM), to obtain an estimated 1.0E+06 copies/ μ L of each ERCC target in the resulting total RNA post extraction.

2.7.1 2D Culture Model – SaOS-2 Mineralisation

Two different passages of SaOS-2 cells (p33 and p36) were subcultured and propagated as per manufacturer's instructions (**2.1.2 Cell Lines**). Cells were maintained at 37 °C, 5% CO₂ for three days. In total, 7× T25 flasks (Corning, Sigma P/N CL S430372) were prepared per passage: three replicate flasks per condition, treatment (differentiation) versus control, and an additional flask for each passage was prepared alongside the experimental flasks for cell enumeration, as previously. This was repeated twice to generate two time points: D1 (24 hrs) and D7 post-treatment. On reaching confluency, the time point was designated day 0 (D0) and 10 mL treatment media was added to the flasks. Differentiation media consisted of 98.8 mL propagation media, 1 mL of 0.2 M β -Glycerophosphate (Sigma P/N G9422, dissolved in dH₂O, Gibco P/N 15230-089), 100 mL of 50 mg/mL Ascorbic acid (Sigma P/N A4544-25G, dissolved in dH₂O) and 100 mL of 10⁻³ M Dexamethasone (Sigma P/N D4902, dissolved in Ethanol, Fisher P/N E/0650DF/17). Control media consisted of propagation media and 1:1000 ethanol. All media was filtered through a sterile 0.2-micron filter (Corning P/N 431229) and incubated at 37°C before use. Treatment media was renewed on the cells after 24 hrs. Cells were maintained at 37 °C, 5% CO₂ until D1 or D7 following onset of differentiation. On D1 and D7, cells were rinsed and collected in 2.5 mL TRIzol lysis buffer, as described in **2.2.2 Cell Line RNA Production for Complex Background**. 2.5 mL lysates were stored at -80°C as 2× 1 mL aliquots.

2.7.2 3D Co-Culture Model

Dr Cleo Bonnet (Cardiff University) performed all work preceding total RNA extraction.

2.7.2.1 Cell Lines

MLO-Y4 osteocyte-like cells were kindly donated by Prof. Lynda Bonewald (University of Missouri, USA) to Dr Deborah Mason's group, part of the pathophysiology and repair division at Cardiff University. These cells have been shown to behave like primary osteocytes as they express high amounts of osteocalcin (OCN), low amounts of alkaline phosphatase (ALP) and type I collagen protein (Col1) and they have complex cytoplasmic processes expressing CD44, CX43 and ONP [232].

MLO-Y4 cells were grown (until 70-80% confluent) in alpha-MEM (Life Technologies P/N 22561-021) supplemented with 100 U/mL penicillin (PenStrep combined, Life Technologies P/N 15140-122), 100 µg/mL streptomycin, 2.5% heat inactivated fetal bovine serum (HIFBS, Life Technologies P/N 10270-106) and 2.5% heat inactivated newborn calf serum (HINBCS, Life Technologies P/N 26010074). Heat inactivation was performed following Cambrex company protocol. Bottles of sera were thawed in a water bath at 56°C for 30 min before use.

SaOS-2 cells were grown in DMEM GlutaMAX™ (Life Technologies P/N 31966-021) supplemented with 100 U/mL penicillin, 100 µg/mL streptomycin and 5% dialysed FBS (DFBS, Sera Laboratories P/N EU-000-HD) until 100% confluent.

2.7.2.2 3D Collagen Co-Cultures

Rat tail tendon type 1 collagen (2.5 mg/mL in 7 mM glacial acetic acid, Sigma P/N C3867) was mixed on ice in a 4:1 ratio with 5× MEM containing 11 g/L sodium

bicarbonate (NaHCO_3 , Sigma, S-6297) and neutralised to pH 7.4 with 1 M Tris (hydroxymethyl)aminomethane (Tris) base (pH 11.5, Sigma P/N T1378) to give a 2 mg/mL collagen solution. MLO-Y4 cells ($1.5\text{E}+06$ cells/mL gel) were diluted in their alpha MEM medium (less than 10% of the total gel volume) and mixed thoroughly into the collagen solution on ice. The collagen-cell mix was dispensed into wells in silicone plates (250 μL /well), which had been previously coated overnight with the Sigma collagen and incubated at 37°C in 5% CO_2 for 1 hr for polymerisation. Each well in the silicone plates has the same dimensions as a standard 48-well plate. Eight hundred μL of DMEM GlutaMAX medium was added on top of the gels before incubation overnight at 37°C in 5% CO_2 . Media was removed the next day and SaOS-2 cells ($1.0\text{E}+05$ cells/well) were layered on top of the collagen gels in DMEM GlutaMAX medium (**Figure 2.2**). Co-cultures were incubated for 5 days prior to loading and subsequent termination. Media was changed every 2-3 days. Three gels were prepared per plate, with one plate per condition: loaded and control. The experiment was repeated three times on different days with cells of different passage.

2.7.2.3 Mechanical Loading of 3D Co-cultures

Preparation and validation of the mechanical loading system and software, including the silicon plate, was prepared and described previously by Vazquez *et al.* [233,234].

On D5 of incubation the media was replaced (DMEM GlutaMAX) 1 hr before loading. The silicone plate for loading was attached to a BOSE EletroForce® loading instrument by a custom-made device in order to stretch the plate on one side only causing cyclic compression and tension forces at the same time but in perpendicular directions in all wells. A 250 N load cell was used to apply a loading regime of 5 min, 10 Hz, 2.5 N to the 3D collagen co-cultures. Mechanical loading of cultures in the silicone plate was performed using a BOSE ElectroForceController Software® 3200 instrument (Kent, UK) and controlled

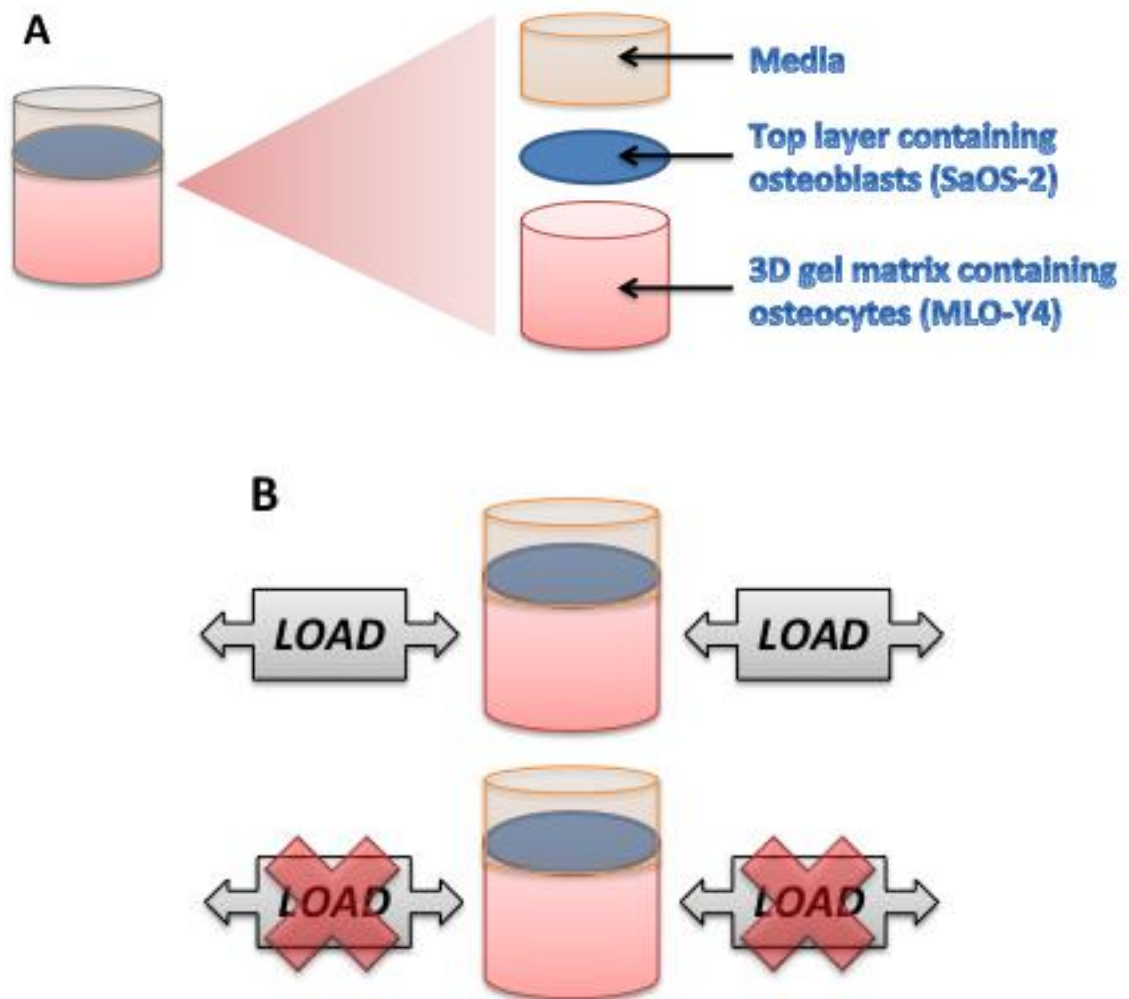


Figure 2.2 Schematic representation of 3D gel co-cultures. (A) Each well contained a 3D collagen gel matrix seeded with MLO-Y4 cells (osteocytes). A surface layer of SaOS-2 cells (osteoblasts) was seeded on top of the 3D matrix. The 3D co-culture was topped with the appropriate media. (B) An illustration of the mechanical loading experiments, with the inclusion of a control plate that was not loaded. A 250 N load cell was used to apply an osteogenic loading regime of 5 min, 10 Hz, 2.5 N to the 3D co-cultures, generating cyclic compression and tension forces at the same time but in perpendicular directions in all wells.

with WinTest® Software 4.1 with TuneIQ control optimisation (BOSE) [233,234]. The control plate was left on the bench next to the loading machine during loading of the test plate. Both silicone plates were returned to the incubator for 4 hrs prior to TRIzol treatment.

2.7.2.4 TRIzol Treatment of 3D Co-cultures

To retrieve the SaOS-2 osteoblastic layer of cells from the 3D gel matrix, the media was removed and 800 µL TRIzol was added to the top of each gel for 10 seconds before transferring to a 1.5 mL Eppendorf. MLO-Y4 cells in the gel were treated with 1 mL of TRIzol until the gel dissolved before transferring to a 1.5 mL Eppendorf (if required for future work). Samples were stored at -80°C. SaOS-2 cell lysates were extracted and DNase treated as described in **2.2.2 Cell Line RNA Production for Complex Background**. RNA pellets were resuspended in 40 µL nuclease-free water.

2.7.3 Clinical Samples – Total Knee Replacement Bone Cores

Clinical samples were collected by the Arthritis Research UK Biomechanics and Bioengineering Centre (Andrea Longman, Helen Roberts, Deborah Mason, Cleo Bonnet) and surgeons (Rhys Williams, Chris Wilson and Sanjeev Argawal) under their ethical approval (Research Ethics Committee for Wales, reference number 10/MRE09/28). Surgical staff collected bone cores during total knee replacement (TKR) surgery from five female patients aged between 44 and 75 years (one patient had a bilateral TKR and so samples were obtained from both the right and left knees, giving six 'patient' samples in total). These samples were used to compare positional mRNA profiles. Each patient set consisted of TKR cores collected in theatre using bone biopsy needles from four different positions, 1 cm below the tibial plateau (**Figure 2.3**). Samples were maintained in RNAlater (Sigma P/N R0901) on dry ice during surgery and stored at -80°C. Samples required thawing to remove excess RNAlater before being frozen on dry ice and subjected to the standard dismembration protocol.

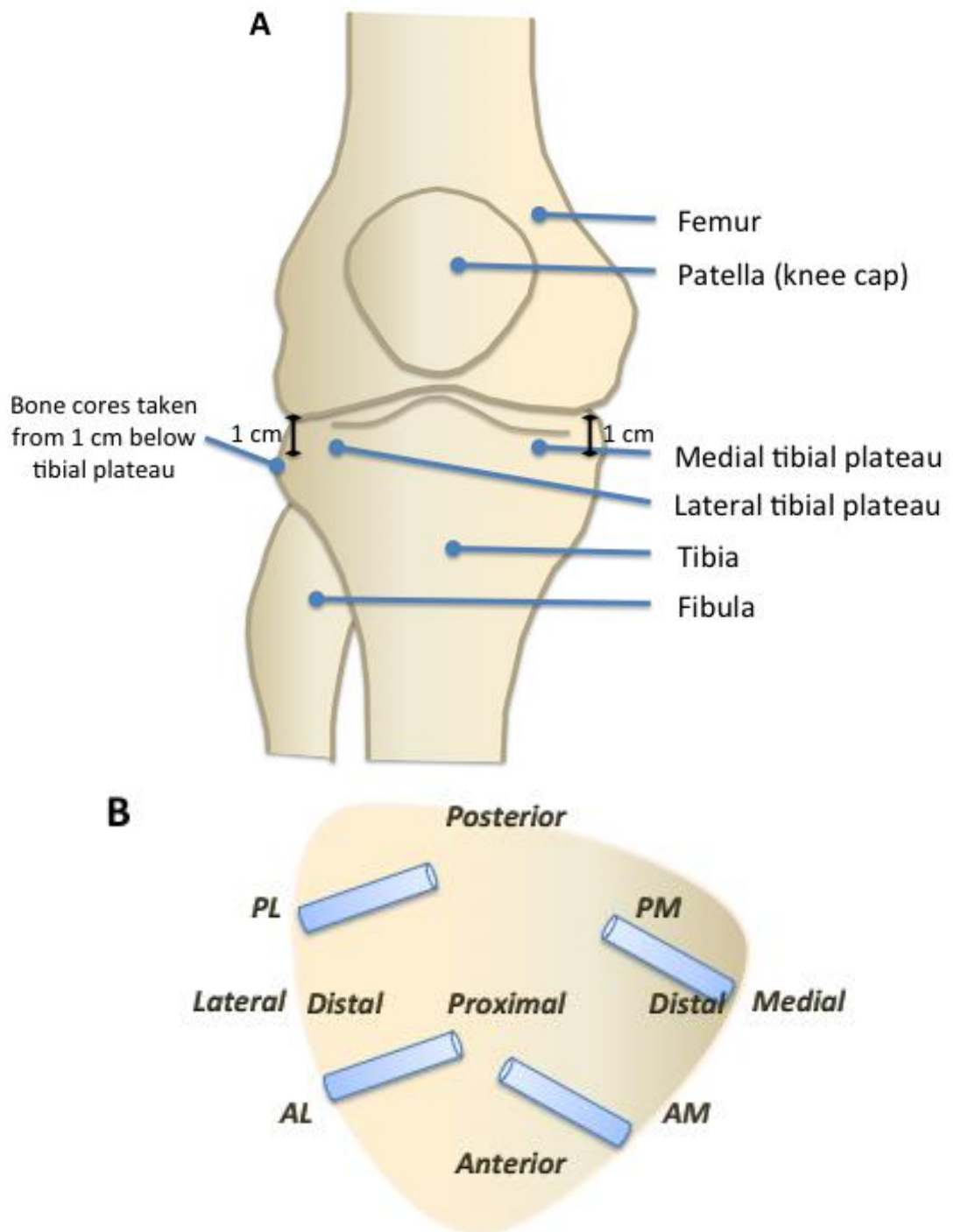


Figure 2.3 Positional schematic of clinical sample regions. (A) Schematic representation of the human knee. (B) Positional schematic of sample sites from the tibial plateau. The four sample sites (blue cores) for each patient included anterior medial (AM), posterior medial (PM), anterior lateral (AL) and posterior lateral (PL). Anterior: toward the front of the body. Posterior: toward the back of the body. Medial: a structure toward the midline of the body. Lateral: away from that median plane.

2.7.3.1 Dismembrator

It is notoriously difficult to extract nucleic acids from bone material, and special protocols are required [194,201-203]. Clinical bone cores were disrupted using a dismembrator before storage in TRIzol, ready for total RNA extraction.

Unprocessed samples were maintained on dry ice. A steel-shaking flask with matching grinding ball were cleaned using 1 M sodium hydroxide (Fisher P/N S14920160) and rinsed with molecular grade water (Sigma P/N W4502) before use. The shaking flask and grinding ball were pre-cooled in liquid nitrogen. An individual bone core sample was placed in the bottom half of the shaking flask with the grinding ball and immediately immersed (alongside the flask top) in liquid nitrogen. After allowing the sample to freeze for 5-10 s, everything was removed from the liquid nitrogen and 600 μ L of TRIzol was added on top of the sample. The shaking flask was sealed and the sample homogenised using a Mikro-Dimembrator-U, B.Braun (Biotech International) at 200 rpm for 2 min. Sample appearance is powdery until melted, so to aid sample collection 400 μ L of TRIzol was added before transferring the whole volume (1 mL) into a fresh Eppendorf. Samples were maintained on dry ice until all samples were processed. Between samples, the shaking flask and grinding ball were rinsed in water, and cleaned first with 1 M sodium hydroxide followed by absolute ethanol. Lysates were stored at -80°C.

Samples were spiked with sTCM pre-extraction and processed using the TRIzol protocol and DNase treated, as described in **2.2.2 Cell Line RNA Production for Complex Background**. Total RNA was resuspended in 50 μ L nuclease-free water.

2.7.4 Quality Metrics

As described in **2.6.6 RNA Quality Metrics**, all DNase treated samples for both the 3D gel co-culture model and clinical bone cores were subjected to Nanodrop and Bioanalyzer assessment, plus evaluation by *Alu* PCR. All samples were analysed

using the *Alu* assay in triplicate against a six-point, ten-fold, human gDNA standard curve, starting at 10 ng/ μ L (also in triplicate).

2.7.5 Dynamic Array

Fluidigm Biomark Dynamic 48.48 Arrays (P/N BMK-M-48.48) were utilised for the high throughput analysis of both clinical bone core and 3D gel co-culture samples. This enabled an assessment of all samples with 27 different assays. Details of the assays analysed in this experiment are given in **9.1 Appendix 1 - Assay Information**.

Due to the low volume capacity (9 nL), and therefore reduced physical sensitivity of the dynamic array partitions, it is recommended by the manufacturer to perform a preamplification reaction prior to analysis on the dynamic array. This ensures that even minority targets are in sufficient abundance for analysis and detection. As a result of this additional step, RT-qPCR reactions on the dynamic array are performed in a three-step process: RT; preamplification; qPCR. Twenty ng/ μ L of RNA was used in each RT reaction. Six out of the 42 samples had concentrations lower than 20 ng/ μ L and so were used in the RT reaction neat. Triplicate RTs per sample were performed as described previously in **2.4.1 Two-step RT-qPCR**. Alongside the samples, triplicate RTs were also performed for the Calibrant unit. The Calibrant standard curve consisted of four points in 10-fold, RNA serial dilutions.

2.7.5.1 Preamplification

Preamplification (Taq amplification based on 14 cycle PCR) was performed using TaqMan PreAmp master mix (ABI P/N 4391128). All 27 assays were combined in equal volumes to generate a final concentration of 0.2 \times for each gene expression assay. A separate preamplification reaction was performed for each of the triplicate RTs. Ten μ L reactions consisted of 2 \times TaqMan PreAmp master mix, pooled assay mix (final concentration 0.2 \times , each assay) and cDNA (final

Chapter 2 Materials & Methods

concentration 10 ng/ μ L). Reaction conditions: 95°C for 10 min, 14 cycles of 95°C for 15 s and 60°C for 4 min. Preamplified products were stored at -20°C. Before proceeding further, all preamplified products were diluted 1:5 using TE, as per manufacturer's protocol.

2.7.5.2 Dynamic Array Analysis

Fluidigm Dynamic Arrays are performed much like Fluidigm Digital Arrays except that the assay and sample components are prepared separately. Five μ L assay mix comprises 20 \times forward and reverse primers and probe mix, plus 2 \times DA assay loading reagent (Fluidigm, Biomark GE 48.48 Dynamic Array Sample and Loading Reagent Kit P/N 85000800). Five μ L sample mix comprises 2 \times TaqMan Universal master mix, 12.5 \times GE sample loading reagent and 2 μ L pre-amplified product. Both assay and sample mixes were prepared in excess and 10 μ L was subsequently loaded into corresponding inlets on the dynamic array chip (**Figure 2.1B**). Three replicate Dynamic Array chips were analysed, one for each of the RT replicates per sample. ERCC assays were performed as single replicates; all other assays were performed in duplicate. Each sample, including the Calibrant dilutions were performed as single replicates per chip.

The Calibrant was also used to test the linearity of the preamplification reaction. Six point curves of 10-fold serial dilutions were prepared for both preamplified and non preamplified Calibrant. These were analysed in replicates of four using the same assays as above.

Chapter 3

Production & Validation of Novel Transcriptomic Calibration Material

3 Production & Validation of Novel Transcriptomic Calibration Material

3.1 Introduction

Accurate normalisation of mRNA level is an absolute prerequisite for reliable results, especially when the biological significance of subtle differences in mRNA levels is studied [7,235]. As detailed in the introduction to this thesis, there are several strategies employed for the normalisation of RT-qPCR data; the most frequently employed of which is the measurement of internal reference genes. While the best approach maybe to use multiple validated internal reference genes [86], to enable meaningful data comparisons, internal RNA control genes must show constitutive, stable expression across all control groups [236].

Normalisation to externally spiked RNA controls offers an alternative to endogenous reference genes [236-239]. This approach allows normalisation of mRNA level data without the assumption of stably expressed endogenous reference genes [236]. As discussed in the introduction to this thesis, such external controls should be spiked into test samples so that any inhibitory matrix effects for example, are also conferred to the control RNA measurement, otherwise, a difference in such conditions may limit the effectiveness of this strategy.

Indeed, several studies have concluded that external RNA controls are suitable for normalisation of RT-qPCR data [235,236,238,240,241] and that they are able to compensate for inadequate internal RNA reference genes, which may in fact increase the variability associated with the measurement result. Such variation adds to the already complex multiple sources of variation attributed to biology and technology [235,237-239]. Normalisation using external RNA controls should allow for comparisons of mRNA levels across different stages of development [242] and across different types of tissues [236]. Furthermore, the reliability and

impact of external RNA controls would be further strengthened by using multiple external RNA control genes and analysing them using geNorm [236,238,243].

The focus of this thesis is to deconstruct the factors contributing to RNA measurement variability. For that purpose, initial studies detailed in this chapter concentrated on the development of a pilot TCM. The aim of this chapter was to produce in large quantities, highly characterise and validate the TCM, before use in experimental assessment throughout the tenure of this project. It was decided that this TCM should contain both synthetic and endogenous RNA species. The synthetic targets allowed evaluation of absolute quantification and supplied an opportunity to manipulate measurement ratios to challenge methodological sensitivities. The synthetic component also provided an opportunity for exogenous target spikes to monitor and normalise all sample types measured. The endogenous targets provided the opportunity for measurement of biological variability and assessment of normalisation strategies.

3.2 Material & Methods

All cell culture of Hep-G2, Hs 683 and SaOS-2 cell lines, up to and including lysate collection, was performed by Dr Gary Morley and Dr Sabhi Rahman, LGC, Teddington. Culture details are described in **2.1.2 Cell Lines** and **2.2.2 Cell Line RNA Production for Complex Background**. Statistical analysis was performed in collaboration with Dr. Simon Cowen, Dr. Steve Ellison and Dr. Jesus Minguez, Statisticians, LGC, Teddington.

For successful generation of a suitable calibration material, quality control assessments were performed at relevant stages in the preparation of the TCM.

3.2.1 DNA Contamination Assessment

ERCC RNA transcript samples were evaluated for plasmid DNA contamination as DNase treatment is not 100% efficient and residual DNA content would give false positive results. For this purpose, all eight ERCC RNA samples were serially diluted 10-fold (from 5E+08 to 5E+03) and the RT-step prior to qPCR excluded, ensuring any signal generated should be attributable to contaminating residual plasmid DNA (**2.4.1 Two-step RT-qPCR**).

Similarly, cell line RNA extracts were tested by qPCR for residual gDNA content following rDNase I treatment. The *Alu* assay was employed for this purpose due to the high prevalence of conserved *Alu* sequence repeats within 3' UTRs. *Alu* expression was compared in all three cell lines, before and after rDNase I treatment, and when performing standard 50 μ L as well as larger volume rDNase I reaction volumes (used to accommodate complete lysate extraction in one reaction, while maintaining manufacturers recommended total nucleic acid concentration of 200 ng/ μ L. Sample volumes treated: SaOS-2 182 μ L, Hs 683 452 μ L and Hep-G2 2510 μ L). Twenty ng RNA for each cell line and treatment were measured in triplicate by qPCR. A standard dilution series of human gDNA was additionally assessed, also in triplicate. Due to the frequency of *Alu* sequence motifs, it is usual to expect *Alu*-specific positive amplification in NTC samples [244]. Low-level *Alu* contamination permeates most reagents. As such, positive amplification observed in target samples at the same concentration (C_q) as in NTC replicates can be considered background contamination, not attributable to gDNA carryover [244]. Amplification of *Alu* sequences in target samples truly resulting from inefficient DNase treatment will be distinguished by a left shift in C_q , i.e., higher concentration. Such differences in this study are defined by at least a three times standard deviation shift in C_q to be considered different. Less than this and the value falls within the 99% level of confidence and so is not significantly different. NTC samples were analysed in replicates of six.

3.2.2 Assay Cross-Reactivity with Human Targets

Since the TCM for assessment in this project will comprise both ERCC RNA transcripts and human cell line-derived RNA (as disease models and sources of endogenous reference genes and GOI), all eight ERCC assays were tested for potential cross-reactivity with human samples (**2.4.1 Two-step RT-qPCR**).

3.2.3 Carrier Optimisation

DNA and RNA carriers at different concentrations, as well as no carrier, were tested for influence on one-step RT-qPCR efficiency and precision. It is important that such carriers have no sequence similarity with ERCC RNA transcripts or endogenous targets to prevent false positive results attributable to the carrier. The carriers evaluated in this experiment were shown by BLAST analysis to have no sequence homology with ERCC RNA transcripts or endogenous targets. Ten-fold serial dilutions of ERCC-13 RNA, from 5E+08 to 5E+04 copies/reaction, were analysed in triplicate for each carrier condition. A second experiment was additionally performed to further define variability between DNA carrier (sonicated salmon sperm DNA) and RNA carrier (total yeast RNA), when analysing both DNA (plasmid) and RNA (IVT) samples (**2.1.2.1 Carrier Options** and **2.4.1 Two-step RT-qPCR**).

3.2.4 RNA Stability Analysis

To evaluate the effect of storage on both lysate and extracted RNA on the qPCR result, lysate was collected from one T-175 flask of Hep-G2 cells and 12 identical aliquots made. The 12 lysate aliquots were split into three groups of four aliquots and total RNA extracted at monthly intervals; time (T)=0, T=1, T=2 (**2.2.2 Cell Line RNA Production for Complex Background**). Lysates and/or total RNA were stored at -80°C between experiments. Standard quality metrics for quality and quantity were performed for each time point. Total RNA extracts were also assessed by two-step RT-qPCR (RT: oligo d(T)₁₆ priming) at the point of extraction

and at monthly intervals until the end of the three month time course (**2.4.1 Two-step RT-qPCR**). Human universal reference RNA (Ambion) was used as a positive control/calibrant in combination with GAPDH assay-on-demand.

3.2.5 RT Variability

In line with current consensus, an experimental demonstration of RT variability was undertaken. A test of linearity for RNA dilutions versus cDNA dilutions at the RT stage of RT-qPCR was performed by two-step RT-qPCR (**2.4.1 Two-step RT-qPCR**).

3.2.6 Endogenous Target Selection

A panel of 32 control genes were evaluated as candidates for endogenous reference genes shared between the three cell lines (**2.3.1.1 Reference Genes**. See **Appendix 1 - Assay Information** for assay details). Following selection of reference genes, 29 potential GOI were evaluated for suitability across the three cell lines (**2.3.1.2 Genes of Interest**. See **Appendix 1 - Assay Information** for assay details).

3.2.7 Transcriptomic Calibration Material Homogeneity and Stability

The TCM was generated by mixing RNA extracted from Hep-G2, SaOS-2 and Hs 683 cell lines, following the protocol outlined in **2.3 Preparation of Transcriptomic Calibration Material (TCM)**. The TCM has been produced as a prototype reference material for molecular measurements, and the way it has been generated was guided by this ultimate purpose. For this reason, the unit types Unknown 1 and Unknown 2 are referred to as 'Unknown' materials, despite the fact that their composition is known to us (as we produced them). Their intended use would include distributing to laboratories to participate in a trial whereby values are assigned to the named targets in Unknown 1 and Unknown 2 through calibration curve-based assessments (using the Calibrant unit type) or fold change

measurements between the two Unknowns. Completion of this type of study helps to determine measurement capabilities (and validate measurement claims) of the participating laboratories.

TCM sample homogeneity (uniform composition) was evaluated using ten randomly selected aliquots of each unit type, Calibrant, Unknown 1 and Unknown 2 (**2.3 Preparation of Transcriptomic Calibration Material (TCM)**), measured in replicates of eight. One randomised 96 well plate was prepared for each sample (Calibrant, Unknown 1 or Unknown 2) and each assay. Each plate included an RNA standard curve (serially diluted 1:10 from 1.0E+06 to 1.0E+01 copies/ μ L in carrier), plus three no template controls (NTCs). RT-qPCR experiments were performed according to one-step conditions, with inclusion of yeast total RNA carrier (**2.4.2 One-step RT-qPCR**). ERCC-99 and HPRT1 assays were employed as representative of both external and endogenous target populations (**2.3 Preparation of Transcriptomic Calibration Material (TCM)**).

A short-term stability study was undertaken at a range of temperatures to establish the effect of storage time on RNA stability. For each Calibrant, Unknown 1 and Unknown 2 solution, three replicate units were isochronously tested at -80 °C, on dry ice, +4 °C, and +40°C and at time (T) = 0, 7 and 14 days. One-step RT-qPCR was performed (**2.4.2 One-step RT-qPCR**) and the ERCC-99 and HPRT1 C_q values for a particular unit type at the different temperatures and time-points were compared. A longer-term stability study was also performed. For each Calibrant, Unknown 1 and Unknown 2, three replicate units were incubated for one week on dry ice (to simulate a shipping period) before being transferred to either -80°C or -20°C (designated T = 0). Measurements of ERCC-99 and HPRT1 were made at T = 0 and 6 months.

3.3 Results & Discussion

3.3.1 ERCC IVT RNA Quality Control

Following plasmid sample digestion and IVT of ERCC RNA, transcript sizes, concentration and integrity were assessed. ERCC sample concentrations and copy number equivalents estimated by UV A₂₆₀ assessment ranged from approximately 300 to 1000 ng/μL, equating to 9.3E+08 to 3.7E+09 copies/μL in 1 ng/μL preparations (**Table 3.1**). Samples were additionally evaluated for integrity by capillary electrophoresis (**Figure 3.1**). Initial analysis confirmed correct transcript sizes with additional banding patterns (**Figure 3.1A**). Heat denaturation at 70°C removed the excess banding patterns from the transcript profiles (**Figure 3.1B**), with minimal band smearing.

The eradication of superfluous banding when heat-treating ERCC RNA transcripts prior to integrity assessment suggests that the banding observed on the original profile was caused by insufficient denaturation of RNA secondary structure, rather than concatemerisation. The profile of the heat denatured transcripts presented clear bands at the expected sizes, without significant smearing (which may otherwise indicate sample degradation). Additional banding present in **Figure 3.1B** suggests some secondary structures remain intact, despite heat denaturation. No instrument-derived RIN values were generated associated with ERCC RNA transcript analysis due to the lack of 18S and 28S rRNA eukaryotic markers.

3.3.1.1 Assay Validation

Several experiments were performed to validate the qPCR ERCC assay conditions and sample purity. Individual assays were assessed for efficiency and intermediate precision by one-step RT-qPCR, and all, except ERCC-95, were shown to be fit for purpose (based on efficiency and intermediate precision, where replicates were performed on a different day by the same analyst (**Table 3.2**). See also **1.1.2 Accuracy and Measurement Uncertainty**). ERCC-95 was therefore no

Chapter 3 Production & Validation of Novel Transcriptomic Calibration Material

Table 3.1 IVT ERCC RNA standards. Concentration and copy number equivalents following initial preparation.

ERCC-	Concentration (ng/ μ L)	Length with poly(A) tail (bases)	Mw	IVT RNA copies/ μ L	1 ng/ μ L equiv to: (copies/ μ L)
13	318	808	264188	7.26E+11	2.28E+09
25	491	1994	647955	4.56E+11	9.29E+08
42	402	1023	330495	7.33E+11	1.82E+09
84	995	994	323987	1.85E+12	1.86E+09
95	551	521	168589	1.97E+12	3.57E+09
99	299	1350	439632	4.10E+11	1.37E+09
113	958	843	274225	2.10E+12	2.20E+09
171	394	505	164604	1.44E+12	3.66E+09

Mw: molecular weight, equiv: equivalent.

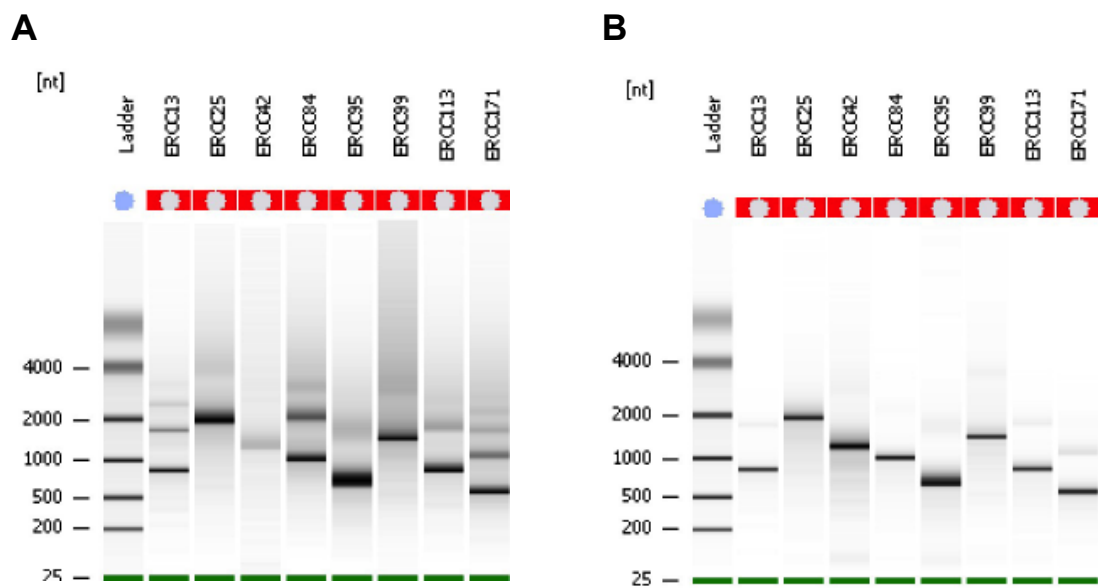


Figure 3.1 Quality control of ERCC IVT RNA. Analysis of IVT transcript sizes was performed using an Agilent 2100 Bioanalyzer. (A) RNA transcripts following RNeasy purification. (B) The same RNA transcript samples following heat-induced denaturation revealed additional bands were attributable to secondary structure motifs in the non-denatured RNA samples. 2100 Bioanalyzer quantification for all synthetic targets was comparable to nanodrop concentration estimates ($p = 0.660$, with an average fold change between the two measurements of 1.02, CV 11.5%).

Chapter 3 Production & Validation of Novel Transcriptomic Calibration Material

Table 3.2 ERCC Assay Efficiencies. Six point RNA standard curve from 5.0E+06 to 5.0E+01 copies/ μ L, triplicate measurements.

Target DNA	Average Efficiency (%) †	CV (%) †	Standard Error of the Mean †
ERCC-13	~109	0.46	0.08
ERCC-25	~104	0.60	0.10
ERCC-42	~102	0.72	0.11
ERCC-84	~99	0.23	0.04
ERCC-95	~140*	0.54	0.09
ERCC-99	~106	0.51	0.09
ERCC-113	~103	0.31	0.05
ERCC-171	~95	0.58	0.11

† As determined by average of three RT-qPCR reactions using the ABI 7900 platform. * An efficiency estimate of ~140% for this assay was criterion for exclusion of the associated target from the panel of standards to be prepared. Efficiency estimates were averaged over three experiments across three months and so this may explain the decrease in precision.

longer included in future studies. Based on our groups' extensive work in this field, acceptable intermediate precision for one-step RNA measurements is < 10%, and for DNA measurements is < 5%, provided > 1000 copies are being quantified. (The coefficients of variance, CV, of qPCR on the LightCycler instrument for DNA measurements have been shown to be approximately 2-5% [245]). Assays with PCR efficiency estimates between 90 and 110% were accepted for this study (**Table 3.2**).

3.3.1.2 Cell Line RNA Quality

Total RNA derived from each cell line was assessed for quality and quantity. Representative yields (pre- and post-DNase treatment) and cell counts per flask are summarised in **Table 3.3**. Hep-G2 lysates produced the highest total RNA yields per T-175 flask (722.25 µg) and SaOS-2 lysates yielded the lowest (46.71 µg; Hs 683: 170.52 µg). Following DNase treatment, these yield relationships were maintained: Hep-G2 645.52 µg/flask, Hs 683 142.36 µg/flask and SaOS-2 33.84 µg/flask (**Figure 3.3**). There was no significant difference observed between pre- and post-DNase yields for any of the three cell lines (all $p > 0.05$). Although cell counts per flask correlated with total RNA yields, the yields per cell also showed the same relationship with Hep-G2 cells yielding the most RNA and SaOS-2 cells yielding the least RNA. All three cell lines, regardless of treatment, produced good quality RNA as assessed by capillary electrophoresis and associated generation of RIN values, all being > 9.9. Additionally, all cell lines showed strong 18S and 28S ribosomal banding, without significant smearing (indicative of non-degraded total RNA; **Figure 3.4**).

The Hs 683 cells were comparatively large and generated a lower total RNA yield per T-175 flask following TRizol extraction than the other two cell lines. The smaller size of the Hep-G2 cells offered an increase in total cell count per T-175 flask and consequently the largest total RNA yield of the three cell lines following TRizol extraction. The SaOS-2 cells were the slowest growing and displayed by far

Chapter 3 Production & Validation of Novel Transcriptomic Calibration Material

Table 3.3 Cell line RNA quantity

Cell line	Estimated cell count per flask	Av. yield/flask pre-DNase (μg)	Av. yield/cell pre-DNase (pg)	% CV	Av. yield/flask post-DNase (μg)	Av. yield/cell post-DNase (pg)	% CV	RIN
Hep-G2	5.90E+07	722.25	12	29.95	645.52	11	31.15	9.9
Hs 683	2.60E+07	170.52	7	35.83	142.36	5	40.94	10
SaOS-2	1.83E+07	46.71	3	36.06	33.84	2	46.03	10

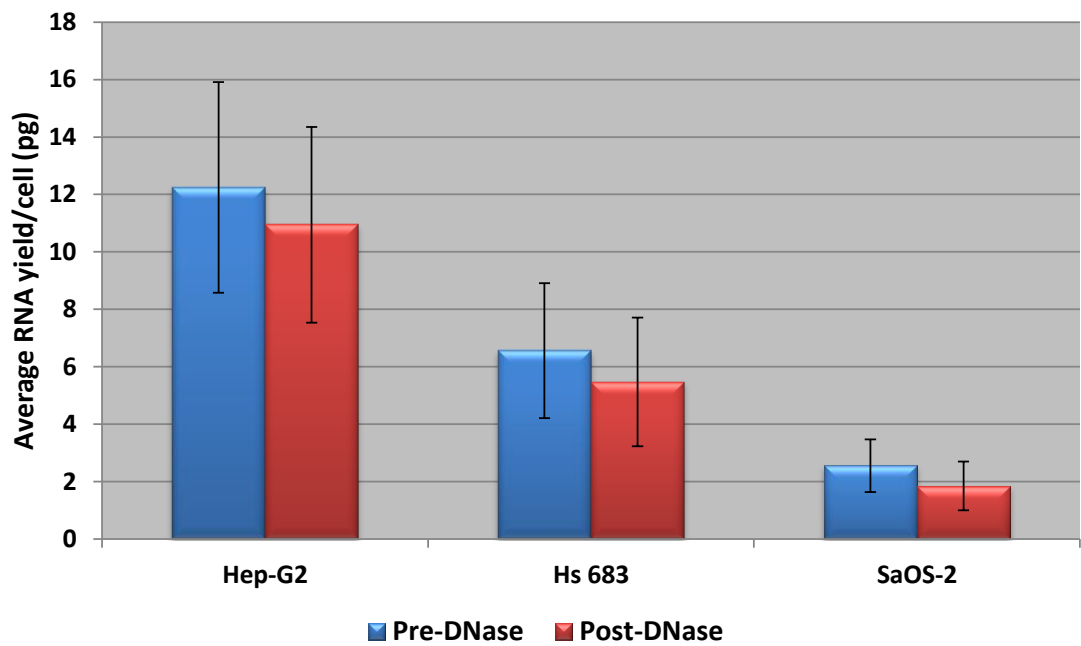


Figure 3.2 RNA yields pre- and post-DNase treatment. Total RNA yields were measured pre- and post-DNase treatment using UV A_{260} for the three cell lines, HepG2 (n = 8), Hs 683 (n = 14) and SaOS-2 (n = 11). The data have been normalised for cell count. Error bars: standard deviation.

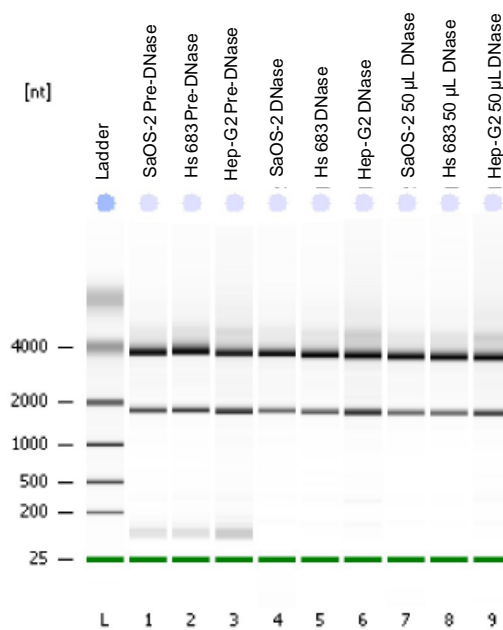


Figure 3.3 Quality control of cell line total RNA. Pre- and post-DNase treatment samples were compared. Analysis of ribosomal bands was performed using an Agilent 2100 Bioanalyzer. All cell lines show strong 18S and 28S ribosomal bands without significant smearing. Low molecular weight bands in lanes 1-3 may be attributable to low level degradation or the 5S precursor.

the lowest yields, despite attempts to extract all cell line flasks at approximately equal (manufacturer recommended) confluency.

3.3.2 DNA Contamination Assessment

Deoxyribonuclease (*DNase*) enzyme treatment of samples is used to degrade contaminating sources of DNA in RNA preparations. This aims to eliminate the possibility of DNA signals being detected in lieu of RNA signals in downstream applications that measure RNA. As with many enzymatic reactions, achievement of 100% efficiency is very difficult, if not impossible to achieve. Consequently, the purpose of this experiment is to examine the efficiency of the *DNase* reaction.

Positive amplification in the absence of RT was observed in ERCC RNA samples 13, 25, 84 and 171 with $5E+08$ and $5E+07$ copies/reaction, at high C_q values ($> 34-37$). ERCC RNA samples -42 and -95 displayed positive amplification for $5E+08$ copies/reaction only, ($C_q > 37$). No positive amplification at any concentration was observed in ERCC RNA samples 99 and 113. For those samples that showed amplification, ERCC-13, -25, -42, -84, -95 and -171, further dilution removed this signal suggesting that DNA contamination was never more than 1 in 5 million copies (diluted to $5E+07$ copies/reaction and below for ERCC-42 and -95, and to $5E+06$ copies/reaction and below for ERCC-13, -25, -84 and -171). Positive control samples (ERCC plasmid DNA at $5E+05$ copies/reaction) presented C_q values between 15 and 20, dependent on ERCC target/assay.

The presence of positive amplification in the RT-negative ERCC samples illustrated that the *DNase* treatment was not 100% efficient in the removal of contaminating plasmid DNA. Such DNA contamination may lead to an overestimation of the RNA A_{260} absorbance measurement [246] and may affect downstream applications. However, the detection of contaminating gDNA indicates the concentration at which the ERCC standards may be used to effectively determine RNA quantification without being obscured by residual gDNA contamination.

Nevertheless, the level of gDNA contamination remaining post-DNase treatment was low and for practical purposes, the efficiency of the DNase treatment was sufficient for downstream applications.

Other studies have also demonstrated the inefficiency of DNase treatment [47,245,247,248], and suggest a trade-off between the completeness of DNA digestion and the preservation of RNA integrity. In this reaction, RNA integrity may be affected by RNase contamination and the method of DNase inactivation [247]. Conversely, Horstmann *et al.*, when evaluating mRNA levels in bladder tissue using laser capture microdissection microscopy, RNA preamplification and qPCR, showed that inclusion of a DNase step both improved the integrity of RNA (observed through increased RIN values) and decreased the C_q values [249]. The observed increase in RIN values was probably because the removal of DNA increased the sample purity, which affects RIN estimation, rather than the DNase step affecting RNA integrity. The latter observation was most likely due to concentration of the sample through a purification procedure post-DNase treatment. Furthermore, due to the higher RIN values observed for the DNase treated samples, it is likely that the higher proportion of less degraded RNA lead to improved preamplification efficiency and thus a decrease in C_q [249].

These data highlight the need for this validation step and subsequently indicated the level at which RNA samples should be assessed for future experiments. In this case, ERCC RNA samples quantified at or below 5E+06 copies/reaction should allow data interpretation without the contribution of plasmid DNA contamination. Of course, it is possible that the DNase used for such experiments may influence the outcome and that different enzymes may exhibit different reaction efficiencies. In addition, the template type and matrix qualities may influence reaction efficiency.

The *Alu* PCR metric for estimating gDNA contamination in cell line derived RNA samples clearly demonstrated the efficacy of different treatments (**Figure 3.4**).

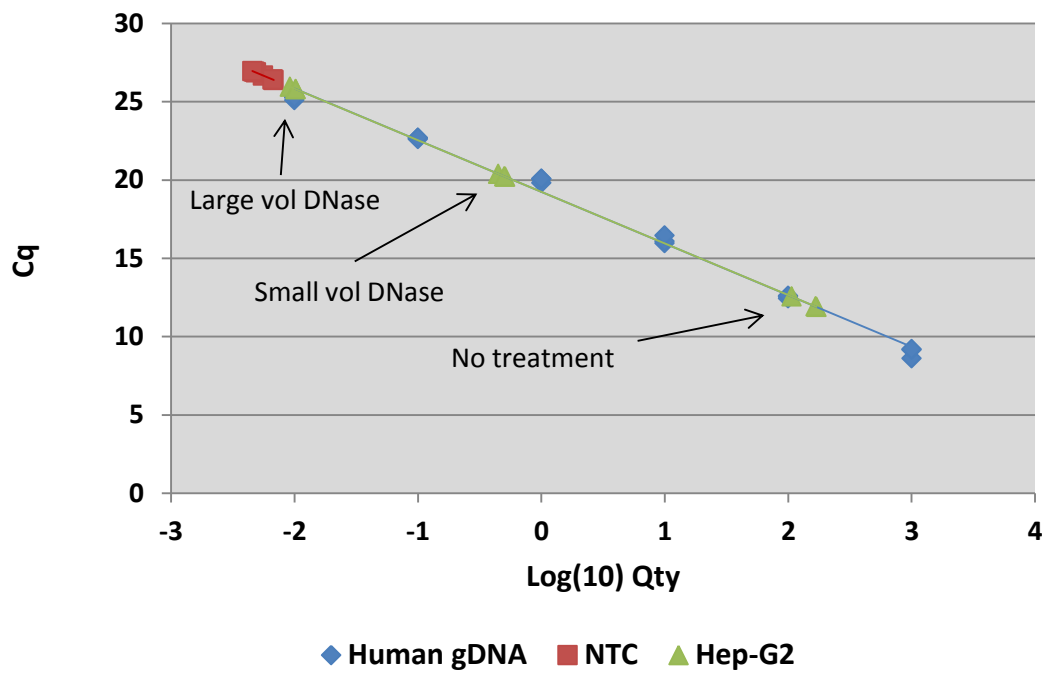


Figure 3.4 DNA Contamination Assessment. *Alu* PCR (no RT) evaluation of Hep-G2 derived RNA samples, with and without DNase treatment. This plot is representative of all three cell lines. Qty: quantity. Log(10) Qty is in pg/reaction.

Pre-treatment samples (no DNase) displayed positive amplification between 12 and 14.5 C_q for all cell lines. Treatment with rDNase I in 50 μL reactions resulted in an increase in C_q (average 5.5 C_q shift), which is indicative of an approximate 2-log reduction of gDNA. When larger volume rDNase I reactions were performed, there was an average increase of 10.6 C_q for all cell lines. This demonstrates that the larger volume reaction works better, with a higher DNase reaction efficiency. In the 50 μL DNase reactions, contaminating gDNA was reduced by 99.67, 91.18 and 96.84% in Hep-G2, Hs 683 and SaOS-2 RNA samples respectively. This is equivalent to 487, 3115 and 725 fg/reaction remaining gDNA contamination. In the larger volume DNase reactions (accommodating the complete lysate extraction in one reaction, while maintaining manufacturers recommended total nucleic acid concentration of 200 ng/ μL), contaminating gDNA was reduced by 99.99, 99.97 and 98.85% in Hep-G2, Hs 683 and SaOS-2 RNA samples respectively. This is equivalent to 10, 11 and 264 fg/reaction remaining gDNA contamination; that's a further reduction of 0.32, 8.79 and 2.01% in Hep-G2, Hs 683 and SaOS-2 RNA samples respectively. Even so, there was still gDNA present and so one should be cautious. Furthermore, these data suggest that the efficiency of the DNase reaction may be in part dependent on the cell line itself that the RNA is derived from. NTC replicates generated the highest C_q values and therefore lowest concentration (average 26.7 C_q).

These findings indicate that the *Alu* metric is suitable for measuring gDNA contamination and may therefore be used as a pre-screen for samples. The fact that *Alu* is a multicopy target gives added confidence to low-level contamination results as (gDNA contamination from) target genes are commonly single copy genes or indeed have a far lower repeated presence in the genome than the *Alu* element and as such would present at even lower concentrations than *Alu* contamination.

Despite the substantial decrease in contaminating gDNA following rDNase I treatment of cell line derived RNA (between 91 and 99%); these data show the

inefficiency of this process. gDNA *Alu* target continued to be detected at levels significantly higher than in background (NTC) samples (NTCs contribute approximately 5-6 fg/reaction of gDNA, whereas the best DNase result leaves approximately 10 fg/reaction of contaminating gDNA and the least efficient leaving approximately 3.1 pg/reaction). Signal in the NTC samples is indicative of gDNA contamination of the reagents.

Based on these data, it is advisable in mRNA studies to dilute RNA samples where possible before processing. Dilution of input RNA is one of the simplest and often effective solutions to alleviate the effects of reversible carryover reaction inhibitors [250]. The ratiometric DNA/RNA would stay the same but by diluting the background any contaminating gDNA should be undetectable. This may be variable by target and should be empirically assessed for each assay/sample type. However, concomitantly, rare mRNA targets may be diluted beyond the limit of detection and so target abundance should be considered before any dilution is undertaken.

Moreover, qPCR assays should be designed to specifically target mRNA transcripts (i.e., crossing exon-exon boundaries) and analysed *in silico* to determine specificity to the chosen target to the exclusion of similar target sequences, including processed pseudo genes [47,48,61,86,122,162,251,252]. These precautions will increase RNA quantification accuracy and so has been done for all assays presented in this chapter. However, when considering secondary structures, designing assays to cover exon-exon boundaries may add too many restrictions. If rigorous and controlled DNase treatment has been performed and the amount of DNA removal assessed, then these precautions may not be necessary. When assessing the abundance of a rare target in a complex background, these tests need to be more rigorous. It may be advisable where possible to design an assay within a loop structure, which is more open, and therefore more cDNA is produced. Large variation is expected for mRNAs with tight structures in which access to primer target sites is restricted [56].

3.3.3 Assay Cross-Reactivity with Human Targets

All eight ERCC assays were tested for potential cross-reactivity with human gDNA. None of the ERCC assays demonstrated positive amplification with 250 ng human gDNA (**2.4.1 Two-step RT-qPCR**). Positive amplification was however observed when ERCC plasmid DNA was assayed (positive controls), as above.

All eight ERCC assays were demonstrated not to exhibit cross-reactivity with human gDNA samples. This was expected following an initial BLAST search (<http://blast.ncbi.nlm.nih.gov/Blast.cgi>, accessed 2011) for ERCC RNA transcript and assay sequence homology to the human sequence database. These samples and assays are therefore suitable for production of mixed, complex units, as the synthetic ERCC targets/assays will not interact with the human RNA background material generated by mixing total RNA from human cell line sources.

3.3.4 Carrier Optimisation

Nucleic acids can stick to plastic and this can affect the concentration of a sample [253,254], particularly low abundance targets. As well as using LoBind® plastic ware the use of carrier solutions (for example, glycogen or nuclease-free tRNA) as diluents when preparing samples, which prevents low copy number molecules from sticking to the plastics, helps preserve integrity and produces greater precision of qPCR data where sensitivity is desired.

All carrier options (including no carrier) exhibited comparable precision (on average, 0.22 C_q standard deviation across all carrier options at all dilutions, n=3) for 5E+08 to 5E+04 copies/reaction (ERCC-13 RNA, 1:10 serial dilution, one-step RT-qPCR reaction) (**Table 3.4**). Similarly, the mean delta (Δ) C_q between subsequent dilutions for all experimental parameters was highly consistent at 3.48 with an average standard deviation of 0.16. A perfectly accurate dilution series would

Chapter 3 Production & Validation of Novel Transcriptomic Calibration Material

Table 3.4 Carrier optimisation. Average, standard deviation and dilution differentials (ΔC_q) of C_q values generated by one-step RT-qPCR for a dilution series of ERCC RNA with and without various carrier types.

		Target Quantity (copies/ μ L)					ΔC_q Mean	ΔC_q StdDev
		5.00E+08	5.00E+07	5.00E+06	5.00E+05	5.00E+04		
Salmon sperm 250 ng	C_q Mean	14.91	18.18	21.52	24.99	28.56	-	-
	C_q StdDev	0.10	0.13	0.21	0.24	0.10	-	-
	ΔC_q	-	3.28	3.34	3.47	3.57	3.41	0.13
Salmon sperm 50 ng	C_q Mean	15.00	18.41	21.62	24.93	28.72	-	-
	C_q StdDev	0.07	0.04	0.29	0.07	0.13	-	-
	ΔC_q	-	3.41	3.21	3.31	3.79	3.43	0.25
Yeast RNA 250 ng	C_q Mean	15.13	18.44	22.08	25.37	28.95	-	-
	C_q StdDev	0.15	0.10	0.04	0.06	0.06	-	-
	ΔC_q	-	3.31	3.65	3.29	3.58	3.46	0.18
Yeast RNA 50 ng	C_q Mean	14.92	18.34	21.82	25.39	28.68	-	-
	C_q StdDev	0.01	0.11	0.18	0.08	0.30	-	-
	ΔC_q	-	3.42	3.48	3.57	3.29	3.44	0.12
Hep-G2 RNA 50 ng	C_q Mean	14.39	18.10	21.44	25.19	28.72	-	-
	C_q StdDev	0.06	0.18	0.08	0.08	0.28	-	-
	ΔC_q	-	3.71	3.34	3.74	3.53	3.58	0.19
No carrier	C_q Mean	14.60	18.14	21.58	25.23	28.89	-	-
	C_q StdDev	0.05	0.13	0.09	0.06	0.15	-	-
	ΔC_q	-	3.54	3.44	3.64	3.67	3.57	0.10

generate ΔC_q values of 3.3 consistently. The difference in these results from the theoretically accurate ΔC_q values for dilutions maybe as a result of pipetting errors, calibration errors and/or inherent inefficiency of the actual system. There was no trend observed between sample concentration and ΔC_q . Two-factor ANOVA (carrier versus dilution) of C_q values revealed that carrier type had a significant impact on the C_q values generated ($p < 0.001$), with yeast total RNA at 250 ng/reaction showing the least variance in C_q values (average C_q variance across all dilutions = $8.06E-03$) and yeast RNA at 50 ng/reaction showing the most variance in C_q values (average C_q variance across all dilutions = $2.79E-02$). While dilution obviously significantly influenced C_q values ($p < 0.001$), there was also an interaction between carrier type and dilution terms ($p < 0.001$). While no carrier appears to have the least variance, this is only for the standard deviation of ΔC_q measurements across all dilutions (final column of **Table 3.4**, this just tells us that the dilutions are consistent), not for the standard deviation of C_q values between replicates (values in bold in **Table 3.4**). It should be noted that reagents themselves often contain carrier, which may go some way to explaining the consistency of results when comparing 'no-carrier' options.

When considering carrier type (250 ng total yeast RNA or 250ng salmon sperm DNA) with regards to sample type (RNA or DNA), almost all data were comparable (**Figure 3.5**). However, it was observed that when measuring low copy ($5E+01$) RNA target, reactions including RNA (yeast) carrier performed better than those including DNA (salmon sperm) carrier. ERCC RNA sample measured at 50 copies/reaction in DNA carrier generated amplification plots and quantification replicates with low precision (average ΔC_q 4.48, ΔC_q standard deviation 2.08, CV 47.5%), while some replicates failed to demonstrate amplification at all (**Figure 3.5A**). Quantification of the same target sample with RNA carrier remained highly consistent even down to 50 copies/reaction (C_q standard deviation was 0.35, at 50 copies/reaction), (**Figure 3.5B**).

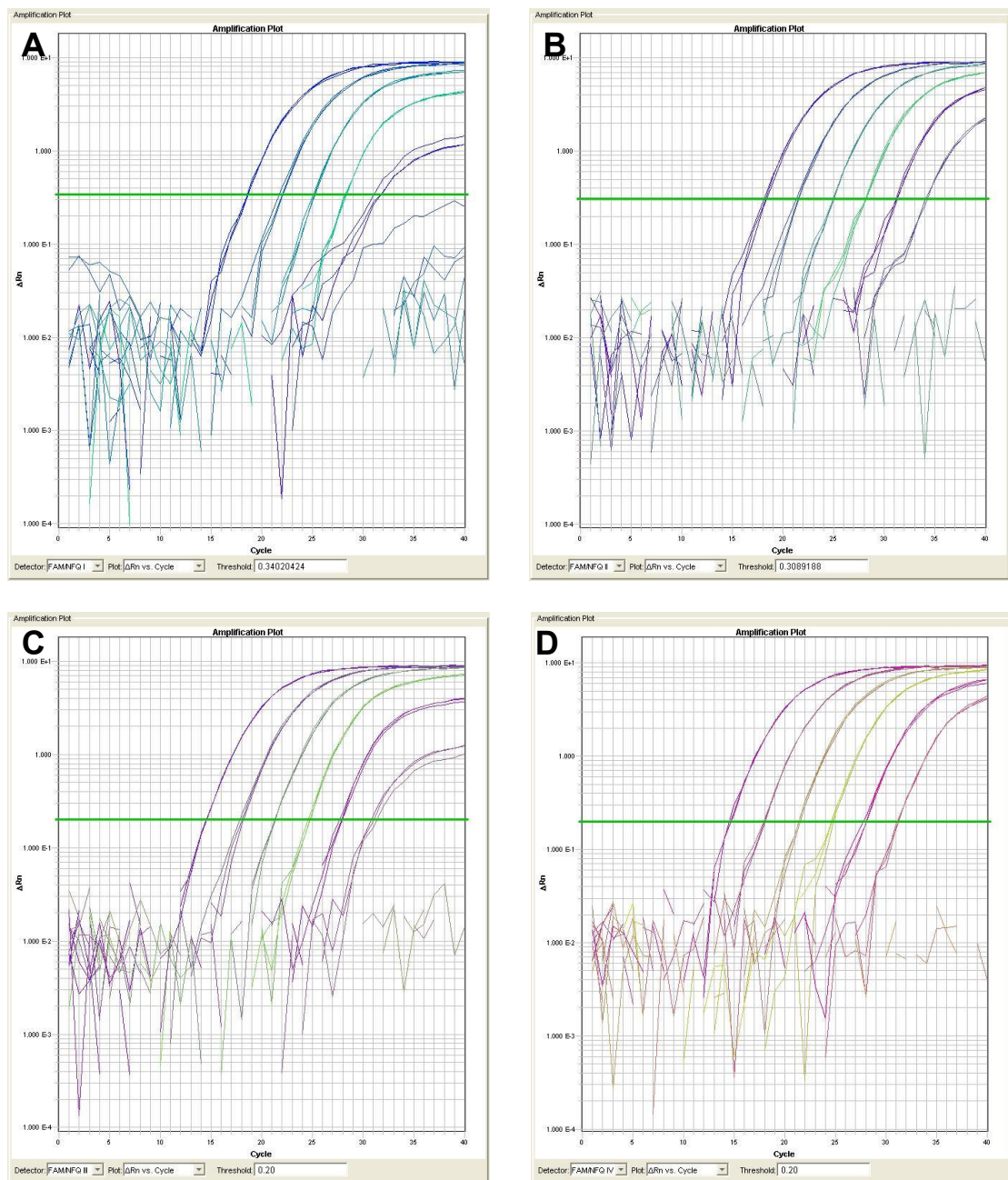


Figure 3.5 Carrier optimisation. ERCC-13 plasmid DNA and IVT RNA were serially diluted (1:10) to produce standard curves from $5E+06$ to $5E+01$ copies per one-step RT-qPCR reaction. Sample was analysed in the presence of 250 ng either total yeast RNA carrier or salmon sperm DNA carrier. (A) ERCC RNA, Salmon Sperm DNA Carrier, (B) ERCC RNA, Yeast Total RNA Carrier, (C) ERCC Plasmid DNA, Salmon Sperm DNA Carrier, and (D) ERCC Plasmid DNA, Yeast Total RNA Carrier.

To summarise the two carrier experiments, all carrier options tested, including no carrier, showed they were fit for purpose when analysing RNA samples between $5E+08$ and $5E+04$ copies/reaction (i.e. linearity of measurement, as demonstrated by ΔC_q consistency across dilution series). However, in a separate experiment when analysing low sample copy numbers (50 copies, **Figure 3.5**) in reactions containing 250 ng of either RNA or DNA carrier, samples that contained DNA carrier experienced increased variability and lower discriminatory power between copy numbers, while those that contained RNA carrier continued to perform well. These data suggest that carrier chosen to match sample type (RNA versus DNA) is preferable for precise quantity estimates, particularly at low target levels. It has been shown previously for DNA measurements that while the inclusion of carrier had no effect on estimated quantity, it did improve measurement precision [103]. Furthermore, the addition of transfer RNA (tRNA) has been shown to significantly increase the sensitivity of quantitative PCR, in part by delaying the appearance of primer artifacts [255] and eliminating, or at least reducing, adsorption artifacts in the sample matrix [56]. tRNA loosely binds through hydrogen bonds to excess primer that is available during the early cycles of the amplification process and thus reduces the possibility of self-priming [255].

The measurements obtained for these carrier experiments were highly precise with small variance, which is why there will always be some significant differences found. In reality, there are no real differences between carrier options. These differences translate to 6.4% difference in efficiency, which in our hands makes no difference. Reagents will most likely contain carrier material, which is one reason why experiments with no added carrier behave so well. By adding a carrier the amount of RNA included in the reaction is normalised, and it is known how much has been added. It is preferable to add RNA carrier because the template type is the same as the templates measured. Therefore, in order to match RNA template utilised throughout this study, yeast total RNA carrier was included in future experiments at 250 ng.

3.3.5 RNA Stability Analysis

All replicate extracts (of the same cell type) over three months of analysis produced high total RNA yields at very good quality; RIN values ≥ 9.9 (**Table 3.5**). Experimental estimation of precision for quantity assessment by UV A_{260} was high, with CV = 3.67% (including replicate extracts over the three month time course). Analysis performed using two-factor ANOVA (month of extraction versus extraction replicates) indicated that there was no significant difference in 260/280 ratios between extraction replicates, ($p = 0.60$), but that 260/230 ratios were significantly different between the same extraction replicates ($p < 0.001$). There was a significant difference observed for both ratios between months of extraction ($p < 0.01$). There was a significant interaction between month of extraction and extraction replicates for the 260/230 ratios ($p < 0.001$), whereas no interaction was observed between the same factors for the 260/280 ratios ($p = 0.173$). The 260/230 ratios appear to decrease in a time-dependent manner. There was a significant difference in quantity between month of extraction and between replicate extracts (both $p < 0.0001$). There was also a significant interaction between the two terms (month of extraction and replicate extract) with $p < 0.001$. A 260/280 ratio of approximately 2.0 and a 260/230 ratio of approximately 1.8-2.2 are generally accepted as pure for RNA [256-258]. However, a nucleic acid sample with 260/280 ratio of 1.8 can contain only 40% RNA, in the presence of other contaminants, such as protein [259-261]. This metric was originally developed for the detection of DNA contamination in protein samples, and it more sensitive when used for this purpose as it takes a relatively large amount of protein contamination to significantly affect the 260:280 ratio in a nucleic acid solution [260,262]. For these samples, 260/280 ratio range was 2.11-2.14 (average 2.13, standard deviation 0.01) and the 260/230 ratio range was 1.06-2.14 (average 1.64, standard deviation 0.33) (**Table 3.5**).

Initial investigations of cell line-derived RNA variability and consistency associated with extraction and following storage, demonstrated that this source of RNA is

Chapter 3 Production & Validation of Novel Transcriptomic Calibration Material

Table 3.5 RNA stability analysis. Average Hep-G2 RNA quantification and quality values for replicate cell lysates of the same cell type extracted over a period of three months.

Samples		Average ng/ μ L	CV (%)	Average 260/280	Average 260/230	Average RIN
Month 1 extracts	A	256	0.32	2.14	1.87	10.0
	B	245	0.58	2.14	2.00	10.0
	C	256	0.76	2.13	1.93	9.9
	D	263	0.31	2.13	2.14	10.0
Month 2 extracts	A	257	0.44	2.12	1.50	10.0
	B	260	3.72	2.12	1.85	10.0
	C	266	0.10	2.13	1.45	10.0
	D	257	0.97	2.11	1.70	10.0
Month 3 extracts	A	240	0.47	2.13	1.33	10.0
	B	239	1.27	2.13	1.29	10.0
	C	250	1.05	2.13	1.53	10.0
	D	243	1.28	2.14	1.06	10.0

stable (according to A_{260} measurement) when these preparation, extraction and storage methods are adhered to. However, the ratio measurements are variable, which may mislead the initial quantity measurement. Other methods are needed to evaluate these findings (**Chapter 5**). While the 260/230 ratios were variable, this could be accounted for by the presence of co-extracted contaminants, which absorb at 230 nm, rather than sample degradation. Carbohydrates and phenol (TRIzol reagent is a phenolic solution) all have absorbance at or near 230 nm; TRIzol also absorbs UV at ~ 270 nm [263]. Presence of such contaminants may influence the concentration estimate as the quality and quantity estimates for this method are intrinsically linked.

The 260/280 ratios were variable between months of extraction. However, this does not necessarily represent a decrease in sample integrity over time as the month 3 samples had higher 260/280 ratios with less variability than the month 2 samples. Despite there being significant differences in 260/280 ratios across the month of extraction, all such ratios are between 2.1 and 2.2, which is indicative of good quality RNA. The significant differences observed may be as a result of the high precision in these data and in reality these differences do not impact the final result.

Both the 260/280 and 260/230 ratios are used as a measure of nucleic acid purity [263]. In addition to affecting quantity estimates, co-purified contaminants may also exhibit inhibitory effects on subsequent enzymatic reactions, namely RT and qPCR [58]. Adjusting the pH and ionic strength of test solutions has been shown to significantly impact the variability of 260/280 ratios and change the ability to detect protein contamination [127]. For these reasons, 260/280 and 260/230 absorbance ratios are not particularly reliable metrics. Despite the variability observed in this metric, 260/280 ratios and RIN values were highly consistent and close to the expected/desired values (~ 2.0 and > 8 , respectively) for good quality RNA. RIN values below 7.0 have been shown to give high variation in C_q values [130,264].

qPCR data was also consistent with high quality RNA, showing good linearity (**Figure 3.6**). Using two-way ANOVA, there was no significant difference observed in RNA concentration between month of extraction ($p = 0.341$) or replicate extractions ($p = 0.552$). No interaction was detected between the two terms, month of extraction and replicate extracts ($p = 0.724$). These data suggest that the RNA remains stable when stored as unprocessed cell lysate over the time course. Furthermore, extractions were highly consistent between replicates (**Figure 3.6B**); precision estimate (CV) between all extraction replicates (A-D) of all extraction time points, CV = 33.99%. RT replicates showed high precision, with the vast majority of replicates displaying ΔC_q variance standard deviation of < 0.5 . It is recommended that qPCR samples should not exceed a variation in between reaction replicates of $> 0.5 C_q$ [252]. This equates to a fold change of 1.4, assuming 100% efficiency ($\text{Efficiency}^{\Delta C_q}$).

The same evaluation was performed using month 1 RNA extracts stored post extraction and additionally analysed at T = 1 and T = 2. There was no significant effect of month of analysis ($p = 0.725$) or replicate extraction ($p = 0.060$) on stored RNA concentration. However both time and extraction replicates ($p < 0.001$ for both) significantly affected RNA concentrations derived from stored lysates. However, no interaction was measured between the two terms, month of analysis and extraction replicates ($p = 0.780$). This suggests that, while cell lysate remains stable, stored RNA maybe more stable than stored lysate and so extracted RNA should be stored in preference to unextracted lysates, when possible. Having said that, inspection of the data in **Figure 3.6** intimates that the lysate data (**Figure 3.6A**) have high precision and as such, is more likely to reveal significant differences between replicates than the RNA data (**Figure 3.6B**). In practical terms, there is no difference in the stability of stored lysates versus stored RNA and so storage at either process stage is equally valid. Overall these data are highly consistent (high precision) and confirm the stability of the extracted RNA when stored at -80°C over this time course. Precision estimates (CV) between all

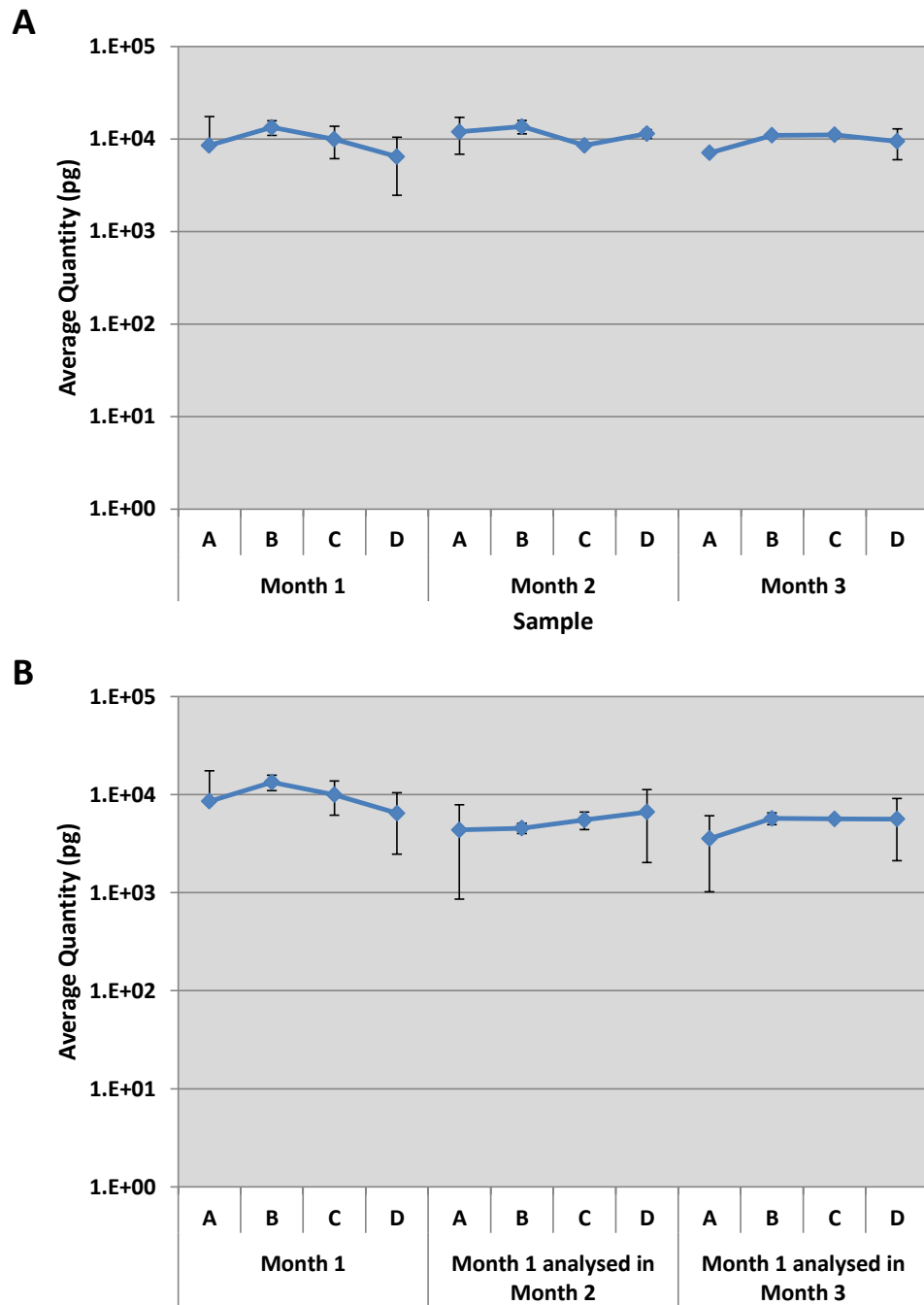


Figure 3.6 RNA Stability Analysis. Stability of Hep-G2 lysate preparations and extracted RNA over a three-month time course. (A) Replicate lysate aliquots from a single cell culture flask were stored for 1, 2 or 3 months before RNA was extracted in replicates (A-D). (B) RNA extracted in month 1 was stored and additionally analysed in month 2 and month 3. Average quantity in pg per qPCR (RNA equivalent), based on human Universal Reference RNA standard curve. n = 2 RT replicates. Error bars = standard deviation.

extraction replicates (A-D) for monthly analysis (n = 3) of month 1 extracts: CV = 56.87%.

These data demonstrated that the assayed mRNA target was not affected by degradation in stored RNA preparations over this time course. The reproducibility observed in terms of total RNA yield was precise (less than 5%, all but one CV < 1.5%, month 2 extract B = 3.72, **Table 3.5**). Sellin Jeffries *et al.* [265] showed RNA kit extraction yield precision estimates (CV) > 6%. According to the user guide (ND-1000 Spectrophotometer v3.3), the reproducibility error (CV) associated with the Nanodrop ND-1000 instrument is 2%. The RNA extract precision estimates were within this range suggesting that in this experiment, extraction did not contribute significant variability to the measurement result. These preliminary experiments paved the way for further production of total RNA from the three chosen cell lines. All samples were extracted and stored as RNA for future experiments.

It is worth considering how relevant cell culture extraction variability (a synthetic situation) is compared to clinical samples. The variability (or lack thereof) observed for these data may not be representative of a clinical sample scenario. Furthermore, different tissues are likely to contain different levels of RNases, and targets with differing susceptibilities to those RNases. Comparison of cell culture and clinical sample variability would be required to evaluate any differences effectively.

3.3.6 RT Variability

This experiment allowed evaluation of inhibition and variability attributable to RT and qPCR steps. In theory, RNA dilutions should minimise any reversible inhibition carried-over from extraction while cDNA dilutions of neat RT product should reduce any reversible inhibition ascribable to extraction carryover and RT reaction components. Furthermore, based on previous publications [47,48,55], qPCR

quantities derived from cDNA dilutions should exhibit greater precision as RT variability is excluded from this measurement and RT has been shown to contribute greater variability. These experiments aimed to test this hypothesis.

The RNA and cDNA dilution series produced very similar standard curves (**Figure 3.7**). An F-test confirmed that there was no significant difference between variances for the RNA versus the cDNA data sets ($p = 0.9707$). A two way ANOVA for dilution type (RNA versus cDNA) and dilution level (1-5) was performed to further analyse these data. There was a significant difference observed in C_q values between dilution types, $p = 0.031$. As values were not normalised for dilution, there was a significant difference detected between dilution levels (dilution 1-5), $p < 0.0001$. However, there was no significant interaction between the two factors (dilution type versus dilution level), $p = 0.127$.

The RNA and cDNA dilutions generated standard curves with different slopes and as such would generate different measurement values for sample unknowns. In order to establish any differences between the two standard curves, a theoretical test sample with a nominal C_q value of 32 was used to calculate corresponding quantity estimates from the RNA and cDNA curves independently. Using arbitrary quantity values assigned to the standard dilutions, the test sample quantities generated were $6.50E+04$, $3.87E+03$ SEM (RNA curve) and $7.30E+04$, $1.74E+03$ SEM (cDNA curve), with a difference between the two values of $7.97E+03$, $4.18E+03$ SEM (arbitrary units). The value generated from the RNA standard curve was 90% of the value generated from the cDNA standard curve. While the difference in the curve gradients appears small, this can equate to a large difference in quantity estimates.

When measuring small fold changes, the relative measurement difference derived from RNA and cDNA standard curves is negligible (for example, for a ΔC_q of 2, both the RNA and cDNA curves yield a fold change measurement of 4). However, when larger differences need to be measured, the difference between the two standard

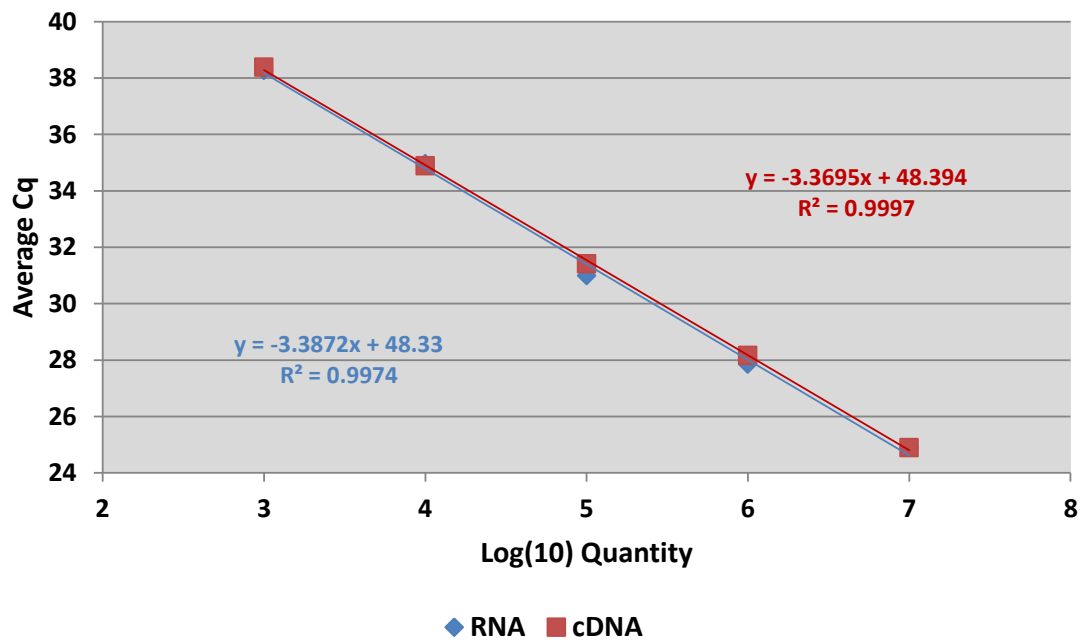


Figure 3.7 RNA versus cDNA Standard Curves. Dilution series generated pre-RT (RNA) and post-RT (cDNA) were compared by qPCR. Quantity values are in arbitrary units. n = 6 per dilution point/dilution type. Error bars: standard deviation.

curves becomes apparent, with ΔC_q values > 7 generating observable differences in fold change measurements (for example, for a ΔC_q of 12, the RNA curve yields a fold change measurement of 3873, while the cDNA curve yields a fold change measurement of 3718. Therefore the relative quantity estimation of samples becomes less comparable between standard curve types as fold change increases.

As the two slopes are almost identical, it would suggest that discrepancies between the two curves are not dependent on the RT and PCR enzymes and that the variation observed between RNA and DNA standard curves is linked to aliquoting nucleic acid, and that no enzymatic variation is contributing. Using this particular experimental set-up, the RTase is both linear and precise and has no effect on the experimental outcome. This shows us the low variability that is possible when experiments are planned with variability contributions in mind and what analysts should be aiming for.

It is clear that when measuring an RNA target, an RNA standard curve should be used to generate the most accurate measurement value. This is because it will include the variability associated with the RT reaction. An RNA standard curve when measuring an RNA target, and a DNA standard curve when measuring a DNA target, would offer the best approximation of the true value, with associated error. While RNA measurements are generally more variable than DNA measurements [56], this offers a true reflection of the variability inherent in the measurement. When performed correctly, both RNA and DNA standard curves may offer linear measurements over a defined range [47,48,55,56]. While a comprehensive assessment of RT variability contributions was not undertaken in this experiment, this is addressed fully in **Chapter 4 Comparison of Different Reverse Transcriptases by Digital PCR**.

It is well established that the RT reaction may contribute greater variability to quantification than qPCR [47,48,55]. Without including variability measurements contributed by all components (including RTases), a true assessment of

measurement uncertainty cannot be performed. Purification procedures post-RT may be time consuming, expensive and more importantly, represent another stage whereby precious RNA yield may be reduced. For that reason, subsequent experimental protocols will include RNA-based dilutions to reflect the variability inherent to this step, which may be observed in the error of associated standard curves.

3.3.7 Endogenous Target Selection

Reference genes with least variable expression across the three different cell types (Hep-G2, SaOS-2 and Hs 683) were selected from 32 candidates for use as a reference target (**Figure 3.8**), as determined by the RefFinder programme [225]. (**Table 2.1, 2.3.1 Endogenous Target Selection and 2.3.2 Assay Design**). Further targets were subsequently assessed on the basis of GOI criteria: the expression of each gene was different between the cell lines. This enabled the generation of different TCM units with different GOI expression profiles.

Initial endogenous target selection experiments were performed using assay-on-demand, commercially bought assays (ABI). Accordingly, the endogenous targets selected were re-designed (based on the amplicon regions detailed by ABI). These assays were validated using optimisation of primer/probe concentrations and cross-reactivity tests with ERCC RNA standards (**Chapter 2 Materials & Methods**). The endogenous reference genes selected and validated were: CASC3, HPRT1 and UBC. GOI were: MMP1, NES and SLC1A3 (**Table 3.6**). GOI targets have previously been shown to be of interest in the selected cell lines, MMP1 in Hep-G2 cells [266], SLC1A3 (GLAST1) in SaOS-2 cells [267] and NES in Hs 683 cells [268].

To complete ERCC assay validation, cross-reactivity with cell line-derived total RNA was assessed. All eight ERCC assays were tested against each of the three cell line-derived total RNA samples, with ERCC plasmid DNA positive controls and GAPDH assay-on-demand (ABI) analysis of cell line-derived RNA positive controls.

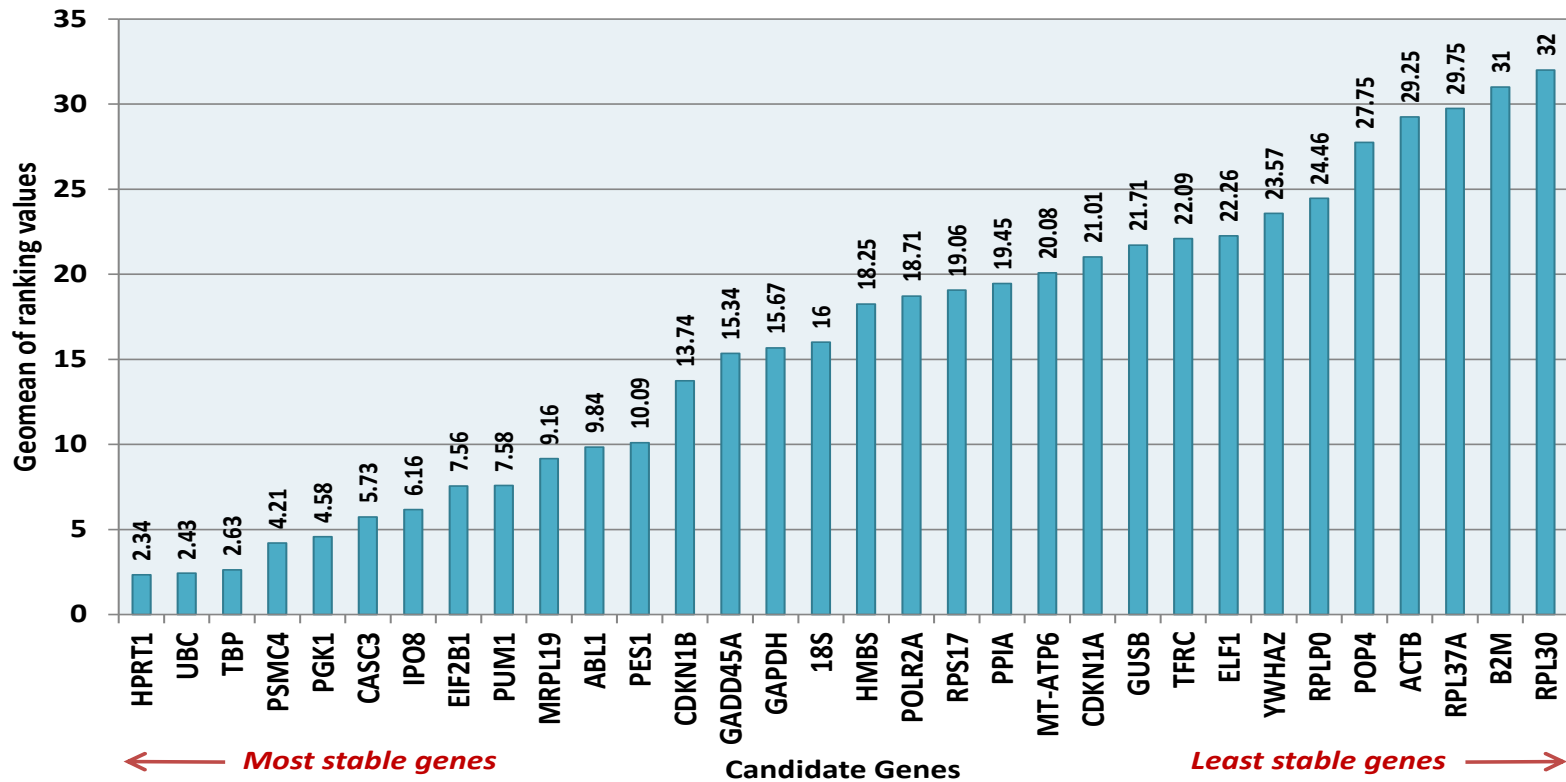


Figure 3.8 Comprehensive gene stability, generated from RefFinder output. Average expression stability values for assessed candidate reference genes measured in the three cell line-derived total RNA samples (Hep-G2, Hs 683 and SaOS-2. n = 3). Based on the rankings from each program (GeNorm [7], Normfinder [137], BestKeeper [226] and the comparative ΔC_t (C_q) method [227]), individual genes are assigned an appropriate weight and the geometric mean of their weights is calculated for the overall final ranking. Starting from the most stable gene at the left, genes are ranked according to decreasing expression stability, ending with the least stable genes on the right.

Table 3.6 Endogenous reference genes and GOI selected and validated

	Target	Name	Function
Reference	CASC3	Cancer susceptibility candidate 3	Protein is involved in nonsense-mediated mRNA decay. Widely expressed. Overexpressed in breast cancers and metastasis, as well as in gastric cancers [269].
	HPRT1	Hypoxanthine phosphoribosyl-transferase 1	Enzyme plays a central role in the generation of purine nucleotides through the purine salvage pathway [270].
	UBC	Ubiquitin C	Encoded protein is a polyubiquitin precursor.
GOI	MMP1	Matrix metalloproteinase 1	Proteins of the MMP family are involved in the breakdown of extracellular matrix in normal physiological processes, such as embryonic development, reproduction, and tissue remodelling, as well as in disease processes, such as arthritis and metastasis.
	NES	Nestin	Gene encodes a member of the intermediate filament protein family. Expressed primarily in nerve cells.
	SLC1A3	Solute carrier family 1 (glial high affinity glutamate transporter) member 3 *	Protein is involved in glutamate transport/signalling.

* Also known as GLAST1 in rats

No PCR products were produced from ERCC assays on cell line derived cDNAs whereas all positive controls produced expected amplicons.

3.3.8 Transcriptomic Calibration Material Homogeneity and Stability

Following large batch production and aliquoting of described TCM (**2.3 Preparation of Transcriptomic Calibration Material (TCM)**); the material was assessed for homogeneity and stability to confirm suitability as a pilot reference material for this study.

RT-qPCR data were analysed by comparing both between and within replicate units (**Figure 3.9**). Several test runs show comparatively extreme outliers (Grubb's test): Calibrant/ERCC-99 unit 1, Calibrant/HPRT1 unit 9, Unknown 1/ERCC-99 unit 8 and Unknown 1/HPRT1 unit 5 (**Figure 3.9A, B, D & E**). Repeating analysis with and without outliers checked the effect of outliers on subsequent analysis; between-unit variance estimates with outliers removed were somewhat more conservative (larger) and values are accordingly reported on an outlier excluded basis. Between-unit variances were calculated by randomising units across the PCR thermocycling block (re-randomised for each replicate plate). Between-unit variation must be bigger than positional variance in order to not be lost in the noise. This approach removes systematic variation of the thermocycling block. A two-factor ANOVA (unit number versus randomised position on qPCR plate) was used to analyse these data. For ERCC-99, the between-unit CV was calculated to be 6.1%, 6.8% and 4.4% for Calibrant, Unknown 1 and Unknown 2 units, respectively, which were found to be statistically significant ($p < 0.05$) for Calibrant and Unknown 1, in other words, these samples showed some signs of inhomogeneity. For HPRT1, the between-unit CV was calculated to be $< 0.01\%$, $< 0.01\%$ and 2.8% for Calibrant, Unknown 1 and Unknown 2 units, respectively.

The TCM homogeneity data are broadly consistent with the material origins (ERCC-99 showed greater variability between units than HPRT1); the ERCC

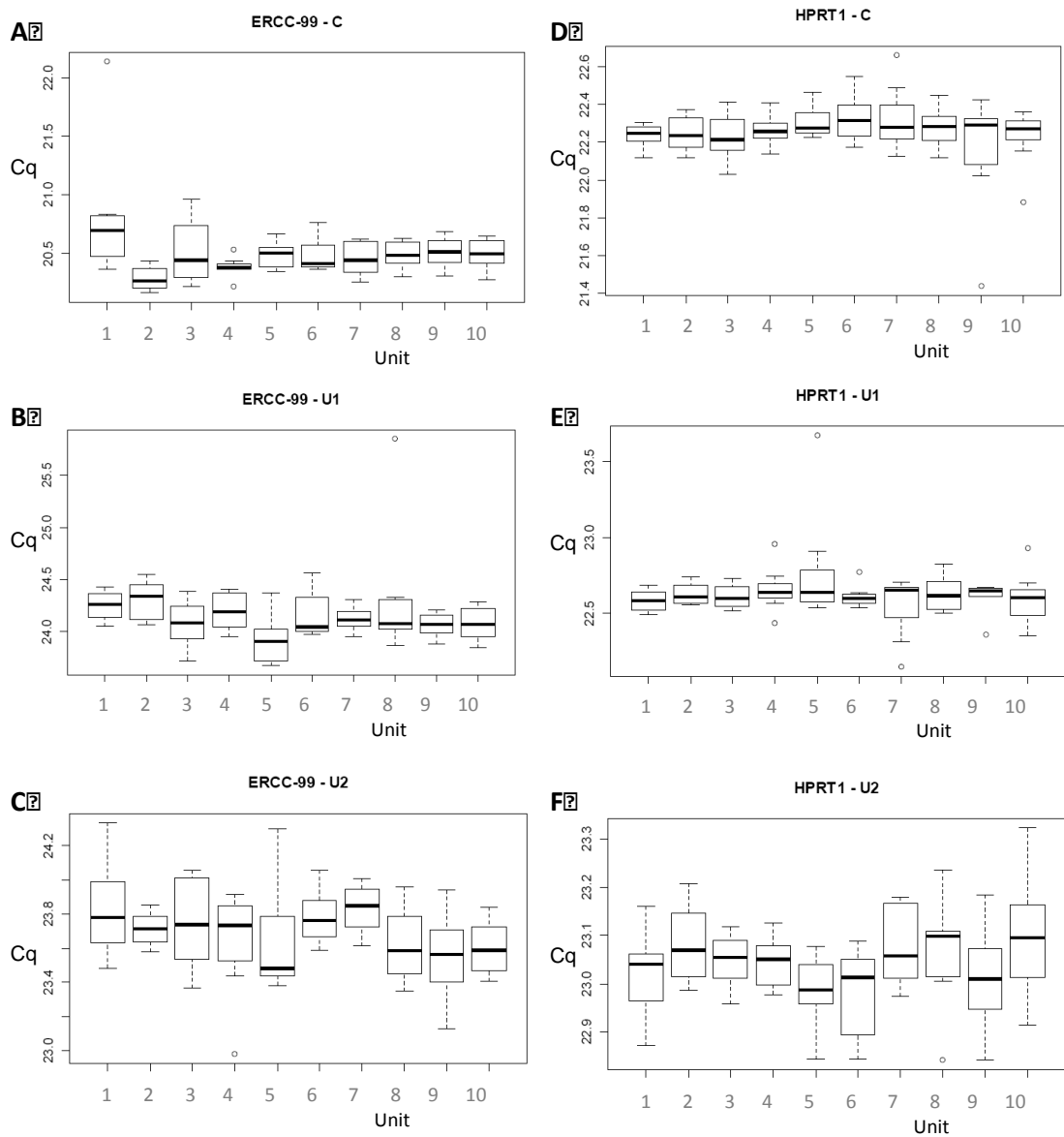
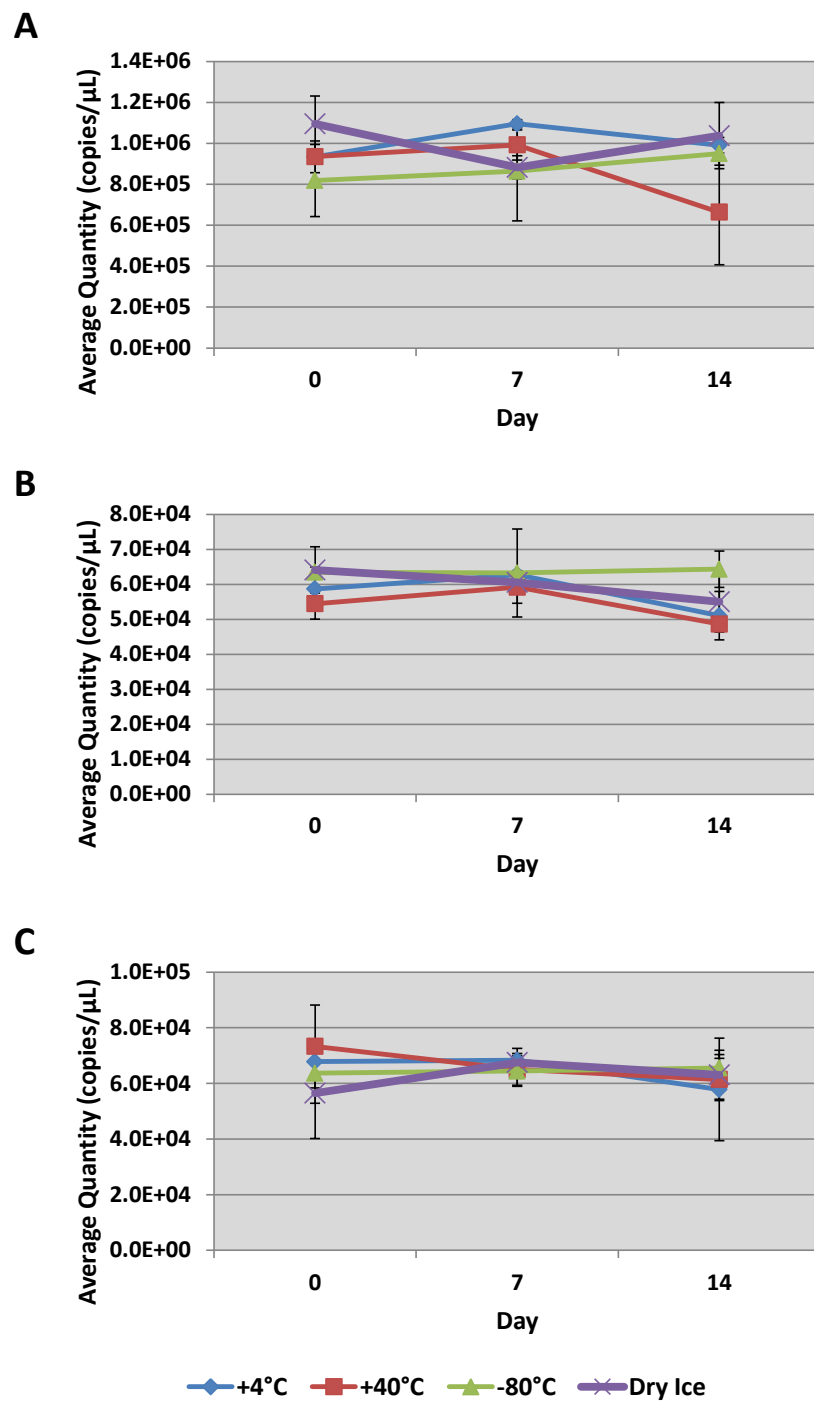


Figure 3.9 Results of Homogeneity study. RT-qPCR measurements ($n = 8$) of ERCC-99 (A-C) and HPRT1 (D-F) were performed on ten units (x-axis 1-10) of each study material (Calibrant, Unknown 1 and Unknown 2). Plots indicate median (bold line), interquartile range (box) and range (up to $1.5 \times$ interquartile range, whiskers) of C_q values for each unit 1-10. Values outside of the $1.5 \times$ interquartile range are plotted as individual points (circle).

material is synthetic and prepared by plasmid digestion, IVT, DNase-treatment, dilution and mixing; the endogenous material required less manipulation and there were fewer opportunities for introducing substantial heterogeneity [271]. The synthetic targets would therefore generate a larger uncertainty contribution to the uncertainty budget than endogenous targets and subsequently a more conservative estimate of target abundance. A synthetic reference material may be less variable than endogenous targets given that it is not influenced by dynamic transcriptomics. While this may be true for endogenous targets in other studies, this is not the case for the pre-prepared TCM as it is pre-prepared/aliquoted. In this case, the addition of synthetic targets generates a more complex background. Synthetic targets have the added benefit of being able to be value assigned before spiking into test material. Homogeneity studies are not generally performed within the wider research community. In the absence of a precedent, it was decided not to perform an assessment of all transcripts in all units (Calibrant, Unknown 1 and Unknown 2). ERCC-99 and HPRT1 targets were selected to be representative of the other ERCC and endogenous targets measured, for which homogeneity has not been individually assessed. In the absence of a homogeneity study that measures all targets therefore, the uncertainty associated with homogeneity was based on the largest between-unit relative standard deviation rounded to one significant figure: ERCC-99 = 0.07, for all ERCC targets in all unit types and HPRT1 = 0.03, for all endogenous targets in all unit types. As assigned values were not calculated for the endogenous gene targets, the HPRT1 results were interpreted as confirmation of acceptable between-unit homogeneity with respect to the endogenous gene targets.

The short-term stability study showed no systematic effects up to and including 4°C (**Figure 3.10**, two-factor ANOVA, storage time versus temperature). Samples stored at 40°C showed a significant ($p = 0.0166$) increase in C_q of 0.019 C_q units/day over all samples and both targets. The use of dry ice had no systematic effect on sample stability, despite the large variability observed in HPRT1, Unknown 1 at day 14 (**Figure 3.10E**). This variability may have been caused by



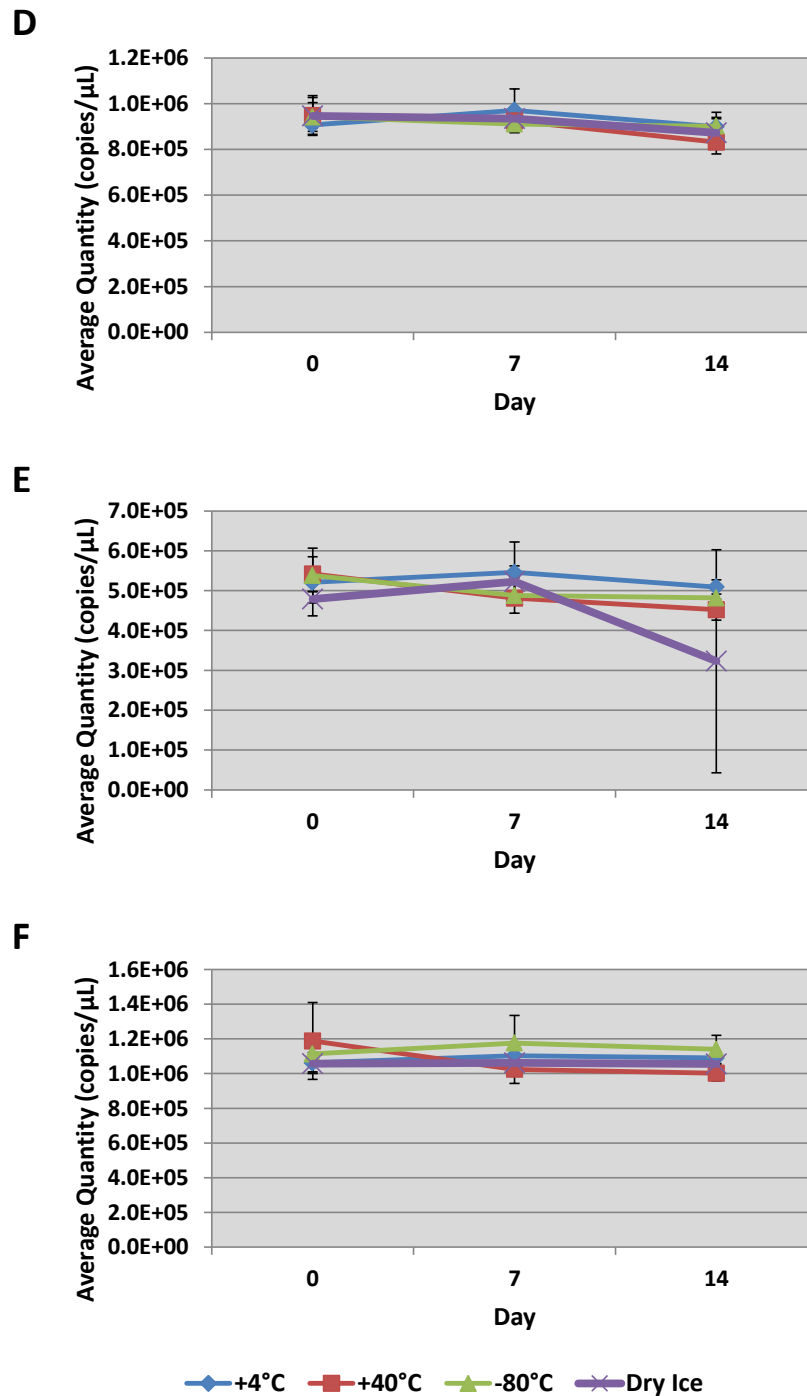


Figure 3.10 Results of Short-Term Stability study. For each Calibrant, Unknown 1 and Unknown 2 solution, three replicate units were isochronously tested after storage at -80 °C, on dry ice, +4 °C, and +40°C at 0, 7 and 14 days. One-step RT-qPCR measurements of ERCC-99 (A-C) and HPRT1 (D-F) were performed per unit. Calibrant (A & D), Unknown 1 (B & E) and Unknown 2 (C & F). Error bars standard deviation.

acidification of the material through penetration of CO₂ through Eppendorf walls [272]. For all other samples there was no evidence of a significant impact on C_q from storage time or temperature (all $p > 0.05$). For potential shipping purposes therefore, there was no evidence of instability in the short-term at 4°C or below.

A longer-term stability study was also performed over six months (**Figure 3.11**, two way ANOVA for storage time versus temperature, applied separately to each transcript/unit combination). The results were checked for a significant time/temperature interaction (indicative of temperature-mediated instability) using two-factor ANOVA applied separately to each transcript and also to each transcript/sample combination. ANOVA demonstrated significant effect of time on copy number in all cases ($p < 0.0001$), however the differences are less than two fold and so are within the range of calibration; temperature was not significant ($p > 0.05$). There was no significant time/temperature interaction at the 95% confidence level ($p > 0.05$) for any of the groups studied.

It is likely that the variability observed was due to an artefact of the analysis; possibly assay variation with time, as the experiments were performed six months apart. There was no evidence of temperature-mediated instability. Studies, including homogeneity and stability assessments, confirmed the suitability of the prepared TCM for the basis of future evaluation. Any variability associated with these materials has been included in the corresponding uncertainty budgets (**Table 3.7**. Discussed below in **3.3.9 Measurement Uncertainty**). Both exogenous and endogenous transcripts will be employed for the identification and characterisation of variability contributors to the experimental measurement of mRNA levels. This is not done routinely, however is a fundamental basis of RM production (the TCM is a pilot RM). To our knowledge, this has never been done on a wholesale material for RNA.

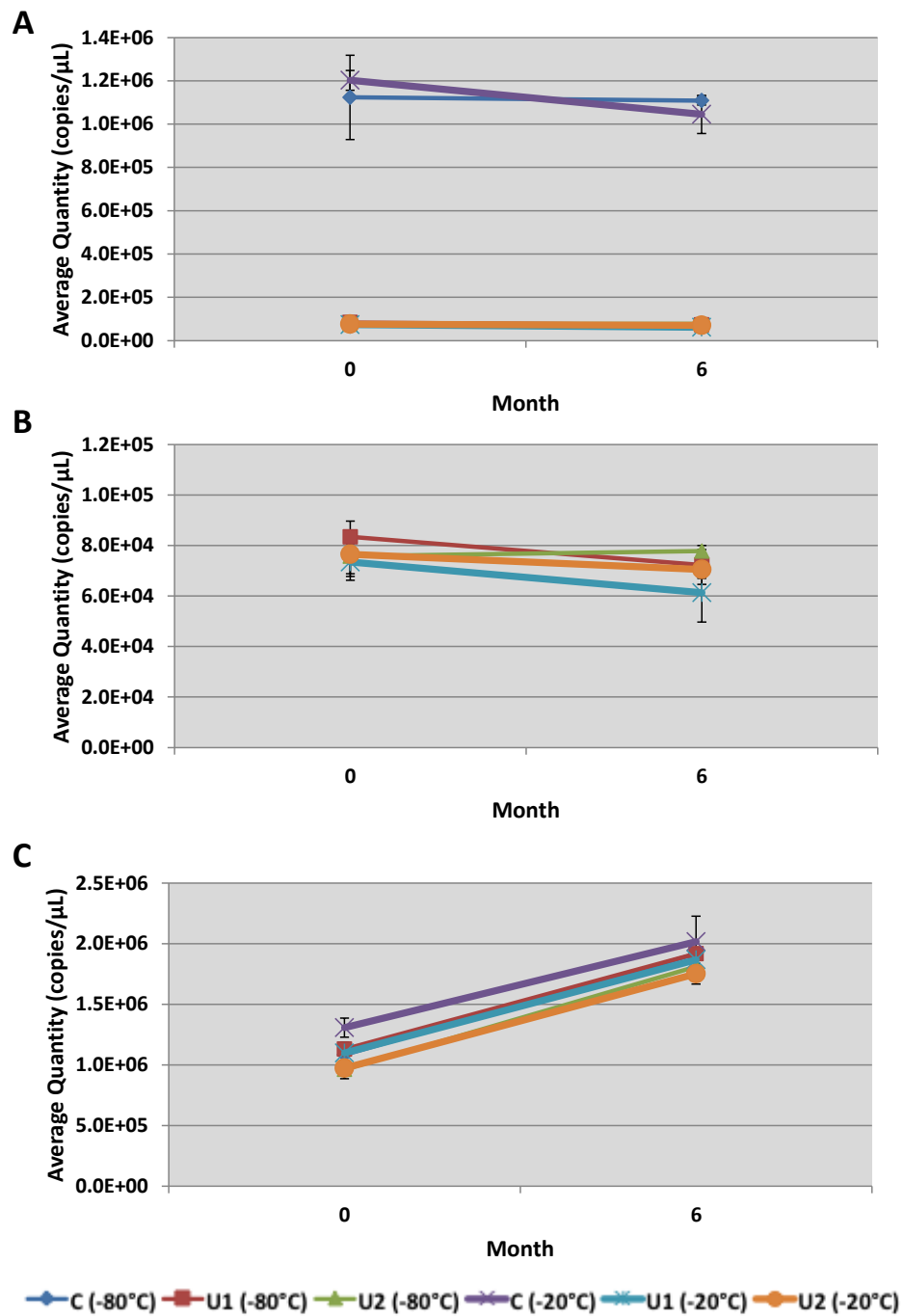


Figure 3.11 Results of Long-Term Stability study. For each Calibrant, Unknown 1 and Unknown 2, three replicate units were incubated for one week on dry ice (to simulate a shipping period) before being transferred to either -80°C or -20°C (designated T = 0). One-step RT-qPCR measurements of (A) ERCC-99 (full data set) (B) ERCC-99 (adjusted scale for visualisation of lower concentration samples) and (C) HPRT1 were performed on each unit at T = 0 and 6 months. Error bars standard deviation.

Chapter 3 Production & Validation of Novel Transcriptomic Calibration Material

Table 3.7 Assigned values and measurement uncertainty of ERCC standards. Uncertainty components common to both Unknown 1 and Unknown 2 are not included in corresponding uncertainty budgets as these contributions cancel out in measurement of combined standard uncertainty of assigned ratios.

Calibrant

ERCC	Assigned value, (copies/ μ L)	Combined Standard Uncertainty, u_c	Expanded Uncertainty, U (k=2) (\pm)	Relative Expanded Uncertainty (%)
ERCC-13	9.48E+05	101704	2.03E+05	21.46
ERCC-25	1.00E+06	87498	1.75E+05	17.50
ERCC-42	1.00E+06	87629	1.75E+05	17.52
ERCC-99	9.86E+05	87160	1.74E+05	17.67
ERCC-113	9.38E+05	87760	1.76E+05	18.70
ERCC-171	9.39E+05	89207	1.78E+05	19.00

Unknown 1

ERCC	Assigned value, (copies/ μ L)	Combined Standard Uncertainty, u_c	Expanded Uncertainty, U (k=2) (\pm)	Relative Expanded Uncertainty (%)
ERCC-13	5.69E+04	4013	8027	14.11
ERCC-25	5.00E+03	354	709	14.17
ERCC-42	1.00E+03	71	143	14.29
ERCC-99	6.90E+04	4870	9740	14.11
ERCC-113	1.97E+04	1395	2790	14.16
ERCC-171	9.39E+04	6633	13266	14.13

Unknown 2

ERCC	Assigned value, (copies/ μ L)	Combined Standard Uncertainty, u_c	Expanded Uncertainty, U (k=2) (\pm)	Relative Expanded Uncertainty (%)
ERCC-13	8.53E+04	6029	1.21E+04	14.14
ERCC-25	5.00E+03	354	7.09E+02	14.17
ERCC-42	7.00E+03	495	9.89E+02	14.13
ERCC-99	6.90E+04	4870	9.74E+03	14.11
ERCC-113	6.57E+03	464	9.28E+02	14.13
ERCC-171	1.88E+04	1330	2.66E+03	14.17

Chapter 3 Production & Validation of Novel Transcriptomic Calibration Material

ERCC Assigned Ratios (Unknown 1/Unknown 2)

ERCC	U1 Assigned value, (copies/ μ L)	U2 Assigned value, (copies/ μ L)	Assigned Ratio (U1/U2)	Combined Standard Uncertainty, u_c	Expanded Uncertainty, U (k=2) (\pm)	Relative Expanded Uncertainty
ERCC-13	56867	85300	0.667	0.0999	0.200	29.965
ERCC-25	5000	5000	1.000	0.1002	0.200	20.045
ERCC-42	1000	7001	0.143	0.1005	0.201	140.684
ERCC-99	69049	69049	1.000	0.0997	0.199	19.949
ERCC-113	19706	6569	3.000	0.1000	0.200	6.668
ERCC-171	93919	18784	5.000	0.1000	0.200	4.001

The reported expanded uncertainty of measurement is stated as the standard uncertainty of measurement multiplied by the coverage factor $k = 2$, which for a normal distribution corresponds to a coverage probability of approximately 95%. The standard uncertainty of measurement has been determined in accordance with EAL Publication EAL-R2 [273].

3.3.9 Measurement Uncertainty

Assigned target concentration values and uncertainty budgets were calculated for all six ERCC targets in all unit types (Calibrant, Unknown 1 and Unknown 2), according to EU recommendations [273]. Summaries of the assigned values and uncertainties (**2.3.3 Measurement Uncertainty Budget**) for each synthetic target and unit type are collated in **Table 3.7**. Comprehensive tables and figures describing measurement uncertainty contributing factors may be found in **9.3 Appendix 3 – Measurement Uncertainty Budgets**. Variability contributions to the assigned values were considered from several sources, which were subsequently included in the uncertainty budget. The factors included in the uncertainty calculation were; Nanodrop calibration, estimated purity (Bioanalyzer), homogeneity, stability and volumetric (error associated with pipetting steps). It should be noted that no extraction component is included in this calculation due to the nature of ERCC preparation. Assigned values for ERCC targets may be used to define variance, precision and accuracy of ERCC target measurements when spiked into test samples. Endogenous quantities could not be assigned by RT-qPCR due to transcript source. This could be achieved by RT-dPCR, but this was not undertaken for this study.

3.4 Conclusions

These preliminary studies were broadly undertaken for the purpose of developing the TCM for application to more in-depth investigations of measurement variability. In the process of this development, there have been several additional findings. The DNase reaction may not be 100% efficient but the effects of remaining gDNA contamination on RT and PCR may be alleviated by sample dilution. Furthermore, DNase efficiency may in part be influenced by sample source, for example, the cell line from which the RNA is derived from. In addition, appropriate assay design to target mRNA transcripts will limit gDNA cross-reactivity.

Chapter 3 Production & Validation of Novel Transcriptomic Calibration Material

The inclusion of carrier nucleic acid may be most valuable for trace detection of minority targets and is most beneficial in terms of increasing precision when carrier is chosen that matches sample type (i.e. RNA sample with RNA carrier as opposed to RNA sample with DNA carrier). Furthermore, the RNA used in this study may be stably stored at -80°C as both unprocessed lysate and extracted RNA for at least two months. RT variability experiments revealed that RNA and cDNA generated standard curves may generate differences in quantity estimates due to differences in curve gradients. From these data it is recommended that sample type (RNA, cDNA etc.) should remain consistent between standard and test samples to ensure associated variabilities are captured appropriately.

The uncertainty budgets assigned to the various synthetic transcripts in the TCM take into account the array of factors contributing to the variability in these measurements and define the level of precision achievable for these measurement spikes.

Evaluation studies have successfully demonstrated that the TCM, including ERCC RNA spikes, is fit for purpose, i.e. it is appropriate to use for characterising variability contributions in mRNA analysis. All assays for selected endogenous and ERCC targets have been well optimised and will be employed to identify and define measurement variabilities associated with RNA measurement. The synthetic ERCC targets allow for an assessment of technical variability contributions at various stages of the experimental process and an opportunity to evaluate different fold change measurement challenges while the endogenous targets enable sample normalisation strategies to be applied to generated data sets and assessment of biological variability.

Chapter 4

Comparison of Different Reverse Transcriptases by Digital PCR

4 Comparison of Different Reverse Transcriptases by Digital PCR

This chapter is adapted from the peer-reviewed publication: Evaluation of digital PCR for absolute RNA quantification. **Sanders R**, Mason DJ, Foy CA, Huggett JF. PLoS One. 2013 Sep 20;8(9):e75296. doi: 10.1371/ journal.pone.0075296. eCollection 2013.

4.1 Introduction

Measuring mRNA by RT-qPCR is an established approach for investigating gene expression and viral diagnostics. It is well known that the RT step, required to transcribe mRNA to complementary DNA (cDNA), is imprecise and that different reverse transcriptase enzymes (*RTase*) can work with considerably different efficiencies [82]. Many of the issues associated with differing *RTase* efficiencies may be sidestepped by taking advantage of the (assumed) linear nature of RT and performing relative quantification, with the results expressed as fold changes, or by comparing to a standard curve that is equally affected by the limitations of the RT.

Digital (d)PCR is continuing to gain recognition in the field as a precise and reproducible method offering the potential for accurate, robust and highly sensitive measurement without the need for a standard curve [274]. Much work has already been done to meticulously evaluate this technique for DNA molecular measurement [103,104,223,275-277]. However, a comprehensive evaluation is yet to be established for applying this method to the measurement of RNA. RT-dPCR may offer the potential to maximise the accuracy, sensitivity and reproducibility of RNA measurements, for capabilities such as diagnostic mRNA profiling, biomarker analysis and monitoring of viral load.

While this may be true, many studies have demonstrated that the variability inherent in the RT component of the process far outweighs that observed from the PCR step when performing qPCR [47,48,55]. The RTase itself has been shown to confer reversible inhibitory effects to downstream PCR, demonstrating a need to limit these effects by, for example, heat inactivating the RTase or diluting the cDNA prior to PCR [71,72]. Improved quantification sensitivity reported for one-step *versus* two-step RT-qPCR for low copy targets or low concentration samples such as single cells may in part be attributed to gene-specific priming in one-step protocols (as opposed to random hexamers or oligo (dT) commonly used in two-step protocols) [71,72,80,81].

In addition to the sensitivity differences between one-step and two-step RT-qPCR, when performing RT-dPCR, one must consider sample partitioning. For two-step protocols, the cDNA is produced before sample partitioning for dPCR. This therefore must rely on the assumption that, even if not 100% efficient, the RT step is linear and so relatively speaking, the number of cDNA molecules accurately represents the actual proportions of target RNA molecules. If this is not the case and the RT is not linear or some target amplification occurs during the RT, significant bias may be introduced. For one-step protocols, the RNA population is partitioned into roughly single copies prior to RT and as such, even if one RNA target molecule is amplified during the RT step, these remain in one partition and so only one positive partition results. This would act to alleviate any bias unintentionally introduced by any amplification of target by the RT enzyme.

This chapter details the investigation of how the RT might affect cDNA production and ultimately influence the dPCR measurement. It is hypothesised that RT variability affects the amount of cDNA and thus subsequent dPCR measurement capabilities. RNA analysis by RT-dPCR was evaluated and repeatability, linearity and sensitivity assessed. The aim was to determine the variability contributions of the RT step in RT-dPCR measurement using different RT enzymes. The Transcriptomic Calibration Material (TCM) documented in **Chapter 3** was utilised

for both synthetic and endogenous target measurements, where RT-dPCR analysis was compared to UV A_{260} , and the performance of different assays and commercially available one-step RT-qPCR kits was evaluated.

4.2 Materials & Methods

The techniques exploited in this chapter include one-step RT-dPCR (**2.5.1 One-Step RT-qPCR Kit Comparison by dPCR** and **2.5.3 Linearity and Sensitivity of RT-dPCR**) and UV A_{260} analysis (**2.5.2 Comparison between dPCR and UV Measurement**).

Synthetic targets ERCC-25 and ERCC-99 and endogenous targets MMP1 and UBC were assessed in both uniplex (ERCCs only) and duplex format, utilising three different commercial one-step RT-qPCR kits. ERCC targets were used to establish quantification sensitivity. Subsequently, quantification of six ERCC targets by one-step RT-dPCR was compared to UV A_{260} measurements.

4.2.1 Statistical Methods

All statistical analyses were performed using MS Excel 2007 and the R statistical programming environment (<http://www.r-project.org/>, ongoing access). Statistical analysis was performed in collaboration with Dr. Simon Cowen, Statistician, LGC, Teddington. Data were tested for normality and equal variance before analysis using ANOVA. Where necessary, data were transformed (square root or weighted regression, as appropriate) in order to obtain a data set in which the within group variances were sufficiently similar for an ANOVA to be performed. These transformed data were analysed using ANOVA.

4.3 Results & Discussion

In this study we used a TCM containing synthetic RNA transcripts in a complex background made of mixtures of human cell line total RNA. This was used to both evaluate dPCR measurement and demonstrate the applicability of the TCM for supporting accurate RNA enumeration by RT-dPCR.

4.3.1 One-Step RT-qPCR Kit & Format Comparison by dPCR using Synthetic RNA Targets

Three commercially available kits were compared for quantitative performance by RT-dPCR. The three kits were initially assessed using both uniplex and duplex formats for quantification of two synthetic RNA targets: ERCC-25 and ERCC-99 (**Figure 4.1**). The type of kit significantly affected RNA quantification ($p < 0.0001$) with the Ambion kit consistently yielding the highest signal. A significant difference in quantification was also observed (single-factor ANOVA) between uniplex and duplex formats for the Qiagen (ERCC-25 $p = 0.045$) and Invitrogen (ERCC-25 $p = 0.025$, ERCC-99 $p = 0.019$) kits but not the one supplied by Ambion (ERCC-25 $p = 0.347$, ERCC-99 $p = 0.736$), (Qiagen ERCC-99 $p = 1.000$); however the difference between uni/multi-plex formats was considerably smaller than the inter kit differences (**Figure 4.1**).

Consistent ratios for ERCC-25:ERCC-99 between uniplex and duplex measurements were not maintained between kits suggesting an assay-dependent as well as a kit associated difference (**Table 4.1**). The ERCC-99 assay consistently resulted in lower estimated copies than that for ERCC-25 (with all kits), despite being added at the same concentration, as estimated by UV.

The findings from the one-step kit comparison by dPCR indicate that there can be large numbers of RNA molecules present within the dPCR partitions that are not being detected with dPCR. This is because either they are not converted to cDNA or

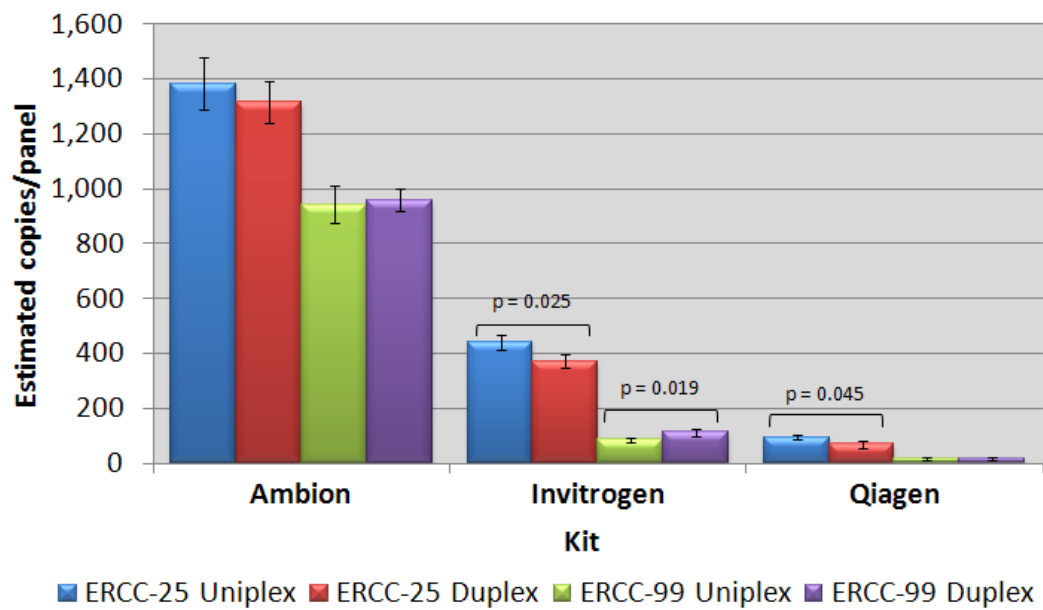


Figure 4.1 One-step kit comparison. Three different one-step RT-qPCR kits were compared in both uniplex and duplex formats, by dPCR. Two synthetic targets, ERCC-25 and ERCC-99 were analysed. Error bars: 95% confidence intervals. n=3 replicate panels. Equivalent UV estimates: ERCC-25 1185.41 copies/panel, 95% CI 17.34. ERCC-99 1185.41 copies/panel, 95% CI 26.19.

Chapter 4 Comparison of Different Reverse Transcriptases by Digital PCR

Table 4.1 Three one-step kit comparison with uniplex and duplex formats. Equivalent UV estimates: ERCC-25 1185.41 copies/panel, 95% CI 17.34. ERCC-99 1185.41 copies/panel, 95% CI 26.19.

Method	Format	ERCC-	Positive Partitions	Copies per panel*	Ratio†	Standard Uncertainty
Ambion	Duplex	25	627	1316	1.37	0.051
		99	546	959		
	Uniplex	25	639	1383	1.47	0.076
		99	541	944		
Invitrogen	Duplex	25	295	373	3.31	0.223
		99	104	113		
	Uniplex	25	335	442	5.18	0.262
		99	81	85		
Qiagen	Duplex	25	68	71	4.22	0.588
		99	17	17		
	Uniplex	25	89	95	5.57	0.906
		99	17	17		

*Copies per panel calculated from the number of positive partitions using the Poisson correction. †Ratio of ERCC-25/ERCC-99 dPCR values with standard uncertainties. Ratios calculated using copies per panel. Standard uncertainty calculated by dividing the standard deviation by the square root of n (number of replicate measurements).

are being converted to cDNA but not being amplified by the PCR. This diminished detection is kit and transcript dependent. However, this assumes that the UV measurement is accurate although in fact UV absorbance may potentially overestimate the initial valuation. This is explored in more detail below.

4.3.2 Comparison Between dPCR and UV Measurement of Synthetic RNA Targets

To investigate this disparity further, RT-dPCR measurements using the Ambion kit were compared when measuring a further four ERCC targets (all six present within the TCM) (**Figure 4.2**). dPCR estimates of ERCC transcript quantities were on average 40% lower than when measured by UV ($p < 0.0001$). Furthermore, despite all six ERCC targets being valued at the same concentration, as estimated by UV spectrophotometry, there was a significant difference between ERCC target concentrations estimated by dPCR ($p = 0.0002$). Bioanalyzer quantification for all six synthetic targets was comparable to nanodrop concentration estimates ($p = 0.660$, with an average difference between the two approaches of 1.02 copies). The significant differences observed in absolute quantification between dPCR and UV were assay/target-specific (**Figure 4.2**). The number of dPCR estimated counts for ERCC-25 was closest to UV at 77.41% agreement, whereas ERCC-99 displayed the lowest agreement at 50.45%. Furthermore, there was no significant inter-plate difference observed despite 5-6 days between independent experiments.

The analysis method was shown to significantly affect the RNA quantification result. There may be a number of reasons explaining the significant difference observed between dPCR and UV methodologies. While dPCR makes an absolute count of specific amplified cDNA target molecules, albeit a small part of a bigger molecule, UV cannot discriminate between nucleic acid species, non-target RNA and fragmented/degraded/non-amplifiable targets [12,47,103,125,126,128]. There is a concordance between UV and the 2100 Bioanalyzer (which utilises a fluorescent dye that interacts with nucleic acids); the Bioanalyser measurement

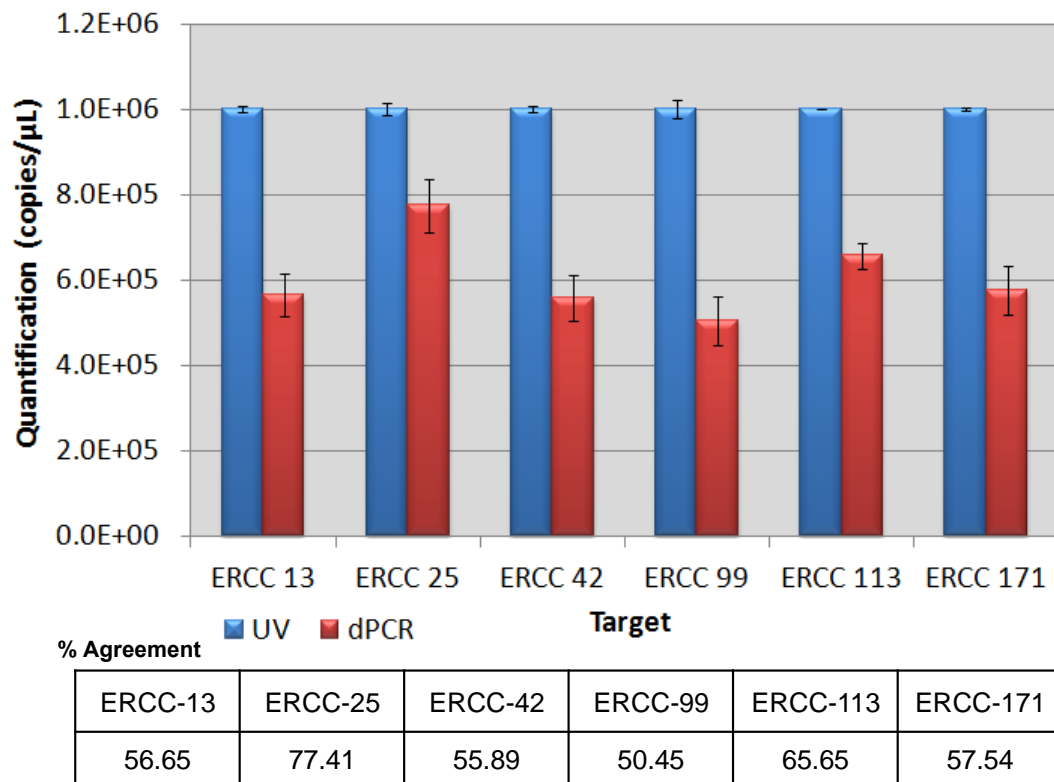


Figure 4.2 dPCR versus UV quantification. Six synthetic targets (ERCC-13, -25, -42, -99, -113 and -171) were assessed by both one-step dPCR, utilising the Ambion one-step RT qPCR kit, and UV measurement. Error bars: 95% confidence intervals. n=3 replicate dPCR experiments or UV measurements.

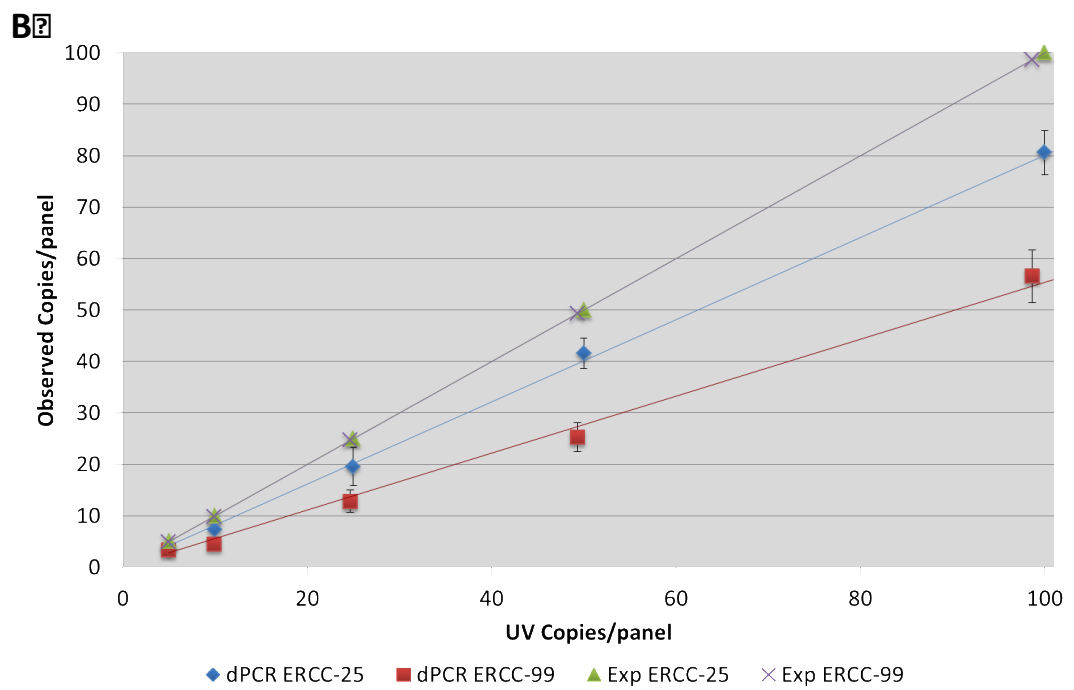
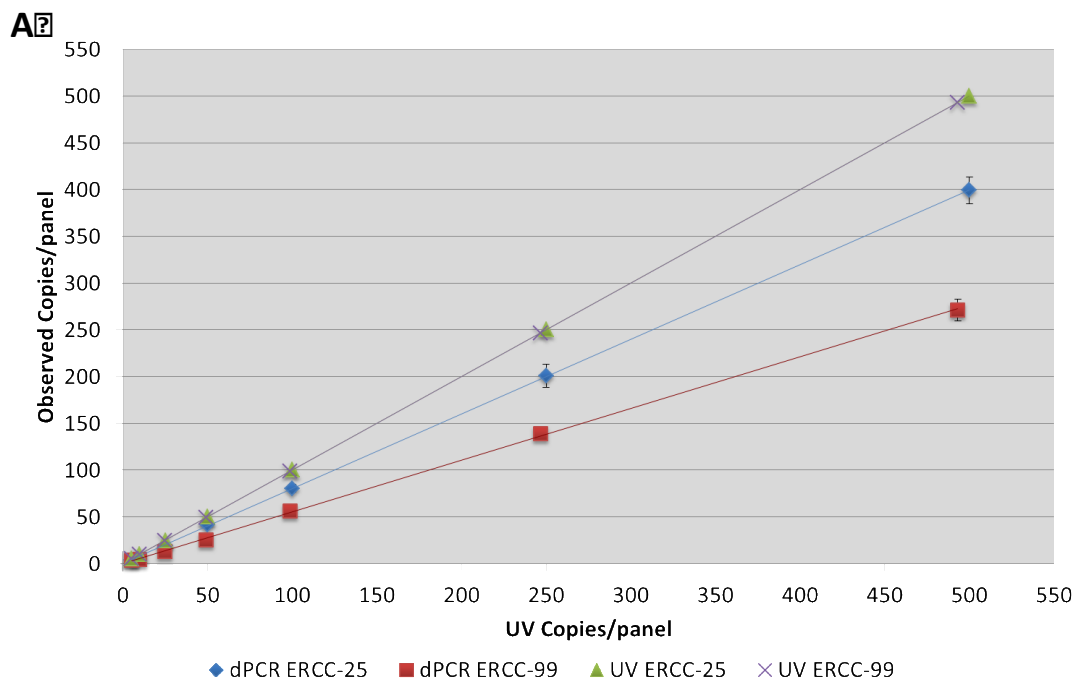
may also be influenced by contaminants and non-target species. This over estimation of RNA target concentration could contribute to the consistent increased RNA concentration estimated by UV. Another explanation for the discrepancy is that the RT-dPCR measurement value is underestimating the true concentration. Quantification of RNA reflects only the number of target cDNA molecules converted from the original RNA. This may or may not give an accurate estimate for the original concentration of the RNA molecules of interest [230]. Given the assumption that the RNA samples analysed are fairly pure in view of the high degree of gDNA removal (**3.3.2 DNA Contamination Assessment**), it is possible that the lower quantification by dPCR reflects the efficiency of the RT reaction. Not only is it shown here that RT sensitivity and variability will affect dPCR estimation, as previously reported when using RT-qPCR [56,82], but previous studies have shown similar disparity between dPCR and UV valuation when measuring DNA targets [103], suggesting the PCR step in the RT-dPCR may also contribute to the observed differences. The quantification divergence of these data demonstrates an assay/target specific bias attributable to the RT and/or dPCR step.

4.3.3 Linearity and Sensitivity of RT-dPCR of Synthetic RNA Targets

In order to identify RT-dPCR sensitivity and linearity of measurement for low copy targets the Ambion kit alone was used, due to its superior capabilities throughout the initial analyses. A dilution series of two synthetic RNA targets, ERCC-25 and ERCC-99, was analysed in duplex (**Figure 4.3**). Dilutions were performed based on UV evaluation, using dH₂O 0.5% v/v Tween 20 as diluent, to generate samples equating to approximately 500, 250, 100, 50, 25, 10 or 5 copies/panel.

There was a significant difference identified in RNA copy number estimates between dPCR and UV values, $p < 0.0001$ (**Figure 4.3A & B**), which concurred with previous observations (**Figure 4.2**). Both ERCC-25 and ERCC-99 displayed linear quantification capabilities, with good precision (CVs of less than 10%) achievable

Chapter 4 Comparison of Different Reverse Transcriptases by Digital PCR



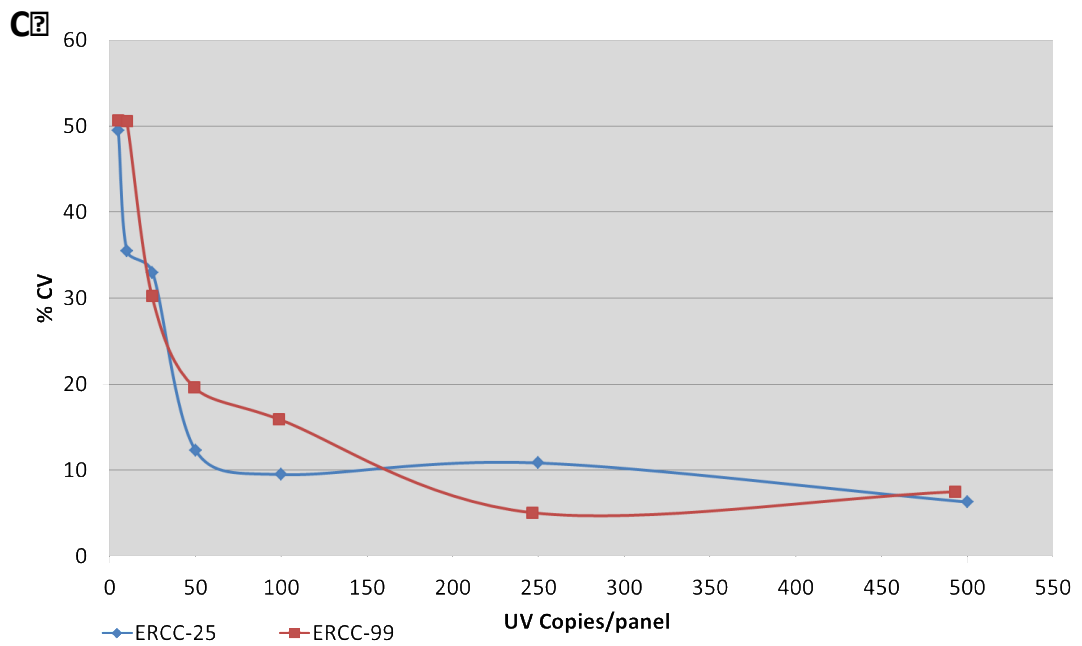


Figure 4.3 dPCR sensitivity for RNA measurement. Assessment of RT-dPCR quantification sensitivity, using independent dilutions and quantifying ERCC-25 and ERCC-99 synthetic targets in a duplex format. n = 6 panels per dilution, in two replicate experiments. UV data based on initial UV quantification of stock and predicted target levels following volumetric dilutions. (A & B) dPCR sensitivity. (B) Focus on lowest level target dilutions. Error bars: 95% confidence intervals. (C) Precision of dPCR quantification compared to UV.

down to 50 UV assigned copies (**Figure 4.3C**).

The linearity and sensitivity data clearly show a pattern of increased variability with the increase of dilution factor below 50-100 estimated copies. We have previously demonstrated that when analysing DNA targets, dPCR is highly precise down to 16 copies/panel [103] suggesting RNA measurement is more variable. (RNA at 50 estimated copies, CV 12-20%. DNA at 16 estimated copies in carrier, CV 24%).

4.3.4 Evaluation of Reverse Transcriptase's Targeting Endogenous mRNA Transcripts

In order to investigate the applicability of these findings to real samples, the same three one-step RT-qPCR kits were tested to compare measurement of endogenous targets alongside synthetic controls in various duplex combinations in the TCM (**Figure 4.4**). Again for each target, there was a significant effect of kit on dPCR quantification (all p values < 0.0001). For endogenous targets, the Ambion kit yielded the highest quantification values, as previously observed with synthetic controls: although the variability observed for UBC (within the Ambion kit) was higher than for the synthetic targets (ERCC 95% CI all <38, UBC 95% CI 100-157).

To establish whether duplex pairings influenced RT-dPCR results, duplex reactions were performed pairing different targets (Duplex A: ERCC-25 + ERCC-99. Duplex B: MMP1 + UBC. Duplex C: ERCC-25 + UBC). As observed above, there was a significant difference between the kits, but no significant difference observed in dPCR values between ERCC-25 or UBC when assessed in different duplex reactions using the Ambion reagents (ABC), p = 0.061 and 0.92, respectively. Therefore, for these targets, assays did not influence the quantification result of their duplex partners. Furthermore, measurement ratios between targets were not maintained owing to the inferior sensitivity of the Invitrogen and Qiagen kits (Ambion, Invitrogen and Qiagen ratios in duplex pairings for ERCC-25:ERCC-99 1.5, 3.26 and

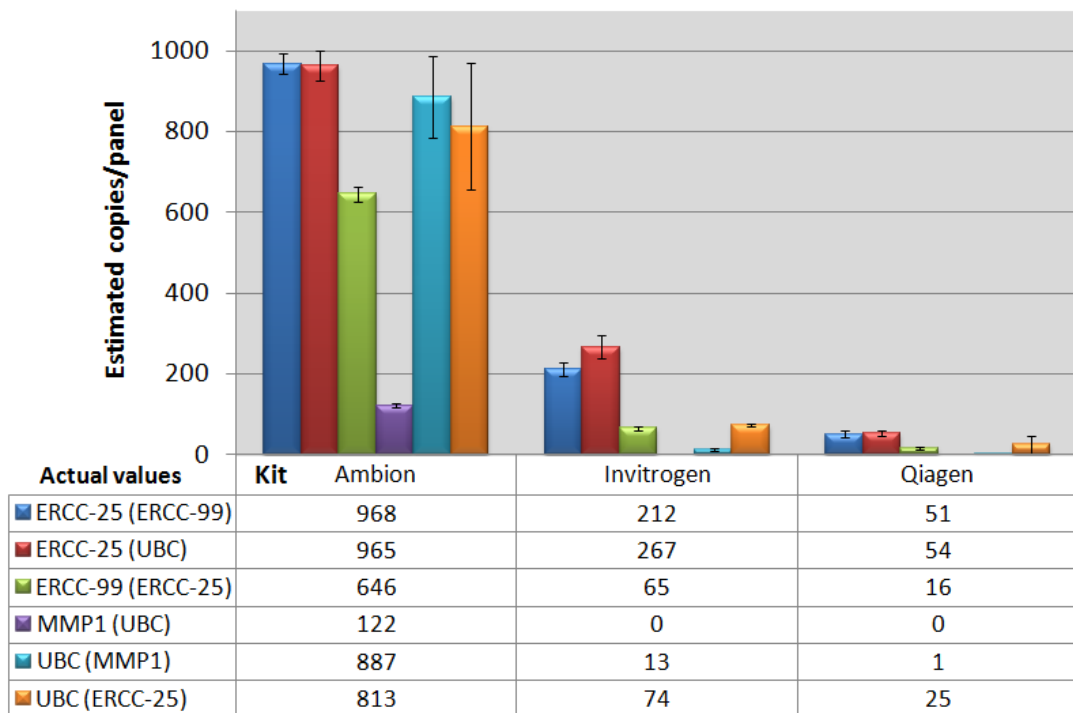


Figure 4.4 Evaluation of Reverse Transcriptases. Three different one-step RT-qPCR kits were compared in different duplex formats, by dPCR. Quantification for synthetic (ERCC-25 and ERCC-99) and endogenous (MMP1 and UBC) targets was evaluated. ERCC-25 with ERCC-99 (duplex A), UBC with MMP1 (duplex B), and ERCC-25 with UBC (duplex C). In the key/tabulated values, the assay in brackets is the duplex partner for the assay whose positive partition values are being displayed. Error bars: 95% confidence intervals. n=3 replicate panels, plus two replicate experiments. Equivalent UV estimates: ERCC-25 1886.10 copies/panel. ERCC-99 1860.30 copies/panel.

3.19, respectively. For ERCC-25:UBC 1.19, 3.61 and 2.16, respectively).

The magnitude of the difference in mean quantification values between kits was not consistent between different targets, both synthetic and endogenous, suggesting an additional assay specific and kit associated bias. There was a greater difference between kits when measuring endogenous targets than for synthetic targets. Furthermore, both Invitrogen and Qiagen kits were unable to detect MMP1 (0 positive partitions) despite being measured with six replicates totalling some 4590 partitions. However, as the Ambion kit only measured on average 112 MMP1 positive partitions, it would suggest that this transcript was below the limit of detection for the two former kits. Measurement, or specifically enzyme, efficiency/sensitivity is an important consideration when measuring low abundance RNA targets, in order to avoid false negative results and these data suggest that choice of kit is crucial for ensuring the most sensitive result when performing RT-dPCR. This also follows when performing RT-qPCR. One of the characterised applications of dPCR is for the detection of minority targets due to its increased sensitivity by increasing the signal to noise ratio (needle in a haystack). Therefore, when applying RT-qPCR for target detection, particularly minority targets, choice of kit is equally critical. It should also be noted that while MMP1 target was present at low abundance in the dilutions tested, evaluation of a more concentrated sample might circumvent the sensitivity issues associated with the two kits. Therefore, this must also be considered when validating protocols if low copy measurements are required.

4.3.5 Causes of Differing RT-dPCR Results

One of the most striking findings of this study is the large inter assay and inter kit difference in the estimated copies for a given target. There are a number of potential causes for these observations. It is clear from these data that some, if not all, of the kits analysed during this study were not measuring all the RNA molecules that were present. There may be a number of different reasons for this.

The assumption that DNA measurement by dPCR can be precise, reproducible, and absolute cannot be readily extrapolated to the measurement of RNA [230]. The RT step may introduce an additional source of variability and bias, with reaction efficiency being both assay and reagent dependent. It is a well-documented fact that RT does not convert all RNA to cDNA [57,278], which may explain these findings. RT inefficiency and variability may account for the majority of this measurement divergence, especially given that qPCR has been shown to be extremely sensitive and efficient [26,86]. In addition, several studies have shown that RT reaction components may have a reversible inhibitory effect on the subsequent qPCR, the magnitude of which depends on the RT system [47,62,69-71]. While it would be hoped that in the one-step kits investigated in this study the RT components would have minimal effect on the PCR step, one cannot rule out the possibility that as well as RNA not being converted to cDNA, failed subsequent amplification of the cDNA may also explain the underestimation. If these biases are global, then the influence of these factors will be removed if data are normalised to validated, internal reference genes.

A recent study documented a dPCR phenomenon termed molecular dropout [279]. This event is characterised as a failure to detect the presence of a target molecule during dPCR. In other words, the target molecule is present in the partition but is not amplified. Given this precedent, it is therefore plausible to assume that molecular dropout, either at the cDNA or RNA stage of the RT-dPCR process, on a much larger scale to that measured by dPCR alone, may explain why copy number detected by dPCR is lower than that predicted by UV. Moreover, it is possible that different enzymes may be affected to different degrees by this phenomenon. Indeed, given the findings of this study, it is possible that molecular dropout may occur on both an assay and kit-specific basis. Several factors may contribute to molecular dropout including reduced assay sensitivity attributable to complex template secondary structures [279], reagent inhomogeneity, whereby primers/probes/enzyme reaction components may not be evenly distributed and

thus not represented in all partitions, and PCR inhibitors that affect one assay more than another [74] (matrix effects).

Template secondary structure and position of the assay along the target length is known to impact on the RT-qPCR [86] and may therefore contribute to this molecular dropout in RT-dPCR. Previous studies [279] have shown an increased prevalence of molecular dropout when analysing gDNA as opposed to linearised plasmid, and this variability was attributed to the increased structural complexity of the gDNA. The potential impact of template secondary structure was assessed [228,229] to evaluate whether this could be a cause for molecular dropout and determine positional influences contributing to assay performance. All templates displayed a degree of secondary structure within the amplicon region (Appendix 2). When concentrating on the regions complementary to the reverse primer (used in the RT to prime cDNA synthesis), all templates exhibited some degree of stem-loop structures. However, the 3' ends of the reverse primer complementary region showed differing secondary structures. For example the 3' end within ERCC-25 was within an open (loop) structure while for ERCC-99, the final base was designed to bind to a closed (stem) region (Appendix 2, H & J). Given that the primers are extended from the 3' end, this may explain why ERCC-25 consistently gave a higher value than ERCC-99 despite their being present at the same copy number. Furthermore, in addition to being a low abundance target, the structure of the MMP1 amplicon region is complex with the largest number of predicted stem-loop structures within this location, which may in part account for the difficulty of some enzymes to detect it. MMP1 also has the longest amplicon size, at 133 bases, whereas ERCC-25 has the shortest, at 67 bases. The assay-specific bias observed between kits for different synthetic and endogenous targets maybe in part explained by predicted template secondary structures and this would also appear to be kit specific.

The recommendation from the MIQE guidelines [86] that RT primers be designed to stem loops to improve qPCR maybe a particularly important consideration when

performing RT-dPCR to improve assay sensitivity; the data presented here suggests choice of reagent has a greater impact on the measurement result (detection of MMP1 transcript was dependent on the one-step kit used for analysis). For this data set, it was not possible to quantify the impact of reagent choice compared to target secondary structure for the detection of MMP1 due to the inability of both the Invitrogen and Qiagen kits to detect it. In order to evaluate which factor (reagent choice or target secondary structure) has the biggest influence on target quantification, a set of assays targeting different regions of the same transcript could be compared to test the influence of secondary structure when using the same template. Furthermore, these assays could be evaluated using the three different one-step kits. This would help discern where the greatest impact lies. This approach would be further aided by the utilisation of a high abundance target, as in the current set-up it cannot be determined whether the low abundance of MMP1 alone influences the detection sensitivity of the one-step kit or whether other factors, such as template secondary structure, precludes its identification when employing particular kits. Further work is required to test the hypothesis that RNA structure will effect RT-dPCR sensitivity, but these findings suggest reaction efficiency may in part reflect the ability of an enzyme to negotiate strong secondary structures and successfully progress the course of the reaction and that this is specific to different kits.

The difference in the RTases themselves is likely to be the primary reason that the three kits performed differently. Both the Ambion (Multiscribe) and Invitrogen (Superscript III) RTases are derived from Moloney murine leukemia virus (MMLV) RTase. Alternatively, the Qiagen (Omniscript and Sensiscript) RTases are derived from a unique source (undisclosed). The Qiagen RTases maintain RNase H activity, while the Ambion and Invitrogen RTases are claimed to have reduced RNase H activity. If RTase pauses during synthesis (for example, when dealing with a complex secondary structure), its RNase H activity has been shown to cleave the template near the 3' terminus of the growing DNA strand [63,64]. High levels of RNase H activity may therefore suppress cDNA yield and restrict its length and thus

Chapter 4 Comparison of Different Reverse Transcriptases by Digital PCR

reduced RNase H activity may be better suited for RT-qPCR [65]. Its purported RNase H activity may be a factor in why the Qiagen kits' performance was comparatively poor. Furthermore, the buffer has an influence on the efficiency of the reaction, and these proprietary components will differ between kits. In addition, the stability of the RT buffer may become compromised following several freeze/thaw cycles.

There may be other factors contributing to RT yields. For example, the samples used were sourced from cell line lysates. Co-extracted inhibitors may affect different reverse transcriptases to different degrees. Furthermore, components of total RNA, such as rRNA and tRNA may additionally inhibit RTase efficiency [65], by competing for reagents and producing undesired products. However, the manufacturers claim that the RTase used in the Invitrogen kit is not significantly inhibited by such total RNA components although this was not specified for the other manufacturers. These considerations taken together may in part explain the disparity displayed between different one-step RT-qPCR kits.

As may be seen from this comparison, despite the precision conferred by dPCR, analysis of RNA using RT-dPCR needs to be approached with caution. While for RNA measurement the precision of the RT-dPCR technique is high, it nonetheless introduces more variability into the measurement value than dPCR alone [103]. The significant differences observed between kit sensitivities, particularly for low abundance and/or structurally complex targets (MMP1), highlight the importance of reagent choice and protocol consistency as critical if data sets are to be meaningfully compared. Furthermore, the inability to detect certain targets may be due to the choice of RTase/kit and all experimental plans should therefore be validated appropriately before embarking upon studies analysing important samples.

For accurate RNA analysis by RT-dPCR it is possible that unknown measurements should be properly correlated to an appropriate measurement standard, with a

well-defined value and uncertainty [1,6,7,230]. It may also be the case that while, unlike RT-qPCR, RT-dPCR may not need a calibration curve to assign a value, some kind of calibration molecule will be required to compensate for the assay/kit differences observed here. Using the data from **Figure 4.4**, normalisation to ERCC-25 generated values with the closest concordance between the kits. Normalisation to: ERCC-25 (analysed with ERCC-99 in duplex A), average RQ (across all targets/kits) 0.650, SD 0.408; ERCC-25 (UBC, duplex C), average RQ 0.603, SD 0.381; ERCC-99 (ERCC-25, duplex A), average RQ 1.607, SD 1.225. While normalisation of these data goes some way to aligning the values generated from different kits, it does not generate values in complete concordance. Normalisation does align Invitrogen and Qiagen kit data more closely, but these values are not in alignment with Ambion kit data. RQ range (across all targets/kits): ERCC-25 (ERCC-99, duplex A) 0.02-1.26; ERCC-25 (UBC, duplex C) 0.02-1.00; ERCC-99 (ERCC-25, duplex A) 0.06-4.11. Furthermore, relative standard deviation (RSD) estimates (standard deviation/mean) of RQ values lay within the RSD range of dPCR quantification estimates (RSD range: 0.628-0.763 for RQs, 0.03-1.57 for dPCR). In this case, normalisation using ERCC targets is limited and may not be fit for purpose for mitigating kit-to-kit differences. It is possible that because the ERCCs are synthetic targets, they do not behave in the same way as the endogenous targets, which is why their use as normalisers (at least in this experiment) is limited. Furthermore, the two ERCCs investigated for this particular comparison (ERCC-25 and ERCC-99) may not be representative of other ERCC synthetic targets in terms of, for example, their secondary structures, and it is therefore possible that other ERCC targets may behave in a more comparable way to endogenous targets. If indeed that were the case, other ERCC synthetic targets may be more appropriate for effective normalisation of endogenous targets.

All samples may be normalised to a calibrator sample, also known as a reference sample, in a similar way as performed for relative quantification by RT-qPCR. It is possible that in some cases where assay bias is observed, only gene specific calibrators will be appropriate. For accurate absolute quantification these data

suggest use of a calibrator sample, with an accurate assigned value, will allow straightforward correction of dPCR data to account for differences in enzyme efficiencies, inhibitors and molecular dropout. Such dPCR-specific calibrator materials are yet to be developed and approaches combining validated synthetic and endogenous control materials, as described here, represent a possible strategy. The full power of this technique may only be realised on their experimental incorporation.

4.4 Conclusions

This study has shown that when compared with RT-qPCR, RT-dPCR is capable of making more precise measurements of synthetic and endogenous RNA molecules in a complex RNA background. RT-dPCR quantification of RNA targets was significantly lower than that derived from UV values suggesting a possible underestimation bias. Furthermore, absolute measurements differed between the three one-step kits assessed, with bias in detection sensitivity. Linearity and precision were sustained for duplex dPCR measurement of synthetic RNA using the Ambion kit, while sensitivities differed between RNA targets. dPCR is unencumbered by the restraints of calibration curve measurements, however, the employment of dPCR-specific calibrant materials (reference samples) would facilitate greater accuracy for absolute quantification. In fact, these data suggest that this is essential to achieve the best accuracy. Furthermore, use of the TCM shows the applicability of RT-dPCR for the target-dependent selection of suitable RT enzymes. This study is novel in demonstrating application of RT-dPCR for absolute quantification of RNA endogenous and synthetic targets. These findings give strong weight to the applicability of RT-dPCR to measurement fields including RNA diagnostics and RNA viral measurement, so that greater levels of accuracy and precision may be achieved.

Chapter 5

Evaluation of the Impact of Extraction Protocol on Target Quantification

5 Evaluation of the Impact of Extraction Protocol on Target Quantification

5.1 Introduction

The experimental starting point for the vast majority of nucleic acid molecular analyses after sample acquisition is nucleic acid extraction, separating RNA and/or DNA from other components constituting a sample. There are numerous methods available for nucleic acid extraction, including both commercial kits and well established, published protocols, utilising organic separation and/or silica membrane separation systems [201,203]. In addition, different sample types (cell culture, solid tissue biopsy, bone, bodily fluids, etc.), present different challenges for successful nucleic acid extraction. Methods may have different efficiencies when applied to different sample types and the samples themselves may present physical (bone) or chemical (matrix components) inhibition to the recovery yield of the chosen method.

Following extraction, standard practices require assessment of RNA quality and quantity [86]. There are several methods available for this purpose, each of which may generate a different measure of such properties. Some methods rely on UV absorbance or fluorescence, such as the Nanodrop (Thermo Scientific) [280] or Qubit (Life Technologies) [281], respectively. Others employ gel electrophoresis for size separation (Bioanalyzer, Agilent) [282] or PCR-based detection, such as *Alu* PCR [283,284] or 3':5' ratio mRNA integrity assay [252]. Some of these methods conveniently offer both quality and quantity assessments in one (such as the Agilent Bioanalyzer), whereas others may only offer one metric and so multiple analyses must be performed in order to obtain both quality and quantity values.

The aim of this chapter was to determine the variability in yield, quality and DNase treatment of RNA across different extraction procedures, and to determine if different approaches were more beneficial when evaluating different sample

sources and/or quantities. The overall intention of this study is to demonstrate how this kind of comparison should be approached. This strategy may be applied to any comparison of methods and is not restricted to the kits evaluated in this chapter. This work helps illustrate the wider problem within the field where comprehensive assessments of the methods/kits available may not be performed in preference of using habitual approaches.

Three different extraction methods were evaluated for the extraction of total RNA from two different cell lines, SaOS-2 and Hs 683, using lysates from different cell densities. The RNA extraction step was evaluated in order to determine its impact on quantification. Furthermore, different quality metrics were applied for comparison; including the Nanodrop 1000, Qubit 2.0, 2100 Bioanalyzer and *Alu* PCR. The utility of these metrics were evaluated.

5.2 Materials & Methods

5.2.1 Lysate preparation

All cell culture of Hs 683 and SaOS-2 cell lines, up to and including lysate collection, was performed by Dr Gary Morley, LGC, Teddington. Culture and further experimental details are described in **2.1.2 Cell Lines** and **2.6 Experimental Details - Extraction Kit Comparison**. Statistical analysis was performed in collaboration with Dr. Simon Cowen, Statistician, LGC, Teddington.

Cell lysates of 17.5 mL were collected from T-175 flasks in aliquots for each cell line and lysate buffer. Four flasks per cell line were produced, one flask per each of three different lysis buffers plus a fourth for cell enumeration (Vi-Cell). The TRIzol experiment was repeated three times for an analysis of batch variability. Seven mL aliquots were prepared and stored at - 80°C.

The ability of a method to extract high quality/yield RNA may be influenced by the concentration of starting material. It is unclear whether the concentration of input lysate versus RNA yield output remains linear at different input concentrations, and whether this influences the integrity of the recovered RNA. The linearity of extraction kits is seldom explored and it is generally assumed that kits perform equally efficiently across the given reference range provided by the manufacturer. It is also worth considering how outputs are affected when input amounts are outside this range (too much or too little). It may be the case that the extent of these differences may be different for different cell types and different extraction kits.

To assess the linearity of each extraction method, lysates were extracted at different dilutions: neat, 1:2 and 1:5. Prior to total RNA extraction, the 7 mL lysate aliquots were thawed, mixed for 10 min on a spiromixer at 4°C and dilutions prepared using the appropriate lysis buffer as diluent. Aliquots of total RNA were reserved for quantification and all extracted samples were stored at - 80°C before DNase treatment.

5.2.2 Total RNA Extraction using TRIzol

Total RNA was extracted from cell lysates by following a standard TRIzol protocol (Invitrogen). One mL TRIzol lysates were incubated for 5 min at room temperature and harvested by centrifugation (12,000 × g for 10 min at 4°C) to pellet DNA and cell debris. Chloroform (Sigma) was mixed with the supernatant (200 µL of chloroform for every 1 mL of TRIzol). Following phase separation using centrifugation (12,000 × g for 15 min at 4°C), RNA was collected in the upper aqueous phase and precipitated at room temperature using 0.5 mL absolute isopropyl alcohol (Sigma) per 1 mL TRIzol. The RNA pellet was washed with 75% ethanol (Sigma) before resuspension in 50 µL nuclease-free water (Life Technologies).

5.2.3 Total RNA Extraction using RNeasy Mini Kit

Total RNA was extracted from cell lysates by following the “Purification of Total RNA from Animal Cells” protocol in the kit handbook [285]. RLT buffer (containing 1% beta-mercaptoethanol) was used to collect lysates, 600 μ L aliquots of which were homogenized using a QIAshredder spin column. One volume of 70% ethanol was mixed with the eluate and transferred to an RNeasy spin column. After separation using centrifugation (8,000 \times g for 15 s), the silica membrane-bound RNA was washed with 700 μ L of RW1 buffer followed by 500 μ L of buffer RPE (both at 8,000 \times g for 15 s). A further 500 μ L of buffer RPE was used to wash the membrane (30 s) and the membrane spun dry for 2 min at full speed. Total RNA was eluted in 50 μ L nuclease-free water (Life Technologies).

5.2.4 Total RNA Extraction using MasterPure RNA Purification Kit

Total RNA was extracted from cell lysates by following the manufacturers’ protocol (Epicentre, Cambio). Fifty μ g Proteinase K (Epicentre and Qiagen) was added to 300 μ L Tissue and Cell Lysis Solution lysates and incubated at 65°C for 15 min with frequent vortexing, before placing samples on ice for 3-5 min. Addition of 175 μ L MPC Protein Precipitation Reagent (a high concentration salt solution containing a precipitation carrier) preceded centrifugation (10,000 \times g for 10 min at 4°C). Total RNA was precipitated from the supernatant using 0.5 mL isopropyl alcohol (Sigma). The RNA pellet was washed with 70% ethanol (Sigma) before resuspension in 35 μ L of TE Buffer. Samples were incubated at 26°C for 15 min to aid resuspension of the pellet.

RNA was eluted or resuspended in nuclease-free water or TE buffer and volume specified by individual kits.

5.2.5 Post-Extraction Treatment

Following total RNA extraction, all samples were DNase treated, purified and subjected to the following quality metrics; Nanodrop, Qubit, 2100 Bioanalyzer and *Alu* PCR, as described in **2.6.6 RNA Quality Metrics**.

5.3 Results & Discussion

Standard procedures require an assessment of RNA quality/integrity and quantity following extraction from test material. Typically, one metric is applied, such as UV absorbance, which will generate an estimate of both RNA yield and integrity. A nanodrop was used for an initial assessment of yield and quality for RNA derived from different extraction kits. Following this initial assessment, different quality metrics were compared.

5.3.1 Effect of Extraction Protocol on RNA Yield

Total RNA extracted from two different cell lines (Hs 683 and SaOS-2) were DNase treated and analysed by UV absorbance for an assessment of yield generated by three different extraction kits (**Figure 5.1**).

Two-factor ANOVA (kit versus dilution) revealed a significant effect of extraction kit for both cell lines, both $p < 0.001$. There was also a significant interaction between the two terms (dilution and kit) for Hs 683 ($p = 0.012$) and SaOS-2 ($p = 0.007$), suggesting the yields of some kits (TRIZol) may be influenced by dilution level. Dilution did not significantly affect Hs 683 total RNA yields ($p = 0.322$), suggesting linear extraction efficiencies across this dilution range for these cells. Dilution significantly influenced SaOS-2 total RNA yields ($p < 0.005$); suggesting extraction efficiencies were not linear across this dilution range (two-factor ANOVA, kit versus dilution). However, on further analysis it was determined that the significant impact of dilution on total RNA yield for the SaOS-2 cell line was attributable to the TRIZol extraction kit alone (single-factor ANOVA, $p = 0.023$),

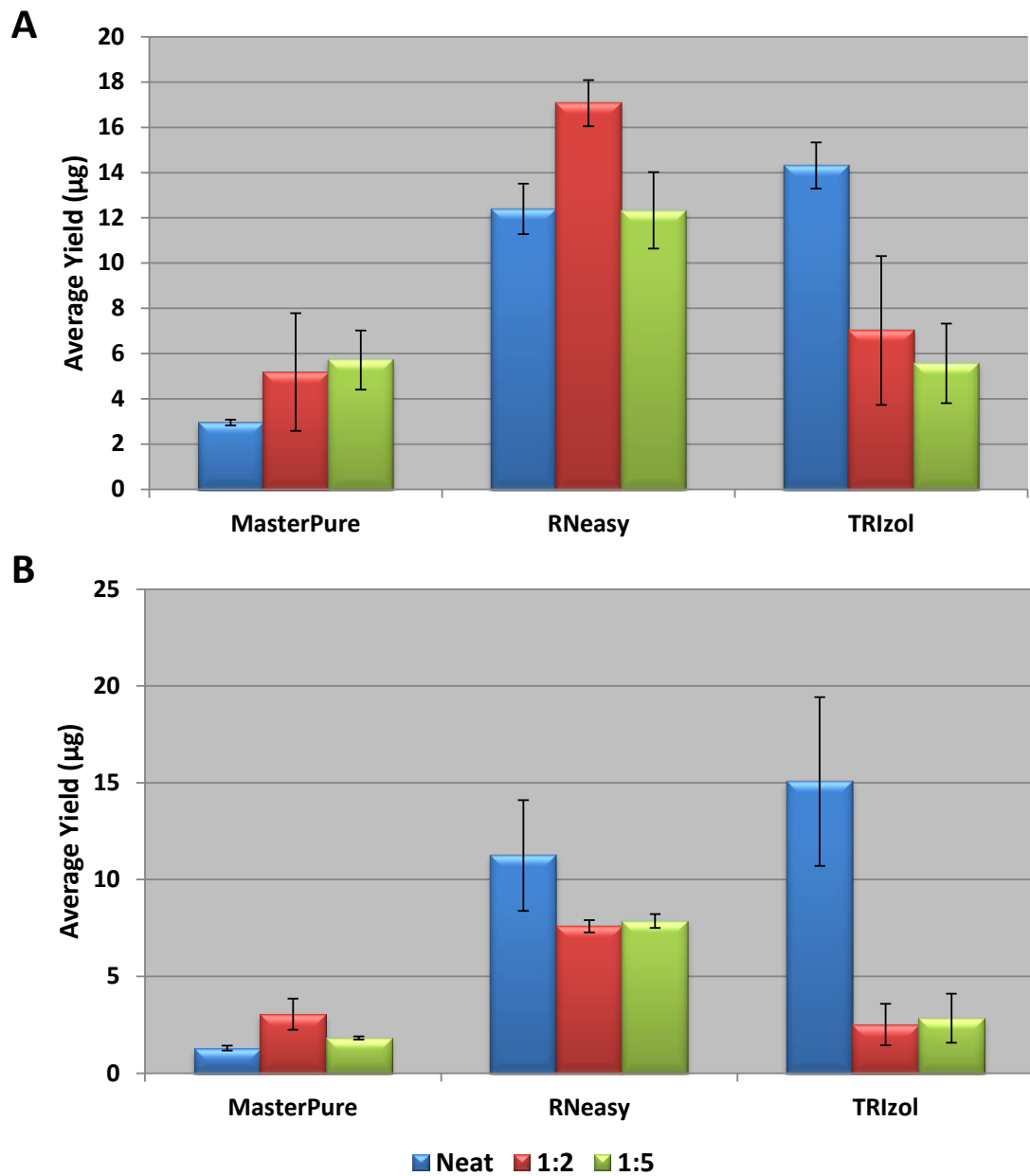


Figure 5.1 Average total RNA extracted by each extraction method. Post DNase RNA yields have been normalised for dilution (multiplied by respective dilution factor). Triplicate extractions were analysed with triplicate UV measurements. (A) Hs 683 cell-derived RNA. (B) SaOS-2 cell-derived RNA. Error bars SEM.

suggesting that the MasterPure and RNeasy kits did in fact maintain linearity in extraction across the dilution range.

The error bars plotted in **Figure 5.1** are SEM. Multiplying the SEM error by an appropriate coverage factor (to give 95% confidence intervals) gives largely overlapping error bars in keeping with statistical outcomes (no significant differences in RNA yields between dilutions for Hs 683). However, these error bars cross zero (y-axis) and so are theoretically not valid, which is why they have not been plotted here. This suggests that the statistical model is not powerful enough to detect true differences, as the extractions do appear to be quite variable. This may be improved in the future by increasing the number of samples analysed.

These data demonstrate that different kits have varying efficiencies when extracting RNA and that not all kits extract RNA in a linear manner. The TRIzol method for example was variable in its RNA extraction yield linearity. Linearity was influenced by sample source (cell line), with Hs 683 cell extracts maintaining linearity throughout the dilution range, while SaOS-2 cell extracts did not. To provide relevant and reliable results, RNA needs to be effectively and reproducibly purified from various heterogeneous materials such as fresh or frozen tissues, cell lines, PCR products or long-term chemically preserved samples [258]. The efficiency of the extraction may be dependent on the concentration of input material, although additional factors such as sample matrix may further affect extraction efficiency [286]. While not all the kits specified a lower limit for sample input (RNeasy kit stated a minimum of 100 cells), all lysate dilutions contained $\geq 1.0E+05$ cells per lysate aliquot extracted. However, amount of input material appeared to be a limiting factor in terms of yield/extraction efficiency. Potential differences in kit yields need to be considered in any comparison studies. The differences between extraction kits are particularly important when limited source material is available (e.g. clinical biopsies), or extractions must be made from difficult material (e.g. bone, formaldehyde-fixed paraffin-embedded (FFPE) samples or compromised samples containing a lot of contaminating material). For

these samples and experiments, the TRIzol extraction yielded the most RNA for the neat extracts ($> 14 \mu\text{g}$), followed by RNeasy ($> 10 \mu\text{g}$) and MasterPure ($< 4 \mu\text{g}$), whereas for diluted samples the RNeasy extraction yielded the most RNA for both 1:2 and 1:5 extracts ($> 7 \mu\text{g}$ for both dilutions), followed by similar yields from TRIzol and MasterPure kits ($< 7 \mu\text{g}$ for both kits and both dilutions).

5.3.2 Effect of Extraction Protocol on RNA Quality

In addition to an assessment of quantity, the same total RNA extracts underwent a quality assessment. This initial assessment was also performed using the UV absorbance measurement. The Nanodrop instrument gives a quality assessment based on UV absorbance ratios at 260/280 and 260/230 nm (**Figure 5.2** and **Table 5.1**).

There was a significant difference observed in Hs683 RNA 260/280 and 260/230 ratios both between dilution levels and between extraction kits (260/280: $p = 0.036$ and $p < 0.001$, respectively. 260/230: both $p < 0.0001$). For 260/280 ratios, there was also a significant interaction between the two terms (dilution level and extraction kit), $p < 0.001$. However, for 260/230 ratios there was no significant interaction between the two terms (dilution level and extraction kit), $p 0.080$.

There was a significant difference observed in SaOS-2 RNA 260/280 and 260/230 ratios both between dilution levels and between extraction kits (260/280: $p = 0.024$ and $p < 0.001$, respectively. 260/230: both $p < 0.0001$). There was also a significant interaction between the two terms for both sets of ratios (dilution level and extraction kit), $p < 0.032$ and $p < 0.015$, 260/280 and 260/230 ratios respectively.

A 260/280 ratio of approximately 2.0 and a 260/230 ratio of approximately 1.8-2.2 are generally accepted as ideal for pure RNA [256-258]. Ratios (for either 260/280 or 260/230) lower than expected maybe as a result of contamination by

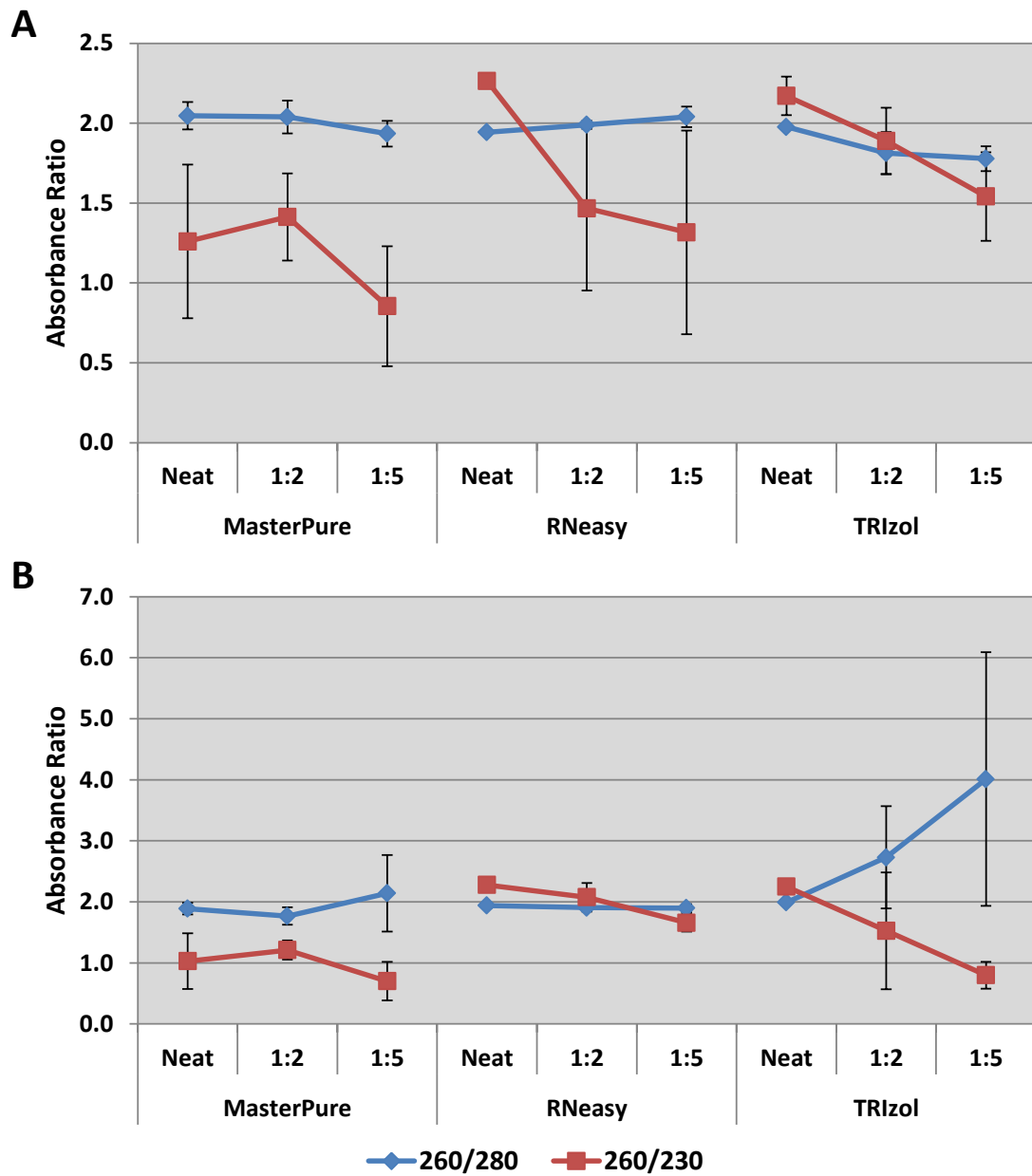


Figure 5.2 RNA Nanodrop quality absorbance assessment. Absorbance ratios at 260/280 and 260/230 nm were compared for RNA extracts performed at different lysate dilutions using different extraction kits. (A) Hs 683 cell-derived RNA. (B) SaOS-2 cell-derived RNA. Error bars 95% CI. Triplicate measurements were performed on triplicate extracts.

Table 5.1 Nanodrop quality assessment based on UV absorbance ratios at 260/280 and 260/230 nm. (A) Average values across all dilutions (neat, 1:2 and 1:5) for each of the extraction kits assessed. (B) Average values across all extraction kits (MasterPure, RNeasy and TRIzol) for each of the dilutions assessed. SEM = standard error of the mean. n = 27 for each comparison.

A

Cell line	Ratio	Kit	Mean	SEM
Hs 683	260/280	MasterPure	2.01	0.02
		RNeasy	1.99	0.01
		TRIzol	1.86	0.03
	260/230	MasterPure	1.18	0.10
		RNeasy	1.68	0.14
		TRIzol	1.87	0.07
SaOS-2	260/280	MasterPure	1.93	0.10
		RNeasy	1.91	0.01
		TRIzol	2.91	0.35
	260/230	MasterPure	0.98	0.09
		RNeasy	2.00	0.06
		TRIzol	1.52	0.18

B

Cell line	Ratio	Dilution	Mean	SEM
Hs 683	260/280	Neat	1.99	0.01
		1:2	1.95	0.03
		1:5	1.92	0.03
	260/230	Neat	1.90	0.11
		1:2	1.59	0.10
		1:5	1.24	0.12
SaOS-2	260/280	Neat	1.94	0.02
		1:2	2.13	0.14
		1:5	2.68	0.35
	260/230	Neat	1.85	0.13
		1:2	1.60	0.16
		1:5	1.05	0.10

residual phenol, guanidine, or other reagents carried over from the extraction protocol [12,125,126,256]. Such contamination might also result in an overestimation of the nucleic acid quantity. High 260/280 purity ratios are not necessarily indicative of a problem. However, a very high ratio can suggest a poor quality blank eliminating too much signal near the 280 nm wavelength [256]. At very low concentrations (less than 10 ng/ μ L) inaccuracies in the nanodrop measurement may also be encountered [256]. This will affect both the concentration estimate and the purity estimate based on absorbance ratios. Small changes in the pH of the solution are also known to cause variability in the 260/280 absorbance ratio [127,258].

The majority of 260/280 measurements are approximately 2.0 (excepting the TRIzol 1:5 dilution for SaOS-2). The majority of 260/230 estimates are below 1.8, which may indicate a degree of contamination or may reflect the low yields in some of these samples (low yields may hinder the accurate estimate of absorbance ratios). Hs 683 TRIzol and SaOS-2 RNeasy samples gave the best approximations to pure RNA [256-258].

Although purity ratios can be indicators of sample quality, the best indicator of nucleic acid quality is functionality in the downstream application of interest. An RNA sample with an absorbance ratio outside the recommended values may still function well for RT-qPCR or other downstream applications [258], as for example, some fragmentation of target may actually open up previously inaccessible regions to PCR enzymes and primers. Likewise there are occasions when the purity ratios are within expected limits, yet there is a problem with sample performance in downstream applications [256]. Nevertheless, these metrics may still give an indication of sample quality and are often estimated concurrently with quantity estimates, required for downstream applications, and so no additional effort or sample is required for their estimation. However, UV absorbance ratio values are not necessarily a robust estimation of quality [130]; quantity alone may be sufficient for downstream applications. Unfortunately, this method of measuring

quantity is linked to the measurement of quality (UV absorbance) and so low quality estimates may influence quantity estimates, potential generating underestimated concentrations. Ideally, measurement of quantity would be independent of quality to prevent introduction of bias. Future studies to evaluate the effect of quality on abundance valuation would include the use of contaminants to adjust quality estimates and compare quantities with control samples. Furthermore, as discussed in the introduction to this chapter, UV absorbance and other methods such as capillary electrophoresis assess the quality of a total RNA population, rather than specifically the mRNA fraction. Methods such as 5'-3' ΔC_q that evaluate the integrity of the mRNA transcripts used as template for RT-qPCR analyses, may be more informative [130,252].

5.3.2.1 Assessment of gDNA Contamination

The *Alu* sequence is highly abundant throughout the genome (approximately 1 million copies) [130] and as such offers an opportunity to measure residual gDNA contamination in total RNA extracts pre- and post-DNase treatment. *Alu* PCR analysis was performed on samples pre- and post-DNase treatment and post RT. Samples measured: Hs 683 post-DNase (all dilutions), SaOS-2 pre-DNase (neat only), SaOS-2 post-DNase (all dilutions), SaOS-2 post-RT (neat only).

A significant difference in *Alu* signal was observed between extraction replicates at any dilution (all $p < 0.05$), different kits at any dilution (all $p < 0.001$) and different dilutions (all $p < 0.001$). Furthermore, an interaction was observed between different dilutions and different kits (all $p < 0.05$) (**Figure 5.3**). Samples appear to show non-linearity, with the 1:2 lysate dilution showing the highest values for genome equivalents in the SaOS-2 cell line (**Figure 5.3B**). The result for neat samples may be attributed to either inhibition or assay/sample saturation, which could be tested by performing a dilution series of the neat lysate preparations pre-PCR [287]. Alternatively, the DNase treatment may be more

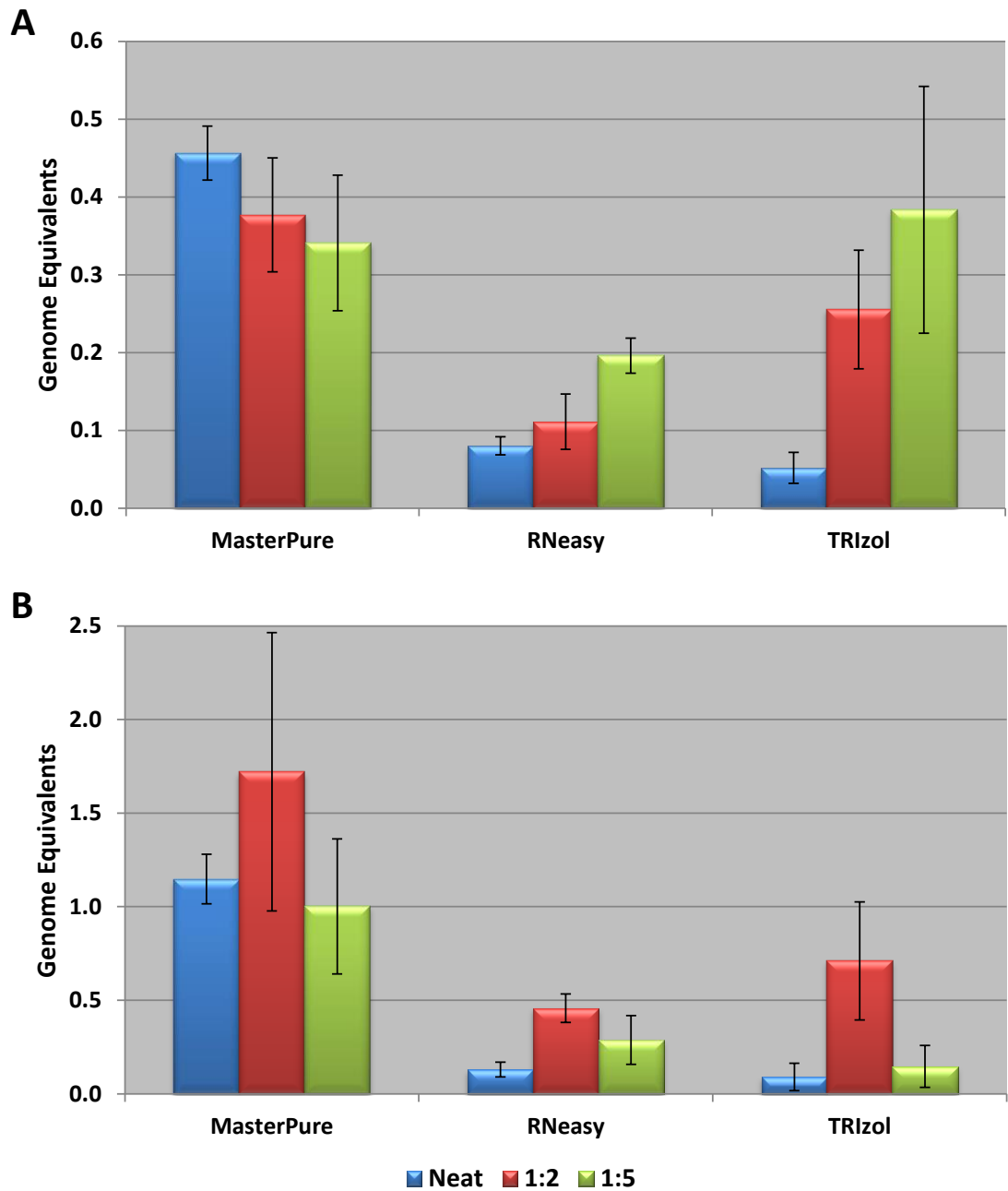


Figure 5.3 *Alu* PCR analysis of samples extracted using different methods. *Alu* PCR Post-DNase. gDNA measured by qPCR was converted to genome equivalents. (A) Hs 683 cell-derived RNA. (B) SaOS-2 cell-derived RNA. Normalised for dilution (multiplied by respective dilution factor). Error bars 95% CI.

efficient in the neat SaOS-2 sample due to a greater availability of DNA substrate, and so have a greater impact on the removal of gDNA.

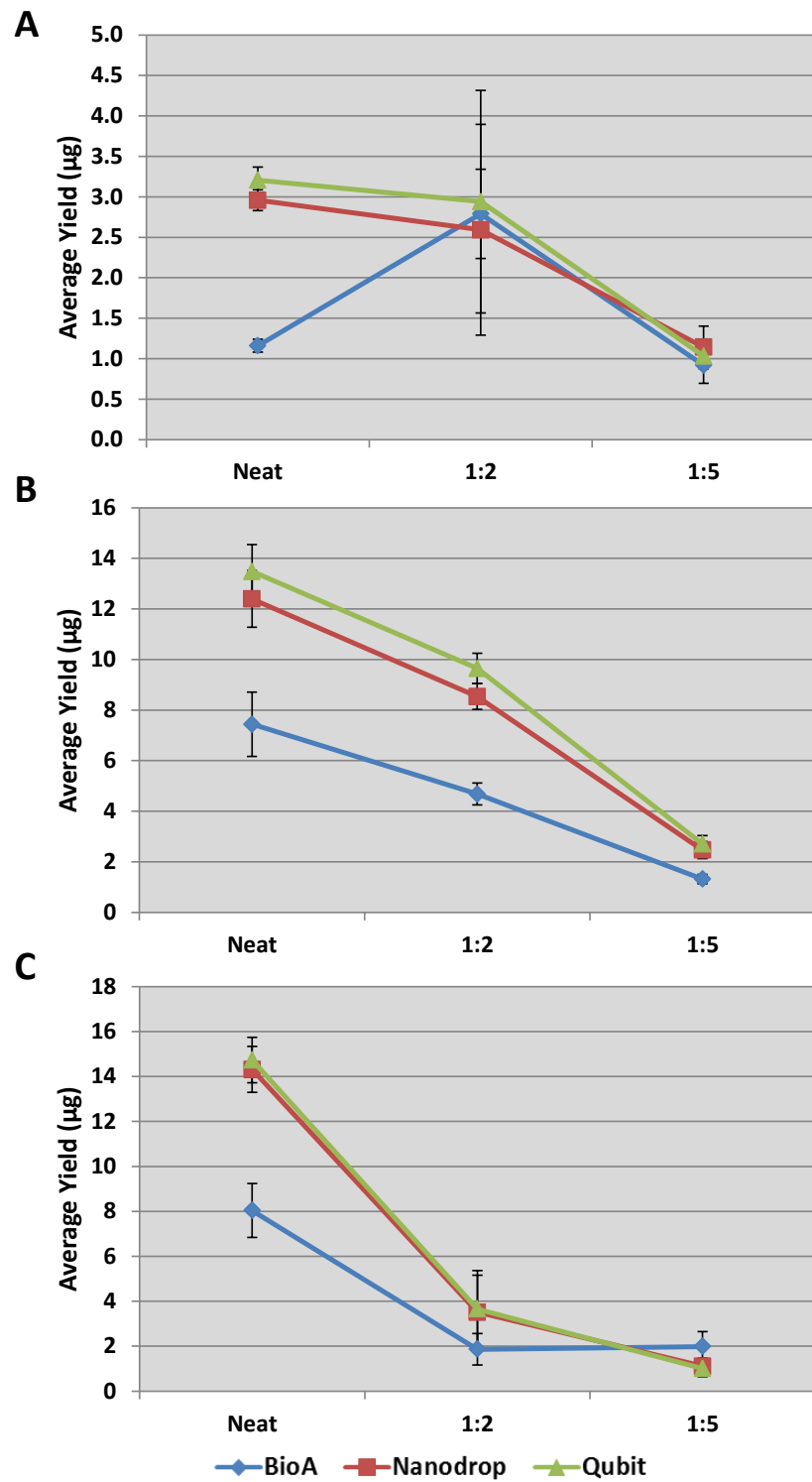
Standard curves for linearity of *Alu* PCR were performed alongside unknown samples. All efficiencies were between 90 and 110%, although this was using a gDNA standard. The assay was linear over the 5 log range measured (all $R^2 > 0.990$. All $p > 0.994$), suggesting neat samples were not assay saturating. Therefore, the differences between neat and 1:2 diluted lysates may be due to inhibition effects or greater efficiency of the DNase treatment in neat samples.

It is observed from the *Alu* PCR data that the DNase treatment was more efficient in removing gDNA contamination in RNeasy and TRIzol extracts than in MasterPure extracts. The components of the extraction buffers and wash solutions used as part of the MasterPure protocol may have an inhibitory effect on DNase activity, resulting in a lower efficiency of gDNA removal. It is unlikely that extraction (or indeed DNase) components inhibited the *Alu* PCR as samples were purified post-DNase treatment.

5.3.3 Effect of Quality Assessment Method on RNA Yield

Total RNA yield estimations were compared between UV absorbance (Nanodrop), fluorescence (intercalating dye, Qubit) and capillary electrophoresis (Bioanalyzer) measurements.

It is clear from these data that the different measurement approaches generated different yield estimates (**Figure 5.4**). There was a significant difference observed in RNA yield estimates for both cell lines and at all dilution levels between different extraction kits and different quantity estimation methods (metric) ($p < 0.05$ for all), except for metric at the 1:5 dilution in Hs 683 cell-derived RNA ($p = 0.796$) and metric at the neat dilution in SaOS-2 cell-derived RNA ($p = 0.066$). However, for Hs 683 neat and 1:2 lysate dilutions, there was no significant



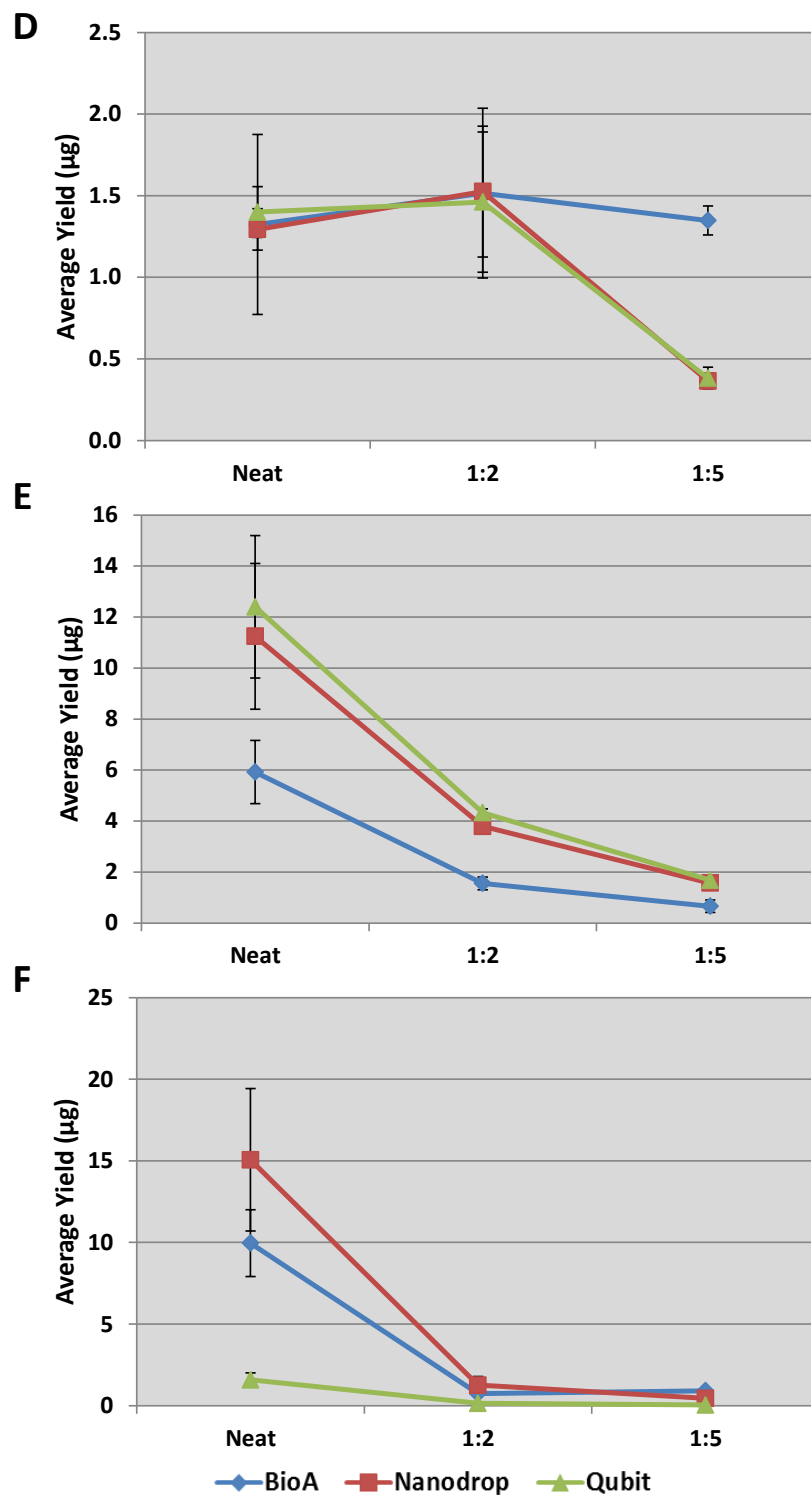


Figure 5.4 RNA yields according to different metrics. (A) Hs 683 cells MasterPure. (B) Hs 683 cells RNeasy. (C) Hs 683 cells TRIzol. (D) SaOS-2 cells MasterPure. (E) SaOS-2 cells RNeasy. (F) SaOS-2 cells TRIzol. Error bars SEM.

interaction between the two terms (extraction kit and metric), $p = 0.094$ and 0.262 , respectively. There was a significant interaction between the two terms for the 1:5 dilution only, $p = 0.034$. For SaOS-2 at all dilution levels, there was a significant interaction between the two terms (extraction kit and metric), $p < 0.01$ for all. All analysis performed using two-factor ANOVA.

The Bioanalyzer estimates were generally lower than for the other two metrics (Nanodrop and Qubit), although these differences were also influenced by dilution level, with the RNA derived from diluted lysate being in better agreement with the Nanodrop and Qubit estimates. It is possible that this discrepancy is due to the calibration of ladder peaks required for the Bioanalyzer measurement. The additional differences between reagent batches have huge implications for the variability between measurements [47,90]. These data are of particular importance when such metrics are to be used for value assignment of a standard solution [12]. Reliance on a particular metric for value assignment may lead to bias in target quantification using a standard curve approach whereby the standard has been value assigned using one of these methods. Where qPCR absolute quantification against a standard curve has been utilised, disparity may become apparent when inter-laboratory comparisons are made where different metrics have been employed in the value assignment of a standard. These biases may not be recognised in originating from the different metric approaches and so differences between laboratories may be wrongly attributed to random variation. Using the yield data in the example above, neat sample quantity estimates were used to simulate a standard curve measurement by RT-qPCR (assuming 100% efficiency) and fold change in test sample quantity estimates based on these standard curves were compared. The biases introduced by the method used for RNA yield evaluation are shown in **Table 5.2**. These biases no longer have an influence if fold change/relative measurements are made instead (using endogenous reference genes).

Nanodrop, Qubit and Bioanalyzer quality metrics are all positively correlated

Table 5.2 qPCR measurement bias introduced by standard curve value assignment.

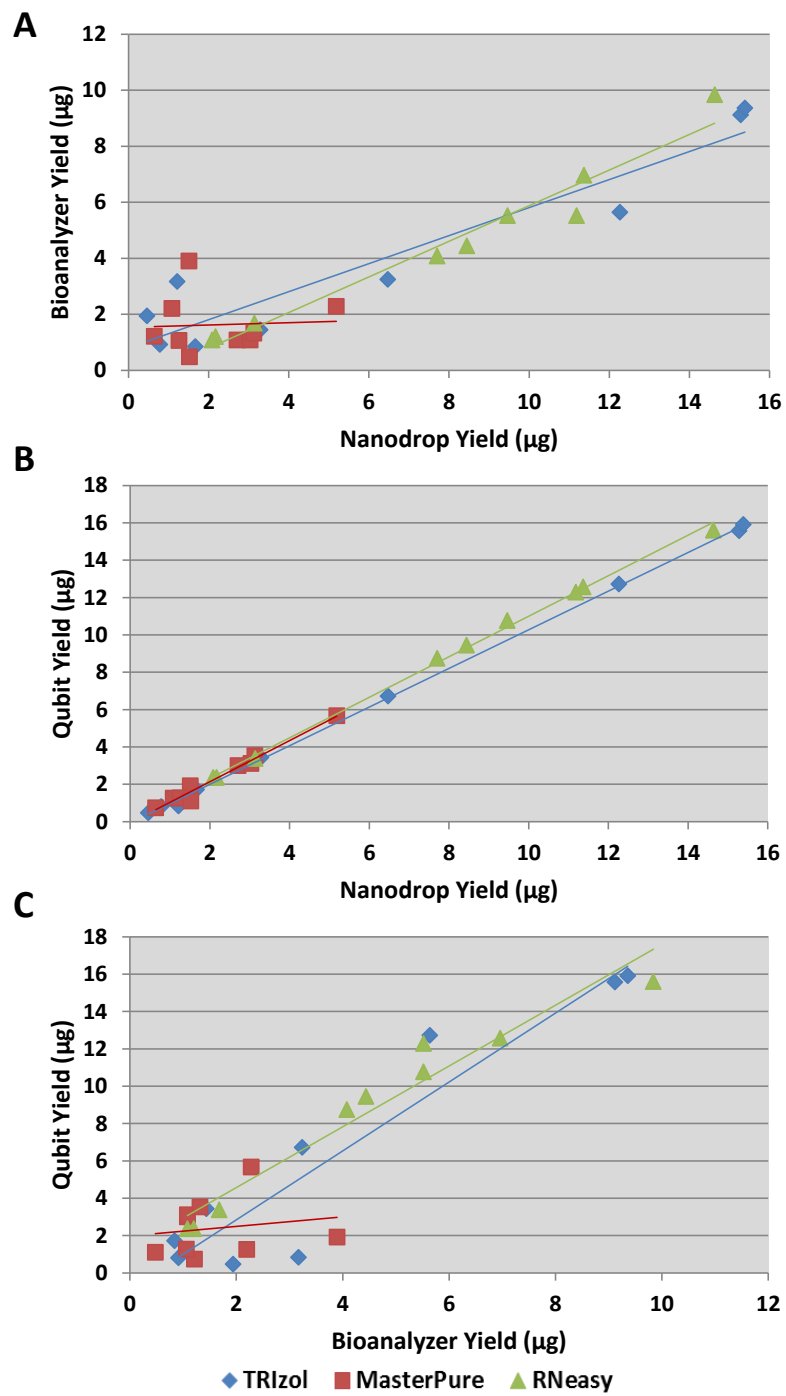
Theoretical fold change measurements of a test sample as a result of using a standard curve that has been value assigned using different RNA quantity metrics. Assuming 100% RT-qPCR efficiency. The Qubit gave the highest quantity measurement estimates for both cell lines and all extraction kits.

Cell line	Kit	Fold change (from Qubit standard curve)		
		Nanodrop	Qubit	Bioanalyzer
Hs 683	MasterPure	0.92	1.00	0.36
	RNeasy	0.92	1.00	0.55
	TRIzol	0.97	1.00	0.55
SaOS-2	MasterPure	0.92	1.00	0.95
	RNeasy	0.91	1.00	0.48
	TRIzol	0.95	1.00	0.63

(>0.9) (**Figure 5.5**), for both cell lines and all dilutions, except for the Bioanalyzer results with the MasterPure kit (no correlation observed with Nanodrop and Qubit). As the MasterPure extracted lysates are diluted, for Bioanalyzer measurements only the extracted concentration was no longer proportional to the number of cells extracted (the ratio was not maintained, **Figure 5.5A, C, D & F**). The Nanodrop and Qubit metrics show much lower yields for the MasterPure extracts. The fact that extraction kit has an effect on the performance of the quality metric may be influenced by extraction factors (such as efficiency) and matrix effects (co-purified contaminants). It may be the case that the Bioanalyzer metric was more sensitive to co-purified contaminants in the MasterPure extracted RNA than the Nanodrop and Qubit metrics, or alternatively, the Bioanalyzer may be less sensitive for measuring low concentrations. Furthermore, the MasterPure kit performed poorly in terms of yield when compared to TRIzol and RNeasy kit yields. This low yield and potential contaminant carryover combination may be particularly unfavourable to the effective application of the Bioanalyzer metric. If the ribosomal bands used for value assignment by the Bioanalyzer are weak, the instrument will struggle to quantify against the ladder. Furthermore, calibration of ladder peaks may explain Bioanalyzer yield discrepancies.

When measuring Hs 683 neat lysate RNA extracts, precision estimates were smallest for Nanodrop and Qubit metrics, with CVs between 7 and 16% for the three extraction kits. Bioanalyzer CVs were highest, between 11 and 30%. The highest CV estimates (lowest precision) were attributable to the RNeasy extracts (13 to 30%). Measuring Hs 683 RNA for all extraction kits, precision in metric measurements decreased (increased CV) when diluted lysate RNA extracts were assessed (between 10 and 87%). Counter to the neat lysate RNA extract measurements, the highest precision (lowest CV) for the diluted lysate RNA extracts was observed for the 1:2 lysate dilution RNeasy extracts, between 10 and 16%.

For SaOS-2 RNA extracts (at all lysate dilutions), precision was lower than for Hs



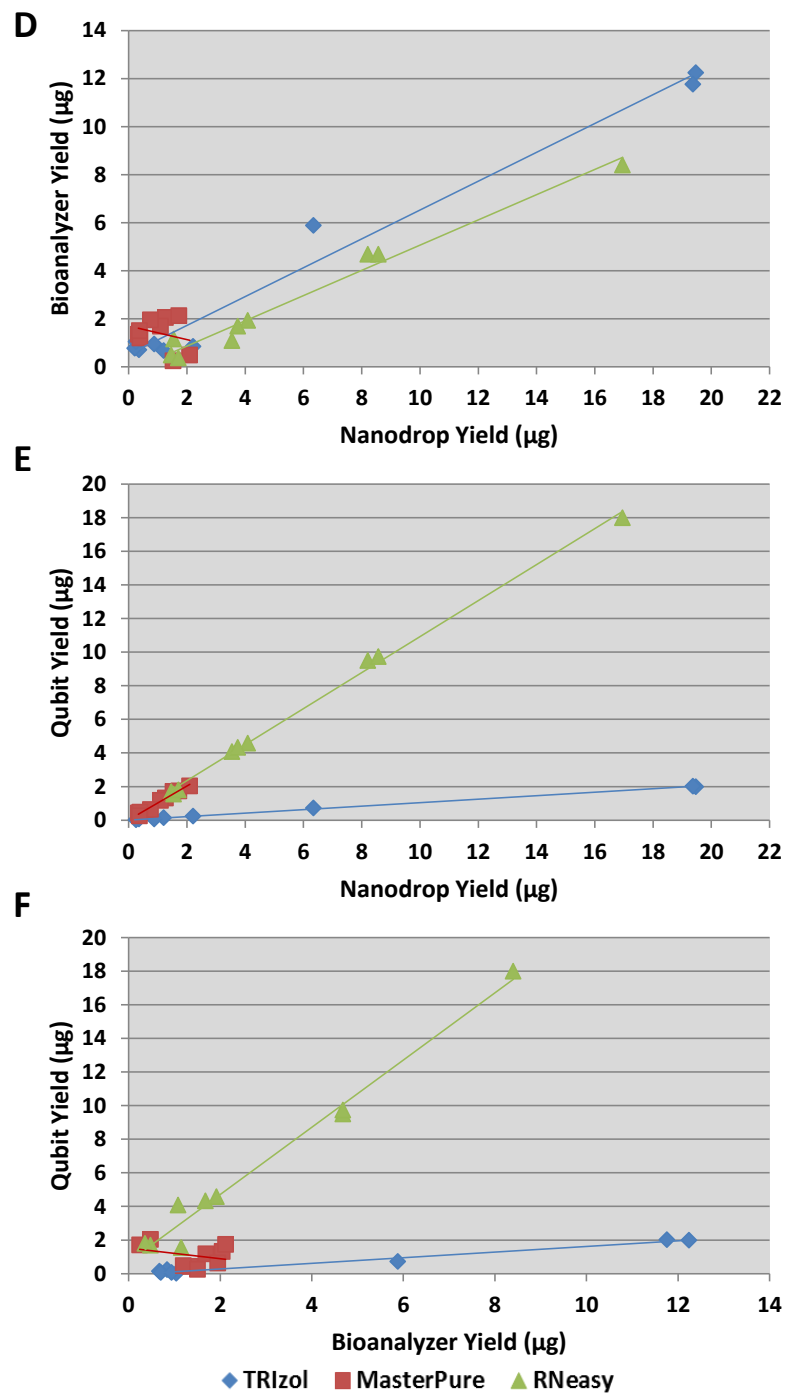


Figure 5.5 Quality Metric Correlation Plots of Yield Estimates. All dilution levels are represented. (A-C) Hs 683 cell-derived RNA. (D-F) SaOS-2 cell-derived RNA. R² values for MasterPure, RNeasy and TRIZOL, respectively: (A) 0.0034, 0.9585, 0.8972 (B) 0.9777, 0.9977, 0.9994 (C) 0.0268, 0.9451, 0.8859 (D) 0.0747, 0.9771, 0.9788 (E) 0.9744, 0.9971, 0.9987 (F) 0.1007, 0.9809, 0.9823.

683 RNA extracts, with CVs between 5 and 89%. However, precision estimates were randomly distributed throughout the sample set, with no apparent trend relating to lysate dilution or extraction kit.

The accuracy of the quantity assessment may be dependent on the composition (purity and integrity) of the extracted material. The different metric methods are estimating quantity by different means (Nanodrop: UV absorbance, Qubit: intercalating dye fluorescence and Bioanalyzer: capillary electrophoresis and intercalating dye fluorescence) and as such, may be affected to different extents by co-purified contaminants such as proteins, phenol and salts, as well as remaining gDNA (inefficient *DNase* treatment). It is well documented that A_{260} measurements are susceptible to extraction contaminants and changes in pH [12,47,103,125-128]. It should be noted that RNA pellets were resuspended in TE buffer for the MasterPure kit, whereas the RNeasy and TRIzol kits used nuclease-free water. This was done according to manufacturer's protocols and it is assumed these recommendations are for optimal results.

Approaches using fluorescent dyes typically require a calibration curve where the calibrator has usually been assigned a value based on A_{260} measurement. In that case, the fluorescent dye approach may propagate the same errors inherent to the A_{260} measurement. As a result, while the Nanodrop and Qubit measurements are in good agreement, they may not be accurate as they may share equal bias. Furthermore, the Qubit may be considered to use an indirect measurement approach, as the bound fluorophore fraction is actually what is being measured. This gives rise to the possibility that not all RNA has fluorophore bound or that contaminants in the RNA sample may affect fluorophore binding or fluorescence.

Gel electrophoresis is not commonly used for quantity estimates where other methods are available due to its subjective nature (based on band intensity). However, with automated capillary electrophoresis systems available, analyst subjectivity is removed in deference to autonomous digital data. The Bioanalyzer

has been shown not to be subject to influence by phenol contamination, but is influenced by low molecular weight DNA contamination [288]. *Alu* PCR analysis (**Figure 5.3**) revealed that removal of gDNA contamination by DNase treatment was more efficient in RNeasy and TRIzol extracts than in MasterPure extracts. This may account for why the Bioanalyzer yield estimates were low compared to Nanodrop and Qubit estimates for the MasterPure kit (residual gDNA may negatively impact of the RNA quantity estimation). While the electropherograms for measured samples looked clear in terms of degraded RNA/gDNA contaminants (**Figure 5.6**), 11 out of a total 18 MasterPure samples were too dilute to be measured by a Bioanalyzer nano chip (were measured by a pico chip). The low abundance of RNA in these samples may be more subject to the contaminating influences of gDNA.

All samples measured (except one: SaOS-2 replicate TRIzol extract of the 1:5 diluted lysate measured by the Qubit) were within the dynamic range of each respective metric. Nanodrop: 2-3000 ng/ μ L, Qubit: 1-1000 ng/ μ L, Bioanalyzer nano chip: 25-500 ng/ μ L, Bioanalyzer pico chip: 50-2000pg/ μ L (from manufacturer's protocols). However, some samples measured were approaching the limit of the dynamic range of these metrics and as such may be subject to increased variability/error in their quantity estimates [289]. It can be assumed therefore, that for the majority of samples the different metrics were linear in their measurement of RNA quantity. Any non-linearity observed therefore, would likely be attributed to a lack of linearity in the RNA extraction itself.

5.3.4 Effect of Quality Assessment Method on RNA Quality

Quality assessment of the RNA extracts was made by 260/280 and 260/230 ratios from the Nanodrop measurement (evaluated in **5.3.2 Effect of Extraction Protocol on RNA Quality**) and the RNA integrity number (RIN) from the Bioanalyzer measurement (evaluated below). The Qubit instrument gives no indication of RNA integrity.

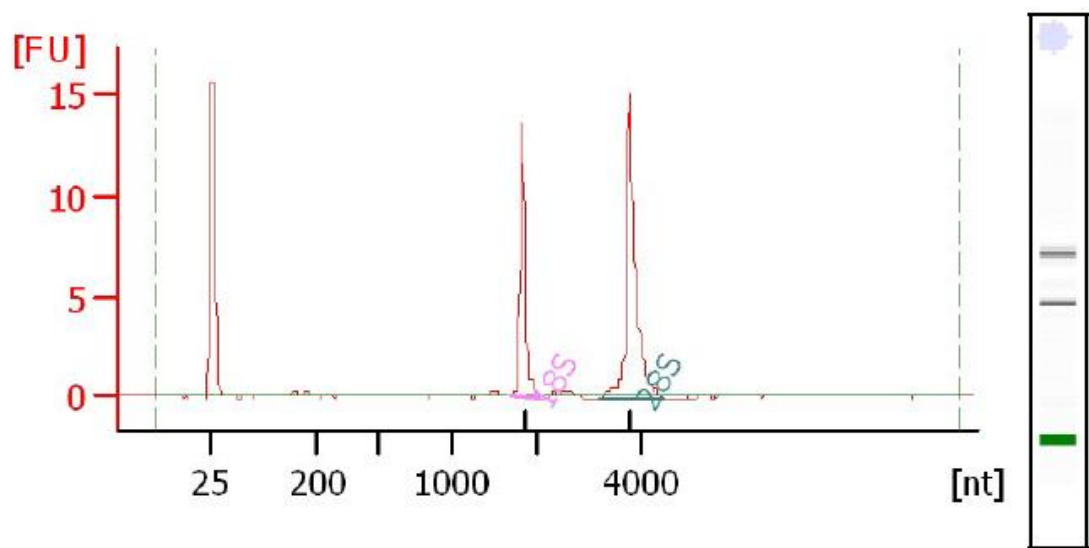


Figure 5.6 Representative Bioanalyzer electropherogram. Measurement of Hs 683 cell-derived RNA extracted from 1:2 diluted lysate using the MasterPure kit. RIN 9.5. 18S and 28S peaks are highlighted. Associated gel image shown alongside the plot. No gDNA or degraded RNA smearing observed.

Figure 5.7 shows the integrity of the various samples as determined by the Bioanalyzer RIN value. The RIN metric indicates the degree of RNA fragmentation, with increasing values representing more intact RNA [290]. Unfortunately, owing to the low concentration of several samples and subsequent analysis using the pico (rather than nano) Bioanalyzer chip, which does not provide an estimation of sample RNA integrity with a RIN value, there were too many data points missing to generate reliable statistical analyses. (Seven Hs 683 and 13 SaOS-2 samples were evaluated using a pico chip). However, on visual inspection of these data all except one sample (SaOS-2 RNA derived from one replicate extract of neat lysate using the MasterPure kit, RIN 4.6), had associated RIN values > 5, which is recognised as sufficient quality for RT-qPCR analysis [265,291]. Furthermore, all Hs 683 samples (20/20) and 79% (11/14) SaOS-2 samples with RIN estimates had values > 7. These data are in concordance with the 260/280 ratios provided by the Nanodrop assessment. However, as discussed above, such quality metrics are possibly misleading and it may be more appropriate to directly assess the quality of the mRNA fraction using for example, 5'-3' ΔC_q assessment [130,252].

5.3.5 Influence of Different Cell Batches

To further determine the variability associated with the extraction step, an assessment of cell batch (replicate cell cultures propagated in independent experiments) was undertaken. Different cryo vials of frozen cell pellets (both Hs 683 and SaOS-2 cell lines) were thawed and propagated in culture before being collected for RNA extraction using TRizol (neat lysates only). The extracted RNA was evaluated using three quality metrics, Bioanalyzer, Nanodrop and Qubit, which were compared for estimates of RNA yield and by *Alu* PCR for an assessment of gDNA contamination.

There was a significant difference in Hs 683 RNA yield (normalised to cell count) between both analysis metric and cell batch, $p < 0.02$ for both (**Figure 5.8**). However, there was no significant difference observed in either factor for SaOS-2

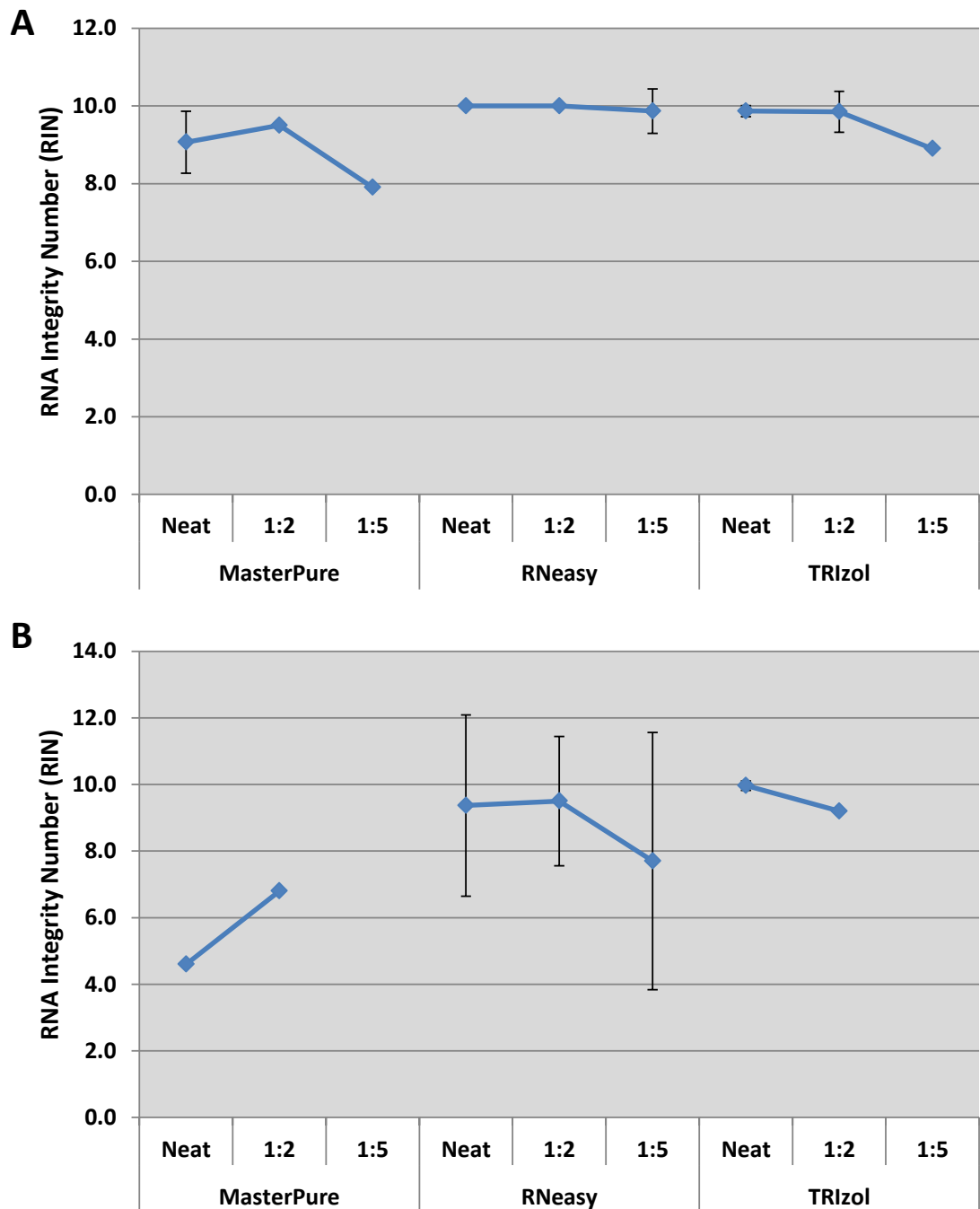


Figure 5.7 RNA Bioanalyzer quality assessment. (A) Hs 683 cell-derived RNA. (B) SaOS-2 cell-derived RNA. Post-DNase assessment. Error bars 95% CI. Missing values are due to low concentration. These samples were analysed on the pico chip (rather than the nano chip) and so no estimation of RNA quality was provided by the instrument. n = 3.

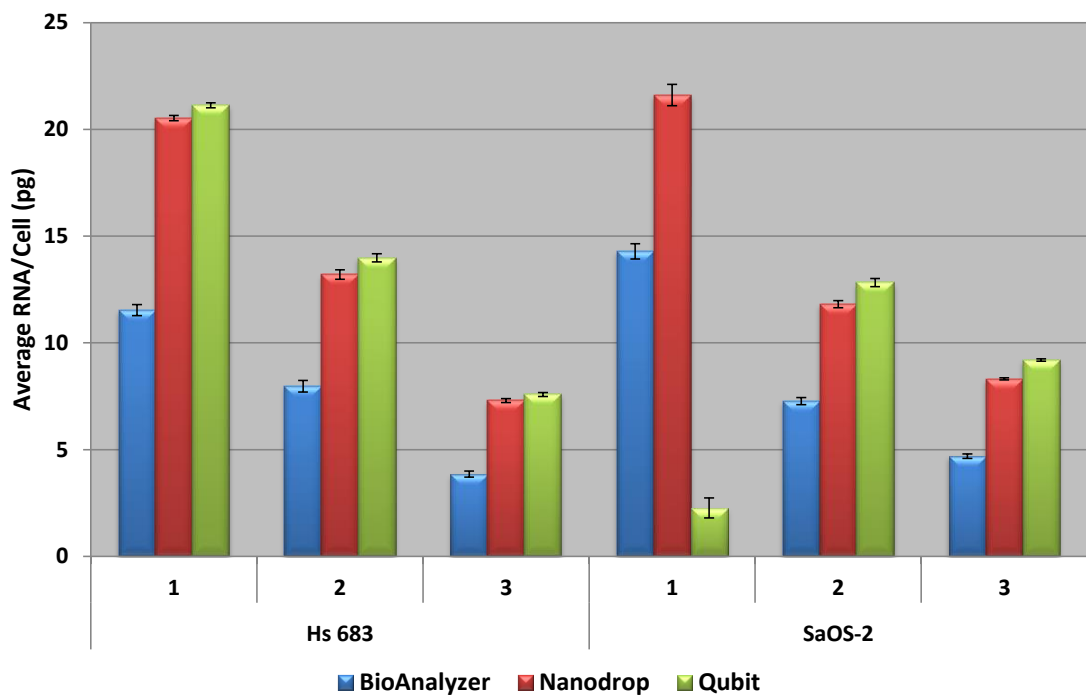


Figure 5.8 Batch Analysis. Different cell batches (1-3) for both Hs 683 and SaOS-2 cell lines were independently propagated before extraction of total RNA using TRIzol (only) and analysed post-DNase treatment for quantity by Bioanalyzer, Nanodrop and Qubit. Error bars SEM.

cell-derived RNA estimates, $p > 0.5$ for both. The lack of significance in the SaOS-2 data may be attributable to the Qubit measurement for batch one, which is low, compared to the trend in measurements. This may be due to operator error when preparing this sample for Qubit measurement or inhomogeneity of the sample. As for previous assessments discussed above, Bioanalyzer quantity estimates were lower than for the other two metrics. Despite normalisation for cell count, different cell batches of Hs 683s generated different yields. This may be attributable to variability in the sample source (biological variability) as well as variability in the TRIzol extraction itself (technical variability) and should be taken into account in downstream measurements.

There was a significant difference in Hs 683 RNA 260/280 ratios between cell batches (TRIzol and neat lysate volume analysed only), $p = 0.027$ (mean 1.97, SEM 0.006). Alternatively, there was no significant difference in Hs 683 RNA 260/230 ratios between cell batches, $p = 0.153$ (mean 2.02, SEM 0.056). There was also a significant difference in SaOS-2 RNA 260/280 and 260/230 ratios between cell batches (TRIzol and neat lysate volume analysed only), $p = 0.004$ (mean 1.99, SEM 0.011) and $p = 0.005$ (mean 1.88, SEM 0.101), respectively. RNA purity and integrity was therefore not consistent between cell batches.

The same samples (assessing variability between cell batches) were additionally analysed by *Alu* PCR (**Figure 5.9**). A significant difference was observed for both cell lines and all sample types (pre-DNase, post-DNase and post-RT) in *Alu* signal between both different cell batches and between extraction replicates (extracted neat with TRIzol only), all $p < 0.001$. A significant interaction was also seen between the two factors (cell batch and extraction replicate) for post-DNase samples (both cell lines) and post-RT samples (SaOS-2 measured only), all $p < 0.001$. However, there was no significant interaction between the terms observed for the pre-DNase samples (SaOS-2 measured only), $p = 0.618$.

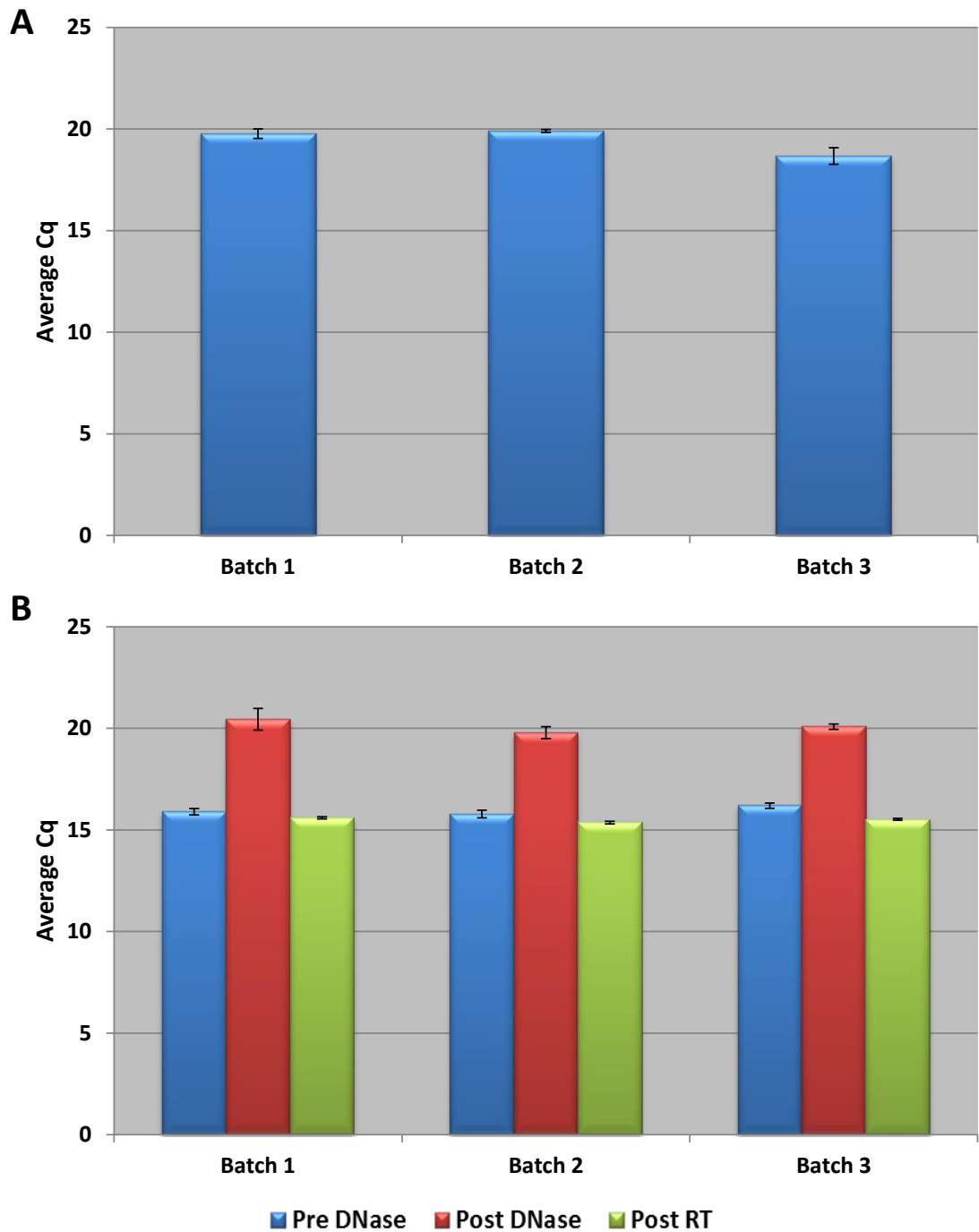


Figure 5.9 *Alu* PCR analysis of different cell batches. Different cell batches extracted using TRIzol. Total RNA was subjected to *Alu* PCR. (A) Hs683 cell-derived RNA, post-DNase treatment only. (B) SaOS-2 cell-derived RNA. Error bars SEM.

To further assess gDNA contamination, *Alu* PCR C_q data was converted to genome equivalents (assuming $1.0E+06$ copies *Alu*/genome, weight of diploid genome 6.6 pg and therefore $1.52E+09$ copies *Alu*/10 ng), (**Figure 5.10**). *Alu* signal increased in post-RT samples as any *Alu* transcribed into RNA will be converted to cDNA (**Figure 5.10B**).

For Hs 683 samples there was a significant difference in genome equivalents between cell batches, $p = 0.0172$ (single-factor ANOVA, **Figure 5.10A**). There was also a significant difference in genome equivalents for SaOS-2 samples between cell batches and stage of treatment (pre-DNase, post-DNase and post-RT), $p < 0.001$ for both factors (two-factor ANOVA, **Figure 5.10B**). Additionally, there was a significant interaction between the two terms (batch and treatment stage), $p < 0.001$. Post-DNase evaluation shows the degree of gDNA removal from the samples was substantial.

These data suggest that the TRIzol extraction method is not consistent between replicates and that different cell batches contribute significant variability to RNA extraction yields, which may in turn contribute significant error to downstream applications.

5.4 Conclusions

These data clearly demonstrate differing yields between extraction methods for the recovery of total RNA. For neat lysates, TRIzol yielded more RNA than either RNeasy or MasterPure kits, while both TRIzol and RNeasy extracted the most pure RNA and had the most efficient removal of gDNA contamination. Dilution did not significantly impact RNA yields, suggesting that extraction efficiencies remained linear across this dilution range (except for the TRIzol kit when extracting SaOS-2 cells). However, linearity was influenced by cell type. Nanodrop quality estimates were also influenced by dilution. Quantity estimates were linear for each of the different metrics and were higher from the Nanodrop and Qubit metrics than the

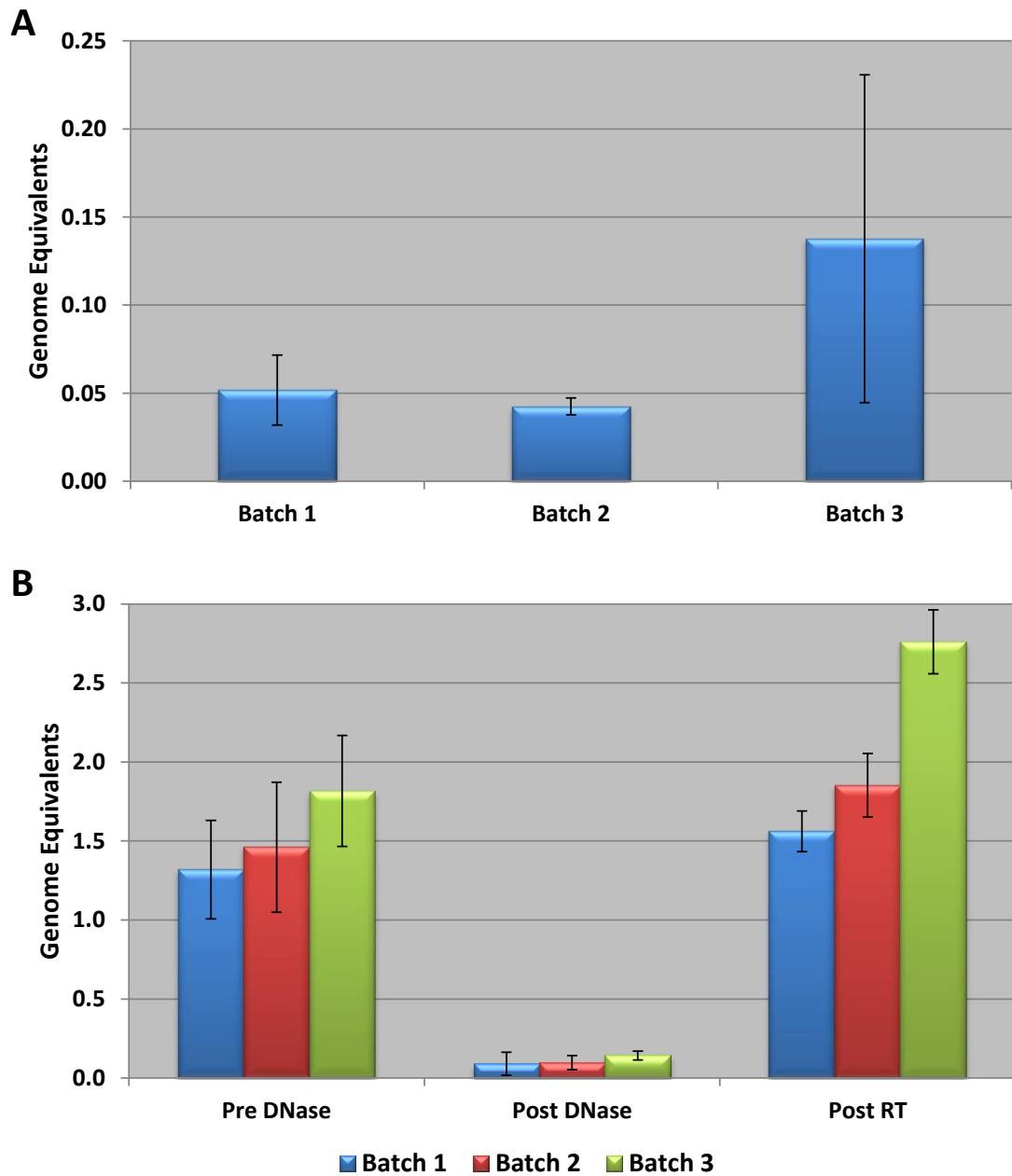


Figure 5.10 *Alu* PCR cell batch analysis: genome equivalents. *Alu* PCR analysis of different cell batches. gDNA measured by qPCR was converted to genome equivalents. (A) Hs683 cell-derived RNA, post-DNase treatment only. (B) SaOS-2 cell-derived RNA. Error bars 95% CI.

Bioanalyzer. However, the Bioanalyzer quality assessments by RIN values were in concordance with the Nanodrop 260/280 ratios and generally good quality RNA was extracted. Precision estimates were dependent on cell line, with Hs 683 RNA measurements decreasing in precision (increasing CV), as lysates were diluted and SaOS-2 precision estimates appearing to be random across dilutions.

The differences observed may be due to a number of factors including the potential of losing the RNA pellet (in relevant methods) and the ability of the extraction kit and/or quality metric to cope with sample contaminants. Furthermore, despite extracting samples with cell counts lower than the recommended maximum for each kit, it appears that some methodologies may be hindered by the extraction of neat lysates (MasterPure) and that they may benefit from a dilution of cell count within the lysate prior to extraction in order for that extraction to be more efficient. This may be due to matrix effects or simply the amount of cell debris. However, making such dilutions may hinder the measurement of rare, low abundance targets as it could adversely affect measurement sensitivity. This should be considered when choosing which extraction method to use for a particular sample type and downstream application. Furthermore, despite normalisation for cell count, different Hs 683 cell batches generated different RNA yields and variable RNA purity and integrity estimates, which may be attributable to both sample and extraction variability (TRIzol).

The *Alu* PCR data suggests that DNase treatment efficiency is at least partly dependant on matrix effects derived from the extraction method used. Co-purified contaminants and extraction buffer compounds (notably used in the MasterPure kit) may have inhibitory contributions to the efficiency of gDNA removal. The same matrix inhibition may also affect the efficiency of the *Alu* PCR. The SPUD assay, utilising an artificial target spiked into the sample and designed to measure C_q differences can be used to determine the extent of inhibition [155] but it is unlikely to be representative of the *Alu* element.

Chapter 5 Evaluation of the Impact of Extraction Protocol on Target Quantification

Despite the differences observed between extraction kits, each one was capable of extracting sufficient RNA quantity of acceptable quality for downstream applications such as RT-qPCR, suggesting RNA yield and quality is unlikely to be a limiting factor for any of the extraction kits analysed. However, for downstream applications requiring higher amounts and/or quality RNA, such as NGS [265,290,291], careful consideration of extraction method must be made before proceeding to ensure optimal RNA is prepared. Propagation of the variability observed between kits and metrics should be accounted for in downstream analyses.

Chapter 6

The Influence of Sample Type on Measurement Variability

6 The Influence of Sample Type on Measurement Variability

6.1 Introduction

There is a plethora of studies detailing the variability in particular measurement parameters [74,76-78,88,90,112,183,278,292,293] (such as stress-inducing treatments in cell lines including hypoxia and drug administration). For an appreciation of the applicability of such studies to basic research, as well as the wider scope of potential biomarkers, preclinical studies and in some cases, successful translation of these findings to a clinical setting, the specific samples in question must be evaluated on an experimentally specific basis. That is to say, experimental findings cannot be inferred to a different experimental set-up without direct empirical evidence. This of course depends on what level of precision is required for a particular experiment, be it large fold-changes over several orders of magnitude (HIV viral load [108]), or small copy number variations (HER2 amplification in breast cancer [223]). The key point is that the correct variability must be captured in order to make clinically relevant and important assertions.

Biologically relevant findings can be facilitated by the use of experimentally specific, validated reference genes. However, conclusions based on inappropriate (particularly single) reference genes that have not been validated for a particular sample set, may be erroneous. The continued use of GAPDH as a normaliser (without testing the assumption that it may be a suitable reference gene), despite years of evidence of its variable expression in a range of circumstances [47,131,142-146], is a clear example of where the utilisation of normalisation bestows confidence in a result that is fundamentally misplaced due to the inappropriate use of an otherwise powerful strategy. This is as damaging (if not more so) to data credibility as the application of no reference gene normalisation

strategy at all. A critical aspect therefore for relevant translation of data and methodologies, is the application of appropriate and effective normalisation.

Findings from a given controlled experiment should be shown to reflect “real-life” scenarios before their applicability to such scenarios can be asserted. One of the principal sources of variability in molecular measurements is the sample itself. The application of experimentally specific and validated reference genes allows technical variability to be unpicked from biological variations. This permits an evaluation of the true biological impact of the experimental parameters (such as drug treatment or clinical intervention). However, use of inappropriate reference genes may introduce measurement bias and may influence the final outcome. Furthermore, what the sample is composed of and where and how it is sourced contributes often unpredictable variations to the final measurement result.

Across disciplines, researchers analyse different sample types while employing the same types of measurements. The challenge is to highlight where the differences are introduced and how methods may be best used in a reproducible and robust manner so that despite analysing different sample types, the techniques are standardised to perform effectively within a study and between different studies. For RT-qPCR-based studies, gross variability in mRNA measurement may be standardised by controlling experimental details such as cell numbers, media, RNA quantity used for RT, rigorous experimental protocol, appropriate controls and standardised storage, handling and processing procedures. For smaller variabilities, appropriate normalisation strategies are needed. Material complexity ranges from a pure, single RNA target (from IVT), to a mixed mRNA population from a single primary cell line, cellular co-cultures or tissues *in vivo*. One might expect the level of error introduced increases from a pure, single RNA target, to a 2D cell model, to a 3D cell model and finally to a clinical scenario, as the level of sample complexity increases. 3D cell models are used as they enable cells to be cultured in a manner more representative of their *in vivo* environment and as such, observed responses may be more biologically relevant [294]. Cell models are used

Chapter 6 The Influence of Sample Type on Measurement Variability

to inform on the clinical situation, and as such how representative they are in terms of error must be delineated. For bone there are multiple culture systems in use including cell lines [232,295-298], co-cultures [234,299-301], explants, isolation of primary cells from tissue – primary cells [294,301-303] and 3D cell scaffolds [304-307].

In this chapter, different sample types and sources were assessed to determine their influence on such variability in the final measurement result. The experimental approach used a series of simple (cell line) to complex (human tissue) samples of bone to investigate our normalisation strategy and the influence of changing different parameters, such as cell passage, addition of stimuli, or anatomical position, to determine the variability contributions of these factors. A 2D cell model was used to evaluate the effect of cell passage and mineralisation on total RNA yields. A 3D co-culture model was used to evaluate the effect of cell batch, mechanical loading and RT on total RNA yields and specific mRNA levels. Bone cores from surgical total knee replacement (TKR) patients were used to evaluate the effect of patient, anatomical position and RT on total RNA yields and specific mRNA levels.

This study makes use of osteoblasts and osteocytes. These cells, along with osteoclasts, are involved in bone formation and remodeling. Bone is a highly dynamic organ that is constantly undergoing remodeling and growth [308]. New bone is formed by osteoblasts (found near the bone surface) [308,309], which secrete osteoid, an unmineralised portion of immature bone matrix rich in collagen [308,310]. Osteoblasts then secrete alkaline phosphatase to create sites for calcium and phosphate deposition, allowing crystals of bone mineral to form [311]. Mineralisation of osteoid results in new bone formation. Osteoclasts are responsible for bone resorption. They travel to specific sites on the surface of bone and secrete acid phosphatase, which unfixes the calcium in mineralised bone to break it down [311]. Osteocytes are osteoblasts that have become trapped in the bone matrix and are no longer located at the bone surface. They are involved in

homeostasis [311] and act as mechanosensors and orchestrators of the bone remodeling process [308,312-315]. Mechanosensor activity, a capacity to detect mechanical pressures and loads, helps the adaptation of bone to daily mechanical forces [308,316-318]. Osteocyte cytoplasmic processes (up to 50 per cell) are connected to other neighboring osteocytes processes, as well as to cytoplasmic processes of osteoblasts, facilitating the intercellular transport of small signaling molecules among these cells [308]. The mechanosensitive function of osteocytes is possible due to this intricate network, which allows communication among bone cells [308].

The aims of these experiments were to apportion variability contributions to different steps in the experimental process, to determine where the sources of error were largest and whether the error sources were different for different sample sources (2D cell culture, 3D co-culture and clinical samples) or transcripts (endogenous versus synthetic). Assessing three different systems enables determination of how the complexity of the sample source affects the variation. This will attribute weight to individual steps in terms of contribution to whole process variability and help inform future studies.

6.1.1 2D Culture Model

Firstly, SaoS-2 cell line was evaluated for differences in RNA yield and variability contributions introduced following mineralisation. This highly characterised, osteoblastic cell line has a mature osteoblast phenotype with high levels of alkaline phosphatase activity [204] and was selected because of its well-known ability to mineralise in culture, forming a calcified matrix typical of woven bone *in vivo* [204,205].

Differentiation is a transforming event that can have a substantial impact on transcriptomic profiles [319-325]. Indeed, transcriptomic profiles also change in order to initiate differentiation [319,320]. It is a key-step in many fields of cell

profiling and as such investigations into the variabilities associated with this step are vital for meaningful comparisons to be made. In this study, bulk changes were evaluated rather than evaluating changes at a single cell level. The transcription factors released by individual cells may have an impact on the mass population and these are the variabilities we concentrated on. Utilisation of the osteoblastic cell line SaOS-2 alleviates the difficulties of RNA extraction from whole bone and offers the additional benefit of being able to mineralise in culture [204,205]. This 2D mineralisation model also represents the simplest model of a bone-forming osteoblast employed in this chapter.

6.1.2 3D Co-Culture Model

A 3D co-culture model system for osteocyte/osteoblast interaction is more representative of physiological conditions than the 2D cell line. Within the body, cells grow in a 3D environment, which itself will have a known impact on their development and potential mRNA profiles [326-328]. Indeed osteocytes *in vivo* only exist embedded within the 3D bone matrix. Not only does the 3D-gel co-culture model more closely mimic the *in vivo* environment than a conventional 2D culture system, but it also allowed an investigation of the impact of a different stimulation (mechanical loading) on mRNA levels and associated error. Osteocytes are the mechanosensitive component of the system and their response to loading direct the expression changes in osteoblasts and therefore the regulation of bone formation [308]. For this reason, a 3D co-culture model allows the interaction between the two cell types to play out in response to mechanical stimuli and informs on the equivalent situation *in vivo* [234]. Comparison of this model with clinical samples will help determine the applicability of the 3D co-culture model error propagation to accurately represent what happens *in vivo*.

The aim was to measure mRNA level variabilities induced by mechanical loading forces on the 3D gel co-culture model system, similar to those experienced by load bearing bones in the body. Mechanical loading models are important for

understanding the mechanisms involved in various common musculoskeletal diseases including osteoarthritis and osteoporosis [233,234,329]. Appreciation of variability contributions in mRNA quantification using this model will allow utilisation of these data to their full potential in interpretation of biological mechanisms relevant to these important diseases.

6.1.3 Clinical Samples

The final stage in these investigations was to evaluate the most complex model employed in this chapter, human tissue *in vivo*, and applies the sTCM in their analysis. For this purpose, a clinical cohort of bone core samples were retrieved from the tibial plateau region of the knee joint that reflected altered mechanical loading from patients undergoing TKR surgery for osteoarthritis (**2.7.3 Clinical Samples – Total Knee Replacement Bone Cores**). These patients would have experienced prolonged unbalanced mechanical loading forces across this region. Cores were taken from four different biopsy positions in each patient (AM, PM, AL, PL) and assessed by dynamic array RT-qPCR. Samples were evaluated using the same markers as used for the 3D gel co-cultures. These clinical samples reflected the bone cells in their most complex, but most representative environment.

Additional to mRNA analysis, 3D gel co-culture samples and clinical bone core samples underwent analysis by *Alu* PCR. RT-qPCR detection of the *Alu* element has been proposed as a new method for normalisation of gene expression data, as a measure for the total mRNA fraction [283]. The *Alu* element is present at more than one million copies interspersed throughout the human genome, with up to 75% of all known genes containing *Alu* insertions within their introns and/or untranslated regions (UTRs) [330]. Therefore, the differential expression of a number of genes in the tissues or cells under investigation will not influence the abundance of expressed *Alu* repeats in the transcriptome [283]. Using this method may alleviate the time and expense associated with testing and validating a panel

of suitable reference genes using an algorithm such as GeNorm [7], and limits use of precious, sometimes limiting, sample material.

6.2 Materials & Methods

6.2.1 2D Culture Model – SaOS-2 Mineralisation

Cell culture of SaOS-2 cell line and mineralisation treatment (up to and including lysate collection) was performed by Dr Gary Morley, LGC, Teddington. Culture details are described in **2.1.2 Cell Lines** and **2.7.1 2D Culture Model – SaOS-2 Mineralisation**.

To assess variability contributions of mineralisation, SaOS-2 cells were analysed at two different passages (p33 and p36), cultured under suppliers' recommended conditions (ATCC), and treated with mineralising media (98.8 mL propagation media, 1 mL of 0.2 M β -Glycerophosphate (Sigma), 100 mL of 50 mg/mL Ascorbic acid (Sigma) and 100 mL of 10^{-3} M Dexamethasone (Sigma)). Control media consisted of propagation media and 1:1000 ethanol. For full details see **2.7.1 2D Culture Model – SaOS-2 Mineralisation**. Following lysate collection 24 hrs or 1-week post initiation of mineralisation, total RNA was extracted using TRIzol reagent and DNase treated (**Chapter 2**). All samples were quantified by UV spectrophotometry.

6.2.2 3D Co-Culture Model

Dr Cleo Bonnet (Cardiff University) performed all 3D co-culture work preceding total RNA extraction (**2.7.2 3D Co-Culture Model**). A mouse osteocyte cell line (MLO-Y4 cells) was grown in 3D collagen gels before being layered with human osteoblasts (SaOS-2 cells). These 3D co-cultures were prepared in silicone plates designed specifically for mechanical loading experiments (**2.7.2.3 Mechanical Loading of 3D Co-cultures**) [234].

Three independent experiments were performed using different cell batches (three different cryo-banked vials of frozen cell pellets) with three replicate gels each for loaded and control treatments in each experiment. Total RNA extraction (TRIzol) and DNase treatment were performed as described in **2.7.2.4 TRIzol Treatment of 3D Co-cultures**.

6.2.3 Clinical Samples

Human samples were used, in collaboration with Dr Mason (Arthritis Research UK Biomechanics and Bioengineering Centre) at Cardiff University, to gain insight into the clinical relevance and power of the TCM for accurate quantification. A 100× mix of synthetic Unknown 1 ERCC RNA (sTCM) was used as a spike for all samples pre-RNA extraction. This enabled an assessment of all stages in the measurement process post cell lysis.

Clinical samples were collected by the Arthritis Research UK Biomechanics and Bioengineering Centre (Andrea Longman, Helen Roberts, Deborah Mason, Cleo Bonnet) and surgeons (Rhys Williams, Chris Wilson and Sanjeev Argawal) under their ethical approval (Research Ethics Committee for Wales, reference number 10/MRE09/28). There were five patients; one patient had a bilateral TKR and so there were six 'patient' sample sets in total. All patients were female aged between 44 and 75 years. Bone cores were extracted in theatre using bone biopsy needles and put into cryo-vials containing RNAlater on dry ice. Samples were transported frozen (in a nitrogen carrier) and stored at -80°C until processing.

Patient and biopsy positional variability contributions were assessed through analysis of TKR patient bone cores, taken from anterior medial (AM), posterior medial (PM), anterior lateral (AL) and posterior lateral (PL) positions (**2.7.3 Clinical Samples – Total Knee Replacement Bone Cores**). Total RNA was extracted (TRIzol) and DNase treatment completed.

6.2.4 RT-qPCR: Dynamic Array

For both 3D gel co-culture and clinical bone core sample sets, triplicate RTs from each sample were performed and the cDNA was preamplified (**2.7.5.1 Preamplification**) before being analysed in duplicate on individual dynamic arrays. Preamplification is part of the Fluidigm Biomark dynamic array protocol. An assessment of preamplification linearity (evaluating preamplified versus non-preamplified samples) was performed for each of the assays used, as described in **2.7.5.2 Dynamic Array Analysis**. A six-point, 10-fold RNA dilution series was performed, with each undergoing RT. Each cDNA was preamplified and subsequently measured (n = 8) by dynamic array qPCR.

The dynamic array output is a C_q value. The efficiency corrected delta C_q method [93] was used to calculate relative quantity values, which were normalised using three validated reference genes. Validation of reference genes is described in **2.3.1.1 Reference Genes**. As described previously (**2.3 Preparation of Transcriptomic Calibration Material (TCM)**), sTCM was spiked into all lysates pre-extraction, enabling measurement of ERCC synthetic transcripts, providing an opportunity to assess the validity of using this synthetic reference gene panel for normalisation of mRNA data. In addition to RT-qPCR analysis of reference genes and GOI, *Alu* PCR was performed on post-DNase samples as an additional quality metric.

6.3 Results & Discussion

6.3.1 Comparison of RNA Yield and Quality from Different Sample Sources

Samples derived from three different sources (2D cell culture with mineralisation treatment, 3D gel co-culture with mechanical loading treatment and clinical TKR bone core samples from different anatomical positions and different patients) underwent extraction of total RNA and yields determined. 2D cell culture samples

were evaluated for process precision factors to define the error contributions of this phase of the analysis. 3D gel co-culture and clinical bone core samples were also analysed by *Alu* PCR before undergoing assessment by RT-qPCR.

6.3.1.1 RNA Yield and Precision

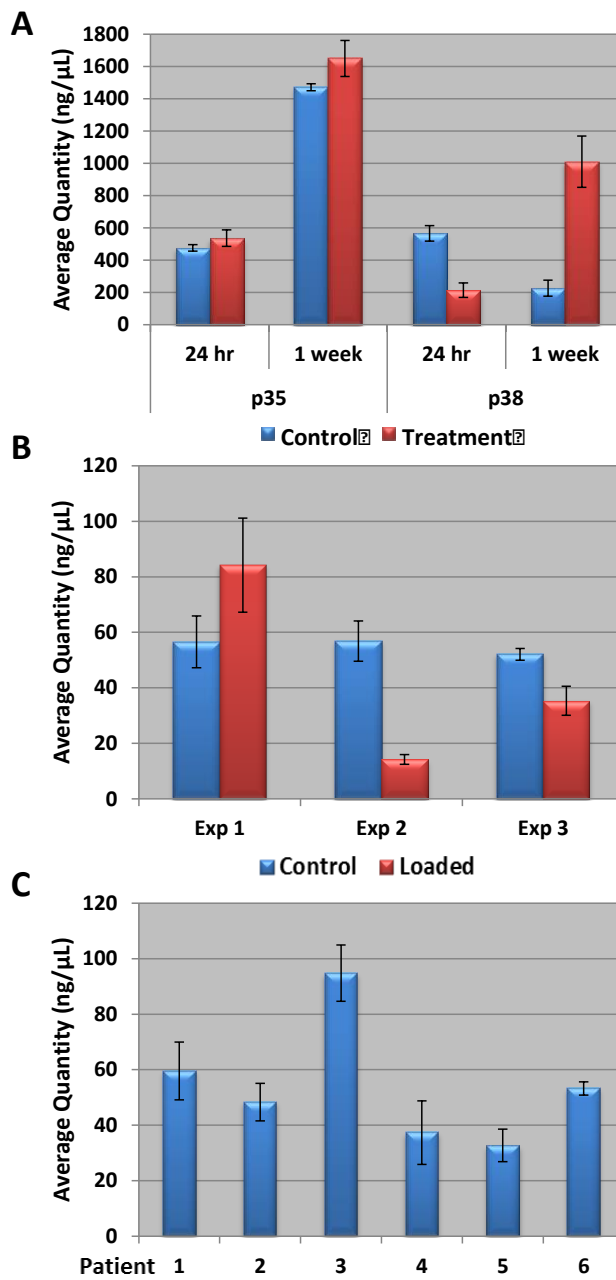
Samples from all sources were first evaluated for total RNA yield and quality following extraction, using the Nanodrop.

6.3.1.1.1 2D Culture Model

Using two-factor ANOVA (time point versus mineralisation treatment), there was a significant difference in total RNA yield between time points for both cell passages (both $p < 0.02$) (**Figure 6.1A**). For p38 there was a significant difference observed in RNA yield between conditions (treatment and control, $p = 0.018$), as well as a significant interaction between the two factors (time point versus condition, $p < 0.0001$). For p35 there was no significant difference ($p = 0.06$) or interaction ($p = 0.349$) in RNA yield observed between conditions.

When considering the condition groups separately (two-factor ANOVA, passage versus time point, performed independently for control and treatment samples), both the control and treatment groups showed a significant difference between both passage and time points, $p < 0.0001$ for all, meaning that both the passage of the cell population and the time post-treatment had a significant impact on the RNA yield; yield increased with time post treatment and decreased between p35 and p38. For the control samples only, there is also a significant interaction between the two factors (passage and time point), $p < 0.0001$, whereas for the treatment samples, there is no significant interaction observed, $p = 0.127$. The variability in these measurements was greater for the later passage (older) cells (**Figure 6.1D**): p35 CV range 6.34-40.62%, p38 CV range 35.87-91.99%.

Chapter 6 The Influence of Sample Type on Measurement Variability



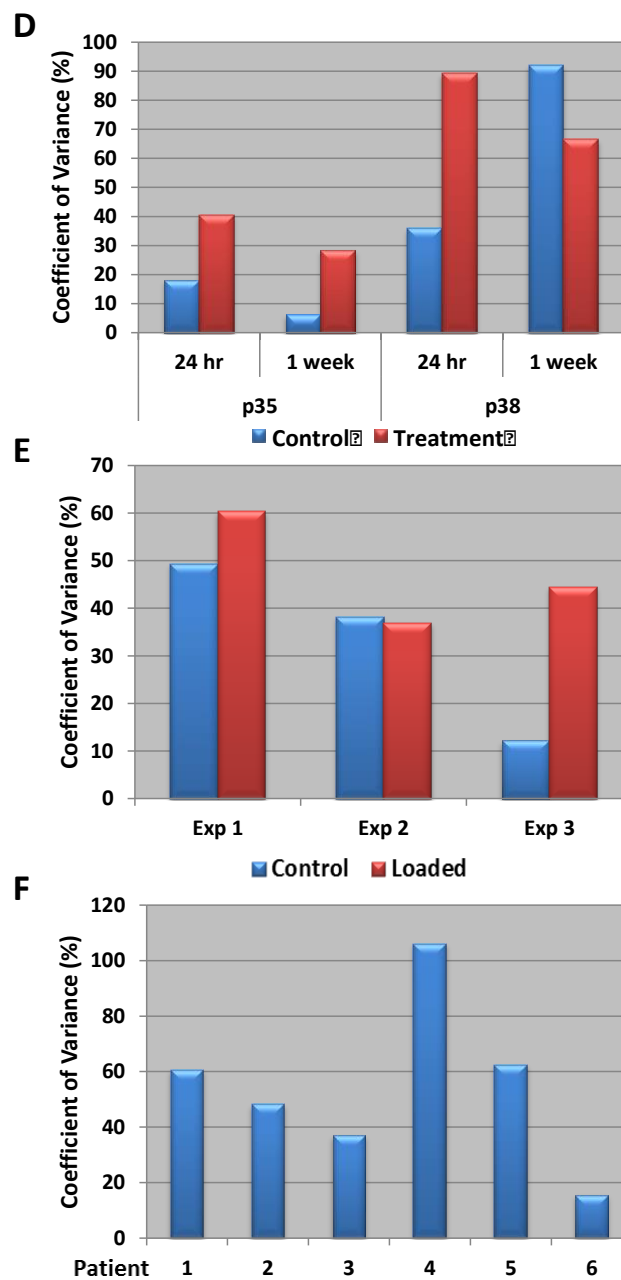


Figure 6.1 Total RNA yields. Post-DNase UV quantification, not corrected for cell count or tissue weight. (A) 2D culture. Average quantity yields 24 hrs and 1-week post initiation of mineralisation for passage 35 and 38. (B) 3D co-cultures. Average quantity yields per experiment for loaded versus control samples. (C) Clinical bone cores. Average quantity yields per patient. (D) Coefficient of variation (multiple extraction and flask replicates) for 2D culture quantity estimates. (E) Coefficient of variation (multiple gels) for 3D co-culture quantity estimates. (F) Coefficient of variation (multiple anatomical positions) for clinical bone core sample quantity estimates. Error bars SEM (A-C). n = 18 (A&D), n = 9 (B&E), n = 12 (C&F).

Chapter 6 The Influence of Sample Type on Measurement Variability

Variability (CV) in the measurement of 2D culture samples was high, with all but two groups being greater than 20%. The variance was significantly different between control and treatment groups for p35 at both time points and p38 at 24 hrs only (all $p < 0.001$, Ftest). In all three instances, treatment group variability was far greater than control group variability, ranging between 2.5 and 5-fold higher. There was no significant difference observed between control and treatment groups for p38 at 1 week ($p = 0.798$, Ftest). Increased variability attributed to the treatment groups may be as a result of mRNA level changes resulting from the treatment itself.

SaOS-2 cells have been characterised as osteoblastic due to the expression of phenotypic markers [331-333] such as alkaline phosphatase (ALP) activity (enzyme involved in mineralisation) [332-334], parathyroid hormone-linked adenylate cyclase [335], osteonectin production [336], specific receptors for 1,25-dihydroxyvitamin D₃ [337], and osteogenic potential as assessed in diffusion chambers [205]. SaOS-2 cells have also demonstrated an ability to deposit an extensive collagenous matrix comprised largely of type I and V collagen, which can mineralise with hydroxyapatite-like crystal formation [338,339]. Mineralisation will cause a reduction in the number of active osteoblasts via osteocyte formation, and a reduction in substrate available for mineralisation as more osteoid becomes mineralised.

The components of the extracellular matrix synthesised by SaOS-2 cells are consistent with a normal osteoblastic phenotype. These include collagen types I and V, the proteoglycans decorin (a small chondroitin sulfate proteoglycan) and a large chondroitin sulfate proteoglycan (CSPG), as well as mRNA encoding bone sialoprotein (BSP) and osteonectin [339]. Osteoblasts become embedded in the extracellular matrix consisting mainly of type I collagen (Coll), and matrix mineralisation begins as mineral deposits extend along and within collagen fibrils [338,340]. Once matrix synthesis begins, cells differentiate as genes encoding osteoblastic markers such as alkaline phosphatase (ALP, differentiation middle-

stage marker) [341], osteocalcin (OCN, differentiation late-stage marker) [340,341] and osteopontin (OPN, the last in a chronological sequence of markers of osteoblastic differentiation) [338,342], are expressed. Factors important for osteoblastic differentiation and modulating osteoblast-specific mRNA levels include bone morphogenic proteins (BMPs), transforming growth factor (TGF), insulin-like growth factor I (IGF-I), vascular endothelial growth factor (VEGF), and glucocorticoids [338,343-348].

Hausser and Brenner [349] previously evaluated phenotypic stability of SaOS-2 cells over 100 passages. Their study demonstrated that higher passage cells exhibited higher proliferation rates and lower specific alkaline phosphatase activities with mineralisation significantly more pronounced in cultures of late passage cells. They also observed differential expression of some targets between early and late passage cells; for example, expression of decorin, a regulator of proliferation and mineralisation was strongly decreased in late passage cells. They concluded that special care is required when results obtained with SaOS-2 cells with different culture history are to be compared [349]. These cells may behave differently in certain experimental situations, depending on their culture history. Such differences in culture history occur, for example, when the cells are propagated in different laboratories [349]. Total RNA yields were not compared between different passages.

The supplier (ATCC) suggested that passaging should not affect RNA yield and purity (personal correspondence). However, no citation can be found to support this claim. It is possible that this question may not have been directly addressed, as most studies focus on target-specific expression levels rather than total RNA abundance. It would therefore be a valid approach to assess this parameter in future experiments. It has been shown that MSC populations become more homogeneous with serial passaging; however, this leads to senescent cell behavior and an impaired capacity for multipotent differentiation [350,351].

While there was no significant difference observed for p35 cells between control and treatment groups in total RNA yield, treatment had a significant impact on RNA yield for p38 cells. It is therefore important to capture this variability (and not just use the mean quantity value) in order to reflect true error propagation and experimental influences. Further work would be required to determine if these findings are reproducible and to elucidate whether cell passage (age) has a consistent impact on the effect of treatment on RNA yield. While RNA yields were not significantly affected by treatment for the earlier passage, p35, this does not necessarily reflect expression profiles of mRNA targets and any changes resulting from such treatment.

6.3.1.1.2 3D Co-Culture Model

Using a two-factor ANOVA (experiment versus gel replicate) there was a significant difference observed in RNA quantity between independent experiments and gel replicates for both treatment conditions (loaded and control), all $p < 0.001$ (**Figure 6.1B**). Furthermore, there was a significant interaction between the two terms (experiment and gel) for both treatment conditions ($p < 0.001$). These data suggest that both cell batch (different experiments) and gel replicates have a significant impact on the total RNA quantity variability for these samples. There was no significant difference observed in RNA quantity between loaded and control sample sets ($p = 0.243$, control sample mean $55.17 \text{ ng}/\mu\text{L}$, standard deviation $20.06 \text{ ng}/\mu\text{L}$, loaded sample mean $44.59 \text{ ng}/\mu\text{L}$, standard deviation $42.08 \text{ ng}/\mu\text{L}$), suggesting that treatment had no impact on total RNA yield (single-factor ANOVA).

The 3D co-culture model was assessed according to experiment and treatment (**Figure 6.1E**). The variability (CV) for these sample groups was high, with all but one (experiment 3, control) being greater than 35%. The variability was highest for experiment 1 groups (loaded and control). This was due to large differences in total RNA yield between different gels. In addition, experiment 2, loaded samples displayed a low average quantity, mainly attributable to a low total RNA

concentration from gel 1. Low concentrations are known to exhibit increased variability on measurement (NanoDrop 1000 Spectrophotometer V3.8 User's Manual).

Total RNA yields varied between samples. This may be explained, as these data cannot be normalised to cell count. The top layer, SaOS-2 cells, of the co-culture was collected directly in TRIzol reagent and as such, a cell count was not possible. However, based on previous studies of this model system, it would be expected that the SaOS-2 osteoblastic cells formed a monolayer over the surface of the collagen gel [234], and therefore the cell counts might expect to be similar.

6.3.1.1.3 Clinical Samples

Two-factor ANOVA (anatomical position versus patient) showed there was a significant difference observed in RNA quantity between anatomical position and between patients, both $p < 0.001$. There was also a significant interaction between the two terms (position and patient), $p < 0.001$. This suggests that both anatomical position and patient introduce significant variability to total RNA yield measurements. However it should be noted that, as for the 3D gel data, a normalisation for cell count or tissue weight was not undertaken due to this information not being available and so at least part of the variability in these measurement values may be due to differing amount of material processed.

Assessing variability per patient (**Figure 6.1F**), all sample groups except one (patient 6) showed variabilities (CV) greater than 35%. Patient 4 showed the greatest variability in total RNA yields, which was attributable to an RNA yield for anatomical position AM being almost twice that of any other anatomical position for the same patient.

There was a degree of variability in total RNA yields not only between patients, but also between biopsy positions within the same patient. In osteoarthritis

development, subchondral bone undergoes an increase in bone turnover (remodelling) and an increased thickness and volume, but is weaker and less mineralised than normal bone (hypomineralisation due to abnormal bone remodeling, reducing its stiffness) [352-359]. These changes result in altered apparent and material density of bone that may adversely affect the joint's biomechanical environment [356,358]. Bone attrition, a depression or flattening of the bony surface, represents remodelling of the subchondral bone envelope, leading to a consequential change in bone shape and/or bone loss [356]. With alterations in its properties, subchondral bone may be less able to absorb and dissipate energy, thereby increasing forces transmitted through the joint and predisposing the articular surface to deformation [356]. As a result, it is likely that the amount of bone (density/cellularity) retrieved from these osteoarthritis patients varied within the same biopsy volumes, which may go some way to explaining the variability in total RNA yields.

Clinical bone core samples were stored at -80°C in RNAlater immediately following collection during surgery and required thawing to remove excess RNAlater before being frozen on dry ice and subjected to the standard dismembration protocol (**2.7.3.1 Dismembrator**). As a result, the yield data could not be normalised according to the weight of the cores collected. This was unavoidable due to the constraints of collecting during surgery and efforts to preserve RNA. In the future, procedures could be put in place to make such weight measurements viable on collection. This is important because a portion of any observed variability may be due to differing amounts of starting material.

It is difficult to compare total RNA yield between sample sources as not all sources can be normalised for cell count and different factors are contributing to the variability in each. However, it is clear from all three sources that RNA extraction yields show a degree of variability, which increases as yields diminish.

Chapter 6 The Influence of Sample Type on Measurement Variability

In order to assess how sample complexity affects variability, total RNA quantities were pooled (all data at all replication levels; therefore process variability included) for all samples per data set (2D cell culture, 3D gel co-culture and clinical bone cores). Measurement variabilities (CV) were estimated as 78.88%, 66.33% and 64.03%, respectively. These data suggest that the least complex model, the 2D cell culture, has the greatest variability between samples, while the 3D co-culture model and clinical bone core samples have similar variability. However, the 2D cell culture experiment included twice as many samples as either of the other two models (48 samples, $n = 144$ due to triplicate A_{260} measurements per sample. 3D gel co-culture: 18 samples, $n = 54$. clinical bone cores: 24 samples, $n = 72$). When evaluating the two cell passages included in the 2D cell culture experiment independently (24 samples, $n = 72$), measurement variabilities (CV) were estimated at 57.63% and 98.00% for p35 and p38, respectively. This agrees with the findings above that the older cells (p38) display greater variability in RNA yields. This needs further investigation to determine whether it is an anomaly in these data or is in fact reproducible, and that cell passage has an impact on RNA yield precision. Considering p35 variability alone, these data suggest that 2D cell culture variability is lowest and sample complexity is positively correlated with RNA yield variability; as sample complexity increases, so does measurement variability of extracted total RNA. The total RNA yields were greatest for the 2D model samples; followed by the clinical bone cores, with the 3D co-culture model returning the lowest total RNA yields (average yields 76.84 ng/ μ L, 10.86 ng/ μ L and 9.98 ng/ μ L, respectively, with associated standard errors 5.05, 0.82 and 0.90 ng/ μ L, respectively).

6.3.1.2 RNA Extraction Process Precision Factors

2D cell culture samples were assessed for variability contributions from sample to extraction (**Figure 6.2**).

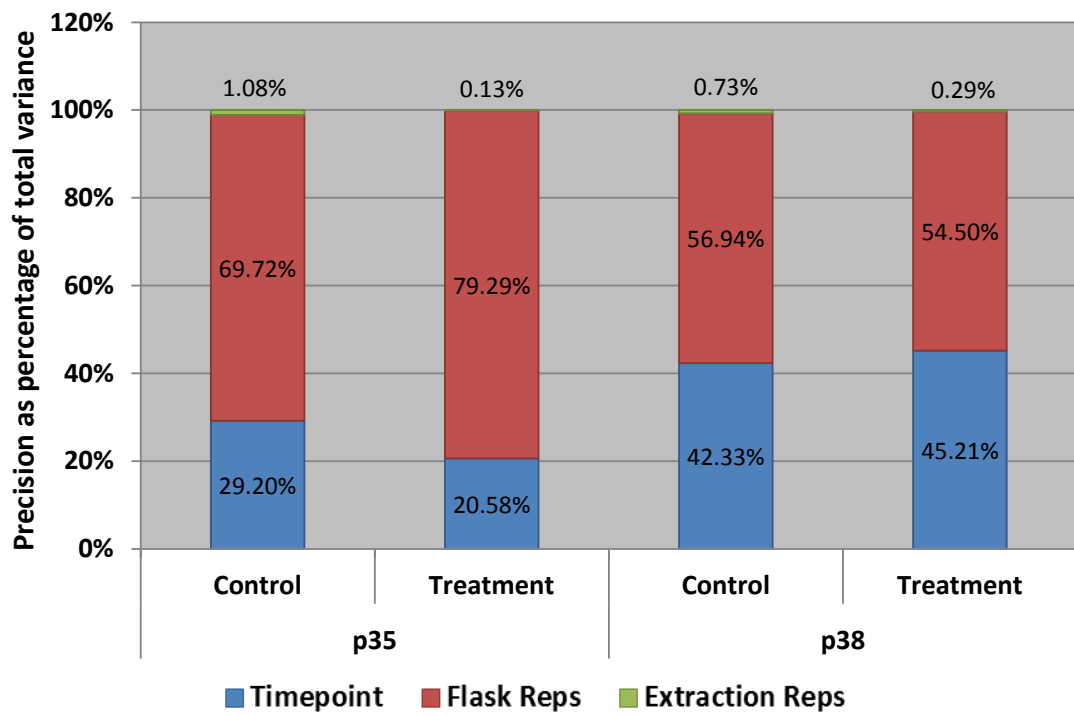


Figure 6.2 SaOS-2 mineralisation process precision contributed by different factors. Nanodrop quantification variability contributions were apportioned to experimental factors in the measurement process, displayed as control versus treatment for two different cell passages (p35 and p38).

Chapter 6 The Influence of Sample Type on Measurement Variability

Average variability contributions to nanodrop RNA quantification were highest for flask replicates (65.1%), followed by time point (34.3%), with the lowest contribution from extraction replicates (0.56%).

These data suggest that the TRIzol extraction replicates in this experimental set-up were highly robust and reproducible, adding little variability to the final RNA quantity measurement. Flask replication contributed the greatest variability to the final measurement followed by time point and as such these factors should be considered as points of replication in similar experimental set-ups. This will ensure variability contributions are taken into account when interpreting measurable changes and results are therefore less likely to become biased. The next step in the analysis of these samples would be to measure specific mRNA changes of suitable GOI targets to discern whether the magnitude of these variability contributions are maintained in the RT-qPCR data and if there are target-specific influences.

6.3.1.3 *Alu* PCR

All 3D gel co-culture and clinical bone core RNA samples were evaluated post DNase treatment using *Alu* PCR as an additional metric for sample quality and measure of gDNA contamination.

6.3.1.3.1 3D Co-Culture Model

Using two-factor ANOVA (condition versus gel replicate, for each independent experiment), a significant difference was observed in *Alu* signal between replicate gels and between treatment conditions for all cell batch replicate experiments (all $p < 0.0001$), except for between treatment conditions for experiment 1 only ($p = 0.085$) (**Figure 6.3A**). There was also a significant interaction observed between the factors (condition and gel replicate) for all cell batch replicate experiments (all $p < 0.006$).

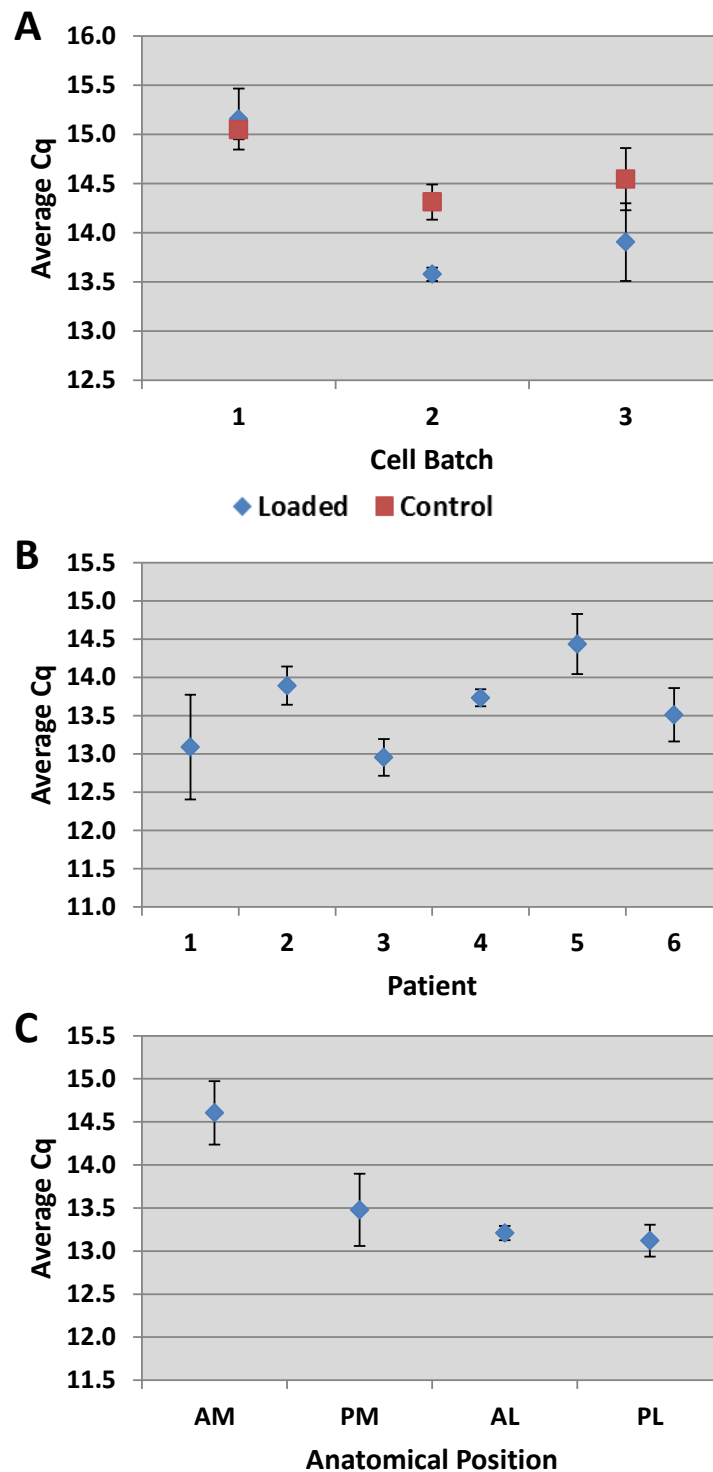


Figure 6.3 *Alu* PCR expression. The extracted total RNA was analysed for *Alu* element expression post-DNase treatment. (A) 3D gel cell batch variability, gel replicate variability captured within condition, n = 9. (B) Clinical bone core patient variability, n = 18. (C) Clinical bone core anatomical position variability, n = 12. Error SEM.

6.3.1.3.2 Clinical Samples

A two-factor ANOVA (anatomical position versus patient) showed a significant difference in *Alu* signal between different positions and between individual patients (all $p < 0.0001$), **Figure 6.3B & C**. Similarly, a significant interaction was measured between the two factors (position and patient), $p < 0.0001$.

6.3.2 Comparison of mRNA Expression Variability from Different Sample Sources

6.3.2.1 Pre-amplification

In order to show the applicability of using a pre-amplification step in the dynamic array protocol, a dilution series of samples with and without pre-amplification were evaluated on an additional dynamic array. This allowed assessment of the linearity of pre-amplification across the dilution range for each of the assays used. The accuracy and precision of qPCR detection for each target was assessed by linear regression, comparing the slope and R^2 of the data to the starting concentration of RNA (**Table 6.1**). Using single-factor ANOVA (non-pre-amplified slopes versus pre-amplified slopes for all assays), there was a significant improvement in the slope of the linear regression of C_q versus quantity value ($p = 0.032$), with the mean slope of pre-amplified targets within 5% of the ideal slope of 1.

The Pearson's correlation for C_q of pre-amplification versus no pre-amplification subsets (per assay) was calculated. Sixteen (of 17) assays had data for more than two of the non-pre-amplified standard dilutions, allowing this comparison to be made. Eight out of the 16 assays had coefficients ≥ 0.94 (**Table 6.1**). There were four assays that were poorly correlated, HPRT1, MMP1, PPIA and RPLPO. It may be expected that both MMP1 and RPLPO would perform poorly in this assessment as both were expressed at low levels and so an accurate evaluation of expression levels in the non-pre-amplified samples was difficult to obtain. PPIA has been used as an endogenous reference gene for normalisation of both 3D gel co-culture and

Table 6.1 Accuracy and Precision between PreAmplified and Non-PreAmplified cDNA. A six-point RNA standard curve was generated using 10-fold serial dilutions of Calibrant. Each dilution point underwent RT. Of the cDNA produced, a proportion was reserved (non-preamplified), while the rest was subject to preamplification using all target assays. All samples for each preamplified and non-preamplified standard curve were analysed by dynamic array qPCR (n = 8). Linear regression was performed with C_q values versus $\log_2(\text{quantity})$ for each target. Pearson's correlation was performed between preamplified and non-preamplified C_q data.

Assay	Slope		R ²		Correlation
	No PreAmp	PreAmp	No PreAmp	PreAmp	
B2M	-0.66	-1.31	-0.99	-0.95	0.99
CASC3		-0.54		-0.91	1.00
GAPDH	-0.66	-0.98	-0.95	-1.00	0.95
HPRT1		-0.92		-1.00	-0.15
MMP1		-1.13		-1.00	-0.79
PPIA		-1.04		-1.00	-0.30
RPLPO		-1.15		-1.00	-0.19
SLC1A3		-0.79		-1.00	
TBP		-1.03		-0.99	1.00
UBC	-0.43	-0.90	-0.87	-0.99	0.83
YWHAZ	-0.41	-0.96	-0.82	-0.99	0.81
ERCC-13	-0.84	-0.94	-1.00	-1.00	0.94
ERCC-25	-1.02	-0.97	-1.00	-1.00	1.00
ERCC-42	-1.00	-0.93	-1.00	-0.99	1.00
ERCC-99	-0.40	-0.70	-0.80	-0.83	0.78
ERCC-113	-1.28	-0.93	-0.98	-1.00	0.70
ERCC-171	-0.77	-0.95	-1.00	-1.00	1.00
Average	-0.75	-0.95	-0.94	-0.98	0.92

PreAmp = preamplification

clinical bone core data sets. It is unclear why PPIA and HPRT1 assays performed poorly in this assessment. The C_q values generated for the non-preamplified samples were not linear. It may be that the stability of the cDNA was compromised during storage (having a greater impact on low abundance targets as a proportion of the total number of low copy molecules) and so did not provide an ideal target for qPCR amplification of the non-preamplified samples. This was not observed for the preamplified samples suggesting the amplicons generated in the preamplification may have provided a more stable and more easily amplifiable template for the qPCR. In addition, the low variability observed for the preamplified samples highlights the variability between samples. Inhibition may also be a factor in the observed difference. It is not known to what extent inhibition may have affected the amplification of these targets and whether or not the preamplified and non-preamplified targets were affected to the same degree. Inhibition evaluation was not performed as part of this study, however, future studies may address this concern by evaluating different target concentrations and measuring a dilution series to determine the influence of reversible inhibition and matrix components [155].

6.3.2.2 Reference Gene Determination

As detailed in the introduction to this thesis (**Chapter 1**), for accurate normalisation of mRNA data, reference genes should be validated experimentally for specific sample sets [132].

6.3.2.2.1 3D Co-Culture Model

Using the RefFinder program, dynamic array C_q data was evaluated for the selection of endogenous reference genes appropriate for the 3D gel co-culture sample set (**Figure 6.4A**). PPIA, GAPDH and YWHAZ were selected with geometric mean of ranking values of 1.57, 3.13 and 3.25, respectively. This ranking value in and of itself does not give an indication of how stable a reference gene is, just a ranking of stability relative to the other potential reference genes analysed.

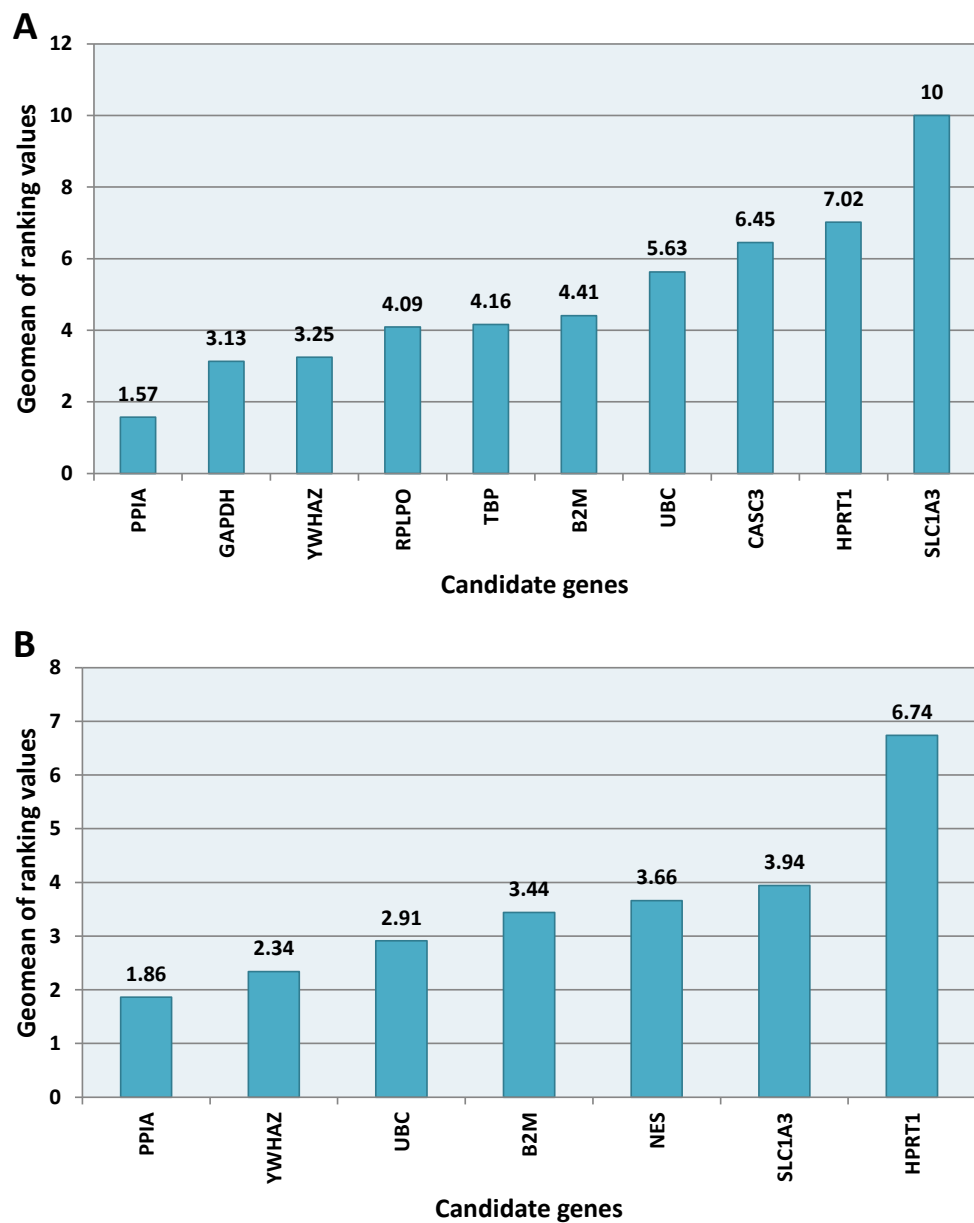


Figure 6.4 Comprehensive gene stability, generated from RefFinder output. Average expression stability values for assessed candidate reference genes. Targets showing expression in all samples (3D gel or bone core) were included (from dynamic array RT-qPCR data set). (A) 3D gel co-culture sample assessment. (B) Clinical bone core sample assessment. Based on the rankings from each program (GeNorm [7], Normfinder [137], BestKeeper [226] and the comparative ΔC_t (C_q) method [227]), individual genes are assigned an appropriate weight and the geometric mean of their weights is calculated for the overall final ranking. Starting from the most stable gene at the left, genes are ranked according to decreasing expression stability, ending with the least stable genes on the right.

However, the RefFinder program does provide a summary of the analysis from each of the programs utilised in the evaluation (GeNorm [7], Normfinder [137], BestKeeper [226] and the comparative ΔC_t (C_q) method [227]). The GeNorm program evaluates the stability of the applied reference genes (and hence the reliability of the normalisation) by calculating the GeNorm stability M-value for each of the potential reference genes analysed [360]. The lower the M-value, the more stably the reference genes are expressed in the tested samples. M-values lower than 0.5 are typically observed for stably expressed reference genes in relatively homogeneous sample panels. For more heterogeneous panels, M-values can increase to 1 [360]. M-values greater than 1.5 are considered as unacceptable levels of expression variability [7]. For the reference genes selected for the 3D gel co-culture sample set, the M-values were 0.079 (PPIA), 0.068 (GAPDH) and 0.084 (YWHAZ). This suggests that all three selected reference genes were stable and therefore suitable for normalisation.

As discussed in **1.3.1.6.2 Internal Reference Genes**, GAPDH may be used as an appropriate normaliser under validated conditions.

6.3.2.2.2 Clinical Samples

As for the 3D gel co-culture sample set, appropriate reference genes were selected for the clinical bone core samples using dynamic array C_q data input to the RefFinder program (**Figure 6.4B**). On this occasion, PPIA, YWHAZ, and UBC were selected as suitable reference genes with geometric mean of ranking values 1.86, 2.34 and 2.91, respectively. The selected reference gene M-values for the clinical bone core sample set were 0.012 (PPIA), 0.012 (YWHAZ) and 0.022 (UBC). These M-values suggest that all three selected reference genes were stable and therefore suitable for normalisation.

6.3.2.3 mRNA Quantification Process Precision Factors

3D gel co-culture and clinical bone core samples were individually assessed for variability contributions from sample to mRNA target quantification. This analysis was performed using C_q values without any normalisation in order to determine the magnitude of variance contributions at the different stages of analysis. As the role of normalisation is to remove much of this variability these differences cannot be easily determined once normalisation has been applied. This approach allows an assessment of where the most benefit would be obtained from replication, i.e. steps contributing the most variability would benefit most from increased replication. This provides a better estimation of the variability of the whole experiment. Once variance contributions have been determined, the impact of normalisation can be assessed.

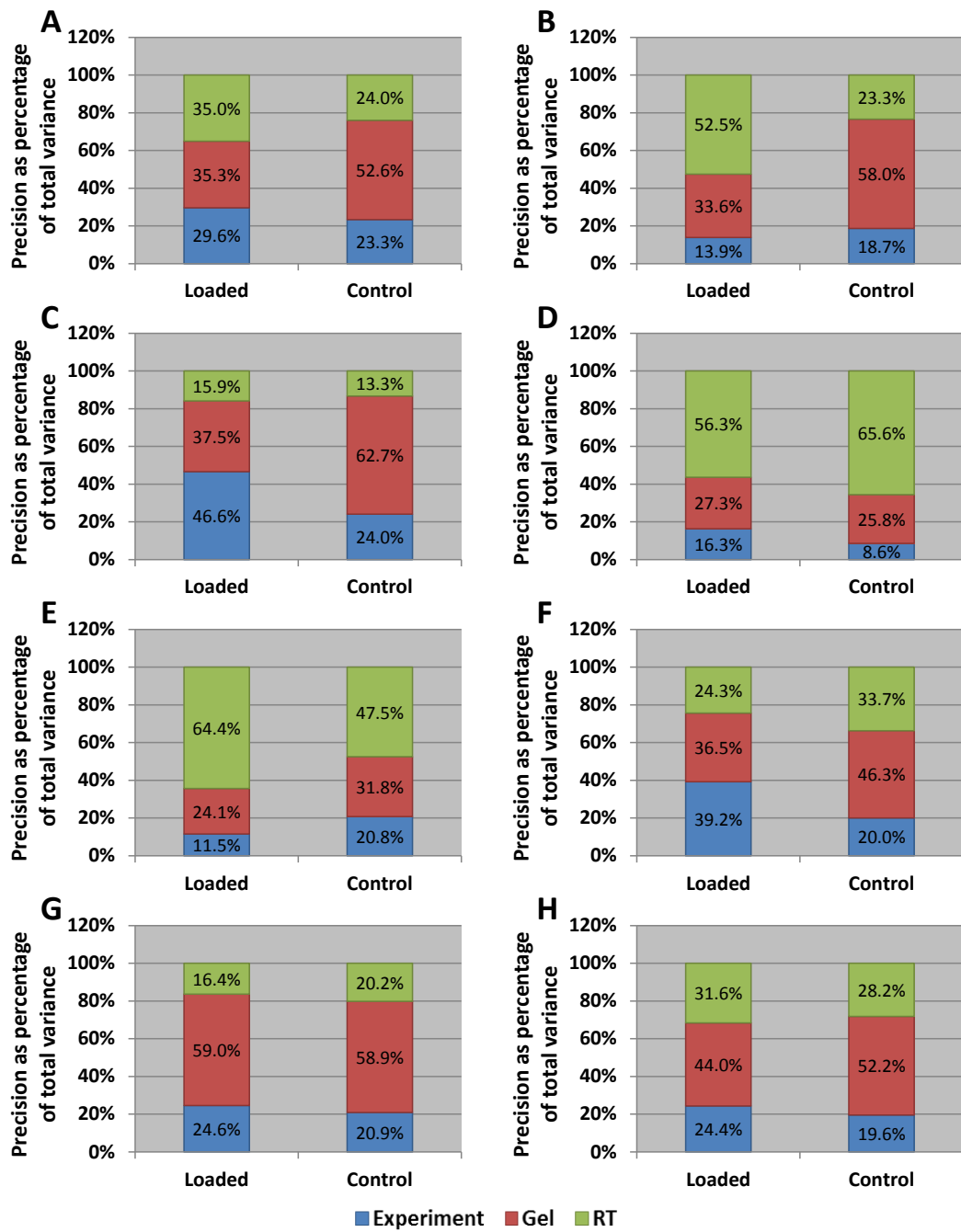
6.3.2.3.1 3D Co-Culture Model

For the 3D gel samples (**Figure 6.5**), the average variance (as a percentage of the total) across all targets was greatest in both the control and loaded samples for the Gel factor (49.1% and 41.2%, respectively) and lowest for the Experiment factor (25.4% and 28.5%, respectively). When considering the ERCC (synthetic) targets only (**Figure 6.5L-P**), the average variance was greatest in both the control and loaded samples for the Gel factor (50.6% and 54.9%, respectively) and lowest for the RT factor (11.9% and 13.3%, respectively). However, when considering the average variance of only the endogenous targets (**Figure 6.5A-K**), the greatest contributing factor for control samples was again Gel replicate (48.4%), but for loaded samples it was RT (37.7%). The lowest variability-contributing factor was Experiment for both control and loaded samples (19.9% and 27.4%, respectively).

6.3.2.3.2 Clinical Samples

For the clinical bone core samples (**Figure 6.6**), the average variance (as a percentage of the total) across all targets was greatest for the patient factor

Chapter 6 The Influence of Sample Type on Measurement Variability



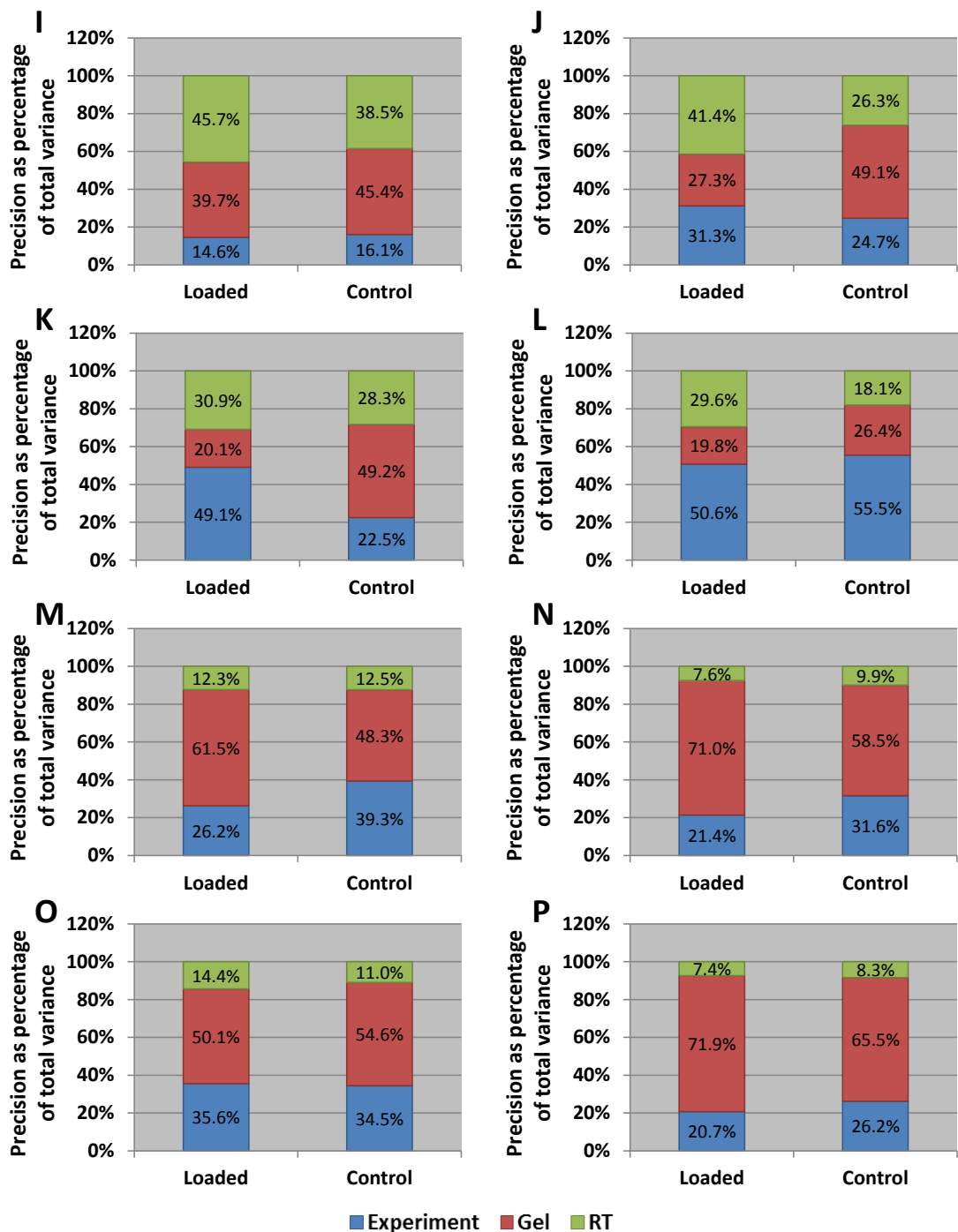


Figure 6.5 3D Gel co-culture process precision contributed by different factors. C_q variability contributions for different transcript targets were apportioned to experimental factors in the measurement process for 3D Gel co-culture samples, displayed as loaded versus control treatments. (A) B2M (B) CASC3 (C) GAPDH (D) HPRT1 (E) NES (F) PPIA (G) RPLPO (H) SLC1A3 (I) TBP (J) UBC (K) YWHAZ (L) ERCC-13 (M) ERCC-25 (N) ERCC-99 (O) ERCC-113 and (P) ERCC-171.

Chapter 6 The Influence of Sample Type on Measurement Variability

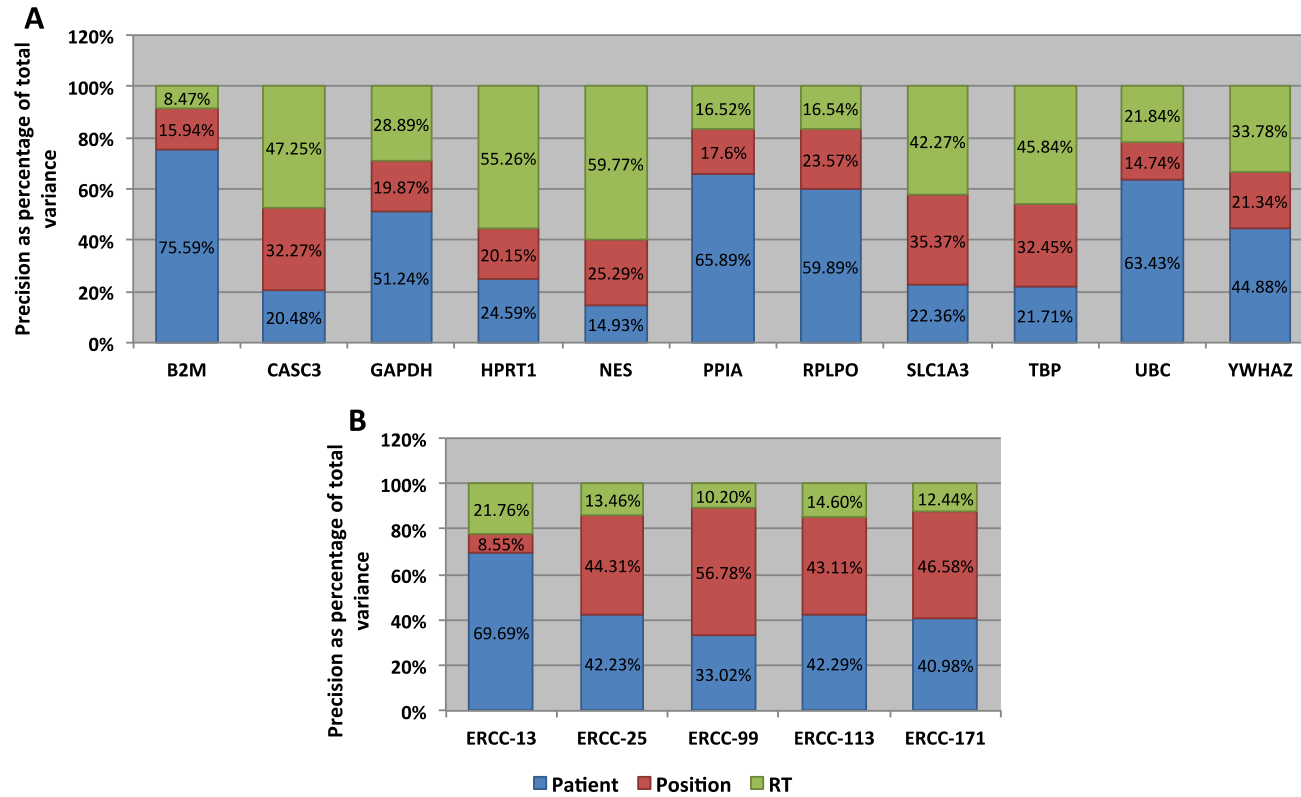


Figure 6.6 Clinical bone core process precision contributed by different factors. C_q variability contributions for different transcript targets were apportioned to experimental factors in the measurement process for 3D clinical bone core samples. (A) Endogenous targets (B) Synthetic targets.

(43.3%) and lowest for the RT factor (28.1%). When only synthetic ERCC targets were compared (**Figure 6.6B**), again the lowest variance attributed was to the RT factor (14.5%) and the greatest variance was attributed to the patient factor (45.6%). However, when only endogenous targets were considered (**Figure 6.6A**), the patient factor contributed the most variability (42.3%), while anatomical position contributed the least (23.5%).

6.3.2.4 Comparison of Factor Variability

Following assessment of process precision factors and validation of reference genes appropriate for normalisation of each sample set, dynamic array RT-qPCR data was normalised and RQ values (relative to sTCM calibrant) compared to determine experimental differences. In this context, ERCCs are not being used as normalisers. By normalising them to the validated endogenous reference genes, we can assess if they remain stable and therefore whether they would be suitable as normalisers.

6.3.2.4.1 3D Co-Culture Model

3D co-culture samples were normalised to the geometric mean of three reference genes: PPIA, GAPDH and YWHAZ (as determined above, **6.3.2.2 Reference Gene Determination**).

There was a significant difference observed in normalised RQ values between loaded and control samples for all synthetic targets (all $p < 0.02$, single-factor ANOVA). There was an average 42-fold difference between control and loaded normalised RQ values for the ERCC targets, with control values being lowest. The levels of these synthetic targets should remain constant, as they were spiked into samples post-stimulation and it is therefore not possible to alter their regulation in response to mechanical loading. Alternative hypotheses for the deviation in synthetic target normalised RQ values post-treatment may include the influence of

changes to the extracellular matrix in response to mechanical loading [361]. The observed effect may be due to factors specifically pertaining to the synthetic origin of the ERCC targets, which are not shared by the endogenous targets. It is also possible that endogenous targets may be protected by cellular mechanisms, not available to the synthetic targets. It therefore brings into question the suitability of the ERCC transcripts for normalisation purposes in such an experiment.

Single-factor ANOVA was used to compare loaded versus control sample data individually for each target (**Figure 6.7**). There was no significant difference in normalised RQ values between loaded and control samples for all but three of the endogenous targets analysed (all $p > 0.08$). For three endogenous targets, GAPDH, PPIA and SLC1A3, there was a significant difference observed between loaded and control data sets ($p = 0.027, 0.003$ and 0.0003 , respectively). SLC1A3, the only GOI detected with sufficient expression, was therefore shown to be influenced by mechanical loading in this experiment. There was a 33-fold difference between loaded and control normalised RQ values for SLC1A3, with loaded values being lowest. This finding is in concordance with previous studies demonstrating the down-regulation of SLC1A3 (also known as EAAT1 and GLAST) in response to mechanical loading [210,362].

Data was analysed further using two-factor ANOVA of gel versus RT for all targets individually and each condition (loaded and control) separately. For all targets and both conditions (except B2M loaded $p = 0.074$ and RPLPO control $p = 0.066$) there was a significant difference in normalised RQ values between gel replicates (all $p < 0.04$). All targets under both conditions showed a significant difference in normalised RQ values between RT replicates (all $p < 0.035$), except for TBP, both loaded and control samples ($p = 0.134$ and 0.178 , respectively) and ERCC-25 and -99, for loaded samples only ($p = 0.156$ and 0.086 , respectively). There was no significant interaction observed for any target between the two factors (gel and RT replicates) for either condition (loaded or control), all $p > 0.06$, except for CASC3,

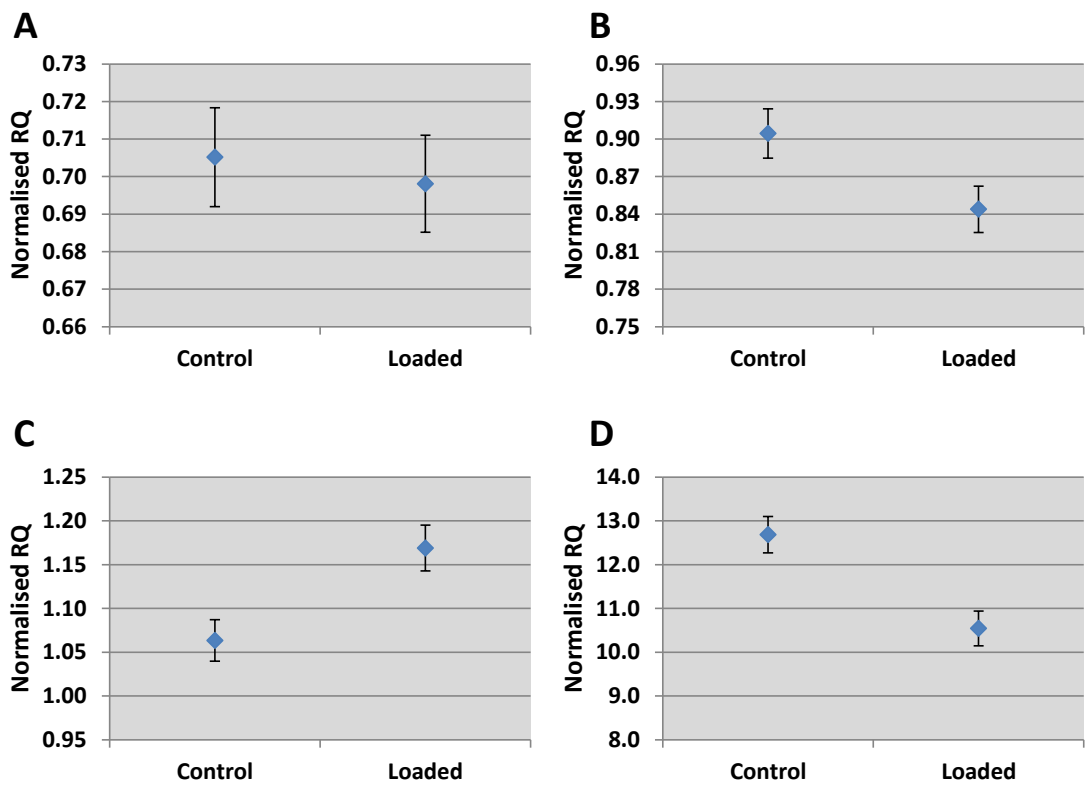


Figure 6.7 3D co-culture treatment variability. Normalised RQ distributions for control versus mechanically loaded 3D gel co-cultures. (A) B2M, representative of no significant difference between conditions (B-D) display a significant difference between loaded and control treatment samples (B) GAPDH (C) PPIA (D) SLC1A3. Error bars SEM, n = 54. Single-factor ANOVA (loaded versus control) p-values: (A) B2M = 0.702, (B) GAPDH = 0.027, (C) PPIA = 0.003 and (D) SLC1A3 = 0.0003.

TBP and UBC control samples only and YWHAZ loaded samples only ($p = 0.003$, 0.045 , 0.008 and 0.017 , respectively).

Gel was determined to be the greatest contributor to whole process variability and so it is not surprising that significant differences were observed between gel replicates. Such large variabilities in sample measurements are not conducive to measurements of small fold changes.

Data were analysed using two-factor ANOVA of experiment versus RT for all targets individually (**Figure 6.8**). For all targets except one (RPLPO, $p = 0.101$, **Figure 6.8A versus B**) there was a significant difference in normalised RQ values between experiments (all $p < 0.002$). All synthetic targets (ERCCs, **Figure 6.8F versus E**) and one endogenous target (TBP, **Figure 6.8D versus C**) showed no significant difference in normalised RQ values between RT replicates (all $p > 0.1$). All other endogenous targets (B2M, CASC3, GAPDH, HPRT1, PPIA, RPLPO, SLC1A3, UBC and YWHAZ) showed a significant difference in normalised RQ values between RT replicates (all $p < 0.001$). There was no significant interaction observed for all but one target (B2M, $p = 0.001$) between the two factors (gel and RT replicates), all $p > 0.09$.

The larger contribution of RT to whole process variation compared to experiment, which had the lowest contribution, is represented in **Figure 6.8A & B** for target RPLPO. From the plot presented according to replicate experiments (**Figure 6.8A**), it is clear that there was no observable difference across the data set. All experimental replicates appeared to have similar normalised RQ values (for this particular target). However, when the same data is presented according to RT replicate, differences between RT replicates are clear. The trend is matched in the loaded and controlled samples for this target data set (RPLPO). These plots nicely demonstrate the influence of the RT on whole process variability. Alternatively, the TBP target data displays the opposite scenario, that is, there was a discernible trend in normalised RQ values across both loaded and controlled samples

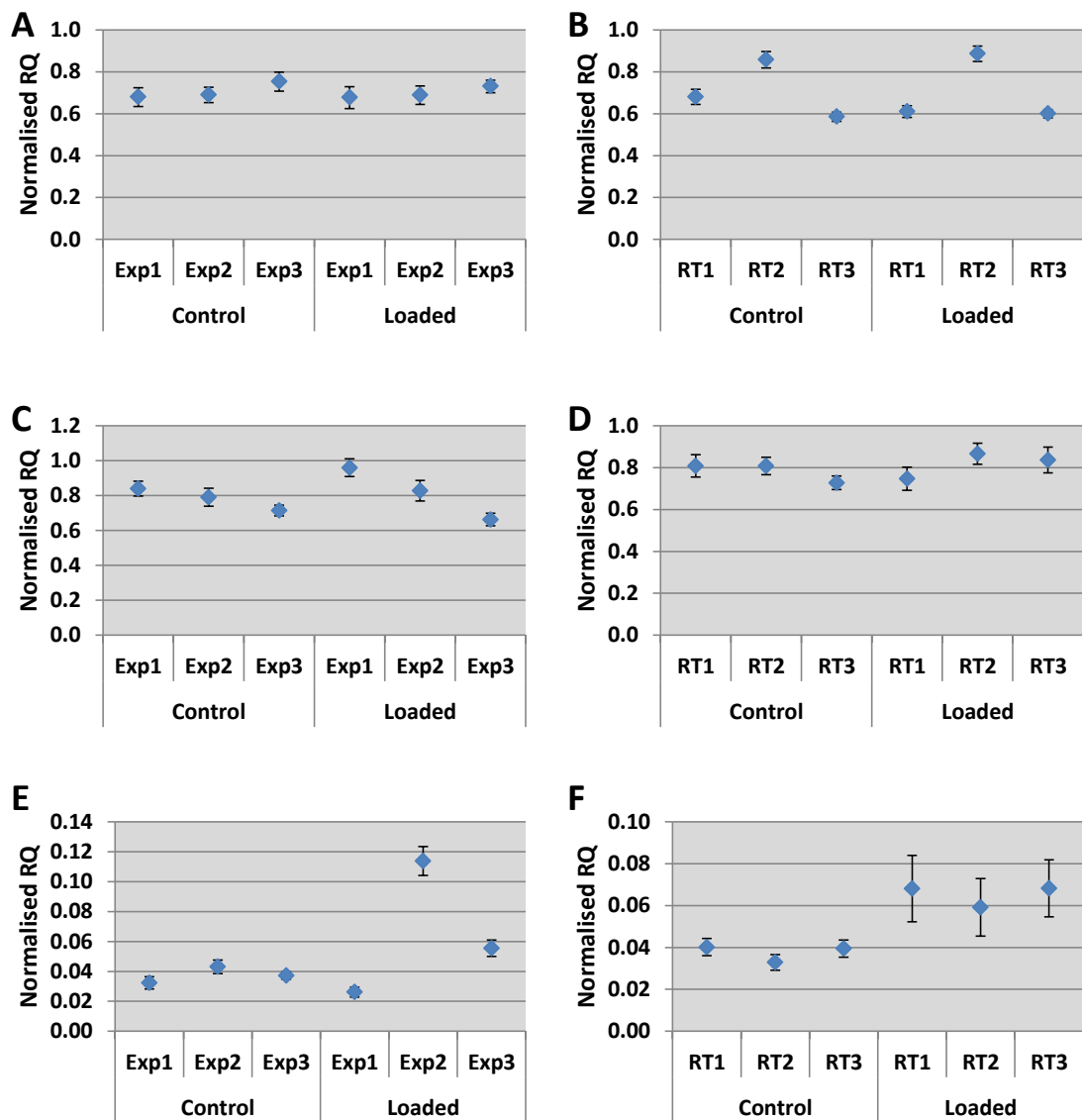


Figure 6.8 3D Gel co-culture variability distributions. Normalised RQ variability for different transcript targets are displayed as loaded versus control treatments according to experimental factors, experiment or RT replicates. (A) RPLPO by experimental replicates (B) RPLPO by RT replicates (C) TBP by experimental replicates (D) TBP by RT replicates (E) ERCC-13 by experimental replicates (F) ERCC-13 by RT replicates. Error bars SEM, n = 18. (A, C & E) RT replicates (from the same RNA sample) and gel replicates are pooled and individual experimental data is plotted. (B, D & F) RT data combines the gel and experimental replicates data. Each of three replicate RTs (from the same RNA sample) is plotted individually.

according to experimental replicates (**Figure 6.8C**), whereas RT replicates appeared to remain consistent, with no significant differences measured (**Figure 6.8D**).

The ERCC targets displayed increased variability for the loaded RT replicates compared with control samples and experimental replicates (**Figure 6.8E & F**, represents ERCC-13). This may have contributed to the lack of a significant difference in normalised RQ values between RT replicates (where significance is found in all but one endogenous target, TBP). ERCC-13 data, displayed in **Figure 6.8E & F** is representative of all the ERCC targets. It is important to note this increase in RT variability for loaded (treated) samples when measuring synthetic targets. No increase in RT variability is observed for loaded (treated) samples when measuring endogenous targets. Since the synthetic targets were spiked into samples after the cells were lysed in TRIzol, their absolute levels should remain constant. It is possible therefore, that the treatment of samples (mechanical loading) stimulated a change in the sample matrix (change in endogenous mRNA and/or protein expression profile), which subsequently affected measurement sensitivity when evaluating ERCC targets. It is possible that all extracts were affected by sample matrix but that this was hidden in the noisier, endogenous data. It is not possible to distinguish between variability contributions from the extraction and RT steps using these protocols. However, the ERCC targets could be utilised for this purpose in future experiments. Suitable reference genes should maintain stable levels, regardless of treatment or matrix effects [47]. It appears that for this particular experimental set-up the ERCC synthetic targets are not suitable reference genes for normalisation of these data.

These data suggest that replicate gels are a major contributory factor to whole process variance, more so than replicate experiments (within experiment is more variable than between experiment). Furthermore, the synthetic ERCC targets do not behave in the same way as the endogenous targets, with experiment contributing more variability to the measurement of synthetic targets than RT;

whereas the opposite is true for endogenous targets (RT is more variable than experiment). However, it must be remembered that the synthetic ERCC targets were spiked into samples pre-extraction and so cannot accurately represent variability contributions in steps prior to this point. Therefore, for the analysis of endogenous targets, RT (three RT reactions from each RNA extraction) contributed more variability to the measurement than experiment. This is an important finding as many cell culture-based studies may replicate an experiment without also replicating the RT step. However, it is extremely difficult to ascertain quite how significant this problem is due to the poor standards of reporting of RT-qPCR technical details [59]. This could lead to an underestimation of the experimental error; possibly biased results and potentially measurement claims of fold changes smaller than actual capability.

6.3.2.4.2 Clinical Samples

Clinical bone core samples were normalised to the geometric mean of three reference genes: PPIA, YWHAZ, and UBC (as determined above, **6.3.2.2 Reference Gene Determination**).

There was a significant difference observed in normalised RQ values between anatomical positions and between patients for all assays (all $p < 0.0001$, two-factor ANOVA per assay), except for between anatomical positions for B2M ($p = 0.0758$) and SLC1A3 ($p = 0.2274$) only (**Figure 6.9 Figure 6.10**). There was a significant interaction between the two terms (patient and anatomical position) for all assays (all $p < 0.00001$). There were similar trends across the patient panel for all the synthetic ERCC assays evaluated (**Figure 6.9**), with patient 4 samples generating higher normalised RQ estimates with increased variability in the measurement. To define these differences, patient 4 samples analysed using ERCC-13 and -99 were plotted to reveal their contributing variance components (**Figure 6.9E & F**). These plots clearly show that the majority of the variability in the patient 4 samples was attributable to the posterior locations, especially the PL anatomical position.

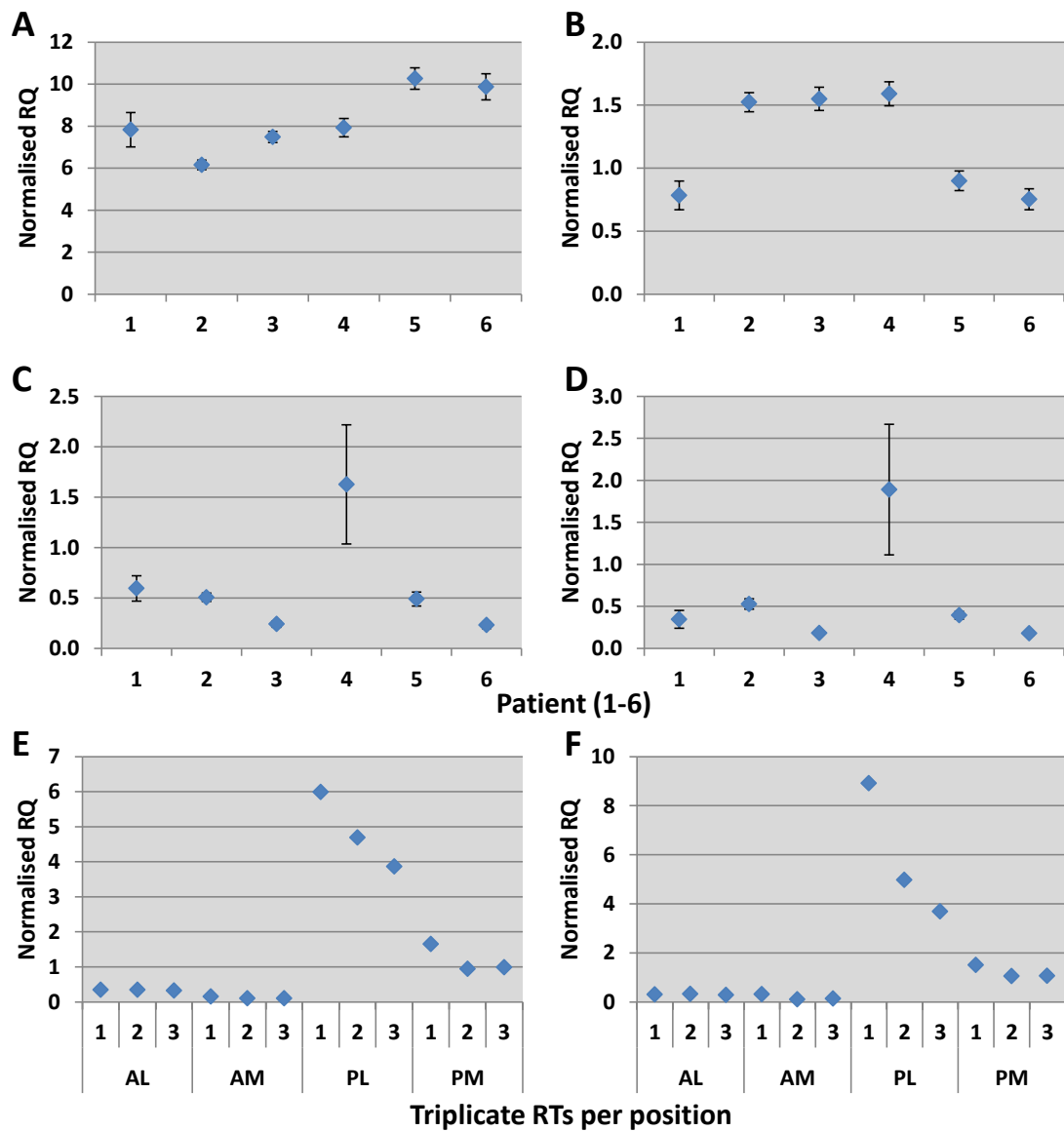


Figure 6.9 Clinical bone core patient variability. Normalised RQ distributions for different patients. (A) B2M (B) UBC (C) ERCC-13 (D) ERCC-99. Error bars SEM, n = 24 (A & B), n = 12 (C & D). Patient 4 for assays ERCC-13 and ERCC-99 are also shown displaying their contributing factors (RT replicate and anatomical position) to display variance contributions attributable to this patient for these targets (E) ERCC-13 (F) ERCC-99. Anatomical Position: Anterior Lateral (AL), Anterior Medial (AM), Posterior Lateral (PL), Posterior Medial (PM).

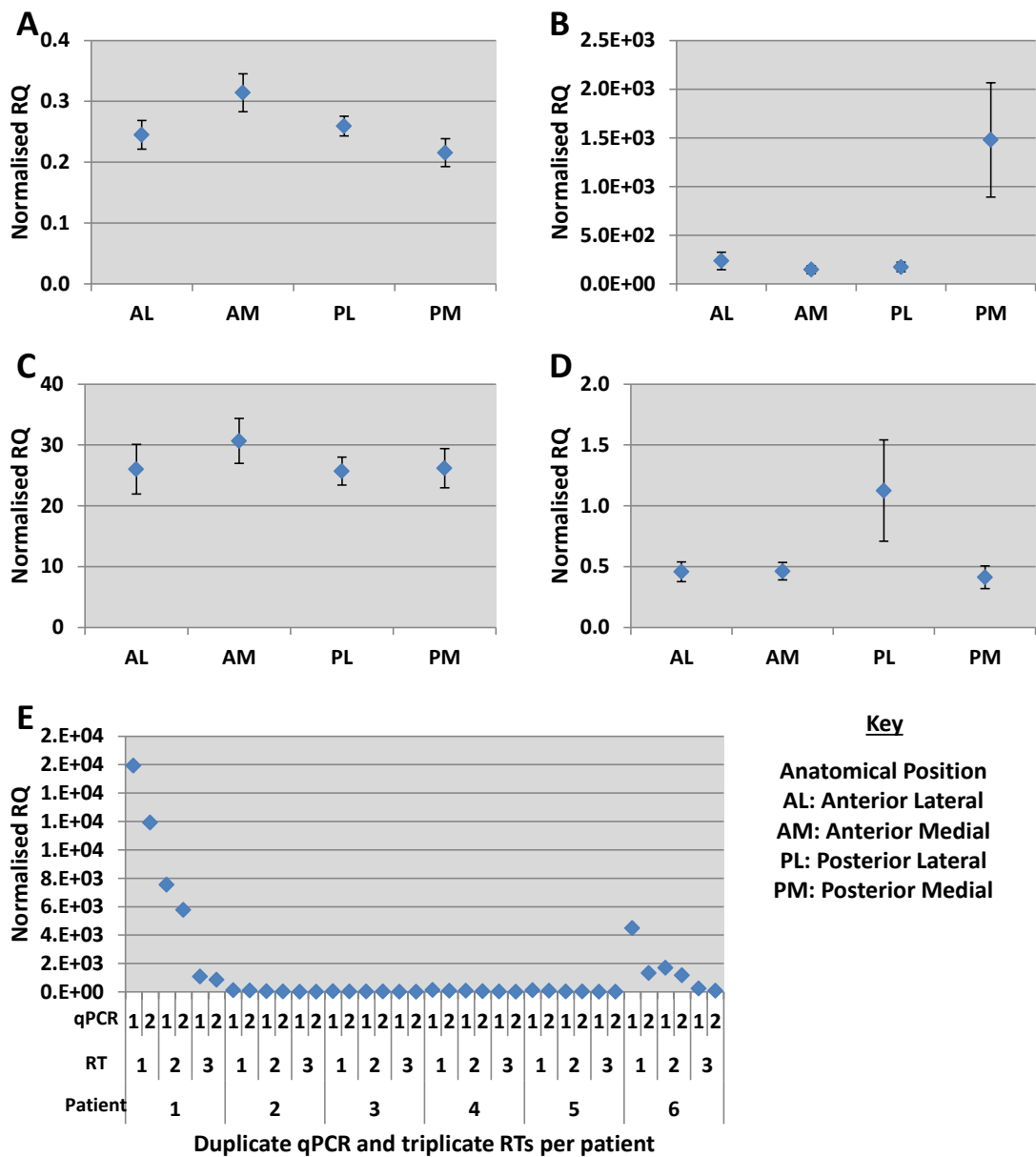


Figure 6.10 Clinical bone core anatomical position variability. Normalised RQ distributions for different biopsies positions of the tibial plateau during TKR surgery. (A) GAPDH (B) NES (C) SLC1A3 (D) ERCC-13. (A & B) Significant difference in normalised RQ between anatomical positions. (C & D) No significant difference in normalised RQ between anatomical positions. Error bars SEM, n = 36 (A-C), n = 18 (D). Anatomical position PM for assay NES is also shown displaying its contributing factors (qPCR replicate, RT replicate and patient) to show variance contributions attributable to this anatomical position for this target (E). The same evaluation for ERCC-13 is shown in **Figure 6.9E** (attributable to patient 4).

Chapter 6 The Influence of Sample Type on Measurement Variability

There was no significant differences observed in normalised RQ values between anatomical positions for all of the assays (all $p > 0.05$, single-factor ANOVA per assay), except GAPDH and NES (all $p < 0.04$), (**Figure 6.10**). The large variability observed for anatomical position PM when analysing samples using NES, was further assessed by plotting contributing variance components (**Figure 6.10E**). This plot suggests that the majority of the variability in the PM position samples was attributable to patients 1 and 6, in particular, RT replicates 1 and 2.

It may be possible that GOI targets would be affected by an uneven gait (and consequently an uneven mechanical load) on osteo-arthritic joints due to varus/valgus deformity (bone or joint is twisted inward/outward from the centre of the body), formation of osteophytes (bony projections that form along the joint margins) and subchondal sclerosis (causes joint pain and numbness due to increased bone density and mass, producing a thin layer of bone beneath the cartilage in the joints in the affected area) [363,364]. Further data, assessing a greater number of patients and several more GOI targets, would be needed to test this hypothesis.

Endogenous targets highlight the variability distribution across all factors considered. In which case, anatomical positional variance was lower than both RT and patient variabilities. Biological variability between patients was the largest contributory factor for overall process variance in this study [365,366].

Given the differential expression observed between loaded and control samples in the 3D co-culture model, and its mechanical regulation as reported in the literature [210,362], GOI SLC1A3 was evaluated for expression differences between anatomical positions for each of the patients (**Figure 6.11**). Comparing the normalised RQ values across anatomical positions for each patient, 44.44% of the lowest normalised RQ values were attributable to the AL position, 30.56% to PM, 13.89% to AM and 11.11% to PL. Alternatively, 27.78% of the highest normalised RQ values was attributed to each AL and PL, and 22.22% each to AM and PM

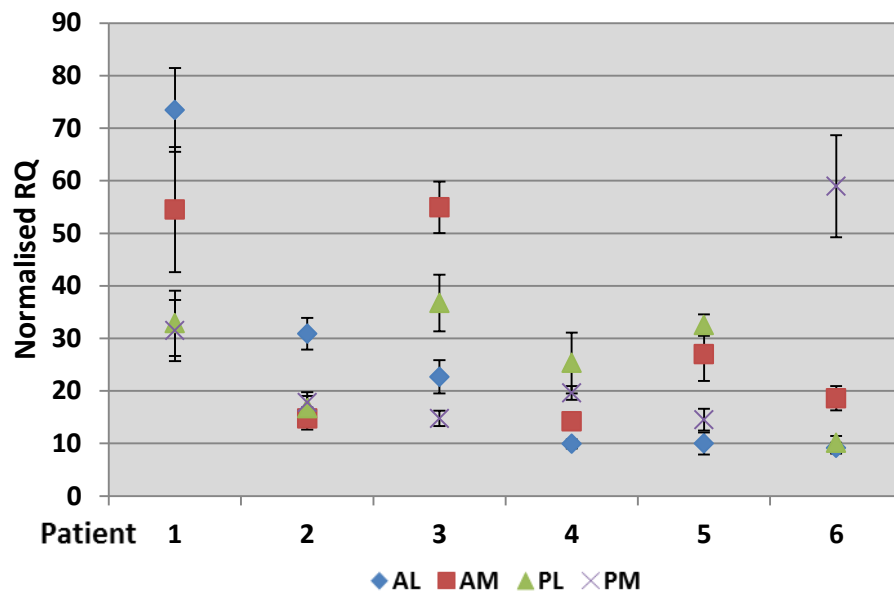


Figure 6.11 Clinical bone core SLC1A3 anatomical position expression variability. Normalised RQ distributions for GOI SLC1A3 between anatomical positions for different patients. Error bars SEM, n = 8. Anatomical Position: Anterior Lateral (AL), Anterior Medial (AM), Posterior Lateral (PL), Posterior Medial (PM). RQ values were calculated relative to sTCM calibrant.

positions. However, replicate RT and preamplification/qPCR samples did not always agree. Therefore, there does not appear to be a pattern between anatomical position and difference in RQ values between individual patients. However, this experiment utilised a small patient cohort, by increasing patient numbers, positional differences may become apparent.

Anatomical positional variance may be low if in fact it does not have much or any influence on mRNA levels. Indeed, the ANOVA evaluation suggested that neither patient nor anatomical position significantly impacted these data. However, there are a couple of points that should be considered. Firstly, anatomical position was assigned solely at the discretion of the surgeon. There was no grid or template for location of a particular position and so locations did not remain uniform across collections. For that reason, the boundaries may be blurred. Secondly, the vast majority of endogenous targets measured were candidate reference genes, and as such, would be hypothesised to remain fairly stable, regardless of anatomical position. Of the targets that were detected with sufficient expression, SLC1A3 was the only one that could be described as a GOI. For this target, the anatomical position factor was more variable than the patient factor (35.4% and 22.4%, respectively). Furthermore, the RT factor was actually the largest contributor to whole process variability (42.3%). Based on this finding, it is possible that mRNA levels are influenced by anatomical position and by extrapolation; this may be due to different mechanical loading pressures at different positions of the joint. In order to test this hypothesis further, a larger cohort of patients could be analysed, considering additional patient factors such as sex, age and medical treatment. A new selection of GOI targets should be assessed to determine if they are affected by mechanical loading in these patients. Mechanical load has been shown to regulate glutamate signalling in bone [210,362,367], and glutamate concentrations are greatly increased in osteoarthritis and rheumatoid arthritis [368], where major disruption in bone remodelling occurs [369]. Additional targets within the glutamate-signalling pathway would therefore be worth investigating in these samples. Such targets may include: AMPA1-3, KA1-2, mGluR1, mGluR5, GluR5,

VGlut1 and NR1 [208-210,362,369,370]. In addition, some effort should be made to maintain consistency between positional collections.

In terms of attributing variability contributions across the whole process, it may be argued that reference genes only should be assessed as they are less biased by biological variations. This would be true if one wanted to assess the contribution of technical factors alone (such as extraction, RT and qPCR), but in order to get the full picture biological variability must also be accounted for. In terms of streamlining a process to reduce as much as possible the technical variability and to assess where best to replicate in order to reflect those variabilities accurately, an assessment of variability contributions may be best made using only multiple validated reference genes. However, in order to fully characterise the true sensitivity to which measurement claims can be made, an assessment of all factors in the process by the analysis of multiple GOIs should be made.

The Cardiff Research team applies a 'molecule to man' approach to investigate normal joint biomechanics and determine how this is influenced by pathology to inform clinical intervention and rehabilitation in musculoskeletal disorders. The work presented here aids in the attainment of the project goals by measuring mRNA profiles in patient bone core samples and defining variability associated with key parameters including inter-patient and positional disparity. This work will act to outline best practice for experimental approaches and highlight key sources of variability that should be considered in order to generate meaningful results reflecting true biological variability. These include patient and RT variability, where replication should be focussed.

6.3.2.5 Assay Troubleshooting

Dynamic array analysis of preamplified clinical bone cores, 3D gel and calibrant (standard curve) samples showed no amplification in seven of the assays chosen for their applicability to bone samples (AMPA1, AMPA2, AMPA3, EAAT1, EAAT3,

KA1 and KA2 – all involved in glutamate signalling). As this result was unexpected, a subset was analysed by qPCR for comparison.

SLC1A3 (which was detected on the dynamic array) and EAAT1 assays actually target the same transcript (accession NM_004172.4). The assays were designed to different regions of the target molecule and were named differently (with recognised synonyms) to avoid confusion. Given that the SLC1A3 assay generated a positive amplification result, EAAT1 would be expected to do the same, as they are linked targets (on the same transcript). EAAT1/SLC1A3 is known to be present at reasonable abundance in the SaOS-2 cell line [267]. It was therefore chosen, alongside GAPDH, which performed consistently well in the dynamic array experiments, to be analysed further by qPCR to test assay performance. Triplicate samples of preamplified calibrant units were analysed alongside non-preamplified human whole bone total RNA (following RT).

These data show presence of both GAPDH (in agreement with the dynamic array data) and EAAT1 (not observed in the dynamic array data, despite positive amplification of the SLC1A3 target) (**Figure 6.12**). This proves that the EAAT1 assay is performing sufficiently, despite the negative result on the dynamic array. Furthermore, the preamplification process is not a cause for concern as the results reflected those expected, i.e. preamplified targets have a lower C_q than non-preamplified targets; the assay is shown to be working. It may be the case that some or all of the seven mRNA targets that failed to demonstrate positive amplification in the dynamic array format may in fact be present, but for some reason, failed in this format. This may be due to assays not being sufficiently optimised, sensitivity problems related to the dynamic array, or other factors yet untested. It is possible that these targets were low abundance and the dynamic array was not sensitive enough to detect them, despite the application of preamplification. This is certainly possible as due to the low reaction volumes utilised by this platform (9 nL), targets are required to be present at concentrations exceeding $1E+04$ to $1E+05$ copies/ $5 \mu\text{L}$ reaction per inlet ($1E+02$ to

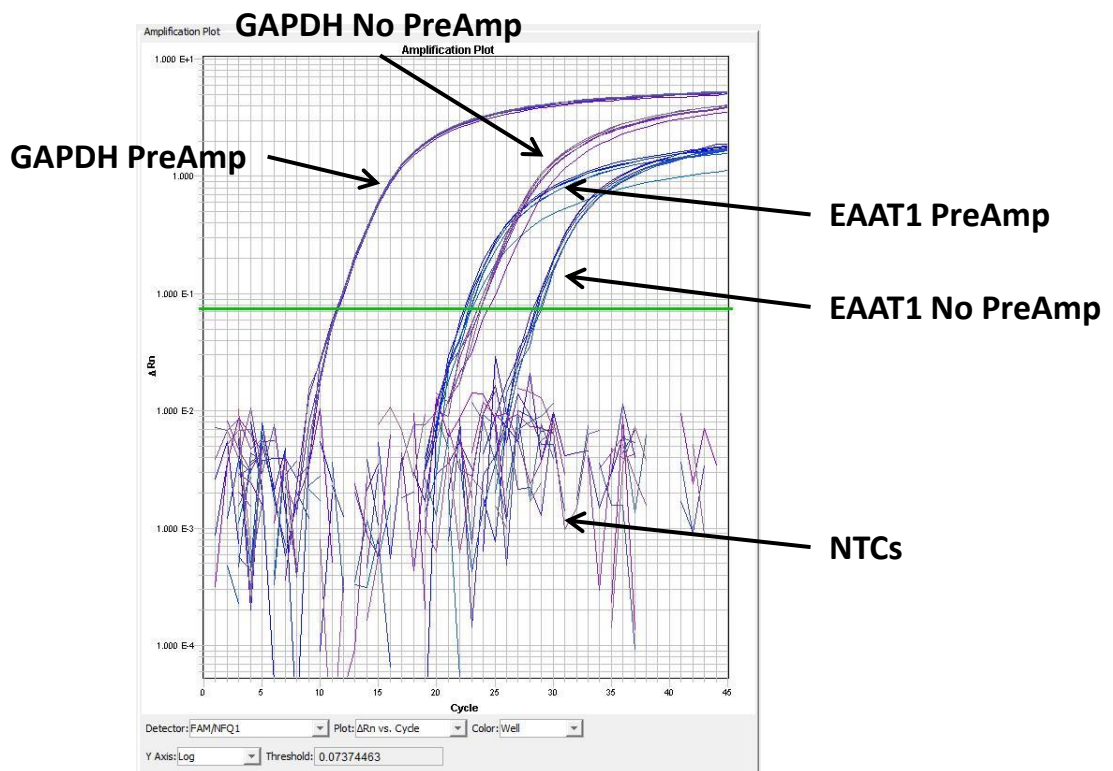


Figure 6.12 RT-qPCR test for abundance. Amplification plots are shown. GAPDH and EAAT1 were analysed for mRNA level in both Calibrant (preamp, preamplified) and human whole bone total RNA (No preamp, non-preamplified) materials.

1E+03 copies/9 nL reaction chamber) in order to be reliably detected [45].

The fact that target was successfully identified using the SLC1A3 assay, but not using the EAAT1 assay (same transcript, different regions targeted) may be explained by the different amplicon positions within the structure of the template. On investigation into the predicted secondary structures (mFold [228]), it appears that the SLC1A3 amplicon region contains more stem-loop structures than the EAAT1 amplicon region (**Figure 6.13**), thus does not explain the difference in assay sensitivity. However, further folding of the transcript may occur in solution, obscuring the primer target sites for the EAAT1 assay, making amplification of the SLC1A3 amplicon more efficient. Furthermore, decreased sensitivity of low copy number targets may arise due to decreased efficiency of the RT (and potentially preamplification), and increased stochastic variation of the qPCR [45,48]. The sequence used for designing the assays was transcript variant 1, which is the longest transcript variant. The SLC1A3 assay crosses exon 2-3. The EAAT1 assay crosses exon 7-8. SLC1A3 transcript variant (GLAST-1a), which is an exon 3 skip transcript, has previously been shown to be expressed in bone [267,371]. It is possible that this transcript variant decreases RT-qPCR detection using the SLC1A3 assay, as this crosses the exon 2-3 boundary and so expression of the variant would not be detected by the SLC1A3 assay (although it would be detected by the EAAT1 assay). However, the SLC1A3 amplicon is amplified whereas the EAAT1 amplicon is not detected and so it is not possible from these data to detect the abundance of the full-length transcript versus the exon 3 skip transcript variant.

Further work required to resolve these issues include analysis of these samples by qPCR. The assays in question were optimised using Human whole bone total RNA (DV Biologics P/N pM007r-107, used at 200 ng/reaction), by qPCR prior to dynamic array analysis. However, these assays were not tested with the clinical samples by RT-qPCR, only on the dynamic array (where observation of amplification failed). The clinical samples should be tested both with and without

Output of sir_graph (©)
mfold_util 4.6

Created Fri Aug

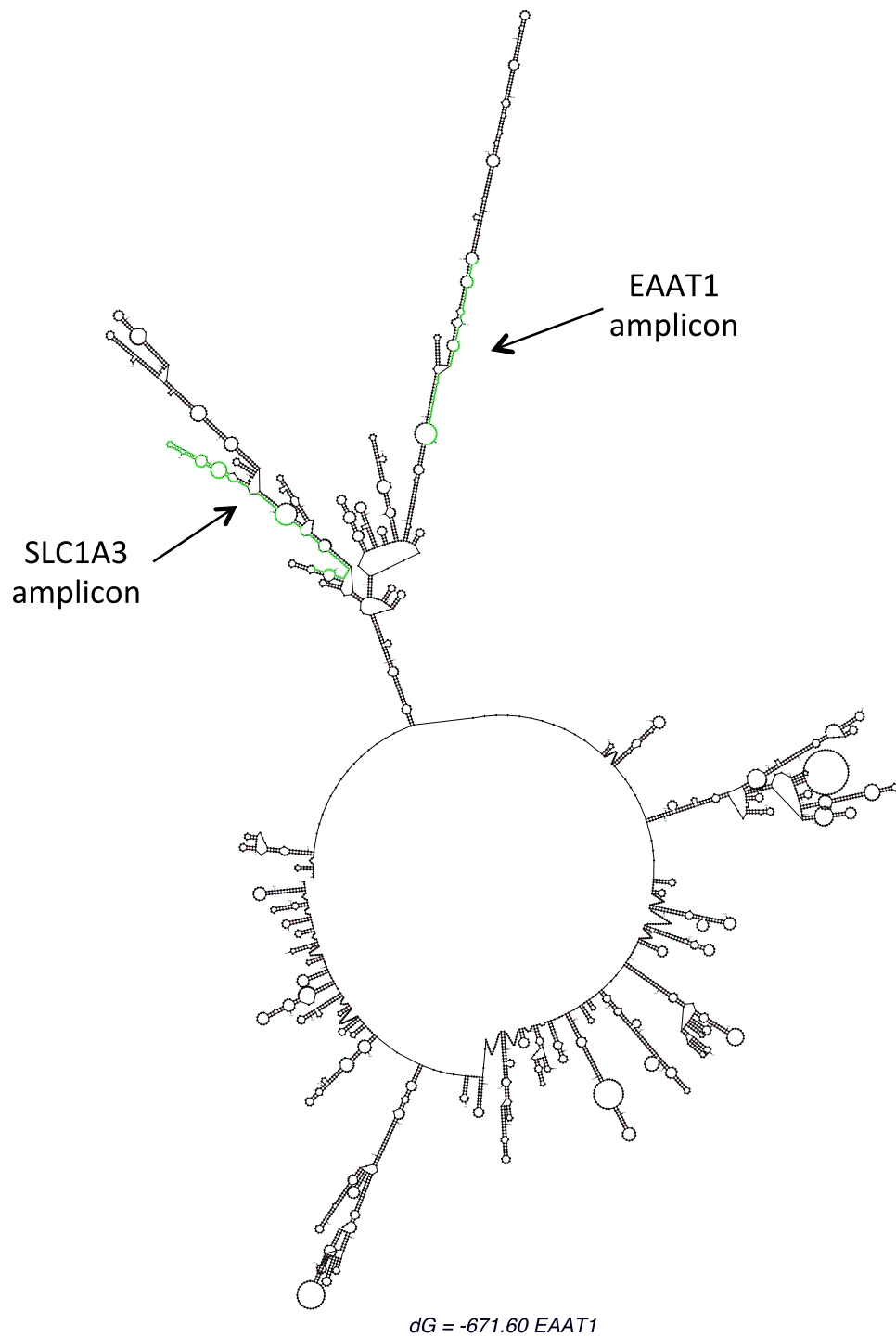


Figure 6.13 EAAT1/SLC1A3 RNA Secondary Structure Prediction from mFold. Green highlighted regions indicate amplicon. Folding predictions were performed at 45°C (temperature of RT step).

preamplification, with relevant positive controls, to fully discern the mRNA level of the targets in question. Furthermore, low abundance targets may benefit from RT-dPCR analysis, which has been shown to be more sensitive than RT-qPCR for detection of minority targets [111,372].

6.4 Conclusions

The 2D cell culture experiment indicated that there was a disparity between different cell passages regarding the impact of treatment on RNA yield, with only older cells showing a significant difference from control populations after treatment. Furthermore, cell passage (age) had an impact on RNA yield precision, with older cell populations displaying greater variability in total RNA measurement. However, this study analysed two different passages and so the variability observed may not be linear. Additional passages (and additional cell lines) would need to be assessed in order to determine whether these cell passage-induced biases are real (cell passage impacts RNA yield precision). Variability contributions suggest that replication efforts should be concentrated at the level of flask repeats followed by time point. Extraction replicates contributed little variability to the total error. If the variability observed for older cells is confirmed through reproducibility experiments, then cell passage should also be taken into account and replicates focused at this level. For the 3D co-culture experiment, treatment appeared to have no impact on total RNA yield, while both cell batch (different experiments) and gel replicates impacted RNA quantity variability. The clinical bone core experiment suggested that both anatomical position and patient introduce significant variability to total RNA yield measurements. Considering earlier cell passage variability alone (2D cell culture), these data suggest that 2D cell culture variability is lowest of the three models tested and sample complexity is positively correlated with RNA yield variability; as sample complexity increases, so does measurement variability of extracted total RNA.

The RT-qPCR experiment analysing 3D co-culture samples revealed that for endogenous targets, the greatest factor contributing to variability for control samples was Gel replicate and for loaded samples was RT, with the lowest variability-contributing factor for both control and loaded samples being Experiment. In similar experimental set-ups, efforts should therefore be made to replicate the gel and RT steps, an important finding as similar cell culture-based studies may replicate an experiment without also replicating the RT step. GOI SLC1A3 was shown to be influenced by mechanical loading, and warrants further investigation into the mechanism of this regulation [208-210,369,373]. The RT-qPCR analysis of clinical bone core samples illustrated that for endogenous targets, biological variability between patients was the largest contributory factor for overall process variance, while anatomical position contributed the least. Replicates should therefore be focussed on the patient and RT level in future studies of similar design. It should be noted that there are several factors relating to the patient variability that have not been taken into account in this study. These include patient age, sex, disease status/progression, medical interventions (drug treatments), etc. These biological variabilities add a layer of complexity beyond that modelled by the 3D co-culture system. A comprehensive assessment of such factors would require a much larger cohort of patient samples. These data combined also suggest that the ERCCs are not suitable for normalisation of values in these experiments as their levels are variable between treatment conditions.

The variability observed in the ERCC targets suggests that these transcripts may be more susceptible to matrix effects/inhibitors than the endogenous reference genes. Furthermore, there may be some influence in terms of enzyme efficiency when dealing with these synthetic targets. Although the ERCC consortium produced them with a mind to generate materials as close to endogenous targets as possible, it is inevitable that differences will be inherent in these synthetic molecules and as a result, their very nature may render them unsuitable (at least as a gold standard) for sample normalisation and comparison by these means.

Chapter 6 The Influence of Sample Type on Measurement Variability

There were some experimental factors that were not highly controlled, such as surgically obtained samples, which could stand to be regulated. This may include standardisation of biopsy sites for bone core sample collection (although the surgeons involved have extensive experience in these collections), weighing bone cores for normalisation of RNA quantity to tissue weight and standardising storage procedures (such as time to snap freezing, thawing for removal of RNAlater, etc.). These measures would aid analysis by improving error measurements and allowing true biological differences to be realised. A key finding of these data has shown very little error between technical replicates. It should be noted that these experimental studies have been well controlled (where possible) and performed very carefully due to the concern for variability. As a result, these investigations may not reflect common study protocols and therefore may not be representative of variabilities typically observed, particularly for cell line and patient replicates, where reported variances are often high [374-377]. These synthetic scenarios have demonstrated good intermediate precision. However, if researchers routinely follow such rigorous methodologies and achieve the same levels of high precision, then data capabilities will be improved. Standardising all aspects of laboratory procedure may not be necessitated if individual studies can maintain consistency in variability measurement and understand the sources of bias and error intrinsic to a particular approach. Ultimately, different methods, whether it be RT-qPCR or RT-dPCR using various different platforms (ABI 7900, Roche Light Cycler, Qiagen Rotor Gene, Fluidigm Biomark, BioRad QX200, Life Sciences Quant Studio 3D, etc.) or other approaches such as RNA-Seq, may be followed and still maintain their relevance through the use of appropriate standardisation and calibration.

The question becomes, if repeatability (experimental replicates under the same conditions with the same operator) can generate very low/negligible error components to a measurement result, even when analysing complex clinical samples from different sources, what is lacking from the normalisation strategy that prevents intermediate precision (different operators) and reproducibility (inter-laboratory) from masking biological variabilities [19,378-385], in other

words, why are multiple validated reference genes not rectifying the situation? Reproducibility attempts will be made easier by choosing to replicate at stages where most variability is introduced, rather than say the qPCR step, which is frequently replicated in preference to other stages. By replicating stages further back in the process, more of the experimental noise will be captured allowing a more comprehensive evaluation of measurement uncertainty. Replication at appropriate stages will remove technical variability, with biological variability remaining. In addition, rather than pursuing external reference gene strategies (given our findings for ERCC target variabilities), it may indeed be prudent to focus efforts on internal target standardisation approaches, whether that is using multiple reference genes, expressed repetitive elements (such as *Alu* repeats), an alternative approach or a combination of such methods. The “Catch 22” in regards to qPCR is that when done correctly, it can be extremely reproducible with low variances. While this is obviously desirable and one of its major selling points, this tight precision may generate a source of bias, whereby the precision that makes it such a successful technique also opens up the variability in measurements between laboratories; the repeatability within a laboratory does not translate to reproducibility between laboratories. In addition to applying replication to appropriate stages of the experimental process, one way to address these biases would be to employ validated internal standards that are used for expression fold change (relative) measurement claims, as differences in absolute quantification values are less relevant if fold change values are maintained.

One aspect that has not been investigated here is the difference between relative and absolute quantification for RT-qPCR approaches and whether or not normalisation strategy influences one approach differently to another. Future work would include evaluating these possibilities for the best approach. For example, if relative changes are maintained regardless of normalisation strategy, differences in absolute values may not be meaningful (dependent on the measurement need).

Chapter 6 The Influence of Sample Type on Measurement Variability

The process precision factors detailed in the variability plots evaluated in this chapter (**Figure 6.2**, **Figure 6.5** and **Figure 6.6**) demonstrate which steps in the experimental process would benefit most from additional replication. This work can be used to guide readers in the approach required to make relevant decisions on process variability contributions and in so doing, make valid improvements to experimental workflow and impact of generated data.

Chapter 7

Final Discussion & Overall Conclusions

7. Final Discussion & Overall Conclusions

Measurement standardisation is a crucial step in maintaining the integrity of scientific studies and is a key feature of robust investigation. Currently, the field of molecular biology is lacking behind other disciplines such as chemistry and physics in terms of the development of measurement standards that can be used for this purpose. However, there have been several standardisation efforts within the field including the International Organization for Standardization (ISO) who develop and publish International Standards [87], Minimum Information About a Microarray Experiment (MIAME) standard guidelines for reporting microarray experiments [386], the Minimum Information for Publication of Quantitative Real-Time PCR Experiments (MIQE) standard guidelines for reporting qPCR experiments [86], the Minimum Information for Publication of Quantitative Digital PCR Experiments (dMIQE) standard guidelines for reporting dPCR experiments [230], Standards, Guidelines and Best Practices for RNA-Seq published by the ENCODE (Encyclopedia of DNA Elements) Consortium to establish best practices for RNA-seq measurements [387] and the Genetic European Variation in Disease (GEUVADIS) Consortium who aim to develop standards on medical genome sequencing, using both RNA (RNA-seq) and DNA (exonSeq) sequencing [388]. Since the publication of these guidelines there has been a concerted effort to increase standardisation within the associated literature [133-135,141,150-152]. This includes both standardised laboratory practices and reporting of methods used as well as appropriate investigation and validation of relevant reference standards within individual studies.

Our recent review of the literature [59] has shown that the qPCR data underlying the vast majority of publications reporting use of this technique are, at the very least, inadequately reported and that the peer review process allows the publication of incomplete experimental protocols, yielding results that are difficult to evaluate independently. When some such studies are reassessed, it may lead to publication retractions [389-392]. This may have contributed to untold quantities

Chapter 7 Final Discussion & Overall Conclusions

of wasted time and money invested in dead ends by researchers following on from these data. Such errors may be particularly difficult to spot when applying findings from one model system to another. For example, findings from cell line based studies or animal models being applied to clinical samples. Disparity in clinical findings compared to a model system may be put down to the inapplicability of the model system, when in fact; the study procedures may be at fault.

Retractions, however, are rare and evidence suggests that this can be due to poor data analysis [59] suggesting that the original data has not been questioned/re-evaluated rather than because such mistakes are infrequent. When standardised practices, both in the laboratory and during data reporting, are not followed, it becomes difficult not only for such results to be successfully reproduced, but also to determine where the causes of erroneous findings lie when they arise. Studies reporting conflicting findings are of concern for this very reason; it may be the case that the second, conflicting study has difficulty getting published at all. Authors of such investigations should endeavor to collaborate in order to resolve such conflicts in data reporting. However, the majority of conflicting reports may be avoided if all laboratories and researchers were to follow standardised and validated procedures within their own laboratories and remain compliant with accepted guidelines (such as MIQE [86]) when reporting data. Of course, it is also possible that some conflicting reports represent the normal reproducibility range.

During the tenure of this thesis, investigations of variability contributions at each stage in the experimental process from RNA sample source to RNA target quantification have been performed with the use of both internal and synthetic experimental standards for normalisation. Possible sources of variability have been scrutinised including, sample source and type, RNA extraction, sample quantification, RT, qPCR and/or dPCR and use of different standards for normalisation. The findings presented here are significant in terms of real-life impact whereby the sources and degree of variability contributions have been

Chapter 7 Final Discussion & Overall Conclusions

examined and shown to be reduced effectively when validated normalisation and standardisation procedures are in place.

The scope of this study has generated many statistically significant findings. dPCR is capable of making precise measurements of synthetic and endogenous RNA molecules in a complex RNA background. A possible underestimation bias exists for RNA measurements; RT-dPCR quantification was significantly lower than that derived from UV values. RT-dPCR has been shown to be more precise than previous methods. However, RT-dPCR was able to highlight the diverse quantification and sensitivity capabilities of different one-step RT-qPCR kits; leading to the conclusion that cDNA prepared using different RT enzymes cannot be meaningfully compared. Not every enzyme is equal in its capabilities and such kits should be validated, particularly when attempting to measure low abundance targets and difficult sample types that may contain inhibitors (such as clinical samples). This study suggests that dPCR may be used to inform and improve practices for qPCR. For example, using dPCR (instead of UV) to value assign standards that will be used for qPCR analysis.

It has been clearly demonstrated that different extraction methods recover RNA with differing efficiencies. Matrix effects, cell debris and/or the quantity of input material, such as the number of cells, may influence this. Extraction efficiencies remained linear across the dilution range; however, linearity was influenced by cell type. This is particularly relevant when evaluating transcripts of low abundance and so experimental-specific validation is important. Furthermore, DNase treatment efficiency may also partly be affected by kit-dependent co-purified contaminants and extraction buffer compounds, as DNase efficiency varied between kits. The ERCC transcripts may be more susceptible to matrix effects/inhibitors than the endogenous reference genes. Both extraction kit/chemistry and yield determination must be maintained in a method specific-manner for sample sets to remain equally valid.

Chapter 7 Final Discussion & Overall Conclusions

The studies evaluating the effect of sample type on process variabilities suggested an impact of cell passage (age) on RNA yield precision, with cell age positively correlating with variability in total RNA measurement. However, with only two passages evaluated, the link between cell passage and RNA yield precision should be further investigated with a range of cell types and passage levels. Furthermore, it was shown that an increase in sample complexity concomitantly increases measurement variability.

A key finding of these data has been the low error between technical replicates. Therefore, concentrating replication on sources determined to contribute greater variability will best capture experimental error and provide accurate estimates of measurement uncertainty. It is worth considering how relevant cell culture extraction variability (a synthetic situation) is compared to clinical samples. The variability (or lack thereof) observed for these data may not be representative of a clinical sample scenario. However, it could explain the very discrepancies mentioned above, i.e. everyone is using precise but varyingly biased methods. The very fact that this study was designed to measure variability contributions necessitates an attention to experimental detail most likely resulting in a consequential decrease in variability. So by 'observing the variability', the measurement result is fundamentally changed, in what might be biology's version of Heisenberg's uncertainty principal.

Overall, this work has shown the level of precision that can be achieved when all sources of error are monitored. When there is maintenance of experimental consistency and an understanding of sources of bias and error, theoretically any methods may be used and be expected to generate the same result. This work could be developed in future to generate power calculations to inform future experimental design. Furthermore, this work provides a guide for the assessment of variability contributions and the translation to reducing experimental error.

Chapter 7 Final Discussion & Overall Conclusions

Based on the findings in this thesis, the author makes the following recommendations:

General best practice guidelines:

- When handling RNA samples at any stage prior to qPCR, experimental procedures should include routine treatment of surfaces/racks/pipettes etc. with a solution to remove RNases (such as RNaseZap, Ambion).
- RNase-free plasticware and water should be used.
- Laboratory space must be separated into at the least two areas comprising PCR set-up (no PCR product handling) and PCR product analysis areas with separate reagents and pipettes.

mRNA measurement by RT-qPCR

- Replication should be performed at all stages of the process (at a minimum $n = 3$), except at the PCR level only.
- If replication can only be performed at limited stages due to cost/resources, it should be focussed at earlier steps in the protocol, i.e. subject/independent experiment replicates should hold the highest priority.
- Samples may be stored at -80°C as either lysate or extracted total RNA.
- For total RNA extraction, organic and silica membrane-based extraction methods are preferable to salt precipitation methods.
- Total RNA extracts should have an aliquot prepared for initial quantification and the rest stored at -80°C . There is no preferred method for this as quantity is not as important as quality (integrity and purity) assessment. Relative levels are sufficient to ensure equal RNA quantities are processed.
- Total RNA should be diluted in a stabilising agent such as RNA storage solution (Ambion), or equivalent.
- Total RNA should always be DNase treated, and preferably assessed for DNase efficiency, for example by using *Alu* PCR or equivalent (samples pre and post DNase treatment).

Chapter 7 Final Discussion & Overall Conclusions

- Total RNA should be tested for integrity, preferably using a 5'-3' assay, for a highly abundant target [252].
- Total RNA purity, in terms of co-extracted inhibitors, should be tested using the SPUD assay [155,157], or equivalent.
- RT may be performed using either one-step or two-step processes. When measuring low abundance targets, oligo d(T)₁₆ or gene specific RT priming is recommended (as opposed to random primers), based on specificity for mRNA or specified targets, respectively.
- Carrier RNA (such as Yeast total RNA) should be added to the RT reaction (both one-step and two-step processes) to ensure linear performance of the RTase.
- The validity of the RTase should be tested for each experimental purpose, particularly when evaluating low abundance targets. Furthermore, when measuring such minority mRNA species, one-step RT-qPCR and RTases lacking RNase H activity should be considered (and validated).
- If a standard curve will be used for quantification of a target, standard dilutions should be performed at the RNA (not cDNA) stage (at a minimum n = 3).
- External controls should be spiked into matrix-matched samples.
- qPCR is highly robust and precise and does not necessarily need to be replicated.

qPCR Assay design:

- If DNase treatment is performed (and validated by *Alu* PCR), assays do not necessarily need to be designed to cross an exon-exon boundary. RT negative controls should be employed as standard.
- Where possible when performing qPCR, probes such as hydrolysis probes, molecular beacons and scorpion probes, can be used to ensure additional specificity. Where intercalating dyes are used, melt curve analysis should always be performed to evaluate specificity.

Additional considerations:

- Passage number of cells should be considered and where possible, matched throughout a study.
- All possible aspects of an experimental set-up should be controlled, e.g. consistency in sample source/type, reagent batches, instrument calibration etc.
- Meaningful comparisons can only be made where the same experimental set-up, reagents and methods are used.
- Published data must include all sample and experimental details to facilitate data reproduction and comparison.
- All sources of variability should be considered and accounted for before conclusions can be made (particularly discriminatory power of the particular experimental process).

7.1. Future Work

Projects following on from this work may include an inter-laboratory study evaluating the reproducibility of RNA measurement from the point of RNA extraction from cell lysates. This would test inter-laboratory capabilities and consistency in RNA extraction as well as all processes downstream. It would also allow for evaluation of normalisation techniques and their ability to control for more variable steps in the process (i.e. the RNA extraction rather than just the RT or qPCR). The next step would be to evaluate RNA measurement reproducibility when starting from tissue samples; an increase in sample complexity. These studies would test the resilience of method standardisation and normalisation techniques to the pressures of increased sample complexity and variability, testing the limits of technical variability and what may be overcome.

The development of a universally applicable RT-qPCR standard for accurate and comprehensive data normalisation could be considered a Holy Grail in the transcriptomics field. Such a material would aim to rectify reproducibility problems and systematic biases, improving the robustness, reliability and

Chapter 7 Final Discussion & Overall Conclusions

applicability of such studies. However, in practical terms, such a material maybe some way off coming to fruition. In the meantime, recognised and accredited standards should be used to improve reproducibility between laboratories, comparisons between which should only be made when the same standards are utilised. This includes calibration materials that have been accurately value assigned using dPCR or a higher order method. dPCR may also be utilised, as shown in this thesis (**Chapter 4**), to determine RT enzyme performance and to ensure that the RT enzyme generates the same result as the PCR enzyme, i.e. counting RNA molecules per cell (without the introduction of bias). The higher precision possible with dPCR methodologies will allow a determination of when an RT enzyme or RNA extraction method is not working efficiently; biases which cannot always be defined using qPCR. Such scrutiny of measurement processes will enable identification of biases allowing improvements to the experimental protocol to be made. Application of dPCR in this way, as a kind of process evaluator, helps to keep those processes faithful to the measurement. It will allow an improvement of all process steps and aid harmonisation of protocols and ultimately improve inter-laboratory reproducibility.

Important continued efforts in this field include the education and uptake of standardised laboratory and reporting practices. When scientists, and people in general, have been doing things a particular way for years it can be tremendously difficult to convince them why they should be doing it differently. Seasoned researchers may be resistant to change, especially with funding pressures and demands to publish. Nevertheless, this may be helped remarkably by requirement of such standards in manuscripts by publishing journals. Furthermore, capturing training and newly qualified young scientists, and ensuring they are schooled in the importance of such standardisation approaches, will go a long way to safeguarding the integrity of future scientific endeavor.

7.2. Overall Impact

The findings reported in this thesis give strong weight to the applicability of RT-dPCR to measurement fields requiring high precision and determination of small changes such as transcriptomic biomarkers, as well as to the development and validation of new material standards for biological measurement. This work further highlights the need for standardisation in all aspects of methodology. This thesis may be used to guide development of studies investigating sources of variability. The employment of dPCR value assigned calibrant materials (reference samples) would facilitate greater accuracy for absolute quantification by qPCR. Efforts should focus on internal target standardisation approaches, whether that is using multiple reference genes, expressed repetitive elements (such as *Alu* repeats), an alternative approach or a combination of such methods, and be used to investigate the extent of variability contributions. Moreover, in-depth validation and analysis of external synthetic ERCC standards has been completed as a potential augmentation to internal controls for normalisation of data in validated circumstances; while these standards were variable under some experimental conditions, their applicability may still be confirmed in certain experimental approaches.

This thesis contributes to the field by outlining processes that should be followed in order to produce scientifically sound and valid results. Furthermore, it highlights areas where harmonisation of methodologies should be maintained.

Chapter 8

References

8. References

1. Quinn T, Kovalevsky J (2005) The development of modern metrology and its role today. *Philos Transact A Math Phys Eng Sci* 363 (1834):2307-2327.
2. Whitelaw I (2007) *A measure of all things: The story of measurement through the ages*. David & Charles Publications
3. (JCGM) JCGM (2012) *International vocabulary of metrology - Basic and general concepts and associated terms (VIM)*. 3rd Edition, 2008, with minor corrections edn.
4. (JCGM) JCGM (2008) *Evaluation of measurement data - Guide to the expression of uncertainty in measurement (GUM)*.
5. LGC (2008) *Method validation training course*.
6. Perez-Novo CA, Claeys C, Speleman F *et al.* (2005) Impact of RNA quality on reference gene expression stability. *Biotechniques* 39 (1):52, 54, 56.
7. Vandesompele J, De Preter K, Pattyn F *et al.* (2002) Accurate normalization of real-time quantitative RT-PCR data by geometric averaging of multiple internal control genes. *Genome Biol* 3 (7):RESEARCH0034.
8. May W, Parris R, Beck C *et al.* (2000) *Definitions of Terms and Modes Used at NIST for Value-Assignment of Reference Materials for Chemical Measurement*. National Institute of Standards and Technology Special Publication, vol 260. National Institute of Standards and Technology, Gaithersburg, MD
9. Williams RL (2006) Official USP Reference Standards: metrology concepts, overview, and scientific issues and opportunities. *J Pharm Biomed Anal* 40 (1):3-15.
10. Ellison SLR, Rosslein M, Williams A (2000) *EURACHEM/CITAC Guide: Quantifying Uncertainty in Analytical Measurement*. EURACHEM/CITAC Guide, Second edn. National Institute of Standards and Technology, Gaithersburg, MD
11. Deuwer DL, Parris RM, White EW *et al.* (2004) *An Approach to the Metrologically Sound Traceable Assessment of the Chemical Purity of Organic Reference Materials*. NIST Special Publication 1012. National Institute of Standards and Technology, Gaithersburg, MD
12. Bhat S, Curach N, Mostyn T *et al.* (2010) Comparison of methods for accurate quantification of DNA mass concentration with traceability to the international system of units. *Anal Chem* 82 (17):7185-7192.

Chapter 8 References

13. Donald CE, Qureshi F, Burns MJ *et al.* (2005) An inter-platform repeatability study investigating real-time amplification of plasmid DNA. *BMC Biotechnol* 5:15.
14. Holden MJ, Rabb SA, Tewari YB *et al.* (2007) Traceable phosphorus measurements by ICP-OES and HPLC for the quantitation of DNA. *Anal Chem* 79 (4):1536-1541.
15. Nielsen K, Mogensen HS, Hedman J *et al.* (2008) Comparison of five DNA quantification methods. *Forensic Sci Int Genet* 2 (3):226-230.
16. Stevenson J, Hymas W, Hillyard D (2005) Effect of sequence polymorphisms on performance of two real-time PCR assays for detection of herpes simplex virus. *J Clin Microbiol* 43 (5):2391-2398.
17. WHO. <http://www.who.int/en/>. 2015
18. Haynes RJ, Kline MC, Toman B *et al.* (2013) Standard reference material 2366 for measurement of human cytomegalovirus DNA. *J Mol Diagn* 15 (2):177-185.
19. White H, Deprez L, Corbisier P *et al.* (2015) A certified plasmid reference material for the standardisation of BCR-ABL1 mRNA quantification by real-time quantitative PCR. *Leukemia* 29 (2):369-376.
20. Joint Research Centre Reference Materials for GMO Analysis. <https://ec.europa.eu/jrc/en/research-topic/reference-materials-gmo-analysis>. 2015
21. BIPM Consultative Committee for Amount of Substance: Metrology in Chemistry and Biology (CCQM). <http://www.bipm.org/en/committees/cc/ccqm/>. 2011
22. Higuchi R, Fockler C, Dollinger G *et al.* (1993) Kinetic PCR analysis: real-time monitoring of DNA amplification reactions. *Biotechnology (N Y)* 11 (9):1026-1030.
23. Mullis KB (1990) The unusual origin of the polymerase chain reaction. *Sci Am* 262 (4):56-61, 64-55.
24. Mullis KB, Faloona FA (1987) Specific synthesis of DNA in vitro via a polymerase-catalyzed chain reaction. *Methods Enzymol* 155:335-350.
25. Saiki RK, Scharf S, Faloona F *et al.* (1985) Enzymatic amplification of beta-globin genomic sequences and restriction site analysis for diagnosis of sickle cell anemia. *Science* 230 (4732):1350-1354.
26. Valasek MA, Repa JJ (2005) The power of real-time PCR. *Adv Physiol Educ* 29 (3):151-159.

Chapter 8 References

27. Mulvey MC, Sacksteder KA, Einck L *et al.* (2012) Generation of a novel nucleic acid-based reporter system to detect phenotypic susceptibility to antibiotics in *Mycobacterium tuberculosis*. *MBio* 3 (2).
28. Mannonen L, Markkula E, Puolakkainen M (2011) Analysis of *Chlamydia pneumoniae* infection in mononuclear cells by reverse transcription-PCR targeted to chlamydial gene transcripts. *Med Microbiol Immunol* 200 (3):143-154.
29. Botelho-Souza LF, Dos Santos AD, Borzacov LM *et al.* (2013) Development of a reverse transcription quantitative real-time PCR-based system for rapid detection and quantitation of hepatitis delta virus in the western Amazon region of Brazil. *J Virol Methods* 197C:19-24.
30. Delarue S, Didier E, Damond F *et al.* (2013) Highly sensitive plasma RNA quantification by real-time PCR in HIV-2 group A and group B infection. *J Clin Virol* 58 (2):461-467.
31. Katsoulidou A, Manesis E, Rokka C *et al.* (2013) Development and assessment of a novel real-time PCR assay for quantitation of hepatitis D virus RNA to study viral kinetics in chronic hepatitis D. *J Viral Hepat* 20 (4):256-262.
32. Shahzamani K, Merat S, Rezvan H *et al.* (2010) Development of a low-cost real-time reverse transcriptase-polymerase chain reaction technique for the detection and quantification of hepatitis C viral load. *Clin Chem Lab Med* 48 (6):777-784.
33. Takahashi S, Miura N, Harada T *et al.* (2010) Prognostic impact of clinical course-specific mRNA expression profiles in the serum of perioperative patients with esophageal cancer in the ICU: a case control study. *J Transl Med* 8:103.
34. Bennour A, Ouahchi I, Moez M *et al.* (2012) Comprehensive analysis of BCR/ABL variants in chronic myeloid leukemia patients using multiplex RT-PCR. *Clin Lab* 58 (5-6):433-439.
35. Moore FR, Rempfer CB, Press RD (2013) Quantitative BCR-ABL1 RQ-PCR fusion transcript monitoring in chronic myelogenous leukemia. *Methods Mol Biol* 999:1-23.
36. Devonshire AS, Sanders R, Wilkes TM *et al.* (2013) Application of next generation qPCR and sequencing platforms to mRNA biomarker analysis. *Methods* 59 (1):89-100.
37. Inc GH OncotypeDX Breast Cancer Assay. <http://www.oncotypedx.com>. 2013
38. Knezevic D, Goddard AD, Natraj N *et al.* (2013) Analytical validation of the Oncotype DX prostate cancer assay - a clinical RT-PCR assay optimized for prostate needle biopsies. *BMC Genomics* 14:690.

Chapter 8 References

39. Sapino A, Roepman P, Linn SC *et al.* (2013) MammaPrint Molecular Diagnostics on Formalin-Fixed, Paraffin-Embedded Tissue. *J Mol Diagn.*
40. Ru Y, Dancik GM, Theodorescu D (2011) Biomarkers for prognosis and treatment selection in advanced bladder cancer patients. *Curr Opin Urol* 21 (5):420-427.
41. Glaubitz J, Sizmann D, Simon CO *et al.* (2011) Accuracy to 2nd International HIV-1 RNA WHO Standard: assessment of three generations of quantitative HIV-1 RNA nucleic acid amplification tests. *J Clin Virol* 50 (2):119-124.
42. Sanders R, Mason DJ, Foy CA *et al.* (2014) Considerations for accurate gene expression measurement by reverse transcription quantitative PCR when analysing clinical samples. *Anal Bioanal Chem* 406 (26):6471-6483.
43. Ellison S, Barwick V (1998) Using validation data for ISO measurement uncertainty estimation, Part 1: Principles of an approach using cause and effect analysis. *Analyst* 123:1387-1392.
44. Ellison S, Williams A (2012) Eurachem/CITAC guide: Quantifying Uncertainty in Analytical Measurement. Third edn.
45. Devonshire AS, Elaswarapu R, Foy CA (2011) Applicability of RNA standards for evaluating RT-qPCR assays and platforms. *BMC Genomics* 12:118.
46. Bustin SA (2000) Absolute quantification of mRNA using real-time reverse transcription polymerase chain reaction assays. *J Mol Endocrinol* 25 (2):169-193.
47. Bustin SA (2002) Quantification of mRNA using real-time reverse transcription PCR (RT-PCR): trends and problems. *J Mol Endocrinol* 29 (1):23-39.
48. Bustin SA, Nolan T (2004) Pitfalls of quantitative real-time reverse-transcription polymerase chain reaction. *J Biomol Tech* 15 (3):155-166.
49. Vermeulen J, Pattyn F, De Preter K *et al.* (2009) External oligonucleotide standards enable cross laboratory comparison and exchange of real-time quantitative PCR data. *Nucleic Acids Res* 37 (21):e138.
50. Carter LE, Kilroy G, Gimble JM *et al.* (2012) An improved method for isolation of RNA from bone. *BMC biotechnology* 12:5.
51. Bar-Joseph Z, Gitter A, Simon I (2012) Studying and modelling dynamic biological processes using time-series gene expression data. *Nature reviews Genetics* 13 (8):552-564.
52. Ma Y, Dai H, Kong X (2012) Impact of warm ischemia on gene expression analysis in surgically removed biosamples. *Anal Biochem* 423 (2):229-235.

Chapter 8 References

53. Taylor S (2013) A Map to More Reliable RT-qPCR Results Using MIQE Guidelines. American Laboratory
54. Holland NT, Smith MT, Eskenazi B *et al.* (2003) Biological sample collection and processing for molecular epidemiological studies. *Mutat Res* 543 (3):217-234.
55. Bustin SA, Beaulieu JF, Huggett J *et al.* (2010) MIQE precis: Practical implementation of minimum standard guidelines for fluorescence-based quantitative real-time PCR experiments. *BMC Mol Biol* 11:74.
56. Stahlberg A, Hakansson J, Xian X *et al.* (2004) Properties of the reverse transcription reaction in mRNA quantification. *Clinical chemistry* 50 (3):509-515.
57. Curry J, McHale C, Smith MT (2002) Low efficiency of the Moloney murine leukemia virus reverse transcriptase during reverse transcription of rare t(8;21) fusion gene transcripts. *Biotechniques* 32 (4):768, 770, 772, 754-765.
58. Opel KL, Chung D, McCord BR (2010) A study of PCR inhibition mechanisms using real time PCR. *Journal of forensic sciences* 55 (1):25-33.
59. Bustin SA, Benes V, Garson J *et al.* (2013) The need for transparency and good practices in the qPCR literature. *Nat Methods* 10 (11):1063-1067.
60. Bustin SA (2010) Why the need for qPCR publication guidelines?--The case for MIQE. *Methods* 50 (4):217-226.
61. Huggett JB, SA. (2011) Standardisation and reporting for nucleic acid quantification. *Accred Qual Assur.*
62. Levesque-Sergerie JP, Duquette M, Thibault C *et al.* (2007) Detection limits of several commercial reverse transcriptase enzymes: impact on the low- and high-abundance transcript levels assessed by quantitative RT-PCR. *BMC molecular biology* 8:93.
63. Kotewicz ML, Sampson CM, D'Alessio JM *et al.* (1988) Isolation of cloned Moloney murine leukemia virus reverse transcriptase lacking ribonuclease H activity. *Nucleic Acids Res* 16 (1):265-277.
64. Sambrook JR, David (2001) *Molecular Cloning: A Laboratory Manual*. Chapter 8: In Vitro Amplification of DNA by PCR. Third Ed. edn. Cold Spring Harbor Laboratory Press
65. Gerard GF, Fox DK, Nathan M *et al.* (1997) Reverse transcriptase. The use of cloned Moloney murine leukemia virus reverse transcriptase to synthesize DNA from RNA. *Mol Biotechnol* 8 (1):61-77.

Chapter 8 References

66. Telesnitsky A, Goff SP (1993) RNase H domain mutations affect the interaction between Moloney murine leukemia virus reverse transcriptase and its primer-template. *Proc Natl Acad Sci U S A* 90 (4):1276-1280.
67. Myers TW, Gelfand DH (1991) Reverse transcription and DNA amplification by a *Thermus thermophilus* DNA polymerase. *Biochemistry* 30 (31):7661-7666.
68. Myers RL, Chiu IM (1994) Single primer-mediated polymerase chain reaction. *Methods Mol Biol* 31:307-316.
69. Suslov O, Steindler DA (2005) PCR inhibition by reverse transcriptase leads to an overestimation of amplification efficiency. *Nucleic acids research* 33 (20):e181.
70. Sellner LN, Coelen RJ, Mackenzie JS (1992) Reverse transcriptase inhibits Taq polymerase activity. *Nucleic acids research* 20 (7):1487-1490.
71. Chandler DP, Wagon CA, Bolton H, Jr. (1998) Reverse transcriptase (RT) inhibition of PCR at low concentrations of template and its implications for quantitative RT-PCR. *Appl Environ Microbiol* 64 (2):669-677.
72. Chumakov KM (1994) Reverse transcriptase can inhibit PCR and stimulate primer-dimer formation. *PCR Methods Appl* 4 (1):62-64.
73. Keen CL, Jue T, Tran CD *et al.* (2003) Analytical methods: improvements, advancements and new horizons. *J Nutr* 133 (5 Suppl 1):1574S-1578S.
74. Huggett JF, Novak T, Garson JA *et al.* (2008) Differential susceptibility of PCR reactions to inhibitors: an important and unrecognised phenomenon. *BMC Res Notes* 1:70.
75. Medeiros F, Rigl CT, Anderson GG *et al.* (2007) Tissue handling for genome-wide expression analysis: a review of the issues, evidence, and opportunities. *Arch Pathol Lab Med* 131 (12):1805-1816.
76. Breit S, Nees M, Schaefer U *et al.* (2004) Impact of pre-analytical handling on bone marrow mRNA gene expression. *British journal of haematology* 126 (2):231-243.
77. Almeida A, Paul Thiery J, Magdelenat H *et al.* (2004) Gene expression analysis by real-time reverse transcription polymerase chain reaction: influence of tissue handling. *Analytical biochemistry* 328 (2):101-108.
78. Hewitt SM, Lewis FA, Cao Y *et al.* (2008) Tissue handling and specimen preparation in surgical pathology: issues concerning the recovery of nucleic acids from formalin-fixed, paraffin-embedded tissue. *Arch Pathol Lab Med* 132 (12):1929-1935.

Chapter 8 References

79. Marx V (2013) PCR: living life amplified and standardized. *Nature Methods* 10:391–395.
80. Wacker MJ, Godard MP (2005) Analysis of one-step and two-step real-time RT-PCR using SuperScript III. *Journal of biomolecular techniques* : JBT 16 (3):266-271.
81. De Paula SO, de Melo Lima C, Torres MP *et al.* (2004) One-Step RT-PCR protocols improve the rate of dengue diagnosis compared to Two-Step RT-PCR approaches. *J Clin Virol* 30 (4):297-301.
82. Stahlberg A, Kubista M, Pfaffl M (2004) Comparison of reverse transcriptases in gene expression analysis. *Clinical chemistry* 50 (9):1678-1680.
83. Huggett J, Nolan T, Bustin SA (2013) MIQE: Guidelines for the design and publication of a reliable real-time PCR assay. Horizon Scientific Press, Wymondham, UK
84. Uhlmann V, Martin CM, Sheils O *et al.* (2002) Potential viral pathogenic mechanism for new variant inflammatory bowel disease. *Mol Pathol* 55 (2):84-90.
85. Bustin SA (2008) Real-time quantitative PCR-opportunities and pitfalls. *European Pharmaceutical Review* (4):18–23.
86. Bustin SA, Benes V, Garson JA *et al.* (2009) The MIQE guidelines: minimum information for publication of quantitative real-time PCR experiments. *Clin Chem* 55 (4):611-622.
87. International Organization for Standardization. <http://www.iso.org/iso/home.htm>. 2015
88. Linz U (1990) Thermocycler temperature variation invalidates PCR results. *Biotechniques* 9 (3):286, 288, 290-283.
89. Schoder D, Schmalwieser A, Schauburger G *et al.* (2005) Novel approach for assessing performance of PCR cyclers used for diagnostic testing. *J Clin Microbiol* 43 (6):2724-2728.
90. Bushon RN, Kephart CM, Koltun GF *et al.* (2010) Statistical assessment of DNA extraction reagent lot variability in real-time quantitative PCR. *Lett Appl Microbiol* 50 (3):276-282.
91. Bustin SA, Benes V, Garson JA *et al.* (2011) Primer sequence disclosure: a clarification of the MIQE guidelines. *Clin Chem* 57 (6):919-921.
92. Livak KJ, Schmittgen TD (2001) Analysis of relative gene expression data using real-time quantitative PCR and the 2(-Delta Delta C(T)) Method. *Methods* 25 (4):402-408.

93. Pfaffl MW (2001) A new mathematical model for relative quantification in real-time RT-PCR. *Nucleic Acids Res* 29 (9):e45.
94. Peirson SN, Butler JN, Foster RG (2003) Experimental validation of novel and conventional approaches to quantitative real-time PCR data analysis. *Nucleic Acids Res* 31 (14):e73.
95. Ramakers C, Ruijter JM, Deprez RH *et al.* (2003) Assumption-free analysis of quantitative real-time polymerase chain reaction (PCR) data. *Neurosci Lett* 339 (1):62-66.
96. Ruijter JM, Ramakers C, Hoogaars WM *et al.* (2009) Amplification efficiency: linking baseline and bias in the analysis of quantitative PCR data. *Nucleic Acids Res* 37 (6):e45.
97. Zhao S, Fernald RD (2005) Comprehensive algorithm for quantitative real-time polymerase chain reaction. *J Comput Biol* 12 (8):1047-1064.
98. Nolan T, Huggett JF, Sanchez E (2013) Good Practice Guide for the Application of Quantitative PCR (qPCR). <http://www.nmschembio.org.uk/PublicationArticle.aspx?m=115&amid=7994>. 2013
99. Ruijter JM, Pfaffl MW, Zhao S *et al.* (2013) Evaluation of qPCR curve analysis methods for reliable biomarker discovery: bias, resolution, precision, and implications. *Methods* 59 (1):32-46.
100. Sanders R, Mason DJ, Foy CA *et al.* (2013) Evaluation of digital PCR for absolute RNA quantification. *PLoS One* 8 (9):e75296.
101. Reischl U, Wittwer C, Cockerill F (2002) *Rapid Cycle Real-time PCR: Methods and Applications; Microbiology and Food Analysis*. Springer-Verlag, New York
102. Holden MJ, Haynes RJ, Rabb SA *et al.* (2009) Factors affecting quantification of total DNA by UV spectroscopy and PicoGreen fluorescence. *J Agric Food Chem* 57 (16):7221-7226.
103. Sanders R, Huggett JF, Bushell CA *et al.* (2011) Evaluation of digital PCR for absolute DNA quantification. *Anal Chem*.
104. Bhat S, Herrmann J, Armishaw P *et al.* (2009) Single molecule detection in nanofluidic digital array enables accurate measurement of DNA copy number. *Anal Bioanal Chem* 394 (2):457-467.
105. Corbisier P, Bhat S, Partis L *et al.* (2010) Absolute quantification of genetically modified MON810 maize (*Zea mays* L.) by digital polymerase chain reaction. *Anal Bioanal Chem* 396 (6):2143-2150.

Chapter 8 References

106. Day E, Dear PH, McCaughan F (2012) Digital PCR strategies in the development and analysis of molecular biomarkers for personalized medicine. *Methods*.
107. Coudray-Meunier C, Fraisse A, Martin-Latil S *et al.* (2015) A comparative study of digital RT-PCR and RT-qPCR for quantification of Hepatitis A virus and Norovirus in lettuce and water samples. *International journal of food microbiology* 201:17-26.
108. Gullett JC, Nolte FS (2015) Quantitative nucleic acid amplification methods for viral infections. *Clin Chem* 61 (1):72-78.
109. Racki N, Dreo T, Gutierrez-Aguirre I *et al.* (2014) Reverse transcriptase droplet digital PCR shows high resilience to PCR inhibitors from plant, soil and water samples. *Plant methods* 10 (1):42.
110. Ruelle J, Yfantis V, Duquenne A *et al.* (2014) Validation of an ultrasensitive digital droplet PCR assay for HIV-2 plasma RNA quantification. *Journal of the International AIDS Society* 17 (4 Suppl 3):19675.
111. Takahashi K, Yan IK, Kim C *et al.* (2014) Analysis of extracellular RNA by digital PCR. *Frontiers in oncology* 4:129.
112. Jacobs BK, Goetghebeur E, Clement L (2014) Impact of variance components on reliability of absolute quantification using digital PCR. *BMC bioinformatics* 15:283.
113. Dingle TC, Sedlak RH, Cook L *et al.* (2013) Tolerance of droplet-digital PCR vs real-time quantitative PCR to inhibitory substances. *Clin Chem* 59 (11):1670-1672.
114. Huggett JF, Cowen S, Foy CA (2015) Considerations for digital PCR as an accurate molecular diagnostic tool. *Clin Chem* 61 (1):79-88.
115. Nixon G, Garson JA, Grant P *et al.* (2014) Comparative study of sensitivity, linearity, and resistance to inhibition of digital and nondigital polymerase chain reaction and loop mediated isothermal amplification assays for quantification of human cytomegalovirus. *Anal Chem* 86 (9):4387-4394.
116. Roy NC, Altermann E, Park ZA *et al.* (2011) A comparison of analog and Next-Generation transcriptomic tools for mammalian studies. *Briefings in functional genomics* 10 (3):135-150.
117. Wang Z, Gerstein M, Snyder M (2009) RNA-Seq: a revolutionary tool for transcriptomics. *Nature reviews Genetics* 10 (1):57-63.
118. Nagalakshmi U, Wang Z, Waern K *et al.* (2008) The transcriptional landscape of the yeast genome defined by RNA sequencing. *Science* 320 (5881):1344-1349.

Chapter 8 References

119. Mortazavi A, Williams BA, McCue K *et al.* (2008) Mapping and quantifying mammalian transcriptomes by RNA-Seq. *Nat Methods* 5 (7):621-628.
120. Cloonan N, Forrest AR, Kolle G *et al.* (2008) Stem cell transcriptome profiling via massive-scale mRNA sequencing. *Nat Methods* 5 (7):613-619.
121. Tunbridge EM, Eastwood SL, Harrison PJ (2011) Changed relative to what? Housekeeping genes and normalization strategies in human brain gene expression studies. *Biol Psychiatry* 69 (2):173-179.
122. Huggett J, Dheda K, Bustin S *et al.* (2005) Real-time RT-PCR normalisation; strategies and considerations. *Genes and immunity* 6 (4):279-284.
123. Marullo M, Zuccato C, Mariotti C *et al.* (2010) Expressed Alu repeats as a novel, reliable tool for normalization of real-time quantitative RT-PCR data. *Genome Biol* 11 (1):R9.
124. English CA, Merson S, Keer JT (2006) Use of elemental analysis to determine comparative performance of established DNA quantification methods. *Anal Chem* 78 (13):4630-4633.
125. Blotta I, Prestinaci F, Mirante S *et al.* (2005) Quantitative assay of total dsDNA with PicoGreen reagent and real-time fluorescent detection. *Ann Ist Super Sanita* 41 (1):119-123.
126. Cavaluzzi MJ, Borer PN (2004) Revised UV extinction coefficients for nucleoside-5'-monophosphates and unpaired DNA and RNA. *Nucleic Acids Res* 32 (1):e13.
127. Wilfinger WW, Mackey K, Chomczynski P (1997) Effect of pH and ionic strength on the spectrophotometric assessment of nucleic acid purity. *Biotechniques* 22 (3):474-476, 478-481.
128. Haque KA, Pfeiffer RM, Beerman MB *et al.* (2003) Performance of high-throughput DNA quantification methods. *BMC Biotechnol* 3:20.
129. Leninger AL (1975) *Biochemistry*. 2nd edn. Worth Publishers, New York
130. Vermeulen J, De Preter K, Lefever S *et al.* (2011) Measurable impact of RNA quality on gene expression results from quantitative PCR. *Nucleic Acids Res* 39 (9):e63.
131. Erkens T, Van Poucke M, Vandesompele J *et al.* (2006) Development of a new set of reference genes for normalization of real-time RT-PCR data of porcine backfat and longissimus dorsi muscle, and evaluation with PPARGC1A. *BMC Biotechnol* 6:41.

132. Dheda K, Huggett JF, Bustin SA *et al.* (2004) Validation of housekeeping genes for normalizing RNA expression in real-time PCR. *Biotechniques* 37 (1):112-114, 116, 118-119.
133. Aursnes IA, Rishovd AL, Karlsen HE *et al.* (2011) Validation of reference genes for quantitative RT-qPCR studies of gene expression in Atlantic cod (*Gadus morhua* L.) during temperature stress. *BMC Res Notes* 4:104.
134. Chapuis MP, Tohidi-Esfahani D, Dodgson T *et al.* (2011) Assessment and validation of a suite of reverse transcription-quantitative PCR reference genes for analyses of density-dependent behavioural plasticity in the Australian plague locust. *BMC Mol Biol* 12:7.
135. Hruz T, Wyss M, Docquier M *et al.* (2011) RefGenes: identification of reliable and condition specific reference genes for RT-qPCR data normalization. *BMC Genomics* 12:156.
136. Lovoll M, Austbo L, Jorgensen JB *et al.* (2011) Transcription of reference genes used for quantitative RT-PCR in Atlantic salmon is affected by viral infection. *Vet Res* 42 (1):8.
137. Andersen CL, Jensen JL, Orntoft TF (2004) Normalization of real-time quantitative reverse transcription-PCR data: a model-based variance estimation approach to identify genes suited for normalization, applied to bladder and colon cancer data sets. *Cancer research* 64 (15):5245-5250.
138. Pfaffl MW, Horgan GW, Dempfle L (2002) Relative expression software tool (REST) for group-wise comparison and statistical analysis of relative expression results in real-time PCR. *Nucleic Acids Res* 30 (9):e36.
139. Schmittgen TD, Zakrajsek BA (2000) Effect of experimental treatment on housekeeping gene expression: validation by real-time, quantitative RT-PCR. *J Biochem Biophys Methods* 46 (1-2):69-81.
140. Fox BC, Devonshire AS, Schutte ME *et al.* (2010) Validation of reference gene stability for APAP hepatotoxicity studies in different in vitro systems and identification of novel potential toxicity biomarkers. *Toxicology in vitro : an international journal published in association with BIBRA* 24 (7):1962-1970.
141. Fedrigo O, Warner LR, Pfefferle AD *et al.* (2010) A pipeline to determine RT-QPCR control genes for evolutionary studies: application to primate gene expression across multiple tissues. *PLoS One* 5 (9).
142. Glare EM, Divjak M, Bailey MJ *et al.* (2002) beta-Actin and GAPDH housekeeping gene expression in asthmatic airways is variable and not suitable for normalising mRNA levels. *Thorax* 57 (9):765-770.

Chapter 8 References

143. Ke LD, Chen Z, Yung WK (2000) A reliability test of standard-based quantitative PCR: exogenous vs endogenous standards. *Mol Cell Probes* 14 (2):127-135.
144. Suzuki T, Higgins PJ, Crawford DR (2000) Control selection for RNA quantitation. *Biotechniques* 29 (2):332-337.
145. Yang X, Hatfield JT, Hinze SJ *et al.* (2012) Bone to pick: the importance of evaluating reference genes for RT-qPCR quantification of gene expression in craniosynostosis and bone-related tissues and cells. *BMC Res Notes* 5:222.
146. Zhu G, Chang Y, Zuo J *et al.* (2001) Fudenine, a C-terminal truncated rat homologue of mouse prominin, is blood glucose-regulated and can up-regulate the expression of GAPDH. *Biochem Biophys Res Commun* 281 (4):951-956.
147. Sirover MA (1999) New insights into an old protein: the functional diversity of mammalian glyceraldehyde-3-phosphate dehydrogenase. *Biochim Biophys Acta* 1432 (2):159-184.
148. Tatton WG, Chalmers-Redman RM, Elstner M *et al.* (2000) Glyceraldehyde-3-phosphate dehydrogenase in neurodegeneration and apoptosis signaling. *J Neural Transm Suppl* (60):77-100.
149. Goidin D, Mamessier A, Staquet MJ *et al.* (2001) Ribosomal 18S RNA prevails over glyceraldehyde-3-phosphate dehydrogenase and beta-actin genes as internal standard for quantitative comparison of mRNA levels in invasive and noninvasive human melanoma cell subpopulations. *Anal Biochem* 295 (1):17-21.
150. Maess MB, Sendelbach S, Lorkowski S (2010) Selection of reliable reference genes during THP-1 monocyte differentiation into macrophages. *BMC Mol Biol* 11:90.
151. Zyzynska-Granica B, Koziak K (2012) Identification of suitable reference genes for real-time PCR analysis of statin-treated human umbilical vein endothelial cells. *PLoS One* 7 (12):e51547.
152. Arun A, Baumle V, Amelot G *et al.* (2015) Selection and Validation of Reference Genes for qRT-PCR Expression Analysis of Candidate Genes Involved in Olfactory Communication in the Butterfly *Bicyclus anynana*. *PLoS One* 10 (3):e0120401.
153. Bustin S, Nolan T (2015) Improving the reliability of peer-reviewed publications: We are all in it together. *Biomolecular Detection and Quantification*.
154. Consortium ERC (2005) Proposed methods for testing and selecting the ERCC external RNA controls. *BMC Genomics* 6:150.

Chapter 8 References

155. Nolan T, Hands RE, Ogunkolade W *et al.* (2006) SPUD: a quantitative PCR assay for the detection of inhibitors in nucleic acid preparations. *Anal Biochem* 351 (2):308-310.
156. Honeyborne I, McHugh TD, Phillips PP *et al.* (2011) Molecular bacterial load assay, a culture-free biomarker for rapid and accurate quantification of sputum *Mycobacterium tuberculosis* bacillary load during treatment. *J Clin Microbiol* 49 (11):3905-3911.
157. Ferns RB, Garson JA (2006) Development and evaluation of a real-time RT-PCR assay for quantification of cell-free human immunodeficiency virus type 2 using a Brome Mosaic Virus internal control. *J Virol Methods* 135 (1):102-108.
158. Garson JA, Grant PR, Ayliffe U *et al.* (2005) Real-time PCR quantitation of hepatitis B virus DNA using automated sample preparation and murine cytomegalovirus internal control. *J Virol Methods* 126 (1-2):207-213.
159. Wahlberg KH, J. Sanders, R. Whale, A.S. Bushell, C. Elaswarapu, R. Scott, D.J. and Foy, C.A. (2012) Quality Assessment of Biobanked Nucleic Acid Extracts for Downstream Molecular Analysis. *Biopreservation and Biobanking* 10 (3).
160. Mathieson W, Thomas GA (2013) Simultaneously extracting DNA, RNA, and protein using kits: is sample quantity or quality prejudiced? *Anal Biochem* 433 (1):10-18.
161. Longo MC, Berninger MS, Hartley JL (1990) Use of uracil DNA glycosylase to control carry-over contamination in polymerase chain reactions. *Gene* 93 (1):125-128.
162. Derveaux S, Vandesompele J, Hellemans J (2010) How to do successful gene expression analysis using real-time PCR. *Methods* 50 (4):227-230.
163. Ellison. Ba (2011) The fitness for purpose of randomised experimental designs for analysis of genetically modified ingredients. . *European Food Research and Technology* 233 (1):71-78.
164. Pfaffl M (2014) <http://www.Gene-Quantification.info>. 2014
165. TATAABiocenter. <http://www.tataa.com>. 2014
166. Biogazelle. <http://www.biogazelle.com>. 2014
167. Integromics. <http://www.integromics.com>. 2014
168. Yang ZL, Zheng Q, Yan J *et al.* (2011) Upregulated CD133 expression in tumorigenesis of colon cancer cells. *World J Gastroenterol* 17 (7):932-937.

Chapter 8 References

169. Vermeulen J, Derveaux S, Lefever S *et al.* (2009) RNA pre-amplification enables large-scale RT-qPCR gene-expression studies on limiting sample amounts. *BMC Res Notes* 2:235.
170. Rizzi F, Belloni L, Crafa P *et al.* (2008) A novel gene signature for molecular diagnosis of human prostate cancer by RT-qPCR. *PLoS One* 3 (10):e3617.
171. Foroni L, Wilson G, Gerrard G *et al.* (2011) Guidelines for the measurement of BCR-ABL1 transcripts in chronic myeloid leukaemia. *Br J Haematol.*
172. Gomes AQ, Correia DV, Grosso AR *et al.* (2010) Identification of a panel of ten cell surface protein antigens associated with immunotargeting of leukemias and lymphomas by peripheral blood gammadelta T cells. *Haematologica* 95 (8):1397-1404.
173. Schultz-Thater E, Frey DM, Margelli D *et al.* (2008) Whole blood assessment of antigen specific cellular immune response by real time quantitative PCR: a versatile monitoring and discovery tool. *J Transl Med* 6:58.
174. Kammula US, Marincola FM, Rosenberg SA (2000) Real-time quantitative polymerase chain reaction assessment of immune reactivity in melanoma patients after tumor peptide vaccination. *Journal of the National Cancer Institute* 92 (16):1336-1344.
175. Abdeldaim GM, Stralin K, Korsgaard J *et al.* (2010) Multiplex quantitative PCR for detection of lower respiratory tract infection and meningitis caused by *Streptococcus pneumoniae*, *Haemophilus influenzae* and *Neisseria meningitidis*. *BMC Microbiol* 10:310.
176. Pollara CP, Corbellini S, Chiappini S *et al.* (2011) Quantitative viral load measurement for BKV infection in renal transplant recipients as a predictive tool for BKVAN. *New Microbiol* 34 (2):165-171.
177. Schmid F, Glaus E, Cremers FP *et al.* (2010) Mutation- and tissue-specific alterations of RPGR transcripts. *Invest Ophthalmol Vis Sci* 51 (3):1628-1635.
178. Provenzano M, Panelli MC, Mocellin S *et al.* (2006) MHC-peptide specificity and T-cell epitope mapping: where immunotherapy starts. *Trends in molecular medicine* 12 (10):465-472.
179. Zhou Y, Wei Y, Wang L *et al.* (2011) Decreased adiponectin and increased inflammation expression in epicardial adipose tissue in coronary artery disease. *Cardiovasc Diabetol* 10 (1):2.
180. Geller SE, Koch A, Pellettieri B *et al.* (2011) Inclusion, analysis, and reporting of sex and race/ethnicity in clinical trials: have we made progress? *Journal of women's health* (2002) 20 (3):315-320.

181. Stronks K, Wieringa NF, Hardon A (2013) Confronting diversity in the production of clinical evidence goes beyond merely including under-represented groups in clinical trials. *Trials* 14:177.
182. Hoel AW, Kayssi A, Brahmanandam S *et al.* (2009) Under-representation of women and ethnic minorities in vascular surgery randomized controlled trials. *Journal of vascular surgery* 50 (2):349-354.
183. Bernard S, Cajavec Bernard B, Levi F *et al.* (2010) Tumor growth rate determines the timing of optimal chronomodulated treatment schedules. *PLoS computational biology* 6 (3):e1000712.
184. Chelly J, Concordet JP, Kaplan JC *et al.* (1989) Illegitimate transcription: transcription of any gene in any cell type. *Proc Natl Acad Sci U S A* 86 (8):2617-2621.
185. Sugiyama Y, Farrow B, Murillo C *et al.* (2005) Analysis of differential gene expression patterns in colon cancer and cancer stroma using microdissected tissues. *Gastroenterology* 128 (2):480-486.
186. Fink L, Kohlhoff S, Stein MM *et al.* (2002) cDNA array hybridization after laser-assisted microdissection from nonneoplastic tissue. *Am J Pathol* 160 (1):81-90.
187. Deng G, Lu Y, Zlotnikov G *et al.* (1996) Loss of heterozygosity in normal tissue adjacent to breast carcinomas. *Science* 274 (5295):2057-2059.
188. Bengtsson M, Stahlberg A, Rorsman P *et al.* (2005) Gene expression profiling in single cells from the pancreatic islets of Langerhans reveals lognormal distribution of mRNA levels. *Genome research* 15 (10):1388-1392.
189. Fox BC, Devonshire AS, Baradez MO *et al.* (2012) Comparison of reverse transcription-quantitative polymerase chain reaction methods and platforms for single cell gene expression analysis. *Anal Biochem* 427 (2):178-186.
190. Stahlberg A, Rusnakova V, Forootan A *et al.* (2013) RT-qPCR work-flow for single-cell data analysis. *Methods* 59 (1):80-88.
191. Devonshire AS, Baradez MO, Morley G *et al.* (2014) Validation of high-throughput single cell analysis methodology. *Anal Biochem* 452:103-113.
192. Gutala RV, Reddy PH (2004) The use of real-time PCR analysis in a gene expression study of Alzheimer's disease post-mortem brains. *J Neurosci Methods* 132 (1):101-107.
193. Woolf AD, Pfleger B (2003) Burden of major musculoskeletal conditions. *Bull World Health Organ* 81 (9):646-656.

Chapter 8 References

194. Davoren J, Vanek D, Konjhodzic R *et al.* (2007) Highly effective DNA extraction method for nuclear short tandem repeat testing of skeletal remains from mass graves. *Croat Med J* 48 (4):478-485.
195. Loreille OM, Diegoli TM, Irwin JA *et al.* (2007) High efficiency DNA extraction from bone by total demineralization. *Forensic Sci Int Genet* 1 (2):191-195.
196. Salamon M, Tuross N, Arensburg B *et al.* (2005) Relatively well preserved DNA is present in the crystal aggregates of fossil bones. *Proc Natl Acad Sci U S A* 102 (39):13783-13788.
197. Clayton TM, Whitaker JP, Maguire CN (1995) Identification of bodies from the scene of a mass disaster using DNA amplification of short tandem repeat (STR) loci. *Forensic Sci Int* 76 (1):7-15.
198. Holland MM, Cave CA, Holland CA *et al.* (2003) Development of a quality, high throughput DNA analysis procedure for skeletal samples to assist with the identification of victims from the World Trade Center attacks. *Croat Med J* 44 (3):264-272.
199. Hoss M, Paabo S (1993) DNA extraction from Pleistocene bones by a silica-based purification method. *Nucleic Acids Res* 21 (16):3913-3914.
200. Prado VF, Castro AK, Oliveira CL *et al.* (1997) Extraction of DNA from human skeletal remains: practical applications in forensic sciences. *Genet Anal* 14 (2):41-44.
201. Chomczynski P (1993) A reagent for the single-step simultaneous isolation of RNA, DNA and proteins from cell and tissue samples. *Biotechniques* 15 (3):532-534, 536-537.
202. Chomczynski P, Sacchi N (1987) Single-step method of RNA isolation by acid guanidinium thiocyanate-phenol-chloroform extraction. *Anal Biochem* 162 (1):156-159.
203. Tan SC, Yiap BC (2009) DNA, RNA, and protein extraction: the past and the present. *Journal of biomedicine & biotechnology* 2009:574398.
204. Czekanska EM, Stoddart MJ, Richards RG *et al.* (2012) In search of an osteoblast cell model for in vitro research. *Eur Cell Mater* 24:1-17.
205. Rodan SB, Imai Y, Thiede MA *et al.* (1987) Characterization of a human osteosarcoma cell line (Saos-2) with osteoblastic properties. *Cancer Res* 47 (18):4961-4966.
206. Shum L, Nuckolls G (2002) The life cycle of chondrocytes in the developing skeleton. *Arthritis Res* 4 (2):94-106.

Chapter 8 References

207. Barak MM, Sharir A, Shahar R (2009) Optical metrology methods for mechanical testing of whole bones. *Vet J* 180 (1):7-14.
208. Mason DJ (2004) Glutamate signalling and its potential application to tissue engineering of bone. *Eur Cell Mater* 7:12-25; discussion 25-16.
209. Mason DJ, Huggett JF (2002) Glutamate transporters in bone. *J Musculoskelet Neuronal Interact* 2 (5):406-414.
210. Mason DJ, Suva LJ, Genever PG *et al.* (1997) Mechanically regulated expression of a neural glutamate transporter in bone: a role for excitatory amino acids as osteotropic agents? *Bone* 20 (3):199-205.
211. Hathaway WE, Newby LA, Githens JH (1964) The Acridine Orange Viability Test Applied to Bone Marrow Cells. I. Correlation with Trypan Blue and Eosin Dye Exclusion and Tissue Culture Transformation. *Blood* 23:517-525.
212. Dehn PF, White CM, Connors DE *et al.* (2004) Characterization of the human hepatocellular carcinoma (HepG2) cell line as an in vitro model for cadmium toxicity studies. *In Vitro Cell Dev Biol Anim* 40 (5-6):172-182.
213. Roe AL, Snawder JE, Benson RW *et al.* (1993) HepG2 cells: an in vitro model for P450-dependent metabolism of acetaminophen. *Biochem Biophys Res Commun* 190 (1):15-19.
214. Xia JF, Gao JJ, Inagaki Y *et al.* (2013) Flavonoids as potential anti-hepatocellular carcinoma agents: recent approaches using HepG2 cell line. *Drug Discov Ther* 7 (1):1-8.
215. Kienhuis AS, Bessems JG, Pennings JL *et al.* (2011) Application of toxicogenomics in hepatic systems toxicology for risk assessment: acetaminophen as a case study. *Toxicol Appl Pharmacol* 250 (2):96-107.
216. van IJzendoorn SC, Hoekstra D (2000) Polarized sphingolipid transport from the subapical compartment changes during cell polarity development. *Mol Biol Cell* 11 (3):1093-1101.
217. van IJzendoorn SC, Maier O, Van Der Wouden JM *et al.* (2000) The subapical compartment and its role in intracellular trafficking and cell polarity. *J Cell Physiol* 184 (2):151-160.
218. Le Mercier M, Fortin S, Mathieu V *et al.* (2009) Galectin 1 proangiogenic and promigratory effects in the Hs683 oligodendroglioma model are partly mediated through the control of BEX2 expression. *Neoplasia* 11 (5):485-496.
219. Bianchi MG, Franchi-Gazzola R, Reia L *et al.* (2012) Valproic acid induces the glutamate transporter excitatory amino acid transporter-3 in human oligodendroglioma cells. *Neuroscience* 227:260-270.

Chapter 8 References

220. Jiang YX, Ma Y, Cheng Y (2012) Transcriptome and coexpression network analysis of the human glioma cell line Hs683 exposed to candoxin. *J Int Med Res* 40 (3):887-898.
221. Nitta H, Hauss-Wegrzyniak B, Lehrkamp M *et al.* (2008) Development of automated brightfield double in situ hybridization (BDISH) application for HER2 gene and chromosome 17 centromere (CEN 17) for breast carcinomas and an assay performance comparison to manual dual color HER2 fluorescence in situ hybridization (FISH). *Diagn Pathol* 3:41.
222. Schobesberger M, Baltzer A, Oberli A *et al.* (2008) Gene expression variation between distinct areas of breast cancer measured from paraffin-embedded tissue cores. *BMC cancer* 8:343.
223. Whale AS, Huggett JF, Cowen S *et al.* (2012) Comparison of microfluidic digital PCR and conventional quantitative PCR for measuring copy number variation. *Nucleic acids research* 40 (11):e82.
224. Dhanasekaran S, Doherty TM, Kenneth J (2010) Comparison of different standards for real-time PCR-based absolute quantification. *J Immunol Methods* 354 (1-2):34-39.
225. Xie F SG, Stiller JW, Zhang B (2011) Genome-Wide Functional Analysis of the Cotton Transcriptome by Creating an Integrated EST Database. *PLoS One* 6 (11).
226. Pfaffl MW, Tichopad A, Prgomet C *et al.* (2004) Determination of stable housekeeping genes, differentially regulated target genes and sample integrity: BestKeeper--Excel-based tool using pair-wise correlations. *Biotechnol Lett* 26 (6):509-515.
227. Silver N, Best S, Jiang J *et al.* (2006) Selection of housekeeping genes for gene expression studies in human reticulocytes using real-time PCR. *BMC molecular biology* 7:33.
228. Zuker M mfold. <http://mfold.rna.albany.edu/?q=mfold/RNA-Folding-Form>. 2012
229. Zuker M (2003) Mfold web server for nucleic acid folding and hybridization prediction. *Nucleic Acids Res* 31 (13):3406-3415.
230. Huggett JF, Foy CA, Benes V *et al.* (2013) The Digital MIQE Guidelines: Minimum Information for Publication of Quantitative Digital PCR Experiments. *Clinical Chemistry* 59 (6):892-902.
231. Weaver S, Dube S, Mir A *et al.* (2010) Taking qPCR to a higher level: Analysis of CNV reveals the power of high throughput qPCR to enhance quantitative resolution. *Methods* 50 (4):271-276.

Chapter 8 References

232. Kato Y, Windle JJ, Koop BA *et al.* (1997) Establishment of an osteocyte-like cell line, MLO-Y4. *Journal of bone and mineral research : the official journal of the American Society for Bone and Mineral Research* 12 (12):2014-2023.
233. Vazquez M (2013) Development of a Novel in vitro 3D Osteocyte-Osteoblast Co-culture Model to Investigate Mechanically-Induced Signalling. Cardiff University
234. Vazquez M, Evans BA, Riccardi D *et al.* (2014) A new method to investigate how mechanical loading of osteocytes controls osteoblasts. *Front Endocrinol (Lausanne)* 5:208.
235. Peng R, Zhai Y, Ding H *et al.* (2012) Analysis of reference gene expression for real-time PCR based on relative quantitation and dual spike-in strategy in the silkworm *Bombyx mori*. *Acta biochimica et biophysica Sinica* 44 (7):614-622.
236. Ellefsen S, Stenslokken KO, Sandvik GK *et al.* (2008) Improved normalization of real-time reverse transcriptase polymerase chain reaction data using an external RNA control. *Anal Biochem* 376 (1):83-93.
237. Badiee A, Eiken HG, Steen VM *et al.* (2003) Evaluation of five different cDNA labeling methods for microarrays using spike controls. *BMC Biotechnol* 3:23.
238. Liu ZL, Slininger PJ (2007) Universal external RNA controls for microbial gene expression analysis using microarray and qRT-PCR. *Journal of microbiological methods* 68 (3):486-496.
239. van de Peppel J, Kemmeren P, van Bakel H *et al.* (2003) Monitoring global messenger RNA changes in externally controlled microarray experiments. *EMBO reports* 4 (4):387-393.
240. Karatayli E, Altunoglu YC, Karatayli SC *et al.* (2014) A one step real time PCR method for the quantification of hepatitis delta virus RNA using an external armored RNA standard and intrinsic internal control. *J Clin Virol* 60 (1):11-15.
241. Roberts TC, Coenen-Stass AM, Wood MJ (2014) Assessment of RT-qPCR normalization strategies for accurate quantification of extracellular microRNAs in murine serum. *PLoS One* 9 (2):e89237.
242. Baker PJ, O'Shaughnessy PJ (2001) Expression of prostaglandin D synthetase during development in the mouse testis. *Reproduction (Cambridge, England)* 122 (4):553-559.
243. Kanno J, Aisaki K, Igarashi K *et al.* (2006) "Per cell" normalization method for mRNA measurement by quantitative PCR and microarrays. *BMC Genomics* 7:64.
244. Witt N, Rodger G, Vandesompele J *et al.* (2009) An assessment of air as a source of DNA contamination encountered when performing PCR. *J Biomol Tech* 20 (5):236-240.

Chapter 8 References

245. Stocher M, Berg J (2004) Removal of template DNA from cRNA preparations by combined oligo (dT) affinity chromatography and DNase I digestion. *Biotechniques* 36 (3):480-482.
246. Phongsisay V, Perera VN, Fry BN (2007) Evaluation of eight RNA isolation methods for transcriptional analysis in *Campylobacter jejuni*. *Journal of microbiological methods* 68 (2):427-429.
247. Matthews JL, Chung M, Matyas RJ (2002) Persistent DNA contamination in competitive RT-PCR using cRNA internal standards: identity, quantity, and control. *Biotechniques* 32 (6):1412-1414, 1416-1417.
248. Pinti M, Pedrazzi J, Benatti F *et al.* (1999) Differential down-regulation of CD95 or CD95L in chronically HIV-infected cells of monocytic or lymphocytic origin: cellular studies and molecular analysis by quantitative competitive RT-PCR. *FEBS Lett* 458 (2):209-214.
249. Horstmann M, Foerster B, Brader N *et al.* (2012) Establishment of a protocol for large-scale gene expression analyses of laser capture microdissected bladder tissue. *World J Urol* 30 (6):853-859.
250. Covino JS, Z. and Kelley, M (2011) Solaris RNA Spike Control Kit: Identifying Reaction Inhibition in the RT-qPCR Workflow. Technical Note. Dharmacon RNAi, Gene Expression & Gene Editing
251. Kubista M, Andrade JM, Bengtsson M *et al.* (2006) The real-time polymerase chain reaction. *Mol Aspects Med* 27 (2-3):95-125.
252. Nolan T, Hands RE, Bustin SA (2006) Quantification of mRNA using real-time RT-PCR. *Nat Protoc* 1 (3):1559-1582.
253. Gaillard CS, François. (1998) Avoiding adsorption of DNA to polypropylene tubes and denaturation of short DNA fragments. *Technical Tips Online* 3 (1):63-65.
254. Ellison SL, English CA, Burns MJ *et al.* (2006) Routes to improving the reliability of low level DNA analysis using real-time PCR. *BMC Biotechnol* 6:33.
255. Sturzenbaum SR (1999) Transfer RNA reduces the formation of primer artifacts during quantitative PCR. *Biotechniques* 27 (1):50-52.
256. Thermo Scientific (2012) T123 - Technical Bulletin. Interpretation of Nucleic Acid 260/280 Ratios. NanoDrop Lite.
257. Thermo Scientific (2011) The Future of qPCR Webinar Q&A: Best Practices, Standardization and the MIQE Guidelines. MP008 Rev. 1/2011
258. Vomelova I, Vanickova Z, Sedo A (2009) Methods of RNA purification. All ways (should) lead to Rome. *Folia Biol (Praha)* 55 (6):243-251.

Chapter 8 References

259. Baelde HJ, Cleton-Jansen AM, van Beerendonk H *et al.* (2001) High quality RNA isolation from tumours with low cellularity and high extracellular matrix component for cDNA microarrays: application to chondrosarcoma. *J Clin Pathol* 54 (10):778-782.
260. Glasel J (1995) Validity of nucleic acid purities monitored by 260/280 absorbance ratios. *BioTechniques* 18 (1):62-63.
261. Bustin SA, Nolan T (2004) Template handling, preparation, and quantification. In: *The Real-time PCR Encyclopaedia A-Z of Quantitative PCR*. International University Line, La Jolla, CA
262. Sambrook, Russell (2001) *Molecular Cloning: A Laboratory Manual*. 3rd edn. Cold Spring Harbor Laboratory Press
263. Thermo Scientific (2008) T009-Technical Bulletin: 260/280 and 260/230 Ratios. NanoDrop 1000 & 8000.
264. Jahn CE, Charkowski AO, Willis DK (2008) Evaluation of isolation methods and RNA integrity for bacterial RNA quantitation. *Journal of microbiological methods* 75 (2):318-324.
265. Sellin Jeffries MK, Kiss AJ, Smith AW *et al.* (2014) A comparison of commercially-available automated and manual extraction kits for the isolation of total RNA from small tissue samples. *BMC Biotechnol* 14:94.
266. Takeda S, Liu H, Sasagawa S *et al.* (2013) HGF-MET signals via the MLL-ETS2 complex in hepatocellular carcinoma. *J Clin Invest* 123 (7):3154-3165.
267. Huggett JF, Mustafa A, O'Neal L *et al.* (2002) The glutamate transporter GLAST-1 (EAAT-1) is expressed in the plasma membrane of osteocytes and is responsive to extracellular glutamate concentration. *Biochemical Society transactions* 30 (Pt 6):890-893.
268. Branle F, Lefranc F, Camby I *et al.* (2002) Evaluation of the efficiency of chemotherapy in in vivo orthotopic models of human glioma cells with and without 1p19q deletions and in C6 rat orthotopic allografts serving for the evaluation of surgery combined with chemotherapy. *Cancer* 95 (3):641-655.
269. Degot S, Regnier CH, Wendling C *et al.* (2002) Metastatic Lymph Node 51, a novel nucleo-cytoplasmic protein overexpressed in breast cancer. *Oncogene* 21 (28):4422-4434.
270. Keebaugh AC, Sullivan RT, Thomas JW (2007) Gene duplication and inactivation in the HPRT gene family. *Genomics* 89 (1):134-142.
271. R Development Core Team (2011) *R: A language and environment for statistical computing*. R Foundation for Statistical Computing. Vienna, Austria

Chapter 8 References

272. Murphy BM, Swarts S, Mueller BM *et al.* (2013) Protein instability following transport or storage on dry ice. *Nat Methods* 10 (4):278-279.
273. European Co-operation for Accreditation (1997) EAL R2:1997. Expression Of The Uncertainty Of Measurement In Calibration.
274. White RA, 3rd, Blainey PC, Fan HC *et al.* (2009) Digital PCR provides sensitive and absolute calibration for high throughput sequencing. *BMC Genomics* 10:116.
275. Burns MJ, Burrell AM, Foy CA (2010) The applicability of digital PCR for the assessment of detection limits in GMO analysis. *Eur Food Res Technol* 231 (3):353–362.
276. Fan HC, Quake SR (2007) Detection of aneuploidy with digital polymerase chain reaction. *Anal Chem* 79 (19):7576-7579.
277. Lo YM, Lun FM, Chan KC *et al.* (2007) Digital PCR for the molecular detection of fetal chromosomal aneuploidy. *Proc Natl Acad Sci U S A* 104 (32):13116-13121.
278. Barragan-Gonzalez E, Lopez-Guerrero JA, Bolufer-Gilabert P *et al.* (1997) The type of reverse transcriptase affects the sensitivity of some reverse transcription PCR methods. *Clin Chim Acta* 260 (1):73-83.
279. Whale AS, Cowen S, Foy CA *et al.* (2013) Methods for applying accurate digital PCR analysis on low copy DNA samples. *PLoS One* 8 (3):e58177.
280. Thermo Scientific (2010) The MIQE Guidelines and Assessment of Nucleic Acids Prior to qPCR and RT-qPCR. *NanoDrop Spectrophotometers T097-Rev 6/7/2010*.
281. Invitrogen (2014) Comparison of fluorescence-based quantitation with UV absorbance measurements. *Qubit® fluorometric quantitation*.
282. Agilent Technologies (2014) Applications for DNA, RNA, Protein and Cell Analysis. *Agilent 2100 Bioanalyzer System: Application Compendium*.
283. Marullo M, Zuccato C, Mariotti C *et al.* (2010) Expressed Alu repeats as a novel, reliable tool for normalization of real-time quantitative RT-PCR data. *Genome Biol* 11 (1):R9.
284. Pineda GM, Montgomery AH, Thompson R *et al.* (2014) Development and validation of InnoQuant, a sensitive human DNA quantitation and degradation assessment method for forensic samples using high copy number mobile elements Alu and SVA. *Forensic Sci Int Genet* 13:224-235.
285. Qiagen (2012) RNeasy® Mini Handbook. <https://www.qiagen.com/gb/resources/resourcedetail?id=14e7cf6e-521a-4cf7-8cbc-bf9f6fa33e24&lang=en>. 2012

Chapter 8 References

286. Thatcher SA (2015) DNA/RNA preparation for molecular detection. *Clin Chem* 61 (1):89-99.
287. Stahlberg A, Aman P, Ridell B *et al.* (2003) Quantitative real-time PCR method for detection of B-lymphocyte monoclonality by comparison of kappa and lambda immunoglobulin light chain expression. *Clin Chem* 49 (1):51-59.
288. Samar Lightfoot (2002) Quantitation comparison of total RNA using the Agilent 2100 bioanalyzer, ribo- green analysis and UV spectrometry. Agilent Technologies, Application Note 5988-7650EN.
289. Svec D, A. T, Novosadova V *et al.* (2015) How good is a PCR efficiency estimate: Recommendations for precise and robust qPCR efficiency assessments. *Biomolecular Detection and Quantification* 3:9-16.
290. Schroeder A, Mueller O, Stocker S *et al.* (2006) The RIN: an RNA integrity number for assigning integrity values to RNA measurements. *BMC Mol Biol* 7:3.
291. Fleige S, Pfaffl MW (2006) RNA integrity and the effect on the real-time qRT-PCR performance. *Mol Aspects Med* 27 (2-3):126-139.
292. Bhat S, McLaughlin JL, Emslie KR (2011) Effect of sustained elevated temperature prior to amplification on template copy number estimation using digital polymerase chain reaction. *Analyst* 136 (4):724-732.
293. Hou Y, Zhang H, Miranda L *et al.* (2010) Serious overestimation in quantitative PCR by circular (supercoiled) plasmid standard: microalgal pcna as the model gene. *PLoS One* 5 (3):e9545.
294. Gurkan UA, Krueger A, Akkus O (2011) Ossifying bone marrow explant culture as a three-dimensional mechanoresponsive in vitro model of osteogenesis. *Tissue Eng Part A* 17 (3-4):417-428.
295. Kato Y, Boskey A, Spevak L *et al.* (2001) Establishment of an osteoid preosteocyte-like cell MLO-A5 that spontaneously mineralizes in culture. *Journal of bone and mineral research : the official journal of the American Society for Bone and Mineral Research* 16 (9):1622-1633.
296. Addison WN, Nelea V, Chikatun F *et al.* (2015) Extracellular matrix mineralization in murine MC3T3-E1 osteoblast cultures: an ultrastructural, compositional and comparative analysis with mouse bone. *Bone* 71:244-256.
297. Bakker AD, Kulkarni RN, Klein-Nulend J *et al.* (2014) IL-6 alters osteocyte signaling toward osteoblasts but not osteoclasts. *J Dent Res* 93 (4):394-399.
298. Mullen CA, Vaughan TJ, Voisin MC *et al.* (2014) Cell morphology and focal adhesion location alters internal cell stress. *J R Soc Interface* 11 (101):20140885.

Chapter 8 References

299. Wu L, Feyerabend F, Schilling AF *et al.* (2015) Effects of extracellular magnesium extract on the proliferation and differentiation of human osteoblasts and osteoclasts in coculture. *Acta Biomater.*
300. Krishnan V, Vogler EA, Mastro AM (2015) Three-dimensional in vitro model to study osteobiology and osteopathology. *J Cell Biochem.*
301. Chan ME, Lu XL, Huo B *et al.* (2009) A Trabecular Bone Explant Model of Osteocyte-Osteoblast Co-Culture for Bone Mechanobiology. *Cell Mol Bioeng* 2 (3):405-415.
302. Xiao JJ, Zhao WJ, Zhang XT *et al.* (2015) Bergapten promotes bone marrow stromal cell differentiation into osteoblasts in vitro and in vivo. *Mol Cell Biochem.*
303. Bertin A, Hanna P, Otarola G *et al.* (2015) Cellular and molecular characterization of a novel primary osteoblast culture from the vertebrate model organism *Xenopus tropicalis*. *Histochem Cell Biol* 143 (4):431-442.
304. Wang Y, Uemura T, Dong J *et al.* (2003) Application of perfusion culture system improves in vitro and in vivo osteogenesis of bone marrow-derived osteoblastic cells in porous ceramic materials. *Tissue Eng* 9 (6):1205-1214.
305. Mathews S, Bhonde R, Gupta PK *et al.* (2014) Novel biomimetic tripolymer scaffolds consisting of chitosan, collagen type 1, and hyaluronic acid for bone marrow-derived human mesenchymal stem cells-based bone tissue engineering. *J Biomed Mater Res B Appl Biomater* 102 (8):1825-1834.
306. Bouet G, Cruel M, Laurent C *et al.* (2015) Validation of an in vitro 3D bone culture model with perfused and mechanically stressed ceramic scaffold. *Eur Cell Mater* 29:250-266; discussion 266-257.
307. Chuenjitkuntaworn B, Osathanon T, Nowwarote N *et al.* (2015) The efficacy of polycaprolactone/hydroxyapatite scaffold in combination with mesenchymal stem cells for bone tissue engineering. *J Biomed Mater Res A.*
308. Florencio-Silva R, Sasso GR, Sasso-Cerri E *et al.* (2015) Biology of Bone Tissue: Structure, Function, and Factors That Influence Bone Cells. *Biomed Res Int* 2015:421746.
309. Capulli M, Paone R, Rucci N (2014) Osteoblast and osteocyte: games without frontiers. *Arch Biochem Biophys* 561:3-12.
310. Damoulis PD, Hauschka PV (1997) Nitric oxide acts in conjunction with proinflammatory cytokines to promote cell death in osteoblasts. *Journal of bone and mineral research : the official journal of the American Society for Bone and Mineral Research* 12 (3):412-422.

Chapter 8 References

311. University of Cambridge (2015) Formation and remodelling of bone. <http://www.doitpoms.ac.uk/tlplib/bones/formation.php>. 2015
312. Clarke B (2008) Normal bone anatomy and physiology. *Clin J Am Soc Nephrol* 3 Suppl 3:S131-139.
313. Karsenty G, Kronenberg HM, Settembre C (2009) Genetic control of bone formation. *Annu Rev Cell Dev Biol* 25:629-648.
314. Teitelbaum SL (2007) Osteoclasts: what do they do and how do they do it? *Am J Pathol* 170 (2):427-435.
315. Bonewald LF (2011) The amazing osteocyte. *Journal of bone and mineral research : the official journal of the American Society for Bone and Mineral Research* 26 (2):229-238.
316. Dallas SL, Prideaux M, Bonewald LF (2013) The osteocyte: an endocrine cell ... and more. *Endocr Rev* 34 (5):658-690.
317. Rochefort GY, Pallu S, Benhamou CL (2010) Osteocyte: the unrecognized side of bone tissue. *Osteoporos Int* 21 (9):1457-1469.
318. Bonewald LF (2007) Osteocytes as dynamic multifunctional cells. *Ann N Y Acad Sci* 1116:281-290.
319. Costa A, Henrique D (2015) Transcriptome profiling of induced hair cells (iHCs) generated by combined expression of Gfi1, Pou4f3 and Atoh1 during embryonic stem cell differentiation. *Genom Data* 6:77-80.
320. Farhy C, Elgart M, Shapira Z *et al.* (2013) Pax6 is required for normal cell-cycle exit and the differentiation kinetics of retinal progenitor cells. *PLoS One* 8 (9):e76489.
321. Shang J, Fan X, Shanguan L *et al.* (2015) Global Gene Expression Profiling and Alternative Splicing Events during the Chondrogenic Differentiation of Human Cartilage Endplate-Derived Stem Cells. *Biomed Res Int* 2015:604972.
322. Stute P, Sielker S, Wood CE *et al.* (2012) Life stage differences in mammary gland gene expression profile in non-human primates. *Breast Cancer Res Treat* 133 (2):617-634.
323. Uren PJ, Lee JT, Doroudchi MM *et al.* (2014) A profile of transcriptomic changes in the rd10 mouse model of retinitis pigmentosa. *Mol Vis* 20:1612-1628.
324. van Dartel DA, Schulpen SH, Theunissen PT *et al.* (2014) Dynamic changes in energy metabolism upon embryonic stem cell differentiation support developmental toxicant identification. *Toxicology* 324:76-87.

325. Wallner S, Grandl M, Konovalova T *et al.* (2014) Monocyte to macrophage differentiation goes along with modulation of the plasmalogen pattern through transcriptional regulation. *PLoS One* 9 (4):e94102.
326. Bellis SL (2004) Variant glycosylation: an underappreciated regulatory mechanism for beta1 integrins. *Biochim Biophys Acta* 1663 (1-2):52-60.
327. Benton G, George J, Kleinman HK *et al.* (2009) Advancing science and technology via 3D culture on basement membrane matrix. *J Cell Physiol* 221 (1):18-25.
328. Luca AC, Mersch S, Deenen R *et al.* (2013) Impact of the 3D microenvironment on phenotype, gene expression, and EGFR inhibition of colorectal cancer cell lines. *PLoS One* 8 (3):e59689.
329. Taylor AF, Saunders MM, Shingle DL *et al.* (2007) Mechanically stimulated osteocytes regulate osteoblastic activity via gap junctions. *Am J Physiol Cell Physiol* 292 (1):C545-552.
330. Yulug IG, Yulug A, Fisher EM (1995) The frequency and position of Alu repeats in cDNAs, as determined by database searching. *Genomics* 27 (3):544-548.
331. Parfitt AM (1977) The cellular basis of bone turnover and bone loss: a rebuttal of the osteocytic resorption--bone flow theory. *Clin Orthop Relat Res* (127):236-247.
332. Whyte MP (1994) Hypophosphatasia and the role of alkaline phosphatase in skeletal mineralization. *Endocr Rev* 15 (4):439-461.
333. Mornet E, Stura E, Lia-Baldini AS *et al.* (2001) Structural evidence for a functional role of human tissue nonspecific alkaline phosphatase in bone mineralization. *J Biol Chem* 276 (33):31171-31178.
334. Murray E, Provvedini D, Curran D *et al.* (1987) Characterization of a human osteoblastic osteosarcoma cell line (SAOS-2) with high bone alkaline phosphatase activity. *Journal of bone and mineral research : the official journal of the American Society for Bone and Mineral Research* 2 (3):231-238.
335. Fukayama S, Bosma TJ, Goad DL *et al.* (1988) Human parathyroid hormone (PTH)-related protein and human PTH: comparative biological activities on human bone cells and bone resorption. *Endocrinology* 123 (6):2841-2848.
336. Villarreal XC, Mann KG, Long GL (1989) Structure of human osteonectin based upon analysis of cDNA and genomic sequences. *Biochemistry* 28 (15):6483-6491.
337. Ikeda K, Imai Y, Fukase M *et al.* (1990) The effect of 1,25-dihydroxyvitamin D3 on human osteoblast-like osteosarcoma cell: modification of response to PTH. *Biochem Biophys Res Commun* 168 (3):889-897.

Chapter 8 References

338. Huh JE, Yang HR, Park DS *et al.* (2006) Puerariae radix promotes differentiation and mineralization in human osteoblast-like SaOS-2 cells. *J Ethnopharmacol* 104 (3):345-350.
339. McQuillan DJ, Richardson MD, Bateman JF (1995) Matrix deposition by a calcifying human osteogenic sarcoma cell line (SAOS-2). *Bone* 16 (4):415-426.
340. Franceschi RT, Iyer BS (1992) Relationship between collagen synthesis and expression of the osteoblast phenotype in MC3T3-E1 cells. *Journal of bone and mineral research : the official journal of the American Society for Bone and Mineral Research* 7 (2):235-246.
341. Aubin JE, Liu F, Malaval L *et al.* (1995) Osteoblast and chondroblast differentiation. *Bone* 17 (2 Suppl):77S-83S.
342. Hunter GK, Hauschka PV, Poole AR *et al.* (1996) Nucleation and inhibition of hydroxyapatite formation by mineralized tissue proteins. *Biochem J* 317 (Pt 1):59-64.
343. Gerber HP, Vu TH, Ryan AM *et al.* (1999) VEGF couples hypertrophic cartilage remodeling, ossification and angiogenesis during endochondral bone formation. *Nat Med* 5 (6):623-628.
344. Goad DL, Rubin J, Wang H *et al.* (1996) Enhanced expression of vascular endothelial growth factor in human SaOS-2 osteoblast-like cells and murine osteoblasts induced by insulin-like growth factor I. *Endocrinology* 137 (6):2262-2268.
345. Hughes FJ, Collyer J, Stanfield M *et al.* (1995) The effects of bone morphogenetic protein-2, -4, and -6 on differentiation of rat osteoblast cells in vitro. *Endocrinology* 136 (6):2671-2677.
346. McCarthy TL, Centrella M, Canalis E (1989) Regulatory effects of insulin-like growth factors I and II on bone collagen synthesis in rat calvarial cultures. *Endocrinology* 124 (1):301-309.
347. Midy V, Plouet J (1994) Vasculotropin/vascular endothelial growth factor induces differentiation in cultured osteoblasts. *Biochem Biophys Res Commun* 199 (1):380-386.
348. Spelsberg TC, Subramaniam M, Riggs BL *et al.* (1999) The actions and interactions of sex steroids and growth factors/cytokines on the skeleton. *Mol Endocrinol* 13 (6):819-828.
349. Hausser HJ, Brenner RE (2005) Phenotypic instability of Saos-2 cells in long-term culture. *Biochem Biophys Res Commun* 333 (1):216-222.

Chapter 8 References

350. Kim M, Kim C, Choi YS *et al.* (2012) Age-related alterations in mesenchymal stem cells related to shift in differentiation from osteogenic to adipogenic potential: implication to age-associated bone diseases and defects. *Mech Ageing Dev* 133 (5):215-225.
351. Schellenberg A, Stiehl T, Horn P *et al.* (2012) Population dynamics of mesenchymal stromal cells during culture expansion. *Cytherapy* 14 (4):401-411.
352. Buckland-Wright C (2004) Subchondral bone changes in hand and knee osteoarthritis detected by radiography. *Osteoarthritis Cartilage* 12 Suppl A:S10-19.
353. Grynblas MD, Alpert B, Katz I *et al.* (1991) Subchondral bone in osteoarthritis. *Calcif Tissue Int* 49 (1):20-26.
354. Li B, Aspden RM (1997) Composition and mechanical properties of cancellous bone from the femoral head of patients with osteoporosis or osteoarthritis. *Journal of bone and mineral research : the official journal of the American Society for Bone and Mineral Research* 12 (4):641-651.
355. Li B, Aspden RM (1997) Mechanical and material properties of the subchondral bone plate from the femoral head of patients with osteoarthritis or osteoporosis. *Ann Rheum Dis* 56 (4):247-254.
356. Neogi T (2012) Clinical significance of bone changes in osteoarthritis. *Ther Adv Musculoskelet Dis* 4 (4):259-267.
357. Radin EL, Rose RM (1986) Role of subchondral bone in the initiation and progression of cartilage damage. *Clin Orthop Relat Res* (213):34-40.
358. Burr DB (2004) The importance of subchondral bone in the progression of osteoarthritis. *J Rheumatol Suppl* 70:77-80.
359. Li G, Yin J, Gao J *et al.* (2013) Subchondral bone in osteoarthritis: insight into risk factors and microstructural changes. *Arthritis Res Ther* 15 (6):223.
360. Hellemans J, Mortier G, De Paepe A *et al.* (2007) qBase relative quantification framework and software for management and automated analysis of real-time quantitative PCR data. *Genome Biol* 8 (2):R19.
361. Mantila Roosa SM, Liu Y, Turner CH (2011) Gene expression patterns in bone following mechanical loading. *Journal of bone and mineral research : the official journal of the American Society for Bone and Mineral Research* 26 (1):100-112.
362. Szczesniak AM, Gilbert RW, Mukhida M *et al.* (2005) Mechanical loading modulates glutamate receptor subunit expression in bone. *Bone* 37 (1):63-73.
363. Griffin TM, Guilak F (2005) The role of mechanical loading in the onset and progression of osteoarthritis. *Exerc Sport Sci Rev* 33 (4):195-200.

364. Castaneda S, Roman-Blas JA, Largo R *et al.* (2012) Subchondral bone as a key target for osteoarthritis treatment. *Biochem Pharmacol* 83 (3):315-323.
365. Cheung VG, Conlin LK, Weber TM *et al.* (2003) Natural variation in human gene expression assessed in lymphoblastoid cells. *Nat Genet* 33 (3):422-425.
366. Morley M, Molony CM, Weber TM *et al.* (2004) Genetic analysis of genome-wide variation in human gene expression. *Nature* 430 (7001):743-747.
367. Ho ML, Tsai TN, Chang JK *et al.* (2005) Down-regulation of N-methyl D-aspartate receptor in rat-modeled disuse osteopenia. *Osteoporos Int* 16 (12):1780-1788.
368. McNearney T, Baethge BA, Cao S *et al.* (2004) Excitatory amino acids, TNF- α , and chemokine levels in synovial fluids of patients with active arthropathies. *Clin Exp Immunol* 137 (3):621-627.
369. Brakspear KS, Mason DJ (2012) Glutamate signaling in bone. *Front Endocrinol (Lausanne)* 3:97.
370. Bonnet CS, Williams AS, Gilbert SJ *et al.* (2015) AMPA/kainate glutamate receptors contribute to inflammation, degeneration and pain related behaviour in inflammatory stages of arthritis. *Ann Rheum Dis* 74 (1):242-251.
371. Huggett J, Vaughan-Thomas A, Mason D (2000) The open reading frame of the Na(+)-dependent glutamate transporter GLAST-1 is expressed in bone and a splice variant of this molecule is expressed in bone and brain. *FEBS Lett* 485 (1):13-18.
372. White RA, 3rd, Quake SR, Curr K (2012) Digital PCR provides absolute quantitation of viral load for an occult RNA virus. *J Virol Methods* 179 (1):45-50.
373. Skerry TM (2002) Neurotransmitter functions in bone remodeling. *J Musculoskelet Neuronal Interact* 2 (3):281.
374. Also-Rallo E, Alias L, Martinez-Hernandez R *et al.* (2011) Treatment of spinal muscular atrophy cells with drugs that upregulate SMN expression reveals inter- and intra-patient variability. *Eur J Hum Genet* 19 (10):1059-1065.
375. Feuerstein P, Puard V, Chevalier C *et al.* (2012) Genomic assessment of human cumulus cell marker genes as predictors of oocyte developmental competence: impact of various experimental factors. *PLoS One* 7 (7):e40449.
376. Lambert DW, Lambert LA, Clarke NE *et al.* (2014) Angiotensin-converting enzyme 2 is subject to post-transcriptional regulation by miR-421. *Clin Sci (Lond)* 127 (4):243-249.

Chapter 8 References

377. Roberfroid S, Vanderleyden J, Steenackers H (2016) Gene expression variability in clonal populations: Causes and consequences. *Crit Rev Microbiol*:1-16.
378. Boehm AB, Van De Werfhorst LC, Griffith JF *et al.* (2013) Performance of forty-one microbial source tracking methods: a twenty-seven lab evaluation study. *Water Res* 47 (18):6812-6828.
379. Ebentier DL, Hanley KT, Cao Y *et al.* (2013) Evaluation of the repeatability and reproducibility of a suite of qPCR-based microbial source tracking methods. *Water Res* 47 (18):6839-6848.
380. Fryer JF, Baylis SA, Gottlieb AL *et al.* (2008) Development of working reference materials for clinical virology. *J Clin Virol* 43 (4):367-371.
381. Gouarin S, Vabret A, Scieux C *et al.* (2007) Multicentric evaluation of a new commercial cytomegalovirus real-time PCR quantitation assay. *J Virol Methods* 146 (1-2):147-154.
382. Hayden RT, Yan X, Wick MT *et al.* (2012) Factors contributing to variability of quantitative viral PCR results in proficiency testing samples: a multivariate analysis. *J Clin Microbiol* 50 (2):337-345.
383. Rychert J, Danziger-Isakov L, Yen-Lieberman B *et al.* (2014) Multicenter comparison of laboratory performance in cytomegalovirus and Epstein-Barr virus viral load testing using international standards. *Clin Transplant* 28 (12):1416-1423.
384. Schriewer A, Goodwin KD, Sinigalliano CD *et al.* (2013) Performance evaluation of canine-associated Bacteroidales assays in a multi-laboratory comparison study. *Water Res* 47 (18):6909-6920.
385. Zhang T, Grenier S, Nwachukwu B *et al.* (2007) Inter-laboratory comparison of chronic myeloid leukemia minimal residual disease monitoring: summary and recommendations. *J Mol Diagn* 9 (4):421-430.
386. Brazma A, Hingamp P, Quackenbush J *et al.* (2001) Minimum information about a microarray experiment (MIAME)-toward standards for microarray data. *Nat Genet* 29 (4):365-371.
387. Consortium TE (2011) Standards, Guidelines and Best Practices for RNA-Seq V1.0 (June 2011). https://genome.ucsc.edu/ENCODE/protocols/dataStandards/ENCODE_RNAseq_Standards_V1.0.pdf. 2016
388. Genetic European Variation in Disease (GEUVADIS) Consortium (2010) GEUVADIS: Genetic European Variation in Health and Disease, A European Medical Sequencing Consortium.

Chapter 8 References

<http://www.geuvadis.org/web/geuvadis/home;jsessionid=2CEBF8114F08B01C1E6088522B74C133>. 2016

389. Bohlenius H, Eriksson S, Parcy F *et al.* (2007) Retraction. *Science* 316 (5823):367.

390. Kanadia RN, Cepko CL (2011) Retraction. Alternative splicing produces high levels of noncoding isoforms of bHLH transcription factors during development. *Genes Dev* 25 (12):1344.

391. Ikeda N (2013) Retraction of "Enhanced expression of coproporphyrinogen oxidase in malignant brain tumors: CPOX expression and 5-ALA-induced fluorescence". *Neuro-Oncology* 13(11):1234-1243. *Neuro Oncol* 15 (7):969.

392. Alberts B (2011) Retraction. *Science* 334 (6063):1636.

393. Staroscik A (2004) Calculator for determining the number of copies of a template. <http://cels.uri.edu/gsc/cndna.html>. 2011

394. Scientific TF (2011) Accuracy vs. Reference Spectrophotometer. Performance Data NanoDrop 2000/2000c T095 Rev 5/10.

395. Magnusson B, Ellison SL (2008) Treatment of uncorrected measurement bias in uncertainty estimation for chemical measurements. *Anal Bioanal Chem* 390 (1):201-213.

Chapter 9

Appendices

9 Appendices

9.1 Appendix 1 – Assay Information

Table 9.1 Primer and probe sequences

Target DNA	Gene Accession Number	Primer/Probe Sequence (5' to 3')
Exogenous/synthetic targets:		
ERCC-13	EF011062	(F) CGGACATGGTGTGGTCAAG (R) TTGTTGGGCGGACCGTAA (P) FAM-TGCATGAGGACCCGCAAATTCCTC-BHQ1
ERCC-25	DQ883689	(F) CGGTCGTGAACTGCTATAGGA (R) GGTAGTTTCGCTGGTTCGTT (P) FAM-AGCCTGATACGAGCGCACAACA-BHQ1
ERCC-42	DQ516783	(F) AGAGAGCTTTTGGCAATCCT (R) TCATTTGCTAAGGCAGTTAAAGA (P) FAM-TCACCAGTTCCCATGAATGTTCCAC-BHQ1
ERCC-84	DQ883682	(F) TGGATAAGCGAGGTCAGTCAAG (R) ATGCAGGCAAACGATCTACGT (P) FAM-ATTCGTTGCCTCCGGGTCC-BHQ1
ERCC-95	DQ516759	(F) GAGCGTTTTTATGCAGTTCATCTTT (R) GGATAAGATTGTTGAGTGGGCTTT (P) FAM-ACCTCATCCCACAAAGCCGTTTCTT-BHQ1
ERCC-99	DQ875387	(F) TCGTCCATCCCTCAAGAGAGA (R) CGCAATCGCGTGTGAATG (P) FAM-CATGGAAAGAGCTCGACAAAATTTACTC-BHQ1
ERCC-113	DQ883663	(F) GCGACACCAACATCGTTACG (R) CCGCGCGTGAGCACTT (P) FAM-ACACACCGGACGCTTGGATCAGTG-BHQ1
ERCC-171	DQ854994	(F) TTAGTTTCGTGGCGGGATTT (R) CACGAATCGCACGGATGTT (P) FAM-AGGAAAAGTGC GACTGTTCTTTAACC-BHQ1
Endogenous Targets:		
Alu [130]		(F) CATGGTCAAACCCCGTCTCTA (R) GCCTCAGCCTCCCGAGTAG
CASC3	NM_007359.4	(F) AGCCTTCTTTCCTGCAACCA (R) CATATACACATGGGAGCAGGACC (P) FAM-ACTTCGAGGTATGCCC-MGB
HPRT1	NM_000194.2	(F) CCTTGGTCAGGCAGTATAATCCA (R) AGCTTGCTGGTGAAGGACC (P) FAM-AGATGGTCAAGGTCG-MGB

Chapter 9 Appendices

MMP1	NM_001145938.1	(F) GGCCACAAACCCCAA (R) TCTACCCGGAAGTTGAGCTCA (P) FAM-AAGACAGATTCTACATGCGCA-MGB
NES	NM_006617.1	(F) CCCAAGACTGCCCTGGAAA (R) GAAGAGTCTGACCCTGTTTCCTTG (P) FAM-AGTGCTGAGCCTTCT-MGB
SLC1A3	NM_004172.4	(F) AGTGCAGAACATTACAAAGGAGGAT (R) GATTTACCCTCCGACCATACAGA (P) FAM-TTAAAAGTTACCTGTTTCG-MGB
UBC	NM_021009.5	(F) TTGTGGATCGCTGTGATCGT (R) AGACTCTGACTGGTAAGACCATCACC (P) FAM-ACTTGACAATGCAGATCT-MGB
AMPA1	NM_000827.3	(F) CCTTCTTCTGCACCGGTTTC (R) GAAATAATCCCCGATCTGGAT (P) FAM-TAGGCGCGGTAGTAGG-BHQ1
AMPA2	NM_000826.3	(F) GAGCTCTCCTTAGCTTGATTGAATACTA (R) TTGATAAGCCTCTGTCATGTCATAGA (P) FAM-CAATGGGACAAGTTTGCATA-BHQ1
EAAT1	NM_004172.4	(F) TTTATTGGAGGGTTGCTGCAA (R) GTAGGGTGGCAGAACTTGAAGAG (P) FAM-ACTCATCACCGCTCTG-BHQ1
EAAT3	NM_004170.5	(F) GCGATCCAGAGATGAACATGAC (R) TCCTTTGTTTTGTTCTTGAAATTG (P) FAM-AAGAGTCCTTCACAGCTGT-BHQ1
KA1	NM_014619.2	(F) GAGCTGATCGCTAGGAAAGCA (R) TCAATCACCTTCTCCCGTTCA (P) FAM-AGGCCTCACCATTACA-BHQ1
KA2	NM_002088.4	(F) TTCCAGAATTCACGGTACCAAA (R) TCTTCTGTGCTCTTGACGAACAC (P) FAM-TGGAACATGCAGTCGA-BHQ1
NRI	NM_007327.3	(F) CATAGGCATGCGCAAAGACA (R) CGTGGGACTTGAGGATGGA (P) FAM-AGCAGAACGTCTCCCT-BHQ1

Assay-on-demand* (ABI):

TBP

Hs00920497_m1

(F) forward primer, (R) reverse primer, (P) probe, BHQ1: black hole quencher 1, MGB: minor groove binder. ERCC assays previously described by Devonshire *et al.* (2011) [45]. *Assays on demand, all FAM-MGB probes. All ERCC assays: (F) 900 nM, (R) 900 nM, (P) 180 nM. Alu assay: (F) 250 nM, (R) 250 nM. All other in-house endogenous targets: (F) 900 nM, (R) 900 nM, (P) 250 nM.

Chapter 9 Appendices

Assays used for dynamic array experiments (**Chapter 6**): ERCC-13, -25, -42, -99, -113, -171, CASC3, HPRT1, MMP1, NES, SLC1A3, UBC, AMPA1, AMPA2, EAAT1, EAAT3, KA1, KA2, NR1, TBP, PSMC4, PGK1, B2M, GAPDH, PPIA, RPLP0 AND YWHAZ. Details covered in Tables 9.1 and 9.2.

Table 9.2 Human endogenous control assays, TaqMan Array Plate.

Assay ID	Gene Symbol	Assay ID	Gene Symbol
Hs99999901_s1	18S	Hs00201226_m1	CASC3
Hs99999905_m1	GAPDH	Hs00355782_m1	CDKN1A
Hs99999909_m1	HPRT1	Hs00153277_m1	CDKN1B
Hs99999908_m1	GUSB	Hs00169255_m1	GADD45A
Hs99999903_m1	ACTB	Hs00206469_m1	PUM1
Hs99999907_m1	B2M	Hs00197826_m1	PSMC4
Hs00609297_m1	HMBS	Hs00426752_m1	EIF2B1
Hs00183533_m1	IPO8	Hs00362795_g1	PES1
Hs99999906_m1	PGK1	Hs00245445_m1	ABL1
Hs99999902_m1	RPLP0	Hs00152844_m1	ELF1
Hs99999910_m1	TBP	Hs02596862_g1	MT-ATP6,LOC100133315
Hs99999911_m1	TFRC	Hs00608519_m1	MRPL19
Hs00824723_m1	UBC	Hs00198357_m1	POP4
Hs00237047_m1	YWHAZ	Hs01102345_m1	RPL37A
Hs99999904_m1	PPIA	Hs00265497_m1	RPL30
Hs00172187_m1	POLR2A	Hs00734303_g1	RPS17

Assay ID prefix indicates species: Hs = human. Assay ID suffix indicates assay placement: _m = an assay whose probe spans an exon junction and does not detect genomic DNA; _s = an assay whose primers and probes are designed within a single exon. Such assays, by definition, detect genomic DNA; _g = an assay that may detect genomic DNA. The assay primers and probe may also be within a single exon. (**3.2.6 Endogenous Target Selection**).

Table 9.3 Human endogenous GOI assays

Assay ID	Gene Symbol	Assay ID	Gene Symbol
Hs00180269_m1	BAX	Hs01075667_m1	IL6-R
Hs00153120_m1	CYP1A1	Hs00158148_m1	ITGA2
Hs00366488_m1	SLCO1A2	Hs00233958_m1	MMP1
Hs00234219_m1	SULT2A1	Hs00365167_m1	COL6A2
Hs00358656_m1	ABCC3	Hs00705137_s1	IFITM1
Hs00166123_m1	ABCC2	Hs01110251_m1	HO-1
Hs99999141_s1	JUN	Hs00155249_m1	GCLC
Hs00992441_m1	IL32	Hs00998421_m1	M6PRBP1
Hs00234415_m1	IL11RA	Hs00171993_m1	TNFRSF12A
Hs01556193_m1	BRCA1	Hs00242448_m1	COL6A1
Hs00707120_s1	NES	Hs00174360_m1	IL6ST
Hs00221623_m1	CLDN1*	Hs00934682_m1	GATA6
Hs00415716_m1	SOX2OT		

In-house designed assays		
Target DNA	Gene Accession Number	Primer/Probe Sequence (5' to 3')
GFAP	NM_001131019.1	(F) GAGATGGCCCCGCACTTGCA (R) TGGTGATCCGGTTCTCCTCGCC (P) FAM-CAAGCTGGCCCTGGACATCGA-TAMRA
PDGFRA	NM_006206.4	(F) CGTTCCTGGTCTTAGGCTGTCT (R) GGAAGGATAGAGGGTAATGAAAGCT (P) TCACAGGGCTGAGCCTAATCCTCTGC
PDGFRB	NM_002609.3	(F) ATGAGCGGAAACGGCTCTAC (R) GAATAGTTCTCGGCATCATTAGG (P) CTTTGTGCCAGATCCCACCGT
SLC1A3	As Table 9.1	

Assays highlighted in **BLUE** were used to test the applicability of the mocked up mixed ratio model units (**2.3.1.2 Genes of Interest**). GFAP assay: (F) 900 nM, (R) 900 nM, (P) 250 nM. PDGFRA assay: (F) 300 nM, (R) 900 nM, (P) 200 nM. PDGFRB assay: (F) 900 nM, (R) 900 nM, (P) 200 nM.

Table 9.4 Assay Positions

Target	Transcript Length (bases)*	Base position in transcript (5' to 3')		
		Forward Primer	Probe	Reverse Primer
CASC3	4198	1734-1753	1759-1774	1778-1800
HPRT1	1435	610-632	634-648	651-671
MMP1	1903	802-818	884-904	914-934
NES	5591	4574-4592	4607-4621	4631-4654
SLC1A3	4188	572-596	598-616	670-692
UBC	2594	430-449	451-468	475-500
ERCC-13	808	540-559	563-586	588-605
ERCC-25	1994	1772-1792	1795-1816	1819-1838
ERCC-42	1023	680-699	703-727	730-752
ERCC-99	1350	732-752	756-783	785-802
ERCC-113	843	80-99	103-126	129-144
ERCC-171	505	237-256	258-283	285-303

*Length of transcript including poly(A) tail.

Table 9.5 Sample dilutions analysed during study. Concentrations initially estimated using UV spectrophotometry. Calibrant (C), Unknown 1 (U1), Unknown 2 (U2).

Experiment	Assay	RT-qPCR (steps)	Copies or concentration DNA* target per reaction	Replicates (RT or qPCR)	Concentration carrier
Plasmid Contamination Assessment	All eight ERCC assays	qPCR	~5E+08 to 5E+03 (copies)	1 per dilution, per assay	None
gDNA Contamination Assessment	<i>Alu</i>	qPCR	1 to 1E-05 ng Human gDNA (positive control), 20 ng cell line RNA	3 per cell line/positive control. 6 NTC	None
Human Cross-Reactivity	All eight ERCC assays	qPCR	-	1 per assay	250 ng human gDNA
Carrier Optimisation 1	ERCC-13	RT-qPCR (one-step)	~5E+08 to 5E+04 (copies)	3 per dilution, per carrier	50 or 250 ng salmon sperm DNA or yeast total RNA, or 50 ng Hep-G2 total RNA
Carrier Optimisation 2	ERCC-13	RT-qPCR (one-step)	~5E+06 to 5E+01 (copies)	3 per dilution, per carrier	250 ng salmon sperm DNA or yeast total RNA
RNA Stability Analysis	GAPDH	RT-qPCR (two-step)	20, 2 or 0.2 (ng) RNA equivalent	2 (RT), 3 (qPCR, via dilution)	None (total RNA)
RT Variability	GAPDH	RT-qPCR (two-step)	20, 2 or 0.2 (ng) RNA equivalent	2 (RT and qPCR) per sample extraction (×4) & dilution (×3)	None (total RNA)

Endogenous Target Selection:

Chapter 9 Appendices

Reference Genes	32 control genes (Appendix 1)	RT-qPCR (two-step)	10 ng total cDNA	Triplicates per assay, per cell line	None (total RNA)
Genes of Interest	31 potential GOI (Appendix 1)	RT-qPCR (one-step)	10 ng total RNA	1 per assay, per cell line Mocked up mixed ratio model units U1 & U2 analysed in triplicate	None (total RNA)
TCM Homogeneity	ERCC-99 & HPRT1	RT-qPCR (one-step)	C, U1 & U2	Ten aliquots each of C, U1 and U2, with replicates of 8	250 ng yeast total RNA
TCM Short Term Stability	ERCC-99 & HPRT1	RT-qPCR (one-step)	C, U1 & U2	Three aliquots each of C, U1 and U2, per temperature and time point	250 ng yeast total RNA
TCM Long Term Stability	ERCC-99 & HPRT1	RT-qPCR (one-step)	C, U1 & U2	Three aliquots each of C, U1 and U2, per temperature and time point	250 ng yeast total RNA
One-Step RT-qPCR Kit Comparison by dPCR	ERCC-25 & ERCC-99	RT-qPCR (one-step)	~1896 (copies/panel)	1 panel/assay, 3 replicate chips	250 ng yeast total RNA
Comparison between dPCR and UV	All six ERCCs	RT-qPCR (one-step)	~200-400 (copies/panel)	3 panels/assay	250 ng yeast total RNA
Linearity and Sensitivity of RT-dPCR	ERCC-25 & ERCC-99	RT-qPCR (one-step)	~500, 250 100, 50, 25, 10 or 5 (copies/panel)	6 panels/ dilution/assay, 2 replicate chips	250 ng yeast total RNA
Further Evaluation of Reverse Transcriptase's	ERCC-25, -99, UBC & MMP1	RT-qPCR (one-step)	~1886 (copies/panel)	3 panels/assay duplex, 2 replicate chips	250 ng yeast total RNA
Impact of Extraction Protocol	<i>Alu</i>	qPCR and RT-qPCR (two-step)	20 ng total RNA (or cDNA equivalent)	Triplicates per sample	None

Chapter 9 Appendices

3D Gel Co-cultures	<i>Alu</i>	qPCR	20 ng total RNA	Triplicates per sample	None
	Appendix 1	RT-qPCR (two-step) with §PreAmp	10 ng/μL cDNA per §PreAmp	Triplicate RTs measured per sample	None
Clinical Samples	<i>Alu</i>	qPCR	20 ng total RNA	Triplicates per sample	None
	Appendix 1	RT-qPCR (two-step) with §PreAmp	10 ng/μL cDNA per §PreAmp	Triplicate RTs measured per sample	None

*Dilutions are quoted based on RNA copies or concentration (total RNA equivalent) per qPCR well of a standard 96 well plate, or RNA copies per dPCR panel (where specified). No template controls (NTCs) for every experiment resulted in no amplified signal observed (except for *Alu* assessment, as described, **3.2.1 DNA Contamination Assessment**). RNA concentrations were estimated by UV and converted to copy number using published methods [224]. §PreAmp: Preamplification

Table 9.6 ERCC RNA concentration and copy number estimates

ERCC-	Concentration (ng/ μ L)*	Molecular weight with poly(A) tail (g/mol) [†]	Estimated copy number/ μ L	Estimated copies/ng
13	442	261410	1.02E+12	2.30E+09
25	428	640925	4.02E+11	9.40E+08
42	395	325739	7.30E+11	1.85E+09
99	401	434398	5.56E+11	1.39E+09
113	815	271727	1.81E+12	2.22E+09
171	385	163019	1.42E+12	3.69E+09

*As estimated by UV, n = 3.

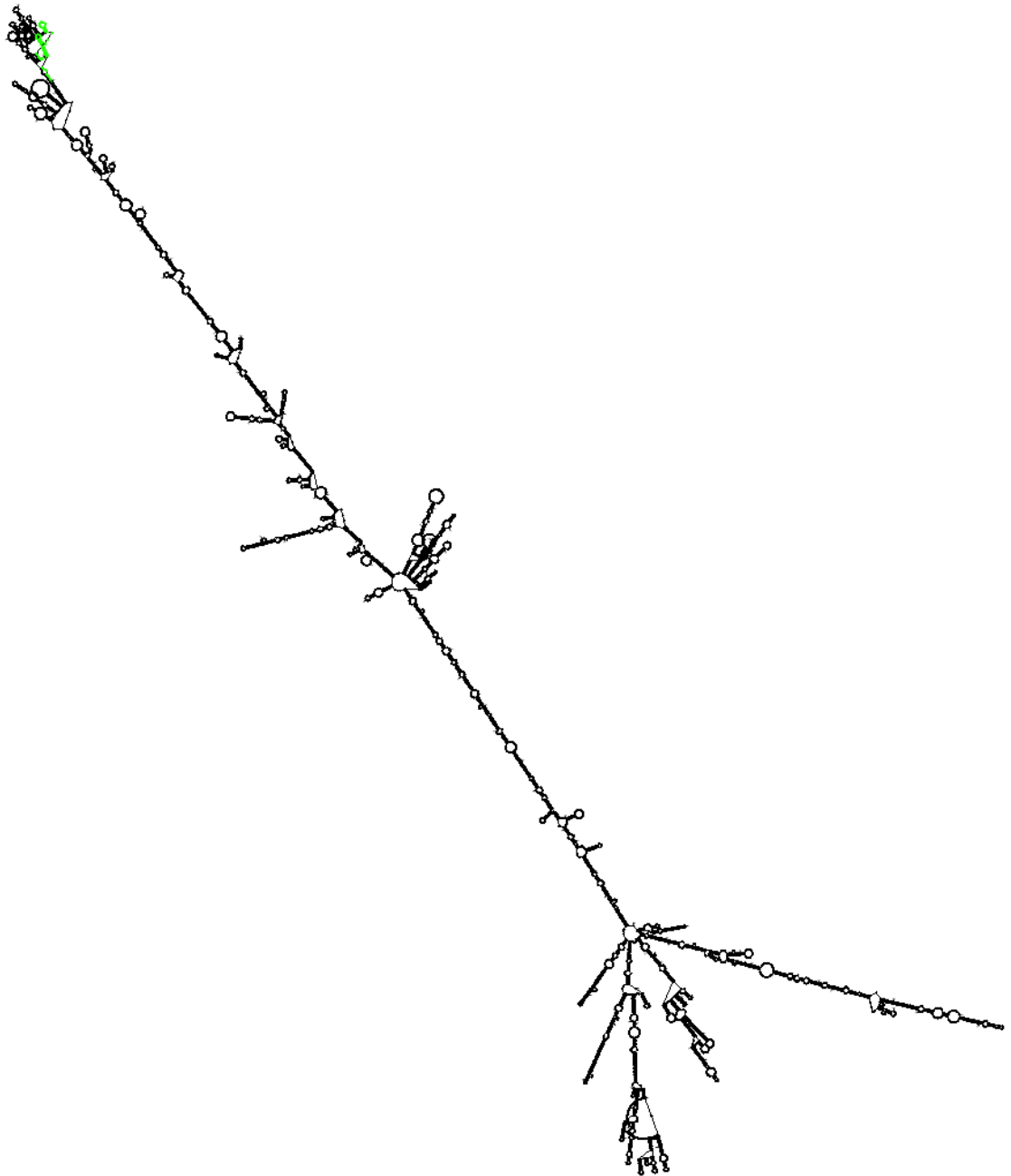
[†]The inverse of the molecular weight (Mw) is the number of moles of template present in one gram of material. By multiplying the moles/gram by Avogadro's number, 6.023E+23 molecules/mole, the number of template molecules per gram can be calculated. The number of template molecules in the sample can be estimated by multiplying copies/gram by 1.0E+09 to convert to ng and multiplying by the amount of template (ng) [393].

9.2 Appendix 2 -Endogenous and ERCC Transcript Predicted Secondary Structures

Output of sir_graph (©)
mfold_util 4.8

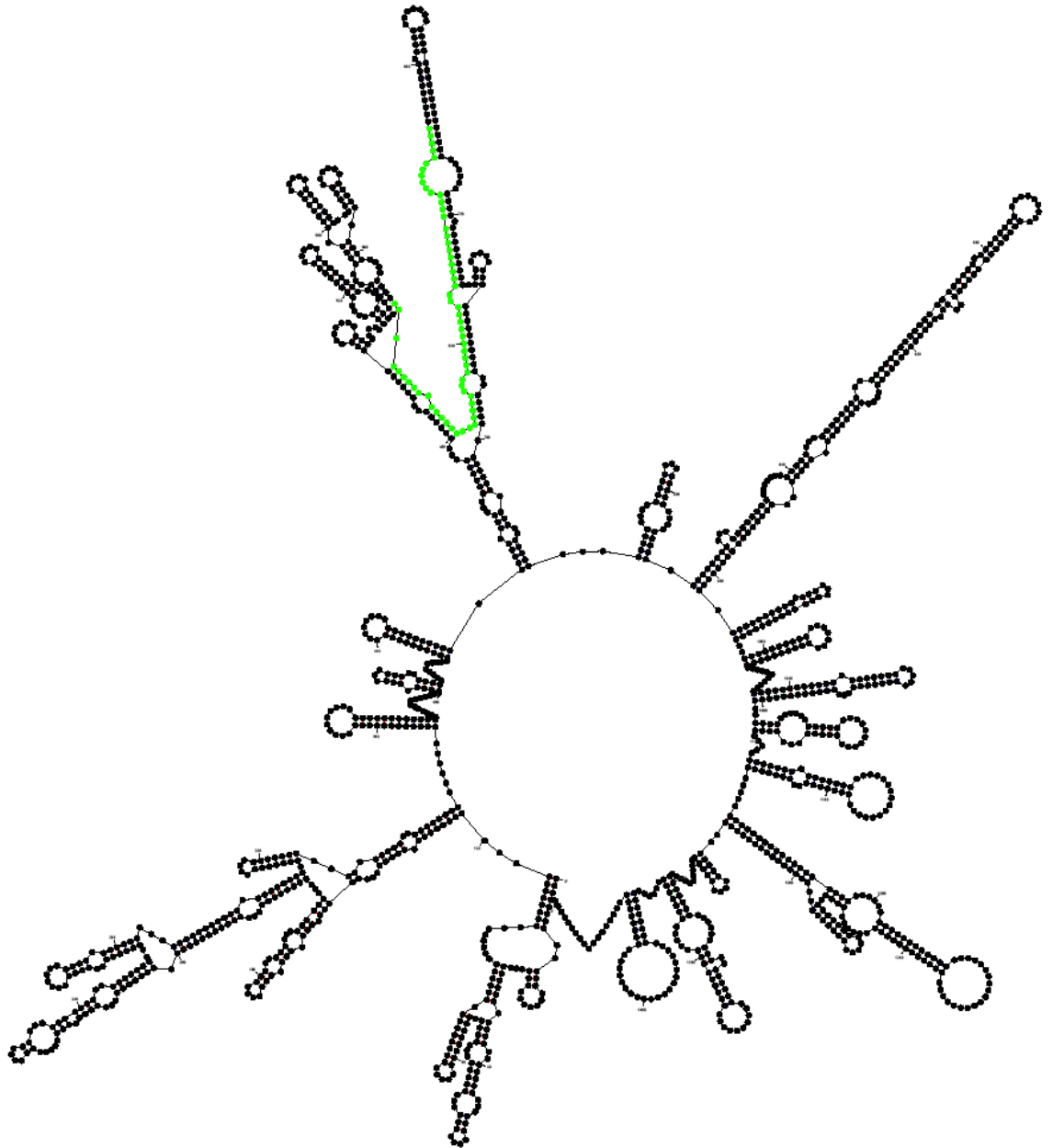
Created Tue Dec 4 12:00:18 2012

A



dG = -930.15 CASC3

B

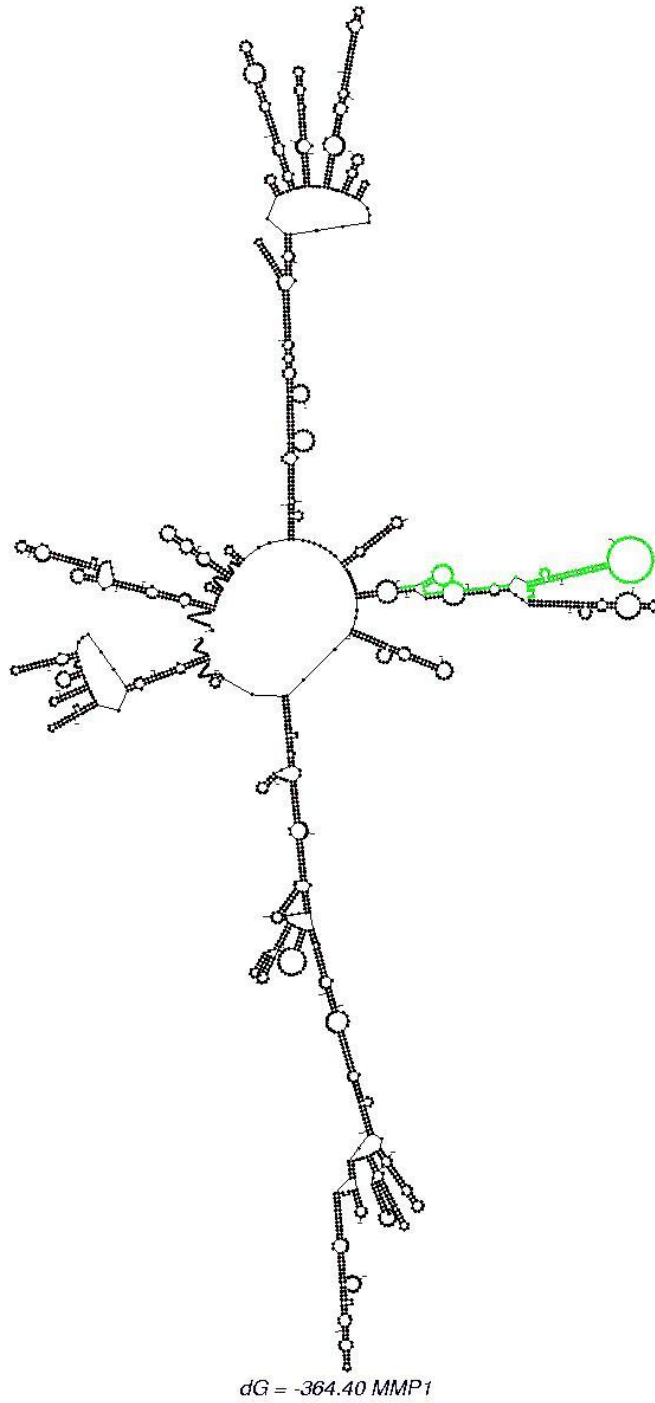


$dG = -251.25$ HPRT1

Output of air_graph (9)
mfold_util 4.6

Created Tue Dec 4 11:54:26 2012

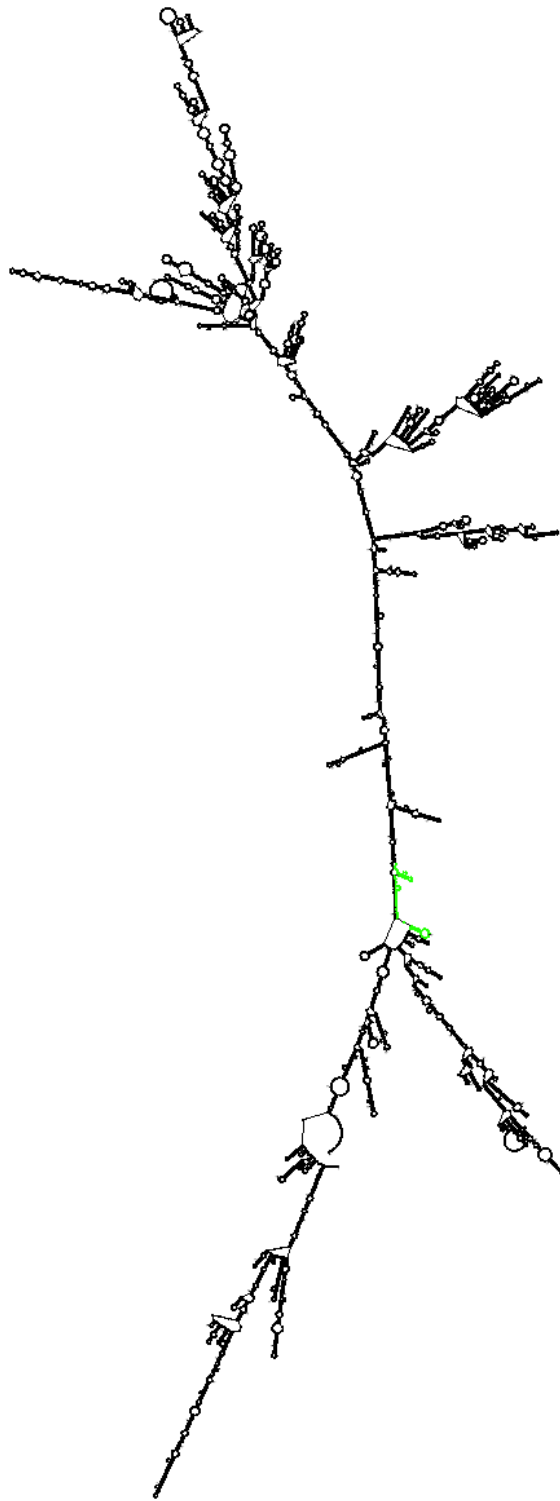
C



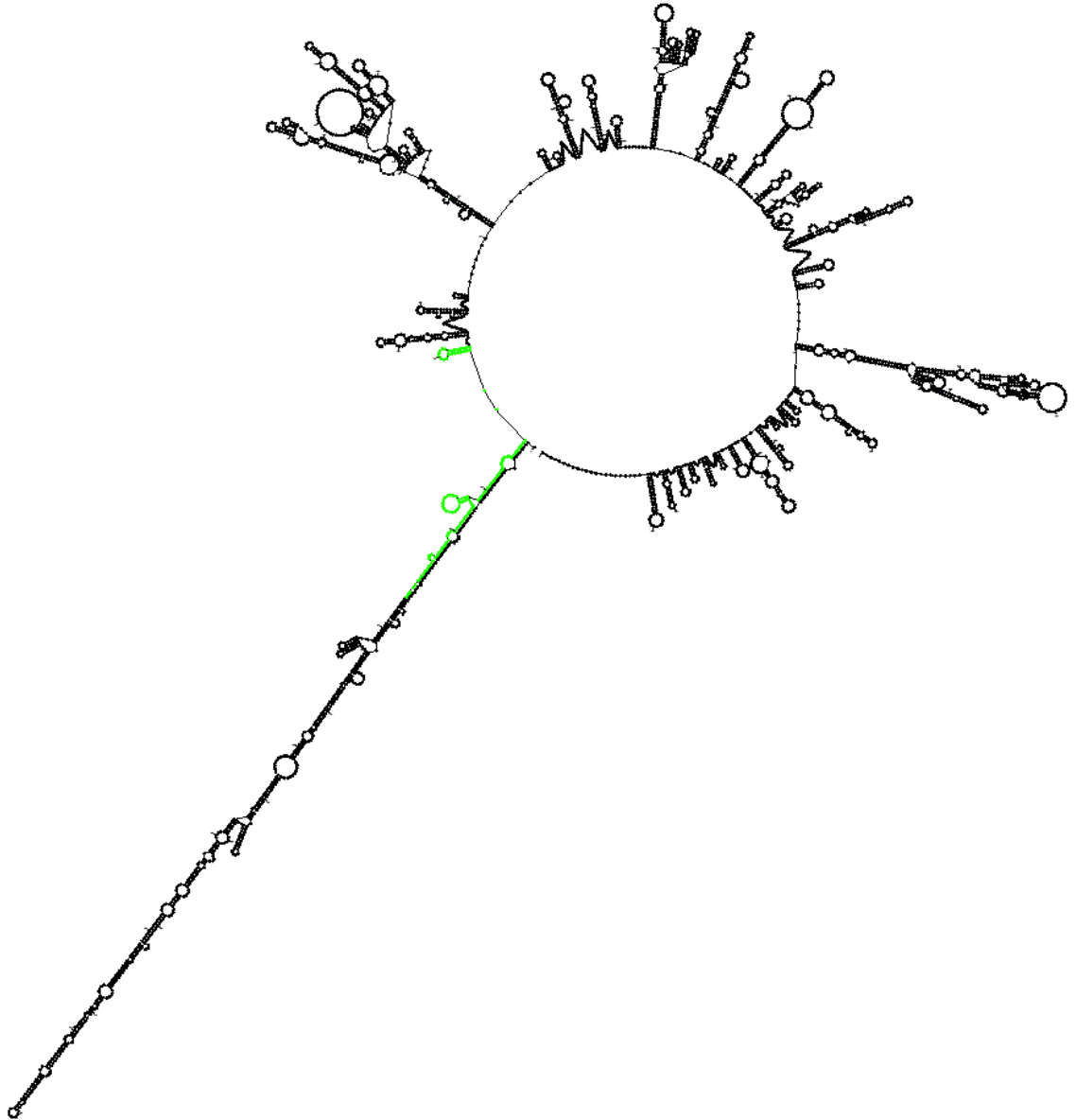
Output of sir_graph (0)
mfold_util 4.6

Created Tue Dec 4 12:58:33 2012

D



E

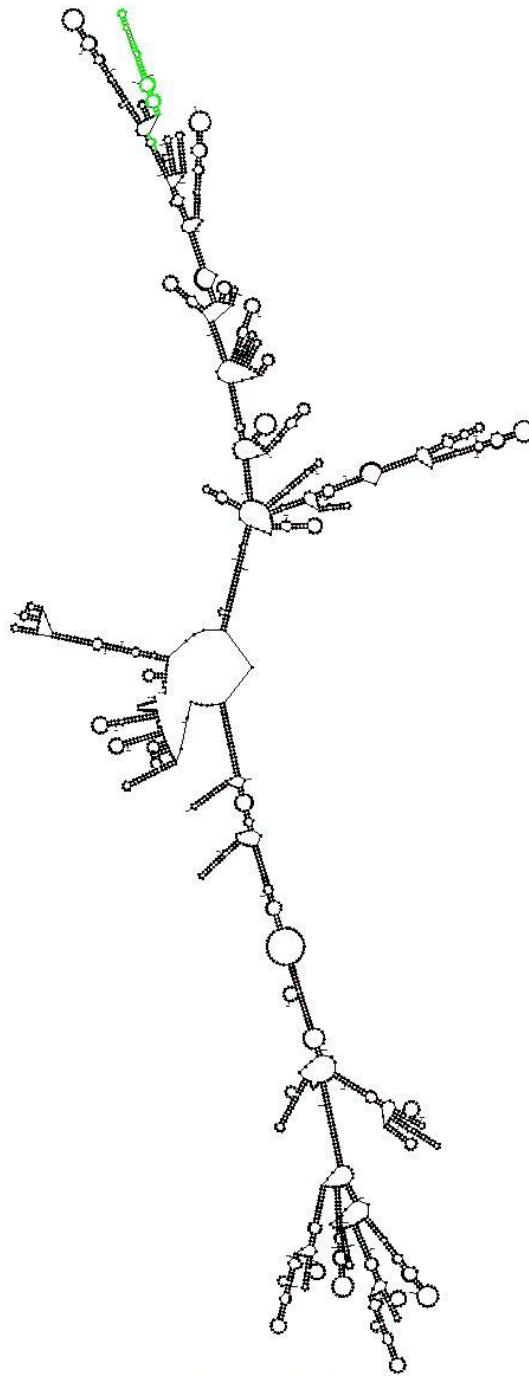


$dG = -571.60$ SLC1A3

Output of air_graph (G)
mfold_util 4.6

Created Tue Dec 4 11:57:46 2012

F

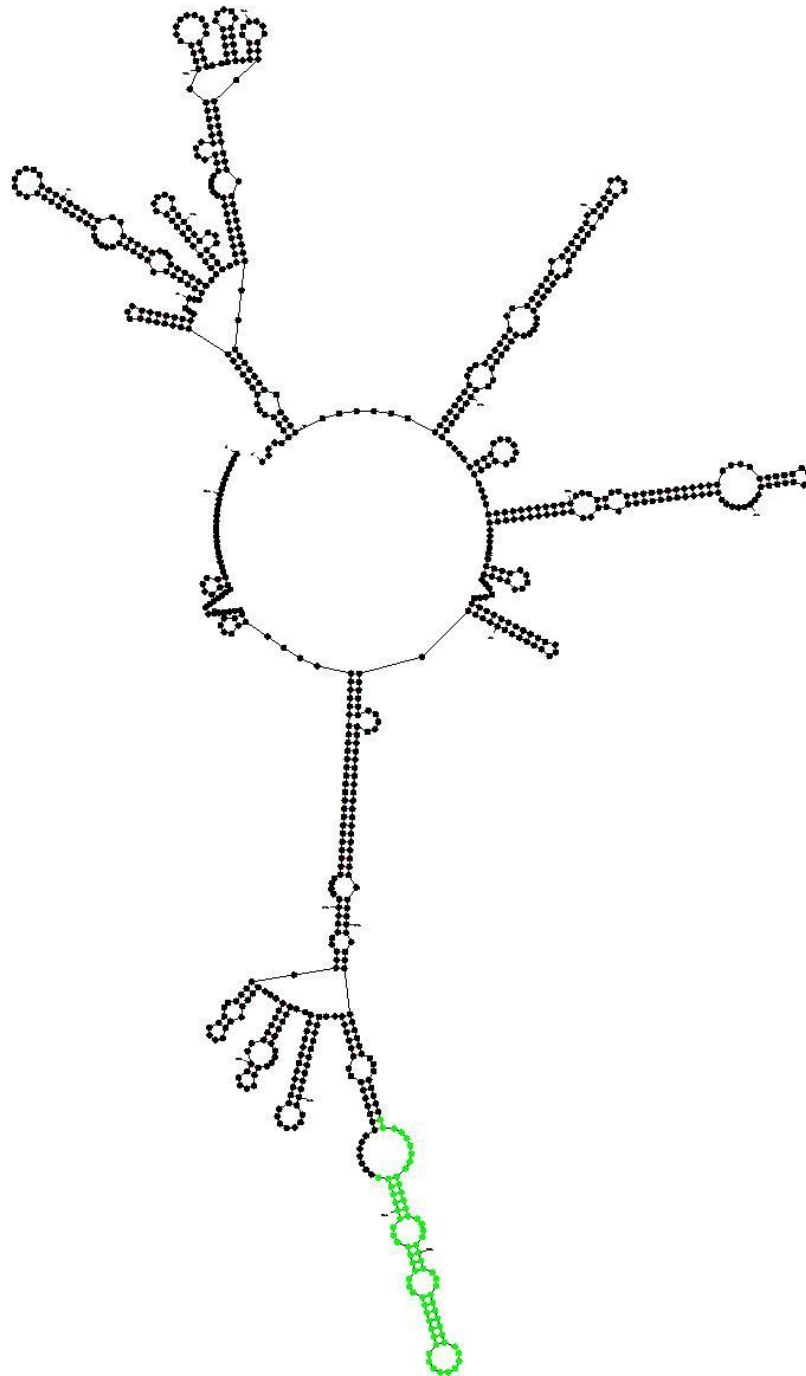


dG = -533.49 UBC

Output of air_graph (G)
mfold_util 4.6

Created Tue Dec 4 11:57:51 2012

G

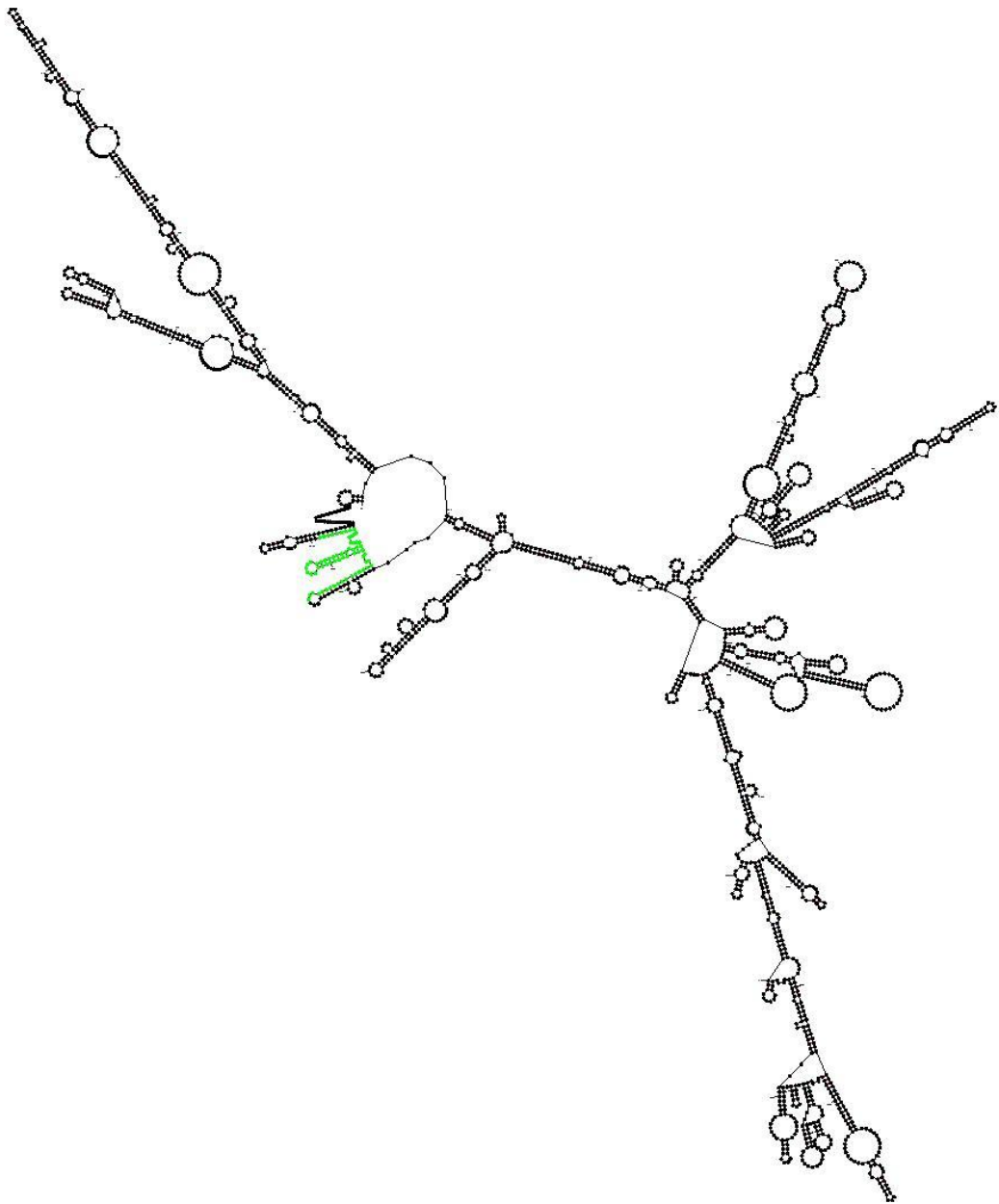


dG = -149.53 ERCC-13

Output of air_graph (G)
mfold_util 4.6

Created Tue Dec 4 12:00:32 2012

H



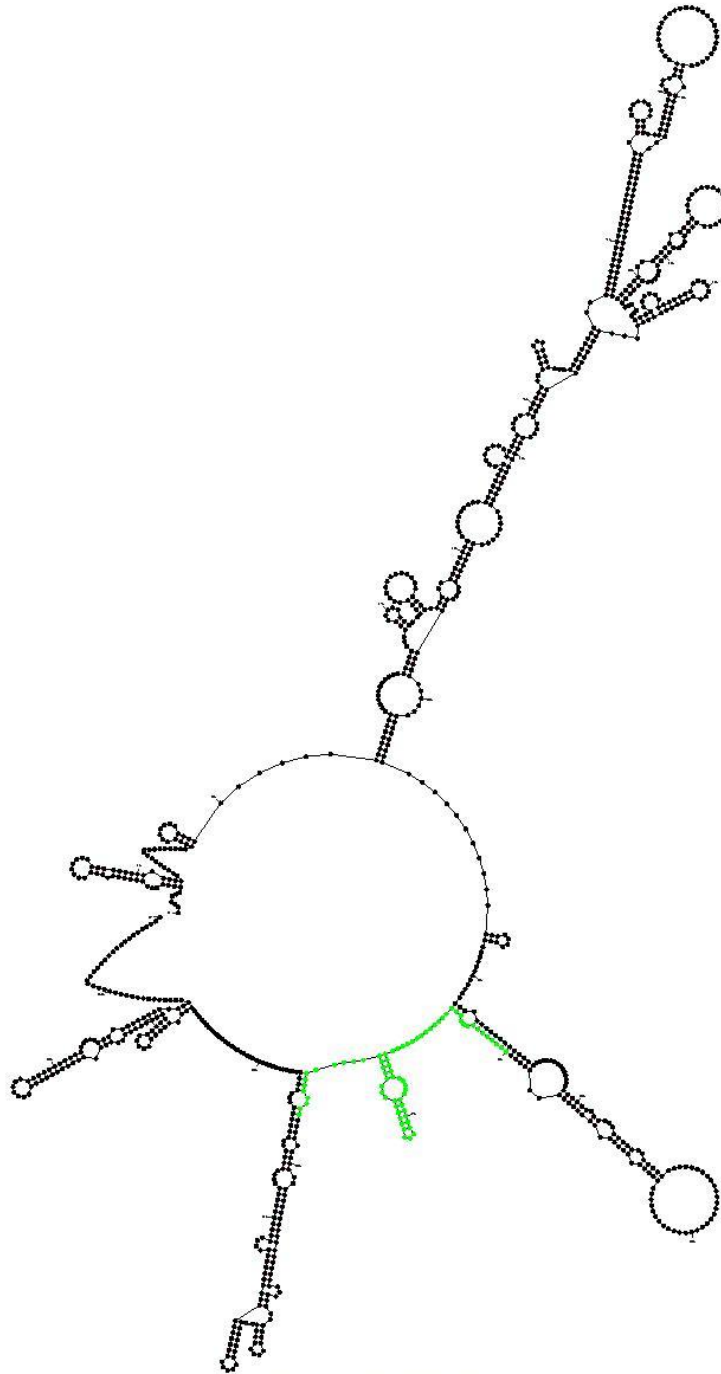
$dG = -395.33$ ERCC-25

Chapter 9 Appendices

Output of air_graph (G)
mfold_util 4.6

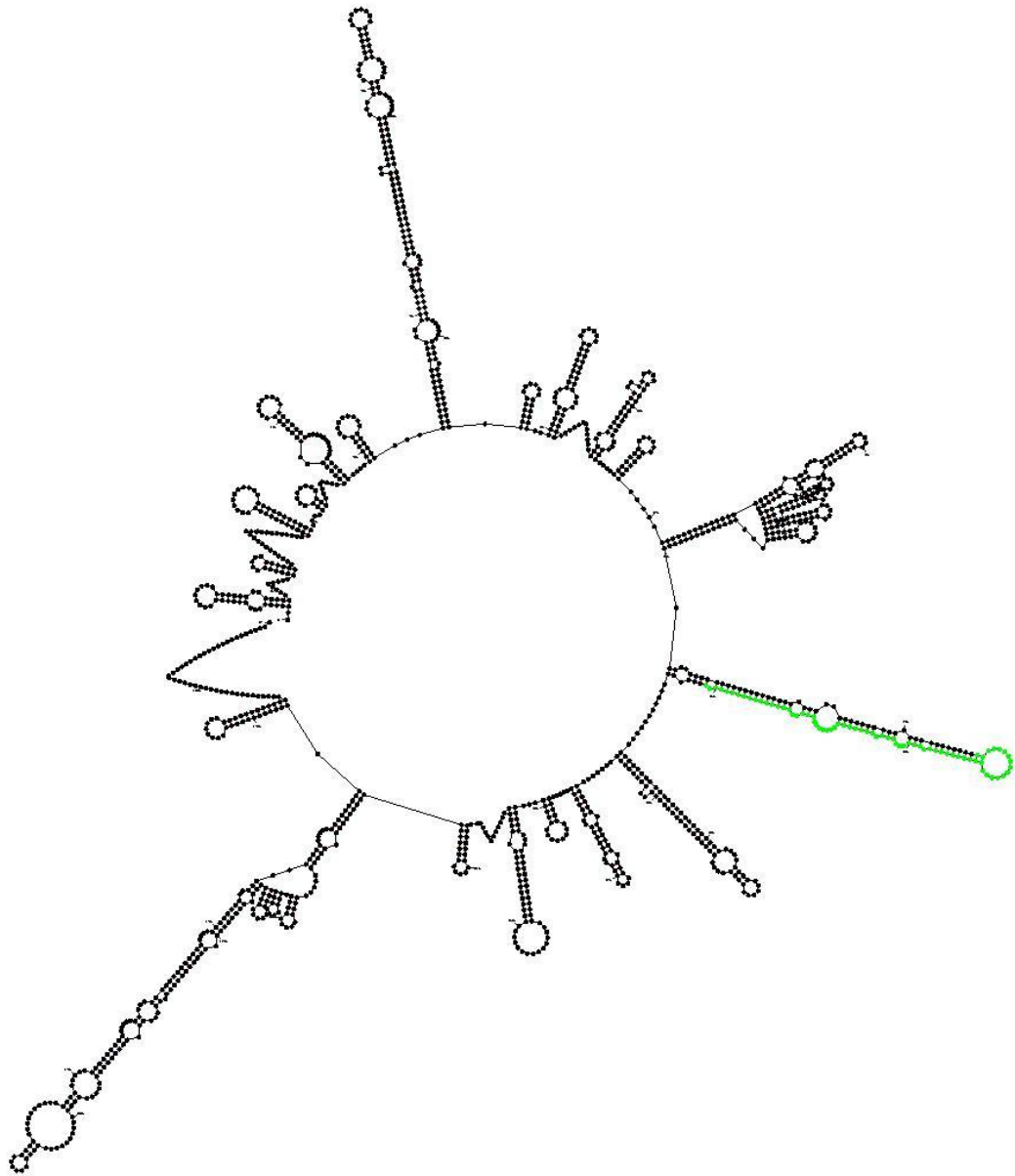
Created Tue Dec 4 11:59:44 2012

I



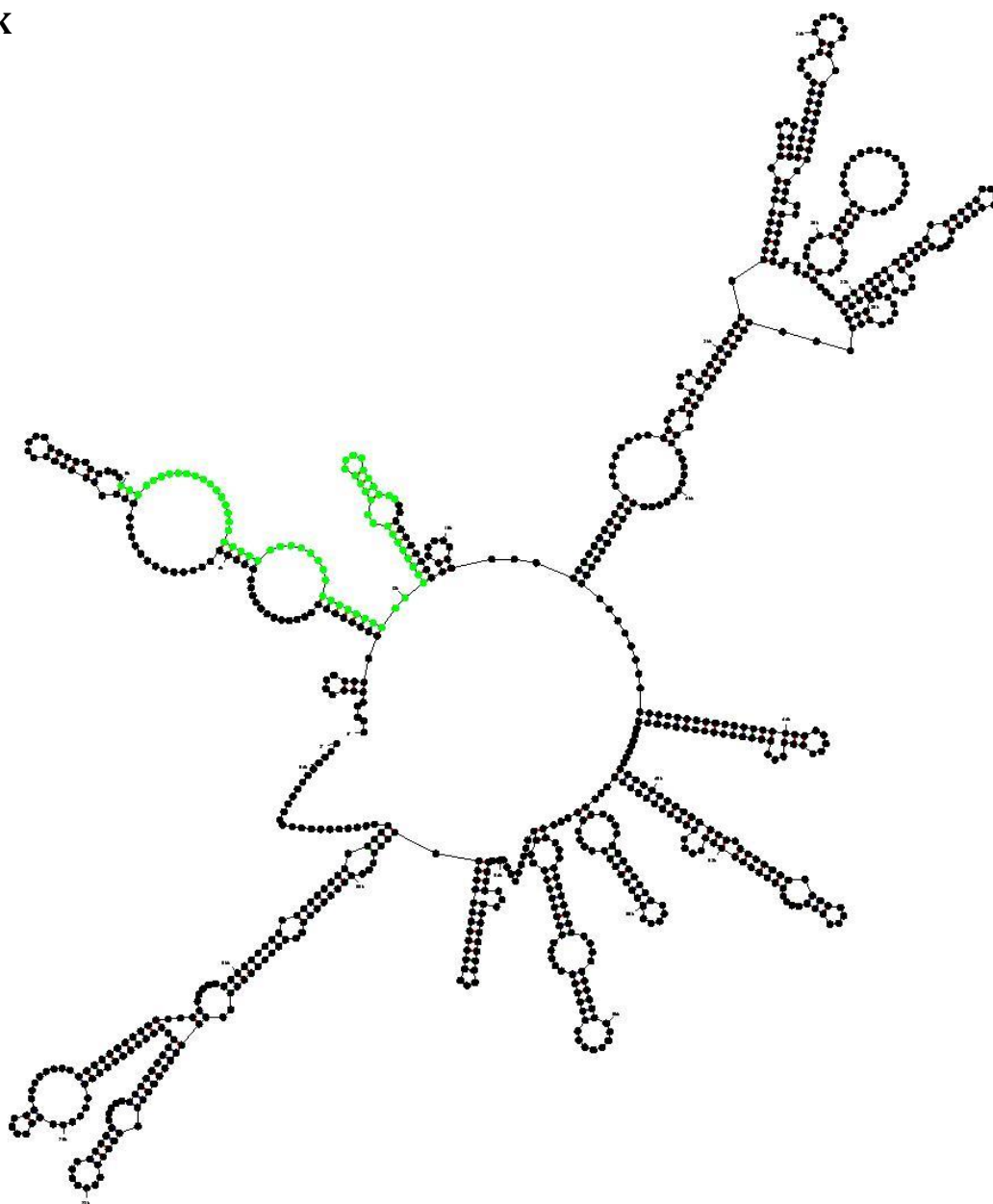
$dG = -153.33$ ERCC-42

J



$dG = -239.52$ ERCC-99

K



dG = -170.25 ERCC-113

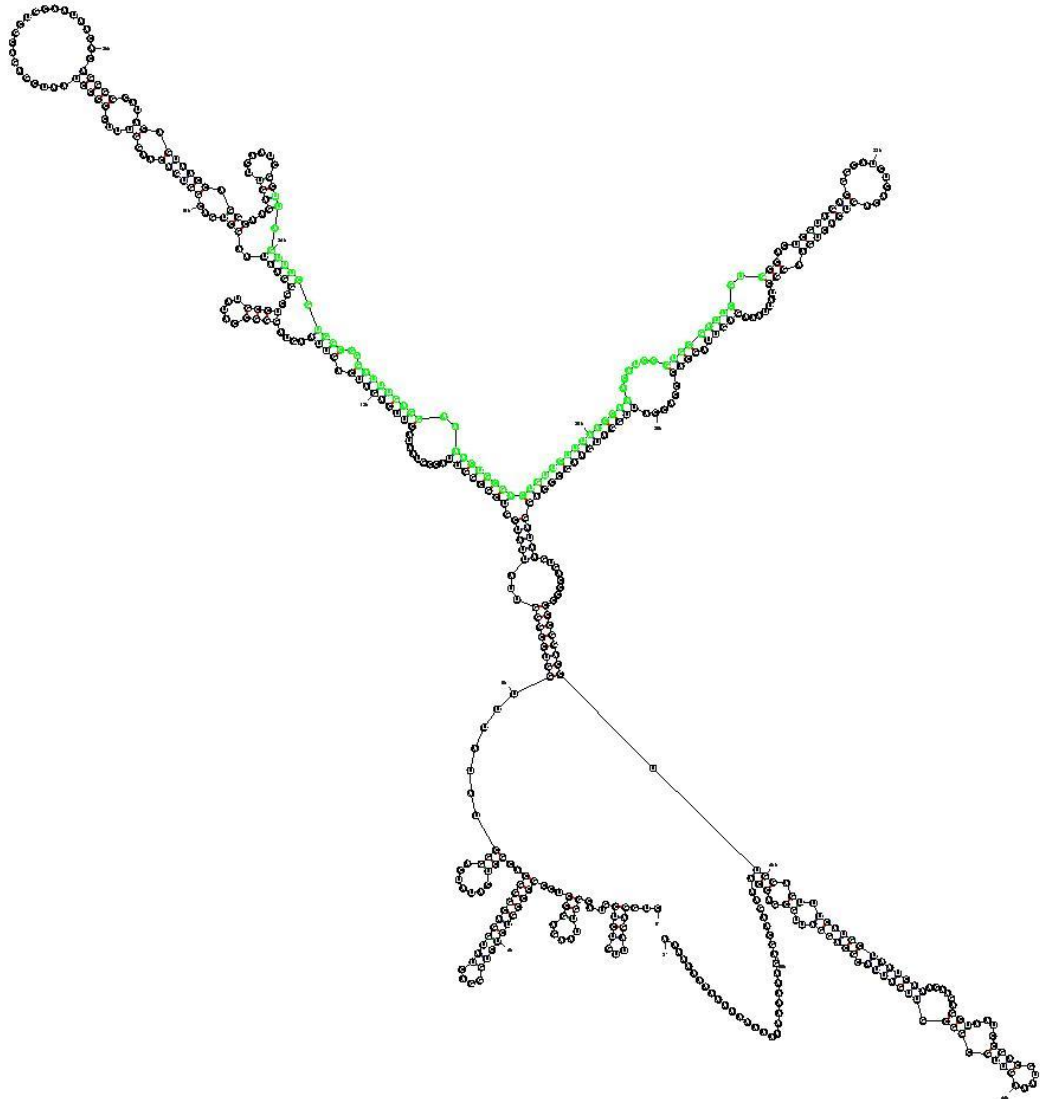
L $dG = -89.66$ ERCC-171

Figure 9.1 RNA Secondary Structure Predictions from mFold. (A) CASC3, (B) HPRT1, (C) MMP1, (D) NES, (E) SLC1A3, (F) UBC, (G) ERCC-13, (H) ERCC-25, (I) ERCC-42, (J) ERCC-99, (K) ERCC-113 and (L) ERCC-171. Green highlighted regions indicate amplicon. Folding predictions were performed at 45°C (temperature of RT step). Structures discussed in **4.3.5 Causes of Differing RT-dPCR Results.**

9.3 Appendix 3 – Measurement Uncertainty Budgets

Table 9.7 Calculation of Calibrant assigned value and measurement uncertainty. u = standard uncertainty, $u'=(u/x)$ = relative standard uncertainty. *Relative to assigned value for additive contributions. **Volumetric Identifiers (equipment:nearest specified volume). 25k denotes $25 \times 1000 \mu\text{L}$.

ERCC-13

	Term	Value x	u	$u'=(u/x)^*$	Remark**
Stock	Estimated stock value (cp)	1.018E+12	2.37E+10	0.023	Nanodrop. u based on observed precision with allowance for between-day effect
Nanodrop Calibration	Nanodrop Calibration (cp)	0	3.94E+04	0.042	Effect modelled as additive correction to final value: Estimated uncertainty based on observed Nanodrop relative bias [394]; Uncertainty (u) calculated as Relative standard uncertainty (RSSu) [395]
Material integrity:					
Impurity	Estimated purity (mass fraction basis)	0.948	0.05961	0.063	Taken from purity assessment. Note that for some ERCC targets purity is taken as 100% with nominal 1% u
Homogeneity	Homogeneity (cp)	0	6.6E+04	0.070	Max observed s[bb]
Stability	Stability	0	0	n/a	No allowance made
Volumetric: (Based on manufacturer's specifications)					
Step 1: Dilution to 1E+11 c/ μL	Aliquot (μL)	5	0.1	0.012	P10:10
	Diluted with (μL) RSS	45.91	0.2	0.005	P100:50
Step 2: Dilution to 1E+9 c/ μL	Aliquot (μL)	5	0.1	0.012	P10:10
	Diluted with (μL) RSS	495	2.4	0.005	P1000:500
Step 4: Mixing of ERCC solutions to prepare 100 \times ERCC solution	Aliquot (μL)	150	0.9	0.006	P200:200
	Diluted with (μL) RSS	600	2.4	0.004	P1000:500
	Diluted with (μL) ERCC-25	150	0.9	0.006	P200:200
	Diluted with (μL) ERCC-42	150	0.9	0.006	P200:200
	Diluted with (μL) ERCC-99	150	0.9	0.006	P200:200
	Diluted with (μL) ERCC-113	150	0.9	0.006	P200:200
Step 5: Preparation of units: Mixing of 100 \times ERCC and Cell line solutions	Aliquot (μL)	367.5	2.4	0.006	P1000:500
	Diluted with (μL) Hep-G2	5000.00	17.8	0.004	P5000:5000
	Diluted with (μL) Hep-G2	549.25	2.4	0.004	P1000:500
	Diluted with (μL) SaOS-2	735.00	2.4	0.003	P1000:500
	Diluted with (μL) Hs683	1000	4.7	0.005	P1000:1000
	Diluted with (μL) Hs683	506.75	2.4	0.005	P1000:500
	Diluted with (μL) RSS	25000	87.1	0.003	P5000:25k
	Diluted with (μL) RSS	1000	4.7	0.005	P1000:1000
	Diluted with (μL) RSS	1000	4.7	0.005	P1000:1000
	Diluted with (μL) RSS	1000	4.7	0.005	P1000:1000
	Diluted with (μL) RSS	591.5	2.4	0.004	P1000:500
	Assigned value (cp):	9.48E+05	1.0E+05	1.07E-01	
	Expanded uncertainty		2.0E+05	2.15E-01	

Chapter 9 Appendices

ERCC-25

Factor	Term	Value x	u	u'=(u/x)*	Remark**
Stock	Estimated stock value (cp)	4.020E+11	9.72E+09	0.024	See Appendix 3, Table 9.7 , ERCC-13
Nanodrop Calibration	Nanodrop Calibration (cp)	0	4.15E+04	0.042	See Appendix 3, Table 9.7 , ERCC-13
Material integrity:					
Impurity	Estimated purity (mass fraction basis)	1.000	0.00999	0.010	See Appendix 3, Table 9.7 , ERCC-13
Homogeneity	Homogeneity (cp)	0	7.0E+04	0.070	See Appendix 3, Table 9.7 , ERCC-13
Stability	Stability	0	0	n/a	No allowance made
Volumetric: (Based on manufacturer's specifications)					
Step 1: Dilution to 1E+11 c/μL	Aliquot (μL)	5	0.1	0.012	P10:10
	Diluted with (μL) RSS	15.1	0.1	0.004	P20:10
Step 2: Dilution to 1E+9 c/μL	Aliquot (μL)	5	0.1	0.012	P10:10
	Diluted with (μL) RSS	495	2.4	0.005	P1000:500
Step 4: Mixing of ERCC solutions to prepare 100× ERCC solution	Aliquot (μL)	150	0.9	0.006	P200:200
	Diluted with (μL) RSS	600	2.4	0.004	P1000:500
	Diluted with (μL) ERCC-13	150	0.9	0.006	P200:200
	Diluted with (μL) ERCC-42	150	0.9	0.006	P200:200
	Diluted with (μL) ERCC-99	150	0.9	0.006	P200:200
	Diluted with (μL) ERCC-113	150	0.9	0.006	P200:200
Step 5: Preparation of units: Mixing of 100× ERCC and Cell line solutions	Diluted with (μL) ERCC-171	150	0.9	0.006	P200:200
	Aliquot (μL)	367.5	2.4	0.006	P1000:500
	Diluted with (μL) Hep-G2	5000.00	17.8	0.004	P5000:5000
	Diluted with (μL) Hep-G2	549.25	2.4	0.004	P1000:500
	Diluted with (μL) SaOS-2	735.00	2.4	0.003	P1000:500
	Diluted with (μL) Hs683	1000	4.7	0.005	P1000:1000
	Diluted with (μL) Hs683	506.75	2.4	0.005	P1000:500
	Diluted with (μL) RSS	25000	87.1	0.003	P5000:25k
	Diluted with (μL) RSS	1000	4.7	0.005	P1000:1000
	Diluted with (μL) RSS	1000	4.7	0.005	P1000:1000
	Diluted with (μL) RSS	1000	4.7	0.005	P1000:1000
	Diluted with (μL) RSS	591.5	2.4	0.004	P1000:500
	Assigned value (cp):	1.00E+06	8.7E+04	8.75E-02	
	Expanded uncertainty		1.7E+05	1.75E-01	

Chapter 9 Appendices

ERCC-42

Factor	Term	Value x	u	u'=(u/x)*	Remark**
Stock	Estimated stock value (cp)	7.305E+11	1.71E+10	0.023	See Appendix 3, Table 9.7 , ERCC-13
Nanodrop Calibration	Nanodrop Calibration (cp)	0	4.15E+04	0.042	See Appendix 3, Table 9.7 , ERCC-13
Material integrity:					
Impurity	Estimated purity (mass fraction basis)	1.000	0.00999	0.010	See Appendix 3, Table 9.7 , ERCC-13
Homogeneity	Homogeneity (cp)	0	7.0E+04	0.070	See Appendix 3, Table 9.7 , ERCC-13
Stability	Stability	0	0	n/a	No allowance made
Volumetric: (Based on manufacturer's specifications)					
Step 1: Dilution to 1E+11 c/μL	Aliquot (μL)	5	0.1	0.012	P10:10
	Diluted with (μL) RSS	31.52	0.2	0.008	P100:50
Step 2: Dilution to 1E+9 c/μL	Aliquot (μL)	5	0.1	0.012	P10:10
	Diluted with (μL) RSS	495	2.4	0.005	P1000:500
Step 4: Mixing of ERCC solutions to prepare 100× ERCC solution	Aliquot (μL)	150	0.9	0.006	P200:200
	Diluted with (μL) RSS	600	2.4	0.004	P1000:500
	Diluted with (μL) ERCC-13	150	0.9	0.006	P200:200
	Diluted with (μL) ERCC-25	150	0.9	0.006	P200:200
	Diluted with (μL) ERCC-99	150	0.9	0.006	P200:200
	Diluted with (μL) ERCC-113	150	0.9	0.006	P200:200
Step 5: Preparation of units: Mixing of 100× ERCC and Cell line solutions	Aliquot (μL)	367.5	2.4	0.006	P1000:500
	Diluted with (μL) Hep-G2	5000.00	17.8	0.004	P5000:5000
	Diluted with (μL) Hep-G2	549.25	2.4	0.004	P1000:500
	Diluted with (μL) SaOS-2	735.00	2.4	0.003	P1000:500
	Diluted with (μL) Hs683	1000	4.7	0.005	P1000:1000
	Diluted with (μL) Hs683	506.75	2.4	0.005	P1000:500
	Diluted with (μL) RSS	25000	87.1	0.003	P5000:25k
	Diluted with (μL) RSS	1000	4.7	0.005	P1000:1000
	Diluted with (μL) RSS	1000	4.7	0.005	P1000:1000
	Diluted with (μL) RSS	1000	4.7	0.005	P1000:1000
	Diluted with (μL) RSS	591.5	2.4	0.004	P1000:500
	Assigned value (cp):	1.00E+06	8.8E+04	8.76E-02	
	Expanded uncertainty		1.8E+05	1.75E-01	

Chapter 9 Appendices

ERCC-99

Factor	Term	Value x	u	u'=(u/x)*	Remark**
Stock	Estimated stock value (cp)	5.559E+11	1.42E+10	0.026	See Appendix 3, Table 9.7 , ERCC-13
Nanodrop Calibration	Nanodrop Calibration (cp)	0	4.10E+04	0.042	See Appendix 3, Table 9.7 , ERCC-13
Material integrity:					
Impurity	Estimated purity (mass fraction basis)	0.986	0.00999	0.010	See Appendix 3, Table 9.7 , ERCC-13
Homogeneity	Homogeneity (cp)	0	6.9E+04	0.070	See Appendix 3, Table 9.7 , ERCC-13
Stability	Stability	0	0	n/a	No allowance made
Volumetric: (Based on manufacturer's specifications)					
Step 1: Dilution to 1E+11 c/μL	Aliquot (μL)	5	0.1	0.012	P10:10
	Diluted with (μL) RSS	22.79	0.2	0.010	P100:50
Step 2: Dilution to 1E+9 c/μL	Aliquot (μL)	5	0.1	0.012	P10:10
	Diluted with (μL) RSS	495	2.4	0.005	P1000:500
Step 4: Mixing of ERCC solutions to prepare 100× ERCC solution	Aliquot (μL)	150	0.9	0.006	P200:200
	Diluted with (μL) RSS	600	2.4	0.004	P1000:500
	Diluted with (μL) ERCC-13	150	0.9	0.006	P200:200
	Diluted with (μL) ERCC-25	150	0.9	0.006	P200:200
	Diluted with (μL) ERCC-42	150	0.9	0.006	P200:200
	Diluted with (μL) ERCC-113	150	0.9	0.006	P200:200
Step 5: Preparation of units: Mixing of 100× ERCC and Cell line solutions	Aliquot (μL)	367.5	2.4	0.006	P1000:500
	Diluted with (μL) Hep-G2	5000.00	17.8	0.004	P5000:5000
	Diluted with (μL) Hep-G2	549.25	2.4	0.004	P1000:500
	Diluted with (μL) SaOS-2	735.00	2.4	0.003	P1000:500
	Diluted with (μL) Hs683	1000	4.7	0.005	P1000:1000
	Diluted with (μL) Hs683	506.75	2.4	0.005	P1000:500
	Diluted with (μL) RSS	25000	87.1	0.003	P5000:25k
	Diluted with (μL) RSS	1000	4.7	0.005	P1000:1000
	Diluted with (μL) RSS	1000	4.7	0.005	P1000:1000
	Diluted with (μL) RSS	1000	4.7	0.005	P1000:1000
	Diluted with (μL) RSS	591.5	2.4	0.004	P1000:500
	Assigned value (cp):	9.86E+05	8.7E+04	8.84E-02	
	Expanded uncertainty		1.7E+05	1.77E-01	

Chapter 9 Appendices

ERCC-113

Factor	Term	Value x	u	u'=(u/x)*	Remark**
Stock	Estimated stock value (cp)	1.807E+12	4.16E+10	0.023	See Appendix 3, Table 9.7 , ERCC-13
Nanodrop Calibration	Nanodrop Calibration (cp)	0	3.90E+04	0.042	See Appendix 3, Table 9.7 , ERCC-13
Material integrity:					
Impurity	Estimated purity (mass fraction basis)	0.938	0.03225	0.034	See Appendix 3, Table 9.7 , ERCC-13
Homogeneity	Homogeneity (cp)	0	6.6E+04	0.070	See Appendix 3, Table 9.7 , ERCC-13
Stability	Stability	0	0	n/a	No allowance made
Volumetric: (Based on manufacturer's specifications)					
Step 1: Dilution to 1E+11 c/μL	Aliquot (μL)	5	0.1	0.012	P10:10
	Diluted with (μL) RSS	85.34	0.5	0.005	P100:100
Step 2: Dilution to 1E+9 c/μL	Aliquot (μL)	5	0.1	0.012	P10:10
	Diluted with (μL) RSS	495	2.4	0.005	P1000:500
Step 4: Mixing of ERCC solutions to prepare 100× ERCC solution	Aliquot (μL)	150	0.9	0.006	P200:200
	Diluted with (μL) RSS	600	2.4	0.004	P1000:500
	Diluted with (μL) ERCC-13	150	0.9	0.006	P200:200
	Diluted with (μL) ERCC-25	150	0.9	0.006	P200:200
	Diluted with (μL) ERCC-42	150	0.9	0.006	P200:200
	Diluted with (μL) ERCC-99	150	0.9	0.006	P200:200
Step 5: Preparation of units: Mixing of 100× ERCC and Cell line solutions	Aliquot (μL)	367.5	2.4	0.006	P1000:500
	Diluted with (μL) Hep-G2	5000.00	17.8	0.004	P5000:5000
	Diluted with (μL) Hep-G2	549.25	2.4	0.004	P1000:500
	Diluted with (μL) SaOS-2	735.00	2.4	0.003	P1000:500
	Diluted with (μL) Hs683	1000	4.7	0.005	P1000:1000
	Diluted with (μL) Hs683	506.75	2.4	0.005	P1000:500
	Diluted with (μL) RSS	25000	87.1	0.003	P5000:25k
	Diluted with (μL) RSS	1000	4.7	0.005	P1000:1000
	Diluted with (μL) RSS	1000	4.7	0.005	P1000:1000
	Diluted with (μL) RSS	1000	4.7	0.005	P1000:1000
	Diluted with (μL) RSS	591.5	2.4	0.004	P1000:500
	Assigned value (cp):	9.38E+05	8.8E+04	9.35E-02	
	Expanded uncertainty		1.8E+05	1.87E-01	

Chapter 9 Appendices

ERCC-171

Factor	Term	Value x	u	u'=(u/x)*	Remark**
Stock	Estimated stock value (cp)	1.421E+12	3.27E+10	0.023	See Appendix 3, Table 9.7 , ERCC-13
Nanodrop Calibration	Nanodrop Calibration (cp)	0	3.90E+04	0.042	See Appendix 3, Table 9.7 , ERCC-13
Material integrity:					
Impurity	Estimated purity (mass fraction basis)	0.939	0.03607	0.038	See Appendix 3, Table 9.7 , ERCC-13
Homogeneity	Homogeneity (cp)	0	6.6E+04	0.070	See Appendix 3, Table 9.7 , ERCC-13
Stability	Stability	0	0	n/a	No allowance made
Volumetric: (Based on manufacturer's specifications)					
Step 1: Dilution to 1E+11 c/μL	Aliquot (μL)	5	0.1	0.012	P10:10
	Diluted with (μL) RSS	66.05	0.2	0.004	P100:50
Step 2: Dilution to 1E+9 c/μL	Aliquot (μL)	5	0.1	0.012	P10:10
	Diluted with (μL) RSS	495	2.4	0.005	P1000:500
Step 4: Mixing of ERCC solutions to prepare 100× ERCC solution	Aliquot (μL)	150	0.9	0.006	P200:200
	Diluted with (μL) RSS	600	2.4	0.004	P1000:500
	Diluted with (μL) ERCC-13	150	0.9	0.006	P200:200
	Diluted with (μL) ERCC-25	150	0.9	0.006	P200:200
	Diluted with (μL) ERCC-42	150	0.9	0.006	P200:200
	Diluted with (μL) ERCC-99	150	0.9	0.006	P200:200
Step 5: Preparation of units: Mixing of 100× ERCC and Cell line solutions	Aliquot (μL)	367.5	2.4	0.006	P1000:500
	Diluted with (μL) Hep-G2	5000.00	17.8	0.004	P5000:5000
	Diluted with (μL) Hep-G2	549.25	2.4	0.004	P1000:500
	Diluted with (μL) SaOS-2	735.00	2.4	0.003	P1000:500
	Diluted with (μL) Hs683	1000	4.7	0.005	P1000:1000
	Diluted with (μL) Hs683	506.75	2.4	0.005	P1000:500
	Diluted with (μL) RSS	25000	87.1	0.003	P5000:25k
	Diluted with (μL) RSS	1000	4.7	0.005	P1000:1000
	Diluted with (μL) RSS	1000	4.7	0.005	P1000:1000
	Diluted with (μL) RSS	1000	4.7	0.005	P1000:1000
	Diluted with (μL) RSS	591.5	2.4	0.004	P1000:500
	Assigned value (cp):	9.39E+05	8.9E+04	9.50E-02	
	Expanded uncertainty		1.8E+05	1.90E-01	

Chapter 9 Appendices



Figure 9.2 Calibrant Unit Measurement Uncertainty Contributing Factors. Purity assessment based on multiple banding (Bioanalyzer).

Table 9.8 Calculation of Unknown 1 assigned value and measurement uncertainty. Measurement uncertainty components common to both Unknown 1 and Unknown 2 are not included in corresponding uncertainty budgets as these contributions cancel out in measurement of combined standard uncertainty of assigned ratios.

ERCC-13

Factor	Term	Value x	u	u'=(u/x)*	Remark**
Stock	Estimated stock value (cp)	1.018E+12	0.00E+00	0.000	See Appendix 3, Table 9.7 , ERCC-13
Nanodrop Calibration	Nanodrop Calibration (cp)	0	0.00E+00	0.042	See Appendix 3, Table 9.7 , ERCC-13
Material integrity:					
Impurity	Estimated purity (mass fraction basis)	0.948	0.00000	0.000	See Appendix 3, Table 9.7 , ERCC-13
Homogeneity	Homogeneity (cp)	0	4.0E+03	0.070	See Appendix 3, Table 9.7 , ERCC-13
Stability	Stability	0	0	n/a	No allowance made
Volumetric: (Based on manufacturer's specifications)					
Step 1: Dilution to 1E+11 c/μL	Aliquot (μL)	5	0.0	0.000	P10:10
	Diluted with (μL) RSS	45.91	0.0	0.000	P100:50
Step 2: Dilution to 1E+9 c/μL	Aliquot (μL)	5	0.0	0.000	P10:10
	Diluted with (μL) RSS	495	0.0	0.000	P1000:500
Step 3: Dilution to 1E+8 c/μL	Aliquot (μL)	20	0.0	0.000	P20:10
	Diluted with (μL) RSS	180	0.0	0.000	P200:200
Step 4: Mixing of ERCC solutions to prepare 100× ERCC solution	Aliquot (μL)	90	0.5	0.005	P100:100
	Diluted with (μL) RSS	1000	4.7	0.005	P1000:1000
	Diluted with (μL) RSS	114.5	0.9	0.008	P200:200
	Diluted with (μL) ERCC-25	7.5	0.1	0.008	P10:10
	Diluted with (μL) ERCC-42	1.5	0.02	0.012	P2:2
	Diluted with (μL) ERCC-99	105	0.5	0.005	P200:100
	Diluted with (μL) ERCC-113	31.5	0.2	0.008	P100:50
Step 5: Preparation of units: Mixing of 100× ERCC and Cell line solutions	Diluted with (μL) ERCC-171	150	0.9	0.006	P200:200
	Aliquot (μL)	367.5	2.4	0.006	P1000:500
	Diluted with (μL) Hep-G2	4000.00	17.8	0.004	P5000:5000
	Diluted with (μL) Hep-G2	116	0.5	0.004	P200:100
	Diluted with (μL) SaOS-2	735.00	2.4	0.003	P1000:500
	Diluted with (μL) Hs683	2000	4.7	0.002	P1000:1000
	Diluted with (μL) Hs683	940	4.7	0.005	P1000:1000
	Diluted with (μL) RSS	25000	87.1	0.003	P5000:25k
	Diluted with (μL) RSS	1000	1.8	0.002	P1000:200
	Diluted with (μL) RSS	1000	1.8	0.002	P1000:200
	Diluted with (μL) RSS	1000	1.8	0.002	P1000:200
	Diluted with (μL) RSS	591.5	2.4	0.004	P1000:500
	Assigned value (cp):	5.69E+04	4.0E+03	7.06E-02	
	Expanded uncertainty		8.0E+03	1.41E-01	

Chapter 9 Appendices

ERCC-25

Factor	Term	Value x	u	u'=(u/x)*	Remark**
Stock	Estimated stock value (cp)	4.020E+11	0.00E+00	0.000	See Appendix 3, Table 9.7 , ERCC-13
Nanodrop Calibration	Nanodrop Calibration (cp)	0	0.00E+00	0.042	See Appendix 3, Table 9.7 , ERCC-13
Material integrity:					
Impurity	Estimated purity (mass fraction basis)	1.000	0.00000	0.000	See Appendix 3, Table 9.7 , ERCC-13
Homogeneity	Homogeneity (cp)	0	3.5E+02	0.070	See Appendix 3, Table 9.7 , ERCC-13
Stability	Stability	0	0	n/a	No allowance made
Volumetric: (Based on manufacturer's specifications)					
Step 1: Dilution to 1E+11 c/μL	Aliquot (μL)	5	0.0	0.000	P10:10
	Diluted with (μL) RSS	15.1	0.0	0.000	P20:10
Step 2: Dilution to 1E+9 c/μL	Aliquot (μL)	5	0.0	0.000	P10:10
	Diluted with (μL) RSS	495	0.0	0.000	P1000:500
Step 3: Dilution to 1E+8 c/μL	Aliquot (μL)	20	0.0	0.000	P20:10
	Diluted with (μL) RSS	180	0.0	0.000	P200:200
Step 4: Mixing of ERCC solutions to prepare 100× ERCC solution	Aliquot (μL)	7.5	0.1	0.008	P10:10
	Diluted with (μL) RSS	1000	4.7	0.005	P1000:1000
	Diluted with (μL) RSS	114.5	0.9	0.008	P200:200
	Diluted with (μL) ERCC-13	90	0.5	0.005	P100:100
	Diluted with (μL) ERCC-42	1.5	0.02	0.012	P2:2
	Diluted with (μL) ERCC-99	105	0.5	0.005	P200:100
	Diluted with (μL) ERCC-113	31.5	0.2	0.008	P100:50
Step 5: Preparation of units: Mixing of 100× ERCC and Cell line solutions	Diluted with (μL) ERCC-171	150	0.9	0.006	P200:200
	Aliquot (μL)	367.5	2.4	0.006	P1000:500
	Diluted with (μL) Hep-G2	4000.00	17.8	0.004	P5000:5000
	Diluted with (μL) Hep-G2	116	0.5	0.004	P200:100
	Diluted with (μL) SaOS-2	735.00	2.4	0.003	P1000:500
	Diluted with (μL) Hs683	2000	4.7	0.002	P1000:1000
	Diluted with (μL) Hs683	940	4.7	0.005	P1000:1000
	Diluted with (μL) RSS	25000	87.1	0.003	P5000:25k
	Diluted with (μL) RSS	1000	1.8	0.002	P1000:200
	Diluted with (μL) RSS	1000	1.8	0.002	P1000:200
	Diluted with (μL) RSS	1000	1.8	0.002	P1000:200
Diluted with (μL) RSS	591.5	2.4	0.004	P1000:500	
Assigned value (cp):		5.00E+03	3.5E+02	7.09E-02	
Expanded uncertainty			7.1E+02	1.42E-01	

Chapter 9 Appendices

ERCC-42

Factor	Term	Value x	u	u'=(u/x)*	Remark**
Stock	Estimated stock value (cp)	7.305E+11	0.00E+00	0.000	See Appendix 3, Table 9.7 , ERCC-13
Nanodrop Calibration	Nanodrop Calibration (cp)	0	0.00E+00	0.042	See Appendix 3, Table 9.7 , ERCC-13
Material integrity:					
Impurity	Estimated purity (mass fraction basis)	1.000	0.00000	0.000	See Appendix 3, Table 9.7 , ERCC-13
Homogeneity	Homogeneity (cp)	0	7.0E+01	0.070	See Appendix 3, Table 9.7 , ERCC-13
Stability	Stability	0	0	n/a	No allowance made
Volumetric: (Based on manufacturer's specifications)					
Step 1: Dilution to 1E+11 c/μL	Aliquot (μL)	5	0.0	0.000	P10:10
	Diluted with (μL) RSS	31.52	0.0	0.000	P100:50
Step 2: Dilution to 1E+9 c/μL	Aliquot (μL)	5	0.0	0.000	P10:10
	Diluted with (μL) RSS	495	0.0	0.000	P1000:500
Step 3: Dilution to 1E+8 c/μL	Aliquot (μL)	20	0.0	0.000	P20:10
	Diluted with (μL) RSS	180	0.0	0.000	P200:200
Step 4: Mixing of ERCC solutions to prepare 100× ERCC solution	Aliquot (μL)	1.5	0.02	0.012	P2:2
	Diluted with (μL) RSS	1000	4.7	0.005	P1000:1000
	Diluted with (μL) RSS	114.5	0.9	0.008	P200:200
	Diluted with (μL) ERCC-13	90	0.5	0.005	P100:100
	Diluted with (μL) ERCC-25	7.5	0.1	0.008	P10:10
	Diluted with (μL) ERCC-99	105	0.5	0.005	P200:100
	Diluted with (μL) ERCC-113	31.5	0.2	0.008	P100:50
Step 5: Preparation of units: Mixing of 100× ERCC and Cell line solutions	Diluted with (μL) ERCC-171	150	0.9	0.006	P200:200
	Aliquot (μL)	367.5	2.4	0.006	P1000:500
	Diluted with (μL) Hep-G2	4000.00	17.8	0.004	P5000:5000
	Diluted with (μL) Hep-G2	116	0.5	0.004	P200:100
	Diluted with (μL) SaOS-2	735.00	2.4	0.003	P1000:500
	Diluted with (μL) Hs683	2000	4.7	0.002	P1000:1000
	Diluted with (μL) Hs683	940	4.7	0.005	P1000:1000
	Diluted with (μL) RSS	25000	87.1	0.003	P5000:25k
	Diluted with (μL) RSS	1000	1.8	0.002	P1000:200
	Diluted with (μL) RSS	1000	1.8	0.002	P1000:200
	Assigned value (cp):	1.00E+03	7.1E+01	7.15E-02	
	Expanded uncertainty		1.4E+02	1.43E-01	

Chapter 9 Appendices

ERCC-99

Factor	Term	Value x	u	u'=(u/x)*	Remark**
Stock	Estimated stock value (cp)	5.559E+11	0.00E+00	0.000	See Appendix 3, Table 9.7 , ERCC-13
Nanodrop Calibration	Nanodrop Calibration (cp)	0	0.00E+00	0.042	See Appendix 3, Table 9.7 , ERCC-13
Material integrity:					
Impurity	Estimated purity (mass fraction basis)	0.986	0.00000	0.000	See Appendix 3, Table 9.7 , ERCC-13
Homogeneity	Homogeneity (cp)	0	4.8E+03	0.070	See Appendix 3, Table 9.7 , ERCC-13
Stability	Stability	0	0	n/a	No allowance made
Volumetric: (Based on manufacturer's specifications)					
Step 1: Dilution to 1E+11 c/μL	Aliquot (μL)	5	0.0	0.000	P10:10
	Diluted with (μL) RSS	22.79	0.0	0.000	P100:50
Step 2: Dilution to 1E+9 c/μL	Aliquot (μL)	5	0.0	0.000	P10:10
	Diluted with (μL) RSS	495	0.0	0.000	P1000:500
Step 3: Dilution to 1E+8 c/μL	Aliquot (μL)	20	0.0	0.000	P20:10
	Diluted with (μL) RSS	180	0.0	0.000	P200:200
Step 4: Mixing of ERCC solutions to prepare 100× ERCC solution	Aliquot (μL)	105	0.5	0.005	P200:100
	Diluted with (μL) RSS	1000	4.7	0.005	P1000:1000
	Diluted with (μL) RSS	114.5	0.9	0.008	P200:200
	Diluted with (μL) ERCC-13	90	0.5	0.005	P100:100
	Diluted with (μL) ERCC-25	7.5	0.1	0.008	P10:10
	Diluted with (μL) ERCC-42	1.5	0.02	0.012	P2:2
	Diluted with (μL) ERCC-113	31.5	0.2	0.008	P100:50
Step 5: Preparation of units: Mixing of 100× ERCC and Cell line solutions	Diluted with (μL) ERCC-171	150	0.9	0.006	P200:200
	Aliquot (μL)	367.5	2.4	0.006	P1000:500
	Diluted with (μL) Hep-G2	4000.00	17.8	0.004	P5000:5000
	Diluted with (μL) Hep-G2	116	0.5	0.004	P200:100
	Diluted with (μL) SaOS-2	735.00	2.4	0.003	P1000:500
	Diluted with (μL) Hs683	2000	4.7	0.002	P1000:1000
	Diluted with (μL) Hs683	940	4.7	0.005	P1000:1000
	Diluted with (μL) RSS	25000	87.1	0.003	P5000:25k
	Diluted with (μL) RSS	1000	1.8	0.002	P1000:200
	Diluted with (μL) RSS	1000	1.8	0.002	P1000:200
	Diluted with (μL) RSS	1000	1.8	0.002	P1000:200
Diluted with (μL) RSS	591.5	2.4	0.004	P1000:500	
Assigned value (cp):		6.90E+04	4.9E+03	7.05E-02	
Expanded uncertainty			9.7E+03	1.41E-01	

Chapter 9 Appendices

ERCC-113

Factor	Term	Value x	u	u'=(u/x)*	Remark**
Stock	Estimated stock value (cp)	1.807E+12	0.00E+00	0.000	See Appendix 3, Table 9.7 , ERCC-13
Nanodrop Calibration	Nanodrop Calibration (cp)	0	0.00E+00	0.042	See Appendix 3, Table 9.7 , ERCC-13
Material integrity:					
Impurity	Estimated purity (mass fraction basis)	0.938	0.00000	0.000	See Appendix 3, Table 9.7 , ERCC-13
Homogeneity	Homogeneity (cp)	0	1.4E+03	0.070	See Appendix 3, Table 9.7 , ERCC-13
Stability	Stability	0	0	n/a	No allowance made
Volumetric: (Based on manufacturer's specifications)					
Step 1: Dilution to 1E+11 c/μL	Aliquot (μL)	5	0.0	0.000	P10:10
	Diluted with (μL) RSS	85.34	0.0	0.000	P100:100
Step 2: Dilution to 1E+9 c/μL	Aliquot (μL)	5	0.0	0.000	P10:10
	Diluted with (μL) RSS	495	0.0	0.000	P1000:500
Step 3: Dilution to 1E+8 c/μL	Aliquot (μL)	20	0.0	0.000	P20:10
	Diluted with (μL) RSS	180	0.0	0.000	P200:200
Step 4: Mixing of ERCC solutions to prepare 100× ERCC solution	Aliquot (μL)	31.5	0.2	0.008	P100:50
	Diluted with (μL) RSS	1000	4.7	0.005	P1000:1000
	Diluted with (μL) RSS	114.5	0.9	0.008	P200:200
	Diluted with (μL) ERCC-13	90	0.5	0.005	P100:100
	Diluted with (μL) ERCC-25	7.5	0.1	0.008	P10:10
	Diluted with (μL) ERCC-42	1.5	0.02	0.012	P2:2
	Diluted with (μL) ERCC-99	105	0.5	0.005	P200:100
Step 5: Preparation of units: Mixing of 100× ERCC and Cell line solutions	Diluted with (μL) ERCC-171	150	0.9	0.006	P200:200
	Aliquot (μL)	367.5	2.4	0.006	P1000:500
	Diluted with (μL) Hep-G2	4000.00	17.8	0.004	P5000:5000
	Diluted with (μL) Hep-G2	116	0.5	0.004	P200:100
	Diluted with (μL) SaOS-2	735.00	2.4	0.003	P1000:500
	Diluted with (μL) Hs683	2000	4.7	0.002	P1000:1000
	Diluted with (μL) Hs683	940	4.7	0.005	P1000:1000
	Diluted with (μL) RSS	25000	87.1	0.003	P5000:25k
	Diluted with (μL) RSS	1000	1.8	0.002	P1000:200
	Diluted with (μL) RSS	1000	1.8	0.002	P1000:200
	Diluted with (μL) RSS	1000	1.8	0.002	P1000:200
Diluted with (μL) RSS	591.5	2.4	0.004	P1000:500	
	Assigned value (cp):	1.97E+04	1.4E+03	7.08E-02	
	Expanded uncertainty		2.8E+03	1.42E-01	

Chapter 9 Appendices

ERCC-171

Factor	Term	Value x	u	u'=(u/x)*	Remark**
Stock	Estimated stock value (cp)	1.421E+12	0.00E+00	0.000	See Appendix 3, Table 9.7 , ERCC-13
Nanodrop Calibration	Nanodrop Calibration (cp)	0	0.00E+00	0.042	See Appendix 3, Table 9.7 , ERCC-13
Material integrity:					
Impurity	Estimated purity (mass fraction basis)	0.939	0.00000	0.000	See Appendix 3, Table 9.7 , ERCC-13
Homogeneity	Homogeneity (cp)	0	6.6E+03	0.070	See Appendix 3, Table 9.7 , ERCC-13
Stability	Stability	0	0	n/a	No allowance made
Volumetric: (Based on manufacturer's specifications)					
Step 1: Dilution to 1E+11 c/μL	Aliquot (μL)	5	0.0	0.000	P10:10
	Diluted with (μL) RSS	66.05	0.0	0.000	P100:50
Step 2: Dilution to 1E+9 c/μL	Aliquot (μL)	5	0.0	0.000	P10:10
	Diluted with (μL) RSS	495	0.0	0.000	P1000:500
Step 3: Dilution to 1E+8 c/μL	Aliquot (μL)	20	0.0	0.000	P20:10
	Diluted with (μL) RSS	180	0.0	0.000	P200:200
Step 4: Mixing of ERCC solutions to prepare 100× ERCC solution	Aliquot (μL)	150	0.9	0.006	P200:200
	Diluted with (μL) RSS	1000	4.7	0.005	P1000:1000
	Diluted with (μL) RSS	114.5	0.9	0.008	P200:200
	Diluted with (μL) ERCC-13	90	0.5	0.005	P100:100
	Diluted with (μL) ERCC-25	7.5	0.1	0.008	P10:10
	Diluted with (μL) ERCC-42	1.5	0.02	0.012	P2:2
	Diluted with (μL) ERCC-99	105	0.5	0.005	P200:100
	Diluted with (μL) ERCC-113	31.5	0.2	0.008	P100:50
Step 5: Preparation of units: Mixing of 100× ERCC and Cell line solutions	Aliquot (μL)	367.5	2.4	0.006	P1000:500
	Diluted with (μL) Hep-G2	4000.00	17.8	0.004	P5000:5000
	Diluted with (μL) Hep-G2	116	0.5	0.004	P200:100
	Diluted with (μL) SaOS-2	735.00	2.4	0.003	P1000:500
	Diluted with (μL) Hs683	2000	4.7	0.002	P1000:1000
	Diluted with (μL) Hs683	940	4.7	0.005	P1000:1000
	Diluted with (μL) RSS	25000	87.1	0.003	P5000:25k
	Diluted with (μL) RSS	1000	1.8	0.002	P1000:200
	Diluted with (μL) RSS	1000	1.8	0.002	P1000:200
	Diluted with (μL) RSS	1000	1.8	0.002	P1000:200
	Diluted with (μL) RSS	591.5	2.4	0.004	P1000:500
	Assigned value (cp):	9.39E+04	6.6E+03	7.06E-02	
	Expanded uncertainty		1.3E+04	1.41E-01	

Chapter 9 Appendices

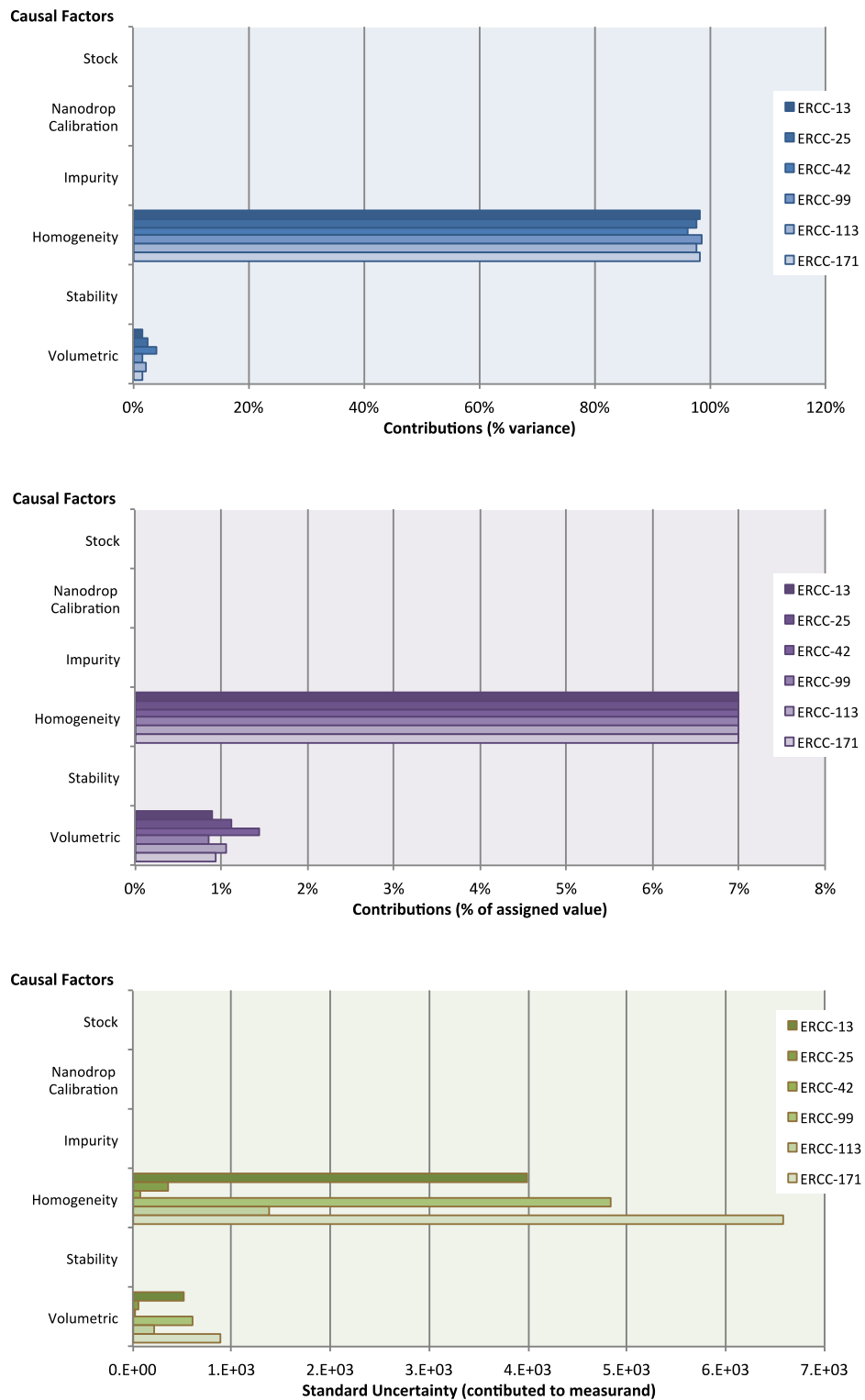


Figure 9.3 Unknown 1 Unit Measurement Uncertainty Contributing Factors. Measurement uncertainty components common to both Unknown 1 and Unknown 2 are not included in corresponding uncertainty budgets as these contributions cancel out in measurement of combined standard uncertainty of assigned ratios.

Table 9.9 Calculation of Unknown 2 assigned value and measurement uncertainty. Measurement uncertainty components common to both Unknown 1 and Unknown 2 are not included in corresponding uncertainty budgets as these contributions cancel out in measurement of combined standard uncertainty of assigned ratios.

ERCC-13

Factor	Term	Value x	u	u'=(u/x)*	Remark**
Stock	Estimated stock value (cp)	1.018E+12	0.00E+00	0.000	See Appendix 3, Table 9.7 , ERCC-13
Nanodrop Calibration	Nanodrop Calibration (cp)	0	0.00E+00	0.042	See Appendix 3, Table 9.7 , ERCC-13
Material integrity:					
Impurity	Estimated purity (mass fraction basis)	0.948	0.00000	0.000	See Appendix 3, Table 9.7 , ERCC-13
Homogeneity	Homogeneity (cp)	0	6.0E+03	0.070	See Appendix 3, Table 9.7 , ERCC-13
Stability	Stability	0	0	n/a	No allowance made
Volumetric: (Based on manufacturer's specifications)					
Step 1: Dilution to 1E+11 c/μL	Aliquot (μL)	5	0.0	0.000	P10:10
	Diluted with (μL) RSS	45.91	0.0	0.000	P100:50
Step 2: Dilution to 1E+9 c/μL	Aliquot (μL)	5	0.0	0.000	P10:10
	Diluted with (μL) RSS	495	0.0	0.000	P1000:500
Step 3: Dilution to 1E+8 c/μL	Aliquot (μL)	20	0.0	0.000	P20:10
	Diluted with (μL) RSS	180	0.0	0.000	P200:200
Step 4: Mixing of ERCC solutions to prepare 100× ERCC solution	Aliquot (μL)	135	0.9	0.007	P200:200
	Diluted with (μL) RSS	1000	4.7	0.005	P1000:1000
	Diluted with (μL) RSS	100	0.5	0.005	P200:100
	Diluted with (μL) RSS	101.5	0.5	0.005	P200:100
	Diluted with (μL) ERCC-25	7.5	0.1	0.008	P10:10
	Diluted with (μL) ERCC-42	10.5	0.06	0.006	P20:10
	Diluted with (μL) ERCC-99	105	0.5	0.005	P200:100
	Diluted with (μL) ERCC-113	10.5	0.1	0.006	P20:10
Step 5: Preparation of units: Mixing of 100× ERCC and Cell line solutions	Diluted with (μL) ERCC-171	30	0.2	0.008	P100:50
	Aliquot (μL)	367.5	2.4	0.006	P1000:500
	Diluted with (μL) Hep-G2	5000.00	17.8	0.004	P5000:5000
	Diluted with (μL) Hep-G2	1000	2.4	0.002	P1000:500
	Diluted with (μL) Hep-G2	600	2.4	0.004	P1000:500
	Diluted with (μL) Hep-G2	382.50	2.4	0.006	P1000:500
	Diluted with (μL) SaOS-2	735	2.4	0.003	P1000:500
	Diluted with (μL) Hs683	73.5	0.5	0.006	P100:100
	Diluted with (μL) RSS	25000	87.1	0.003	P5000:25k
	Diluted with (μL) RSS	1000	4.7	0.005	P1000:1000
	Diluted with (μL) RSS	1000	4.7	0.005	P1000:1000
	Diluted with (μL) RSS	1000	4.7	0.005	P1000:1000
	Diluted with (μL) RSS	591.5	2.4	0.004	P1000:500
	Assigned value (cp):	8.53E+04	6.0E+03	7.07E-02	
	Expanded uncertainty		1.2E+04	1.41E-01	

Chapter 9 Appendices

ERCC-25

Factor	Term	Value x	u	u'=(u/x)*	Remark**
Stock	Estimated stock value (cp)	4.020E+11	0.00E+00	0.000	See Appendix 3, Table 9.7 , ERCC-13
Nanodrop Calibration	Nanodrop Calibration (cp)	0	0.00E+00	0.042	See Appendix 3, Table 9.7 , ERCC-13
Material integrity:					
Impurity	Estimated purity (mass fraction basis)	1.000	0.00000	0.000	See Appendix 3, Table 9.7 , ERCC-13
Homogeneity	Homogeneity (cp)	0	3.5E+02	0.070	See Appendix 3, Table 9.7 , ERCC-13
Stability	Stability	0	0	n/a	No allowance made
Volumetric: (Based on manufacturer's specifications)					
Step 1: Dilution to 1E+11 c/μL	Aliquot (μL)	5	0.0	0.000	P10:10
	Diluted with (μL) RSS	15.1	0.0	0.000	P20:10
Step 2: Dilution to 1E+9 c/μL	Aliquot (μL)	5	0.0	0.000	P10:10
	Diluted with (μL) RSS	495	0.0	0.000	P1000:500
Step 3: Dilution to 1E+8 c/μL	Aliquot (μL)	20	0.0	0.000	P20:10
	Diluted with (μL) RSS	180	0.0	0.000	P200:200
Step 4: Mixing of ERCC solutions to prepare 100× ERCC solution	Aliquot (μL)	7.5	0.1	0.008	P10:10
	Diluted with (μL) RSS	1000	4.7	0.005	P1000:1000
	Diluted with (μL) RSS	100	0.5	0.005	P200:100
	Diluted with (μL) RSS	101.5	0.5	0.005	P200:100
	Diluted with (μL) ERCC-13	135	0.5	0.004	P200:100
	Diluted with (μL) ERCC-42	10.5	0.06	0.006	P20:10
	Diluted with (μL) ERCC-99	105	0.5	0.005	P200:100
	Diluted with (μL) ERCC-113	10.5	0.1	0.006	P20:10
Step 5: Preparation of units: Mixing of 100× ERCC and Cell line solutions	Diluted with (μL) ERCC-171	30	0.2	0.008	P100:50
	Aliquot (μL)	367.5	2.4	0.006	P1000:500
	Diluted with (μL) Hep-G2	5000.00	17.8	0.004	P5000:5000
	Diluted with (μL) Hep-G2	1000	2.4	0.002	P1000:500
	Diluted with (μL) Hep-G2	600	2.4	0.004	P1000:500
	Diluted with (μL) Hep-G2	382.50	2.4	0.006	P1000:500
	Diluted with (μL) SaOS-2	735	2.4	0.003	P1000:500
	Diluted with (μL) Hs683	73.5	0.5	0.006	P100:100
	Diluted with (μL) RSS	25000	87.1	0.003	P5000:25k
	Diluted with (μL) RSS	1000	4.7	0.005	P1000:1000
	Diluted with (μL) RSS	1000	4.7	0.005	P1000:1000
	Diluted with (μL) RSS	1000	4.7	0.005	P1000:1000
Diluted with (μL) RSS	591.5	2.4	0.004	P1000:500	
	Assigned value (cp):	5.00E+03	3.5E+02	7.09E-02	
	Expanded uncertainty		7.1E+02	1.42E-01	

Chapter 9 Appendices

ERCC-42

Factor	Term	Value x	u	u'=(u/x)*	Remark**
Stock	Estimated stock value (cp)	7.305E+11	0.00E+00	0.000	See Appendix 3, Table 9.7 , ERCC-13
Nanodrop Calibration	Nanodrop Calibration (cp)	0	0.00E+00	0.042	See Appendix 3, Table 9.7 , ERCC-13
Material integrity:					
Impurity	Estimated purity (mass fraction basis)	1.000	0.00000	0.000	See Appendix 3, Table 9.7 , ERCC-13
Homogeneity	Homogeneity (cp)	0	4.9E+02	0.070	See Appendix 3, Table 9.7 , ERCC-13
Stability	Stability	0	0	n/a	No allowance made
Volumetric: (Based on manufacturer's specifications)					
Step 1: Dilution to 1E+11 c/μL	Aliquot (μL)	5	0.0	0.000	P10:10
	Diluted with (μL) RSS	31.52	0.0	0.000	P100:50
Step 2: Dilution to 1E+9 c/μL	Aliquot (μL)	5	0.0	0.000	P10:10
	Diluted with (μL) RSS	495	0.0	0.000	P1000:500
Step 3: Dilution to 1E+8 c/μL	Aliquot (μL)	20	0.0	0.000	P20:10
	Diluted with (μL) RSS	180	0.0	0.000	P200:200
Step 4: Mixing of ERCC solutions to prepare 100× ERCC solution	Aliquot (μL)	10.5	0.1	0.006	P20:10
	Diluted with (μL) RSS	1000	4.7	0.005	P1000:1000
	Diluted with (μL) RSS	100	0.5	0.005	P200:100
	Diluted with (μL) RSS	101.5	0.5	0.005	P200:100
	Diluted with (μL) ERCC-13	135	0.5	0.004	P200:100
	Diluted with (μL) ERCC-25	7.5	0.06	0.008	P10:10
	Diluted with (μL) ERCC-99	105	0.5	0.005	P200:100
	Diluted with (μL) ERCC-113	10.5	0.1	0.006	P20:10
Step 5: Preparation of units: Mixing of 100× ERCC and Cell line solutions	Diluted with (μL) ERCC-171	30	0.2	0.008	P100:50
	Aliquot (μL)	367.5	2.4	0.006	P1000:500
	Diluted with (μL) Hep-G2	5000.00	17.8	0.004	P5000:5000
	Diluted with (μL) Hep-G2	1000	2.4	0.002	P1000:500
	Diluted with (μL) Hep-G2	600	2.4	0.004	P1000:500
	Diluted with (μL) Hep-G2	382.50	2.4	0.006	P1000:500
	Diluted with (μL) SaOS-2	735	2.4	0.003	P1000:500
	Diluted with (μL) Hs683	73.5	0.5	0.006	P100:100
	Diluted with (μL) RSS	25000	87.1	0.003	P5000:25k
	Diluted with (μL) RSS	1000	4.7	0.005	P1000:1000
	Diluted with (μL) RSS	1000	4.7	0.005	P1000:1000
	Diluted with (μL) RSS	1000	4.7	0.005	P1000:1000
Diluted with (μL) RSS	591.5	2.4	0.004	P1000:500	
	Assigned value (cp):	7.00E+03	4.9E+02	7.07E-02	
	Expanded uncertainty		9.9E+02	1.41E-01	

Chapter 9 Appendices

ERCC-99

Factor	Term	Value x	u	u'=(u/x)*	Remark**
Stock	Estimated stock value (cp)	5.559E+11	0.00E+00	0.000	See Appendix 3, Table 9.7 , ERCC-13
Nanodrop Calibration	Nanodrop Calibration (cp)	0	0.00E+00	0.042	See Appendix 3, Table 9.7 , ERCC-13
Material integrity:					
Impurity	Estimated purity (mass fraction basis)	0.986	0.00000	0.000	See Appendix 3, Table 9.7 , ERCC-13
Homogeneity	Homogeneity (cp)	0	4.8E+03	0.070	See Appendix 3, Table 9.7 , ERCC-13
Stability	Stability	0	0	n/a	No allowance made
Volumetric: (Based on manufacturer's specifications)					
Step 1: Dilution to 1E+11 c/μL	Aliquot (μL)	5	0.0	0.000	P10:10
	Diluted with (μL) RSS	22.79	0.0	0.000	P100:50
Step 2: Dilution to 1E+9 c/μL	Aliquot (μL)	5	0.0	0.000	P10:10
	Diluted with (μL) RSS	495	0.0	0.000	P1000:500
Step 3: Dilution to 1E+8 c/μL	Aliquot (μL)	20	0.0	0.000	P20:10
	Diluted with (μL) RSS	180	0.0	0.000	P200:200
Step 4: Mixing of ERCC solutions to prepare 100× ERCC solution	Aliquot (μL)	105	0.5	0.005	P200:100
	Diluted with (μL) RSS	1000	4.7	0.005	P1000:1000
	Diluted with (μL) RSS	100	0.5	0.005	P200:100
	Diluted with (μL) RSS	101.5	0.5	0.005	P200:100
	Diluted with (μL) ERCC-13	135	0.5	0.004	P200:100
	Diluted with (μL) ERCC-25	7.5	0.06	0.008	P10:10
	Diluted with (μL) ERCC-42	10.5	0.1	0.006	P20:10
	Diluted with (μL) ERCC-113	10.5	0.1	0.006	P20:10
Step 5: Preparation of units: Mixing of 100× ERCC and Cell line solutions	Diluted with (μL) ERCC-171	30	0.2	0.008	P100:50
	Aliquot (μL)	367.5	2.4	0.006	P1000:500
	Diluted with (μL) Hep-G2	5000.00	17.8	0.004	P5000:5000
	Diluted with (μL) Hep-G2	1000	2.4	0.002	P1000:500
	Diluted with (μL) Hep-G2	600	2.4	0.004	P1000:500
	Diluted with (μL) Hep-G2	382.50	2.4	0.006	P1000:500
	Diluted with (μL) SaOS-2	735	2.4	0.003	P1000:500
	Diluted with (μL) Hs683	73.5	0.5	0.006	P100:100
	Diluted with (μL) RSS	25000	87.1	0.003	P5000:25k
	Diluted with (μL) RSS	1000	4.7	0.005	P1000:1000
	Diluted with (μL) RSS	1000	4.7	0.005	P1000:1000
	Diluted with (μL) RSS	1000	4.7	0.005	P1000:1000
	Diluted with (μL) RSS	591.5	2.4	0.004	P1000:500
Assigned value (cp):		6.90E+04	4.9E+03	7.05E-02	
Expanded uncertainty			9.7E+03	1.41E-01	

Chapter 9 Appendices

ERCC-113

Factor	Term	Value x	u	u'=(u/x)*	Remark**
Stock	Estimated stock value (cp)	1.807E+12	0.00E+00	0.000	See Appendix 3, Table 9.7 , ERCC-13
Nanodrop Calibration	Nanodrop Calibration (cp)	0	0.00E+00	0.042	See Appendix 3, Table 9.7 , ERCC-13
Material integrity:					
Impurity	Estimated purity (mass fraction basis)	0.938	0.00000	0.000	See Appendix 3, Table 9.7 , ERCC-13
Homogeneity	Homogeneity (cp)	0	4.6E+02	0.070	See Appendix 3, Table 9.7 , ERCC-13
Stability	Stability	0	0	n/a	No allowance made
Volumetric: (Based on manufacturer's specifications)					
Step 1: Dilution to 1E+11 c/μL	Aliquot (μL)	5	0.0	0.000	P10:10
	Diluted with (μL) RSS	85.34	0.0	0.000	P100:100
Step 2: Dilution to 1E+9 c/μL	Aliquot (μL)	5	0.0	0.000	P10:10
	Diluted with (μL) RSS	495	0.0	0.000	P1000:500
Step 3: Dilution to 1E+8 c/μL	Aliquot (μL)	20	0.0	0.000	P20:10
	Diluted with (μL) RSS	180	0.0	0.000	P200:200
Step 4: Mixing of ERCC solutions to prepare 100× ERCC solution	Aliquot (μL)	10.5	0.1	0.006	P20:10
	Diluted with (μL) RSS	1000	4.7	0.005	P1000:1000
	Diluted with (μL) RSS	100	0.5	0.005	P200:100
	Diluted with (μL) RSS	101.5	0.5	0.005	P200:100
	Diluted with (μL) ERCC-13	135	0.5	0.004	P200:100
	Diluted with (μL) ERCC-25	7.5	0.06	0.008	P10:10
	Diluted with (μL) ERCC-42	10.5	0.1	0.006	P20:10
	Diluted with (μL) ERCC-99	105	0.5	0.005	P200:100
Step 5: Preparation of units: Mixing of 100× ERCC and Cell line solutions	Diluted with (μL) ERCC-171	30	0.2	0.008	P100:50
	Aliquot (μL)	367.5	2.4	0.006	P1000:500
	Diluted with (μL) Hep-G2	5000.00	17.8	0.004	P5000:5000
	Diluted with (μL) Hep-G2	1000	2.4	0.002	P1000:500
	Diluted with (μL) Hep-G2	600	2.4	0.004	P1000:500
	Diluted with (μL) Hep-G2	382.50	2.4	0.006	P1000:500
	Diluted with (μL) SaOS-2	735	2.4	0.003	P1000:500
	Diluted with (μL) Hs683	73.5	0.5	0.006	P100:100
	Diluted with (μL) RSS	25000	87.1	0.003	P5000:25k
	Diluted with (μL) RSS	1000	4.7	0.005	P1000:1000
	Diluted with (μL) RSS	1000	4.7	0.005	P1000:1000
	Diluted with (μL) RSS	1000	4.7	0.005	P1000:1000
	Diluted with (μL) RSS	591.5	2.4	0.004	P1000:500
	Assigned value (cp):	6.57E+03	4.6E+02	7.07E-02	
	Expanded uncertainty		9.3E+02	1.41E-01	

Chapter 9 Appendices

ERCC-171

Factor	Term	Value x	u	u'=(u/x)*	Remark**
Stock	Estimated stock value (cp)	1.421E+12	0.00E+00	0.000	See Appendix 3, Table 9.7 , ERCC-13
Nanodrop Calibration	Nanodrop Calibration (cp)	0	0.00E+00	0.042	See Appendix 3, Table 9.7 , ERCC-13
Material integrity:					
Impurity	Estimated purity (mass fraction basis)	0.939	0.00000	0.000	See Appendix 3, Table 9.7 , ERCC-13
Homogeneity	Homogeneity (cp)	0	1.3E+03	0.070	See Appendix 3, Table 9.7 , ERCC-13
Stability	Stability	0	0	n/a	No allowance made
Volumetric: (Based on manufacturer's specifications)					
Step 1: Dilution to 1E+11 c/μL	Aliquot (μL)	5	0.0	0.000	P10:10
	Diluted with (μL) RSS	66.05	0.0	0.000	P100:50
Step 2: Dilution to 1E+9 c/μL	Aliquot (μL)	5	0.0	0.000	P10:10
	Diluted with (μL) RSS	495	0.0	0.000	P1000:500
Step 3: Dilution to 1E+8 c/μL	Aliquot (μL)	20	0.0	0.000	P20:10
	Diluted with (μL) RSS	180	0.0	0.000	P200:200
Step 4: Mixing of ERCC solutions to prepare 100× ERCC solution	Aliquot (μL)	30	0.2	0.008	P100:50
	Diluted with (μL) RSS	1000	4.7	0.005	P1000:1000
	Diluted with (μL) RSS	100	0.5	0.005	P200:100
	Diluted with (μL) RSS	101.5	0.5	0.005	P200:100
	Diluted with (μL) ERCC-13	135	0.5	0.004	P200:100
	Diluted with (μL) ERCC-25	7.5	0.06	0.008	P10:10
	Diluted with (μL) ERCC-42	10.5	0.1	0.006	P20:10
	Diluted with (μL) ERCC-99	105	0.5	0.005	P200:100
Step 5: Preparation of units: Mixing of 100× ERCC and Cell line solutions	Diluted with (μL) ERCC-113	10.5	0.1	0.006	P20:10
	Aliquot (μL)	367.5	2.4	0.006	P1000:500
	Diluted with (μL) Hep-G2	5000.00	17.8	0.004	P5000:5000
	Diluted with (μL) Hep-G2	1000	2.4	0.002	P1000:500
	Diluted with (μL) Hep-G2	600	2.4	0.004	P1000:500
	Diluted with (μL) Hep-G2	382.50	2.4	0.006	P1000:500
	Diluted with (μL) SaOS-2	735	2.4	0.003	P1000:500
	Diluted with (μL) Hs683	73.5	0.5	0.006	P100:100
	Diluted with (μL) RSS	25000	87.1	0.003	P5000:25k
	Diluted with (μL) RSS	1000	4.7	0.005	P1000:1000
	Diluted with (μL) RSS	1000	4.7	0.005	P1000:1000
	Diluted with (μL) RSS	1000	4.7	0.005	P1000:1000
	Diluted with (μL) RSS	591.5	2.4	0.004	P1000:500
	Assigned value (cp):	1.88E+04	1.3E+03	7.08E-02	
	Expanded uncertainty		2.7E+03	1.42E-01	

Chapter 9 Appendices

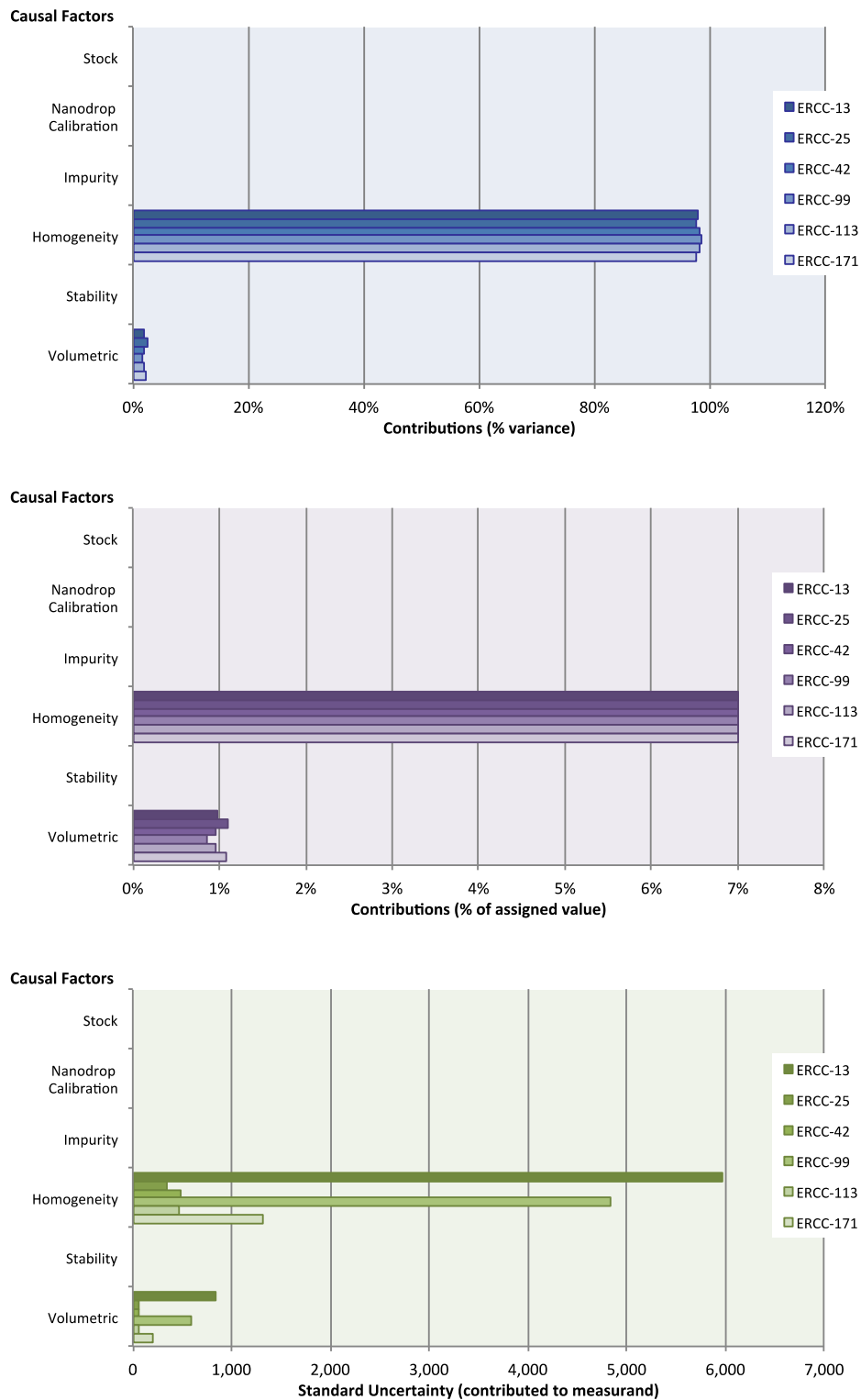
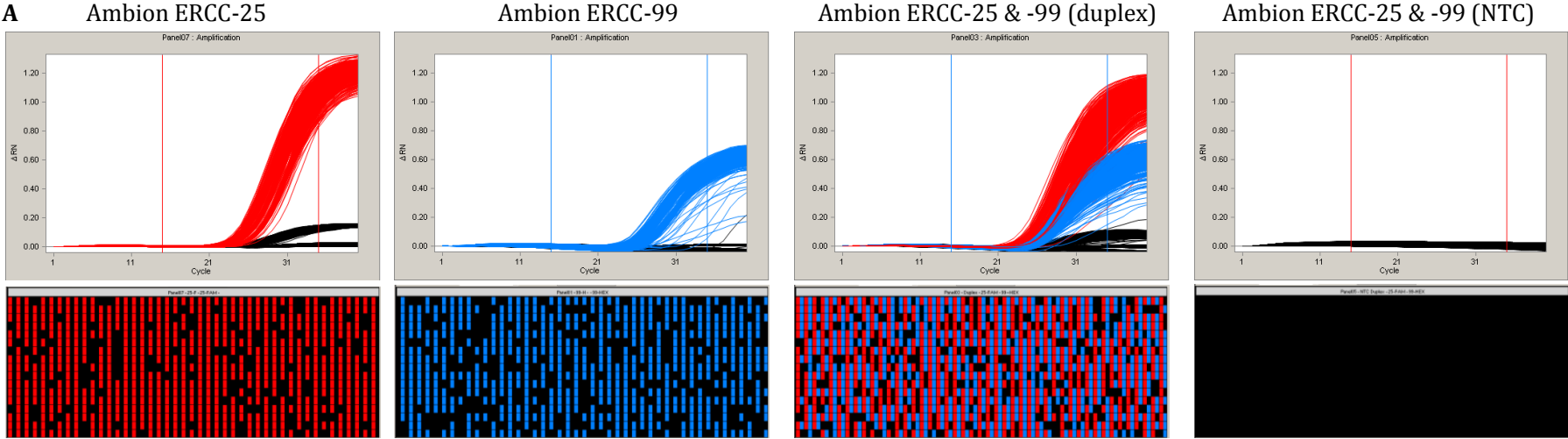


Figure 9.4 Unknown 2 Unit Measurement Uncertainty Contributing Factors. Measurement uncertainty components common to both Unknown 1 and Unknown 2 are not included in corresponding uncertainty budgets as these contributions cancel out in measurement of combined standard uncertainty of assigned ratios.

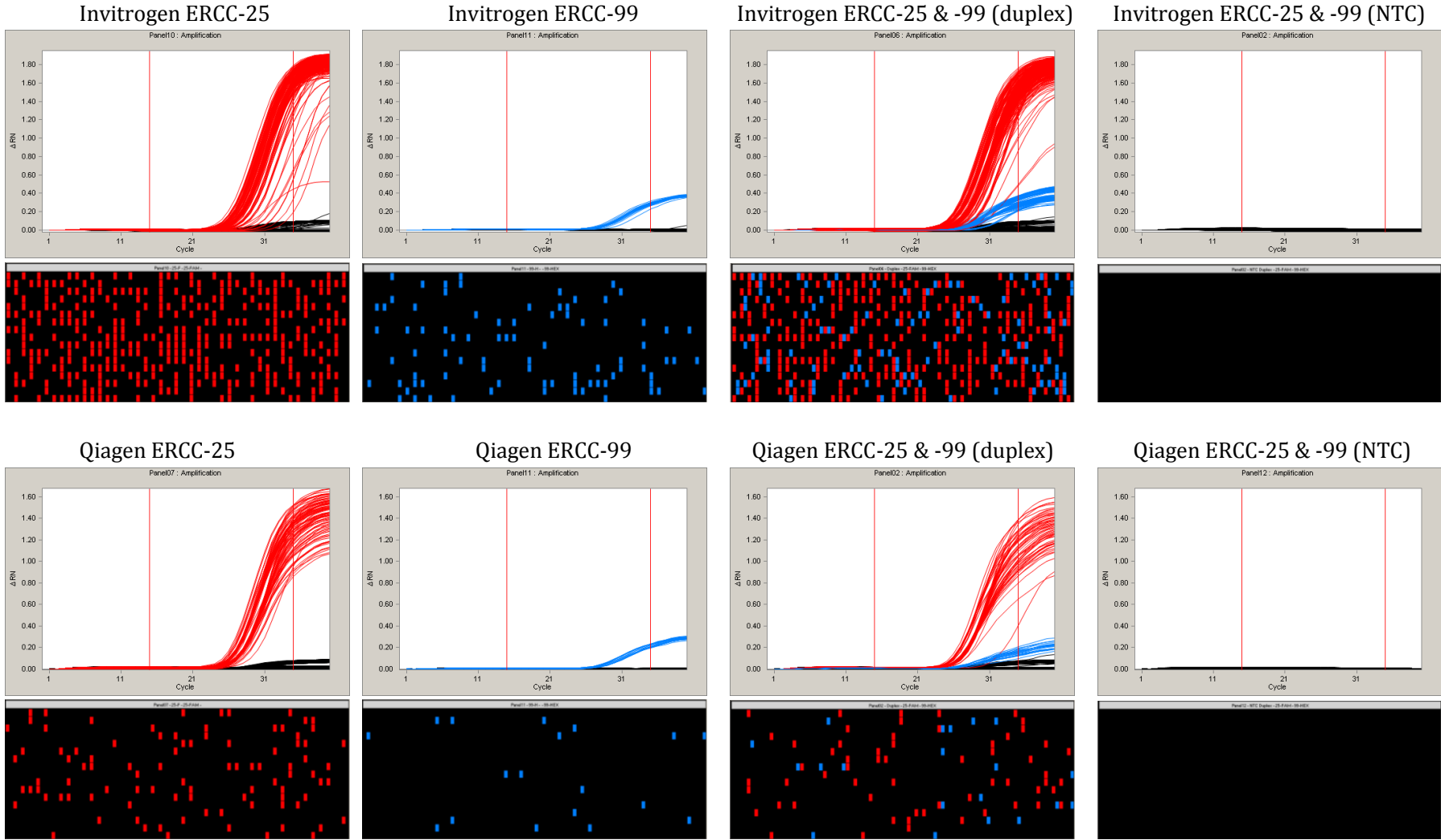
9.4 Appendix 4 – Pilot Reference Material Composition**Table 9.10 Proportions of each cell line included in the pilot RMs.** Hep-G2 and Hs683 total RNA was used at 250 ng/ μ L, and SaOS-2 total RNA was used at 100 ng/ μ L.

Cell Line	Proportions		
	Calibrant	Unknown 1	Unknown 2
Hep-G2 total RNA	0.755	0.56	0.95
SaOS-2 total RNA	0.04	0.04	0.04
Hs683 total RNA	0.205	0.40	0.01

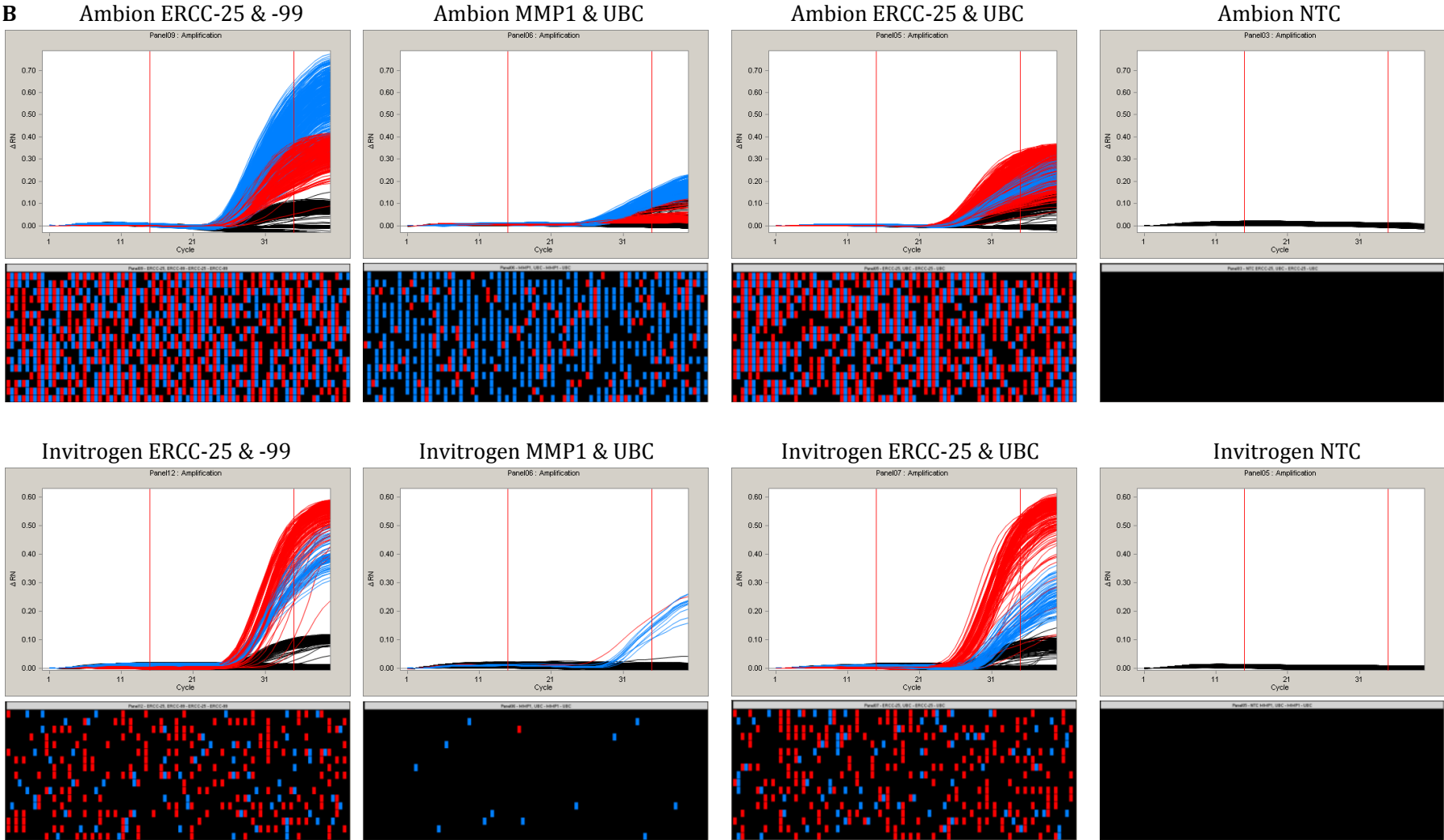
9.5 Appendix 5 – Typical dPCR Output Data



Chapter 9 Appendices



Chapter 9 Appendices



Chapter 9 Appendices

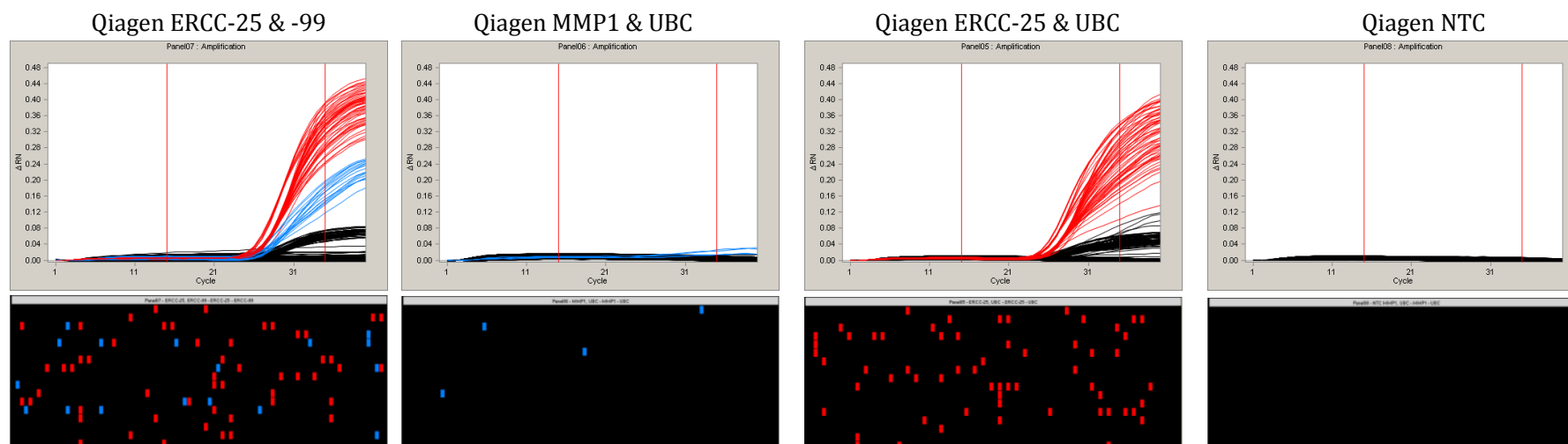


Figure 9.5 Typical dPCR output data from Chapter 4. Both amplification plots and heat maps are shown. Amplification plots display ΔRN versus cycle number. Heat maps are the corresponding schematic representations of positive partitions as detected by the Biomark instrument. Black = no amplification. Red = FAM amplification. Blue = HEX amplification. Threshold was adjusted to eliminate cross talk between the filters (FAM versus HEX). (A) One-Step RT-qPCR Kit Comparison by dPCR. (B) Endogenous versus Synthetic Targets.

9.6 Appendix 6 – Digital MIQE

Table 9.11 dMIQE checklist for authors, reviewers and editors. All essential information (E) must be submitted with the manuscript. Desirable information (D) should be submitted if possible.

ITEM TO CHECK	IMPORTANCE	Checklist	Comments/Where?
EXPERIMENTAL DESIGN			
Definition of experimental and control groups	E	Y	Chapter 2
Number within each group	E	Y	Chapter 2 & Appendix 1
Assay carried out by core lab or investigator's lab?	D	Y	Investigator's lab
Power analysis	D	N	-
SAMPLE			
Description	E	Y	Chapter 2
Volume or mass of sample processed	E	Y	Chapter 2 & Appendix 1
Microdissection or macrodissection	E	N/A	-
Processing procedure	E	Y	Chapter 2
If frozen - how and how quickly?	E	Y	Chapter 2
If fixed - with what, how quickly?	E	N/A	-
Sample storage conditions and duration (especially for FFPE samples)	E	Y	Chapter 2
NUCLEIC ACID EXTRACTION			
Quantification - instrument/method	E	Y	Chapter 2
Storage conditions: temperature, concentration, duration, buffer	E	Y	Chapter 2
DNA or RNA quantification	E	Y	Chapter 2
Quality/integrity- instrument/method; e.g. RIN/RQI and trace or 3':5'	E	Y	Chapters 2-6
Template structural information	E	Y	Chapter 2 & 4
Template modification (digestion, sonication, pre-amplification etc.)	E	Y	Chapters 2-6
Template treatment (initial heating or chemical	E	Y	Chapter 2

Chapter 9 Appendices

denaturation)			
Inhibition dilution or spike;	E	Y	Chapter 2
DNA contamination assessment of RNA sample	E	Y	Chapter 2-3
Details of DNase treatment where performed	E	Y	Chapter 2-6
Manufacturer of reagents used and catalogue number	D	Y	Chapter 2
Storage of nucleic acid: temperature, concentration, duration, buffer	E	Y	Chapter 2
REVERSE TRANSCRIPTION (If necessary)			
cDNA priming method + concentration	E	Y	Chapter 2
One or two step protocol	E	Y	Chapter 2 & Appendix 1
Amount of RNA used per reaction	E	Y	Chapter 2 & Appendix 1
Detailed reaction components and conditions	E	Y	Chapter 2
RT efficiency	D	Y	Chapter 3
Estimated copies measured with and without addition of RT*	D	Y	Alu PCR, Chapter 5
Manufacturer of reagents used and catalogue number	D	Y	Chapter 2
Reaction volume (for two step reverse transcription reaction)	D	Y	Chapter 2
Storage of cDNA: temperature, concentration, duration, buffer	D	Y	Chapter 2
dPCR TARGET INFORMATION			
Sequence accession number	E	Y	Appendix 1
Location of amplicon	D	Y	Appendix 1
Amplicon length	E	Y	Appendix 1
In silico specificity screen (BLAST, etc.)	E	Y	Chapter 2
Pseudogenes, retropseudogenes or other homologs?	D	Y	Chapter 2

Chapter 9 Appendices

Sequence alignment	D	Y	Chapter 2
Secondary structure analysis of amplicon and GC content	D	Y	Chapter 2 & 4, Appendix 2
Location of each primer by exon or intron (if applicable)	E	Y	Appendix 1
Where appropriate, which splice variants are targeted?	E	Y	Appendix 1
dPCR OLIGONUCLEOTIDES			
Primer sequences and/or amplicon context sequence**	E	Y	Appendix 1
RTPrimerDB Identification Number	D	N/A	-
Probe sequences**	D	Y	Appendix 1
Location and identity of any modifications	E	N/A	-
Manufacturer of oligonucleotides	D	Y	Chapter 2
Purification method	D	Y	Chapter 2
dPCR PROTOCOL			
Complete reaction conditions	E	Y	Chapter 2
Reaction volume and amount of RNA/cDNA/DNA	E	Y	Chapter 2 & Appendix 1
Primer, (probe), Mg ⁺⁺ and dNTP concentrations	E	Y	Chapter 2
Polymerase identity and concentration	E	Y	Chapter 2
Buffer/kit Catalogue No and manufacturer	E	Y	Chapter 2
Exact chemical constitution of the buffer	D	N/A	Proprietary
Additives (SYBR Green I, DMSO, etc.)	E	Y	Chapter 2
Plates/tubes Catalogue No and manufacturer	D	Y	Chapter 2
Complete thermocycling parameters	E	Y	Chapter 2
Reaction setup	D	Y	Chapter 2
Gravimetric or volumetric dilutions (manual/robotic)	D	Y	Chapter 2
Total PCR reaction volume prepared	D	Y	Chapter 2
Partition number	E	Y	Chapter 2

Chapter 9 Appendices

Individual partition volume	E	Y	Chapter 2
Total volume of the partitions measured (effective reaction size)	E	Y	Chapter 2
Partition volume variance/standard deviation	D	No	-
Comprehensive details and appropriate use of controls	E	Y	Chapter 2
Manufacturer of dPCR instrument	E	Y	Chapter 2
dPCR VALIDATION			
Optimisation data for the assay	D	Y	Chapter 2 & 3
Specificity (when measuring rare mutations, pathogen sequences etc.)	E	Y	Chapter 3
Limit of detection of calibration control	D	Y	Chapter 2-4
If multiplexing, comparison with singleplex assays	E	Y	Chapter 2 & 4
DATA ANALYSIS			
Average copies per partition (λ or equivalent)	E	Y	Chapter 2-4 & 6
dPCR analysis program (source, version)	E	Y	Chapter 2
Outlier identification and disposition	E		Chapter 3-6
Results of NTCs	E	Y	Chapter 2
Examples of positive(s) and negative experimental results as supplemental data	E	Y	Appendix 5
Where appropriate, justification of number and choice of reference genes	E	Y	Chapter 2-6
Where appropriate, description of normalisation method	E	Y	Chapter 1-6
Number and concordance of biological replicates	D	Y	Chapter 2-6
Number and stage (RT or qPCR) of technical replicates	E	Y	Chapter 2 & Appendix 1
Repeatability (intra-assay variation)	E	Y	Chapter 2-6

Chapter 9 Appendices

Reproducibility (inter-assay/user/lab etc. variation)	D	Y	Chapter 2-6
Experimental variance or confidence interval***	E	Y	Chapter 2-6
Statistical methods used for analysis	E	Y	Chapter 2-6
Data submission using RDML	D	N\A	-

* Assessing the absence of DNA using a no RT assay is essential when first extracting RNA. Once the sample has been validated as DNA-free, inclusion of a no-RT control is desirable, but no longer essential.

** Disclosure of the primer and probe sequence is highly desirable and strongly encouraged. However, since not all commercial pre-designed assay vendors provide this information when it is not available assay context sequences must be submitted [55].

*** When single dPCR experiments are performed, the variation due to counting error alone should be calculated from the binomial (or suitable equivalent) distribution.